Scientific Journals

of the Maritime University of Szczecin ● 48 (120) 2016

Zeszyty Naukowe Akademii Morskiej w Szczecinie

Quarterly

Szczecin, December 2016

Scientific Journals of the Maritime University of Szczecin
Zeszyty Naukowe Akademii Morskiej w Szczecinie
ISSN 1733-8670 (Printed)
ISSN 2392-0378 (Online)

The Scientific Journals of the Maritime University of Szczecin printed version is primary
Wersja drukowana Zeszytów Naukowych Akademii Morskiej w Szczecinie jest wersją pierwotną wydawanego czasopisma

Editorial office: ul. T. Starzyńskiego 8, 70-506 Szczecin, Poland
tel. +48 91 480 96 45, +48 91 480 96 16, e-mail: journals@am.szczecin.pl, http://scientific-journals.eu/

First Edition. 150 copies. 23.75 publishing sheets (ark. wyd.)

Printed by Kampol s.j., ul. Felczaka 17, 71-417 Szczecin, Poland

CONTENTS

Scientific Journals
of the Maritime University of Szczecin

Zeszyty Naukowe
Akademii Morskiej w Szczecinie

2016, 48 (120), 5
ISSN 1733-8670 (Printed)
ISSN 2392-0378 (Online)
DOI: 10.17402/168

Editorial preface

Leszek Chybowski

Maritime University of Szczecin
1–2 Wały Chrobrego St., 70-500 Szczecin, Poland
e-mail: l.chybowski@am.szczecin.pl

Dear Readers,

It is my great pleasure to present the 48th issue of the Scientific Journals of the Maritime University of Szczecin. This issue features recent findings from the fields of marine engineering, sea navigation as well as waterborne and land transportation.

The Marine Technology and Innovation studies address fire safety, modelling the work of marine systems such as steam boilers and dynamic positioning systems, the use of liquid fuels and selected methods for constructing an ontology for automatic communication at sea.

The Navigation and Marine Transport section contains articles focussed on the use of integrated marine navigation systems, optimising sea routes, analysing vessel domains and stochastic simulations for analysing the course of search and rescue missions at sea.

The Transportation Engineering section contains studies examining inland waterway shipping, road infrastructure in the European Union as well as optimising parameters of port areas. The article discussing a theoretical framework for controlled pyrotechnical reactions as an energy source constituting a component for transportation from the sea bed deserves particular attention.

I am also very pleased to announce that that our quarterly has been indexed by Global Impact Factor (GIF), an international database of scientific journals. The quality of the Scientific Journals of the Maritime University of Szczecin has been assessed using an in-depth analysis method to provide a Global Impact and Quality Factor. The journal's scores for the last for years are as follows: 2012 – 0.415; 2013 – 0.528; 2014 – 0.780; 2015 – 0.854. This clearly reflects the increasing quality and standard of the work published by the journal, indeed our scores have increased by 61.7% over the last 2 years.

I strongly invite authors to submit their articles and encourage readers to provide feedback. Access to the online version of this issue and previous issues is available at http://scientific-journals.eu/.

Leszek Chybowski, DSc PhD CRP
Editor-in-Chief

Marine Technology and Innovation

Scientific Journals
of the Maritime University of Szczecin

Zeszyty Naukowe
Akademii Morskiej w Szczecinie

2016, 48 (120), 9–14
ISSN 1733-8670 (Printed)
ISSN 2392-0378 (Online)
DOI: 10.17402/169

Received: 29.04.2016
Accepted: 19.07.2016
Published: 15.12.2016

Analysis of selected methods for building an ontology for a system of automatic communication at sea

Paulina Hatłas✉, Zbigniew Pietrzykowski

Maritime University of Szczecin, Faculty of Navigation
1–2 Wały Chrobrego St., 70-500 Szczecin, Poland
e-mail: {p.hatlas; z.pietrzykowski}@am.szczcin.pl
✉ corresponding author

Key words: ontology of communication, the ontology of navigational information, communication, negotiation, methods of constructing an ontology, the automatic communication

Abstract
Automatic communication can help reduce errors in communication between navigators, and, consequently, increase the level of navigation safety. This article reviews some methods for the development of an ontology and looks into processes for communication at sea. Three basic elements of ontology can be distinguished: navigational information, communication and interface. The possibility of applying these methods for the construction of ontology was analyzed for a system of automatic communication at sea.

Introduction

One of the main tasks in navigation is to ensure its safety by avoiding dangers throughout an entire voyage. One of the causes of dangerous situations in maritime transport is the lack of proper communication between navigators. The most common cause of navigational accidents is human error. The 80/20 rule (Harrald et al., 1998) states that 80% of accidents are due to human error, and 20% are technical incidents. Automation of communication processes, particularly negotiation, may contribute to the prevention of navigationally dangerous situations, or if they occur, to more prompt and effective solutions. IT systems are increasingly used to support processes that characterize maritime transport. In addition, the emergence of new technologies in the IT services market forces changes in IT solutions designed to support management. It is necessary to adjust the best possible IT solutions to current information needs (Gładysz, 2015) and to implement automation in two shipboard areas: the acquisition, selection, processing and presentation of information, and communication processes. So far, these tasks have been mainly by navigators conducting their ships and land-based center personnel (Pietrzykowski et al., 2014). The automation of these processes requires the development of a relevant communication ontology.

Methods of constructing an ontology

Ontology is a theory that may be applied to any area, in which concepts are described in a hierarchical manner to determine the semantic relations in a given domain. One of its characteristics is a logical theory that introduces limits to logical models. According to one of its definitions, ontology can be viewed as conceptualization (Gruber, 2008). Ontology should effectively convey the intended meaning of its concepts. There are several basic approaches to ontology (Basser, 2004):

- Inductive approach − using the generalization of a particular case. Although it is characterized by relatively low costs, the resultant ontology may not be applicable to other cases;
- Deductive approach − using general, universally accepted rules and principles derived from the

analyzed field. It gives rise to the considerably large, work-intensive ontology;
- Inspirational approach − characterized by individual approach to the modelled field. The created ontology is not necessarily universally accepted, but revolutionary in the way of understanding the field;
- Synthetic approach − uses the synthesis of several ontologies, each one describing a part of the modelled field;
- Co-operation-based approach − ontology is created in the mode of group work, based on the experiences of designers and future users.

The analysis of ontology construction methods presented by Sobczak (Sobczak, 2004) indicates that within a few years highly diversified versions were created. The user wishing to implement an IT system must adapt it to his requirements. In order to streamline this process, one can use the methods already available for building an ontology.

There are various attempts to organize ontology construction methods and work out a methodology associated with the formation of ontology. Although the so-called 'from scratch' approach is frequently proposed, it is usually suggested to use existing ontologies. Attempts to partially automate the process of acquiring knowledge for the ontology are also often made. The literature on the subject proposes many solutions, some of which are presented below.

Uschold and King Method

M. Uschold and M. King, later joined by M. Grüninger (Uschold & Grüninger, 1996) presented the guidelines for the construction of an enterprise knowledge-oriented ontology. The procedure to build an ontology can be described through three steps:
1. Capture – identification of the key concepts, generalization and specialization in order to derive the remaining hierarchy of concepts.
2. Coding – explicit representation of the conceptualization captured in the previous stage in some formal language.
3. Integrating existing ontologies – the issue of reuse of existing ontologies.

CYC method

The method was developed by Microelectronics and Computer Technology Corporation.

The key features of this method of building an ontology are:
- Common-sense knowledge as a source of information;
- Manual coding of this knowledge;
- Simplified processes of knowledge feeding and updating.

Grüninger and Fox method

The method was created using the experience and M.Grüninger and M. Fox (Grüninger & Fox, 1995) under the TOVE project. Providing the Design and Engineering Enterprise environment, it allows users to build a wide range of projects in the IT industry. In the process of building an ontology it is important to:
- Create motivational scenarios that will permit the description of the set of requirements for ontology verification;
- Develop informal competency questions, on the basis of which the ontology completeness can be verified during the final construction stage.

KACTUS method

The method was developed by Amay Bernarc, who aimed at examining the use of knowledge of complex information systems and the role of ontologies in these systems. Ontology in this case represents the knowledge required for a specific IT system.

SENSUS method

The approach adopted in the SENSUS method promotes knowledge sharing because it implies acceptance of the same base ontology for all newly created domain ontologies. An interesting feature of the method is the simplicity of creating ontology processes.

ON-TO-KNOWLEDGE method

The purpose of creating this method was to facilitate knowledge management in large distributed organizations. Three main processes were identified: knowledge meta process, human resource management, and software engineering. It consists of five main phases: feasibility study, kick-off (start), refinement, evaluation, and application and evolution.

This method refers to knowledge management, therefore ontologies created by using it are strongly dependent on their future use.

Methontology

The method enables dynamic control of interconnected ontologies and supports the process of reengineering (i.e. recovery and mapping of the conceptual model of implemented ontology to another appropriate model).

The presented overview of some methods is not exhaustive of the topic under consideration. The use of properly chosen methods for the construction of ontology may contribute to faster and more effective development of navigational information ontology, enabling automation of data analysis processes and the creation of a system for automatic communication at sea.

Ontology of communication

An important aspect of management in marine navigation is to ensure an appropriate level of safety for people, cargo, ship and environment. Today the GMDSS (Global Maritime Distress and Safety System) provides a foundation for maritime communication throughout the world. The system sets out rules and procedures for standardized communication; however, situations frequently arise in which additional information is required or a decision has to be made through intership or shore-ship communication. This involves supplementary information or acquiring data through dialogue. That is why the creation of communication ontology is mostly needed for the shipboard system (Pietrzykowski et al., 2015).

So far, research has covered the processes of communication performed between navigators using IMO-recommended standard marine communication phrases (SZPM, 2009). The examined aspects include the exchange of information, message perception and interaction, e.g. negotiations. Their description uses ontologies of navigational information and communication supplemented by elements of the protoform theory. The processes of inference have been studied in the context of acquisition of (additional) information and conducting negotiations. Computing with words has been used for the modelling of communication processes, including inference processes of inference.

The automation of the selective acquisition of information and negotiation processes requires the analysis and interpretation of the content of navigators' exchanges (dialogues). These tasks, in turn, have two requirements: the knowledge of inference methods and the extension of communication ontology. Intelligent communication should consist in automating both information interpretation and negotiations. Although developments in IT and ICT create such opportunities, there is an additional requirement, namely building the ontology of navigational information, including the ontology of communication.

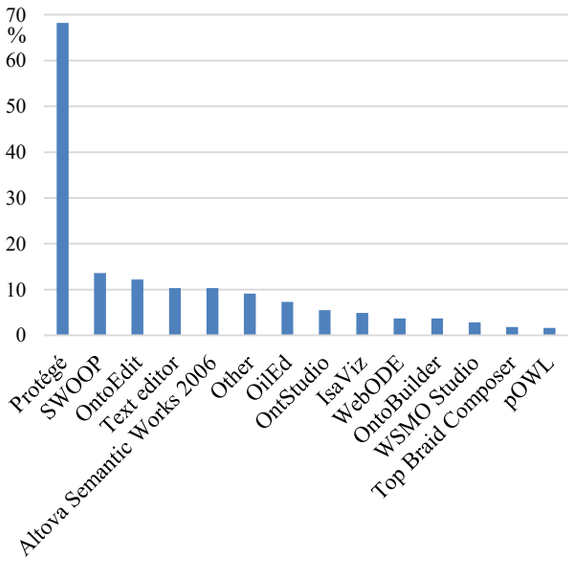

Figure 1. Respondents' use of ontology editors (Cardoso, 2007)

The construction of ontology includes navigational information, communication, and so-called interface (Wójcik, Hatłas & Pietrzykowski, 2016). These aspects are summarized in Table 1.

Ontology is built in the Protégé environment (Figure 2). Statistical data (a questionnaire composed of 14 questions, where the respondent may give more than one answer) gathered for the IEEE Intelligent Systems (Cardoso, 2007) have allowed to conclude that the Protégé is the most frequently used editing program, as depicted in Figure 1.

Table 1. Elements of the ontology (Wójcik, Hatłas & Pietrzykowski, 2016)

No.	Element	Comment
1	NAVIGATIONAL INFORMATION	The ontology of navigational information is under construction according to the IMO's standard marine communication phrases and divided into external and on-board communication. Navigation terms are divided into entities (main classes) and instances (elements belonging to specific sets).
2	COMMUNICATION	The ontology of communication is being developed based on fuzzy logic and the protoform theory. Using fuzzy logic, imprecise and ambiguous terms can be formally defined. These terms are often used in verbal language, such as *low risk*, *safe situation*.
3	INTERFACE	The interface is intended as a merger of navigational information and the ontology of communication. It includes message markers, such as QUESTION, REQUEST.

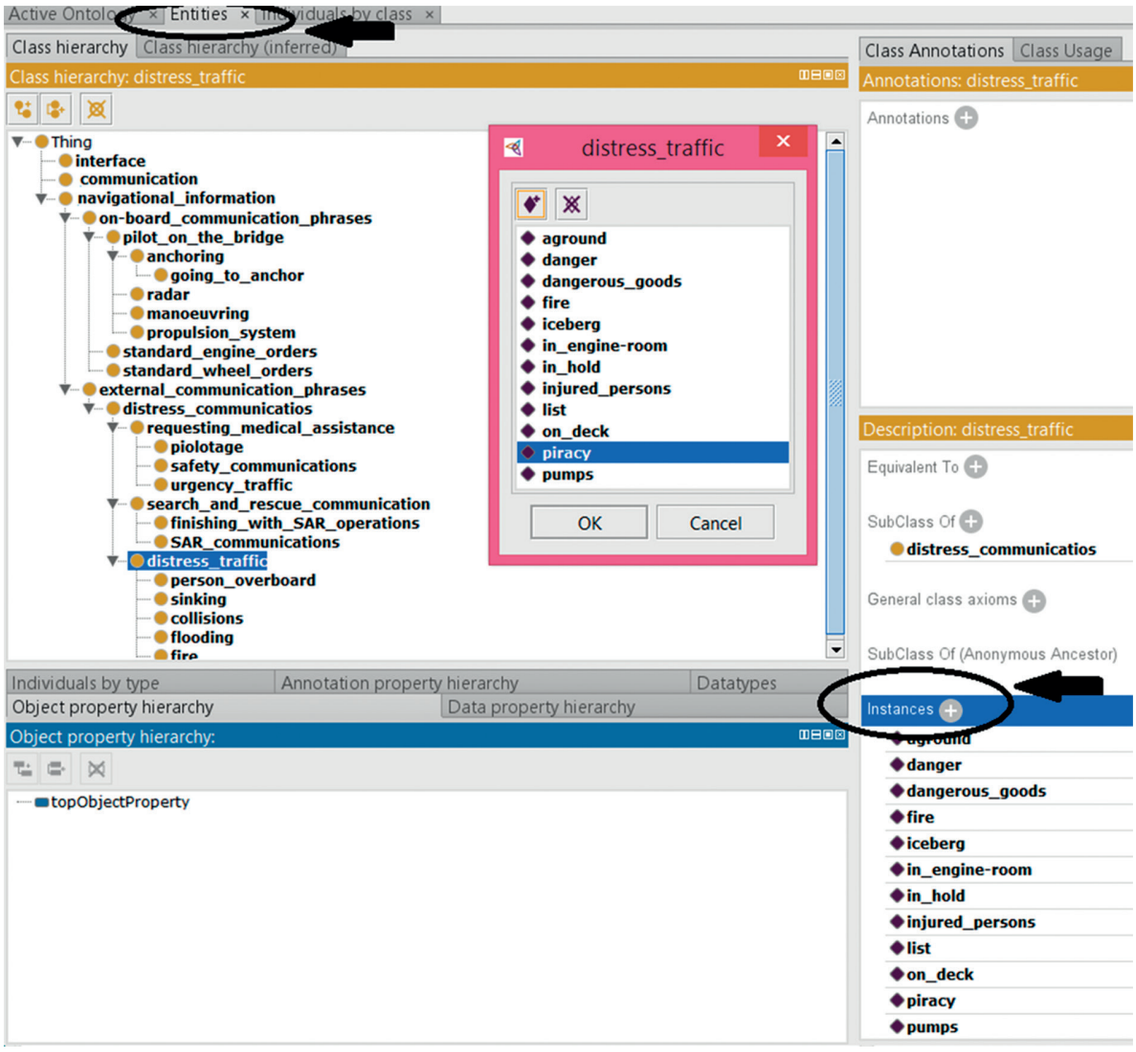

Figure 2. A screenshot displaying communication ontology created in the Protégé program (Wójcik, Hatłas & Pietrzykowski, 2016)

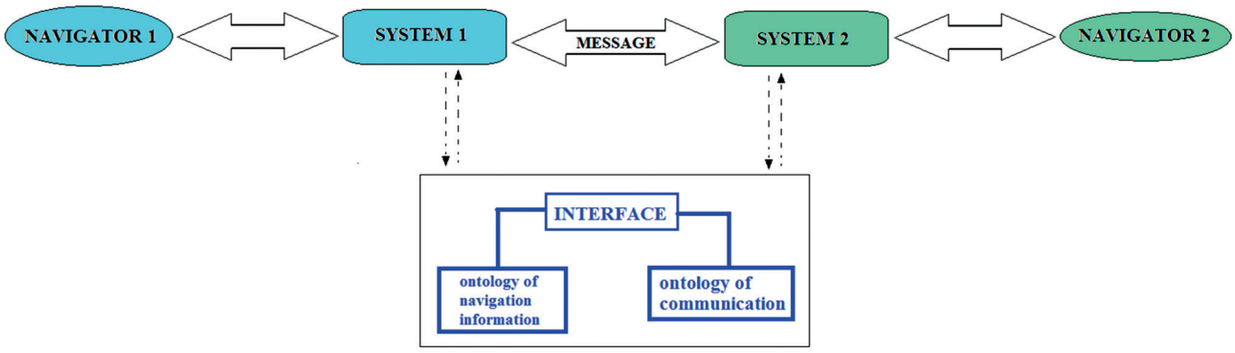

Figure 3. The automatic communication at sea (Pietrzykowski et al., 2015)

The aim of this work is to develop an ontology of communication and knowledge base covering inference processes associated with communication at sea. This will enable the acquisition of additional information and conducting negotiations to solve problematic navigational situations, involving explanations and agreeing on actions to be taken. Constructing such a system (Figure 3) can significantly contribute to the enhancement of safety at sea.

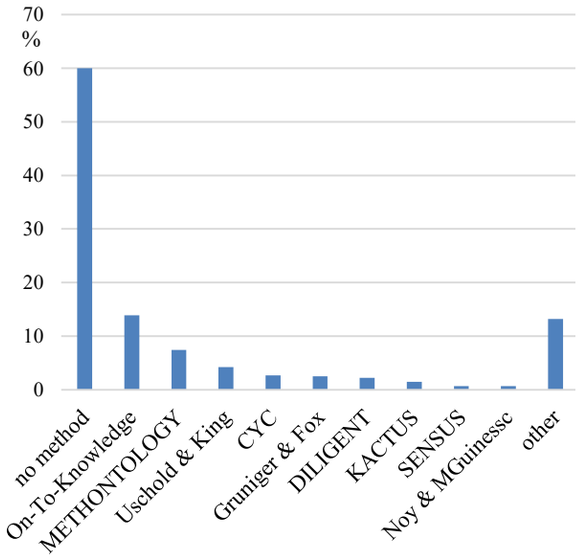

Figure 4. The methods of the ontology and the frequency of their use as a percentage (Cardoso, 2007)

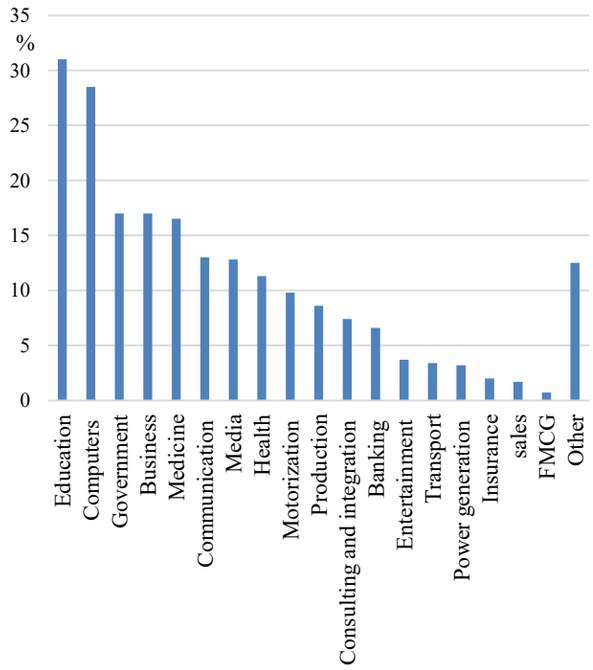

Figure 5. Development of ontologies depending on the field of economic activity (Cardoso, 2007)

The proposed method ontology

One of the propositions (Abramovich, Stolarski & Tomaszewski, 2010) emphasized that the use of ontologies and starting operations on semantic models will broaden possibilities relating to the collection and processing of information. However, it is important to choose the appropriate method for the given domain. Figure 4 implies that 60% of companies do not use any particular method, and are constructing an ontology on an individual basis.

The most commonly chosen method is that of ON-TO-KNOWLEDGE (Figure 4). This method was created under the project, bearing its same name, implemented by Y. Sure, S. Staab and R. Studer (Sure, Staab & Studer, 2004) and aimed at facilitating knowledge management in large distributed organizations. Bearing that in mind, we chose to use the On- To- Knowledge method to build an ontology for a system of automatic communication at sea (Figure 5, Table 2).

Conclusions

The construction of a communication ontology based on the ON-TO-KNOWLEDGE method may contribute to the development of automatic communication systems to be used in shipping, an important link in the global transport chain. This method is

Table 2. Analysis of ON-TO-KNOWLEDGE method applications for a system of automatic communication at sea (Sure, Staab & Studer, 2004)

No.	Stage		COMMENT
1	**Refinement** – aimed to produce mature application – oriented ontology following the specifications given in the initial process. It consists of two sub-processes:		Knowledge and experience of navigators (*method of case studies: analysis of selected dialogues and methods used to formulate utterances*) to create terminology to be used in the word resource of the ontology; recorded in the Protégé program
	knowledge acquisition by domain experts – iterative process used by many experts, who fill in (add details) their skeletal version of the ontology in specific areas of their expertise	formalization – process of recording knowledge in a particular ontology language chosen to suit specific requirements the ontology has to meet	
2	**Evaluation** – process repeated in multiple cycles allows continuous improvement of ontology, at the same time verifies and evaluates the base ontology by subprocesses:		*Experimental method: simulation of the negotiation process* (*simulators at the Maritime University of Szczecin*)
	checking the requirements and competency questions	testing of the ontology in the environment of the target application	
3	**System care** – determines who will be responsible and how the administration of ontology will be provided, including the updating of the knowledge contained therein		

most frequently used by respondents who in practice expect a tool that facilitates knowledge management in large distributed organizations. The primary advantages of the proposed method are its three final phases: refinement, evaluation, and application and evolution. For this reason, ontologies created using this method heavily depend on their future use.

The article analyses selected applications of ontology. The authors present an overview of approaches and methods of ontology construction and consider processes of communication at sea. Based on an analysis of the methods' applicability, the ON-TO-KNOWLEDGE method has been chosen for building the ontology system for automatic communication at sea.

Acknowledgments

This research outcome has been achieved under the research project No. 3/MN/ITM/2016 financed from a subsidy of the Ministry of Science and Higher Education for statutory activities of Maritime University of Szczecin.

References

1. Abramovich, W., Stolarski, P. & Tomaszewski, T. (2010) Ontologies as a tool to build models of insurance information systems. *Wiadomości Ubezpieczeniowe* 02 (Polska Izba Ubezpieczeń). pp. 3–18.
2. Basser, A. (2004) Ontology Engineering. *Newspaper IT* 2 (21). pp. 42–47, 16.
3. Cardoso, J. (2007) *The Semantic Web Vision: Where are We?* IEEE Intelligent Systems, September / October. pp. 22–26.
4. Gładysz, A. (2015) Overview of methods for creating ontologies used to estimate the costs of implementation of information systems. *Logistics* 3. pp. 1479–1487.
5. Gruber, T. (2008) Ontology. Entry in the *Encyclopedia of Database Systems*. Ling Liu and M. Tamer Özsu (Eds.), Springer-Verlag, the Appear in 2008. Provides a definition of ontology as a technical term for computer science, tracing its historical context from philosophy and AI.
6. Grüninger, M. & Fox, M.S. (1995) *Methodology for the design and evaluation of ontologies*. Workshop on Basic Ontological Issues in Knowledge Sharing, International Joint Conference on Artificial Intelligence in 1995, Montreal, Quebec, Canada in 1995.
7. Harrald, J.R. et al. (1998) Using System Simulation Model is the Impact of Human Error in the Maritime Risk Assessment. *Safety Science* 30, 1–2.
8. Pietrzykowski, Z., Banaś, P., Wołejsza, P. & Hatłas, P. (2014) Subontologia communication in process automation exchange of information and negotiations on the sea. *Logistics* 6. pp. 8654–8665.
9. Pietrzykowski, Z., Hatłas, P, Wójcik, A. & Wołejsza, P. (2015) *Subontology of communication in the automation of negotiating processes in maritime navigation*. 16th Marine Traffic Engineering Conference and International Symposium Information on Ships, Maritime University of Szczecin.
10. Sobczak, A. (2004) *Analysis of selected methods of ontology*. Research project KBN number 1 H02D01627.
11. Sure, Y., Staab, S. & Studer, R. (2004) *On-To-Knowledge Methodology (OTKM)*. International Handbooks on Information Systems. pp. 117–132.
12. SZPM (2009) *Standard Marine Communication Phrases* (in English and Polish). Szczecin: Scientific Publishing Maritime University of Szczecin.
13. Uschold, M. & Grüninger, M. (1996) ontologies, Principles of Methods and Applications. *The Knowledge Engineering Review, Cambridge University Press* 11, 02.
14. Wójcik, A., Hatłas, P. & Pietrzykowski, Z. (2016) Modelling communication processes in maritime transport using computing with words. *Transport System Telematics* 9, 4 (Polish Association of Transport Telematics).

Scientific Journals
of the Maritime University of Szczecin

Zeszyty Naukowe
Akademii Morskiej w Szczecinie

2016, 48 (120), 15–21
ISSN 1733-8670 (Printed)
ISSN 2392-0378 (Online)
DOI: 10.17402/170

Received: 29.04.2016
Accepted: 05.12.2016
Published: 15.12.2016

The quality of marine fuels and the safety of navigation: case studies

Włodzimierz Kamiński[1], Paweł Krause[1]✉, Dariusz Gumiński[2], Przemysław Rajewski[1]

[1] Maritime University of Szczecin, Mechanical Faculty
Institute of Marine Propulsion Plants Operation
1–2 Wały Chrobrego St., 70-500 Szczecin, Poland
e-mail: {w.kaminski; p.krause; p.rajewski}@am.szczecin.pl
[2] Rederei Erwin Strahlmann e.K., Branch Office in Poland
43 Narzędziowa St., 70-807 Szczecin, Poland, e-mail: d.guminski@strahlmann.pl
✉ corresponding author

Key words: safety of navigation, fuel samples, quality of marine fuels, procedures of fuel handling on board, requirements, failures

Abstract
The quality of marine fuels is standardised by the international standard ISO 8217. As practice shows, even fuels that meet all standard requirements do not completely guarantee avoiding disruptions in smooth and safe operation of the ship. The future is likely to bring more cases of improper operation of vessels, sometimes leading to main propulsion failures. One cause behind main engine breakdowns is the introduction of new products on the fuel market that are intended to meet the ever-increasing requirements of environmental protection (e.g. low sulphur content). As a result, some fuels are chemically different from the previously used residual fuels. Using them in the engine room requires special care on the part of the ship owner and the ship's crew. The article analyses two cases in which the use of conventional residual fuels resulted in main engine stoppage. The authors, bearing in mind the causes of those failures, focus on technical consequences of using marine fuels produced by currently employed technologies.

Introduction

A breakdown of a ship's propulsion system creates a risk to navigation safety by making the ship unmanoeuvrable. The key to the safe operation of the vessel lies in appropriate technical conditions of the power plant, directly supervised and maintained by the crew of the engine department. The condition of the power plant is also affected by the quality of working fluids, including fuels feeding the main propulsion engines and generating sets. Fuel is a structural component of the engine, which means that its physical and chemical parameters should be within the range of values provided by the engine designer. In addition to the essential requirements for the engine, fuel should meet the requirements for storage and transport installations in specific shipboard conditions.

In the past, a number of institutions analysed individual cases of ship failures in which the main cause was attributed to marine fuel properties. On this basis, regulations and principles were gradually worked out to minimise the risk of engine failure due to poor quality of fuel. In short, these principles prescribe four basic steps: 1. take a representative sample of bunkered fuel in the presence of at least one crew member and supplier, 2. deliver fuel samples to a recognised laboratory for analysis, 3. introduce new fuel to the engine fuel supply system only after receipt of the analysis results and implementing laboratory recommendations, 4. do not mix fuels from different deliveries.

The available documents of institutions dealing with marine fuel usage reveal many cases where poor quality fuel was employed (DNV, 2014a; 2014b; 2014c). Laboratories involved in the so-called

'petroleum services' provide information on cases in which limit values of fuel quality indicators where exceeded in different ports. According to data, DNV PS (now Veritas Petroleum Services) alone reported dozens of such cases. The reports analyse the causes and the consequences of disruption of smooth vessel operation, although the analysis is focused on fuel physical and chemical parameters.

This article aims to consider and discuss the effects of non-compliance with both fuel quality standards and procedures of fuel handling in the engine room, leading to dangerous situations such as the loss of manoeuvrability.

Given the variety of crude oils and various production technologies, fuels of the same composition and properties are hardly encountered. In order to standardise marine fuels on the market, the ISO 8216:1 standard: Petroleum products – Fuels (class F) classification – Part 1: Categories of marine fuels) and ISO 8217 standard: Petroleum products – Fuels (class F) – Specifications of marine fuels were published. The set of limits of physical and chemical parameters as per ISO 8217 is a benchmark for the quality of marine fuels on the market.

The paragraphs that follow describe cases of main propulsion failures of ships due to the use of residual fuels; all these cases led to the loss of the ship's manoeuvrability. Those events are well documented and additionally supported by direct and informal observations of crew members involved. In the descriptions the ship names have been omitted. The laboratories that performed the fuel analyses have not been named either, although they are globally recognised.

Ship No. 1

The failure occurred on a methanol carrier, propelled by the main engine Mitsui Man B&W 7S50MC Mark 6, MCR – 10,010 kW at 127 min^{-1}, CSR – 8510 kW at 120.3 min^{-1} running on ISO-F-RMG 380 fuel. The main propulsion failed during a routine operation of the vessel on a route linking the port of Trinidad and Tobago, where methanol was loaded, and one of the discharge ports in the United States. At the time of the incident the ship had been in operation for 11 months after being launched at a shipyard in Japan. Before the failure, the main engine was in excellent technical condition, as confirmed by periodic inspections of the engine, and current assessment of engine and combustion parameters.

Circumstances preceding the failure

The ship routinely bunkered fuel in US ports, and the supplier of fuel was one of the major companies in the industry. On June 27th 2006 the ship bunkered 1,200 MT (Metric Ton, SI unit: MG) of ISO-F-RMG 380 fuel. A sample of the bunkered fuel was sent, in accordance to the ship owner's procedure, to laboratory No. 1 in order to verify the conformity of the fuel characteristics with the ISO 8217. Three days later an e-mail was received with the results of the fuel sample test. The properties of the fuel samples are presented in Table. 1.

Table 1. Selected data from Fuel Quality Report – ship No. 1

Characteristic	Unit	ISO 8217:1996 RMG 35[1]	Lab 1	
			Supplier's data	Ship's sample 30.06.2006 019701[2]
Density at 15°C	g/cm^3	**Max. 0.991**	0.991	0.9899
Viscosity at 50°C	mm^2/s	**Max. 380**	246	257
Viscosity at 100°C	mm^2/s	**Max. 35**		–
Flash point	°C	**Min. 60**		> 70
Pour point	°C	**+30**		0
Carbon residue	% m/m	**18**		16
Ash	% m/m	**0.15**		0.07
Water	% v/v	**Max. 1.0**		0.2
Sulphur S	% m/m	**Max. 5.0**	3.04	3.7
Al + Si	mg/kg	**Max. 80**		24
Vanadium V	mg/kg	**300**		141
TSP	% m/m	**Max. 0.10**		**0.19**

[1] (ISO-8217:1996); [2] (FQR, 2006)

The results were compared with the ISO 8217:1996 specification for RMG 35 fuel. An exceedingly high value of TSP (Total Sediment Potential, i.e. total quantity of potential deposits after hot filtration) was pointed out, as excess TSP is a signal of possible loss of fuel stability in the conditions prevailing in the engine room. The following operational advice was included in the analysis: "TSP – Fuel stability is suspect and increased sludging is likely to occur. Observe centrifuge operation closely. If sludging is excessive, decrease the time between sludge discharges. If possible operate two centrifuges parallel with minimum throughput. If sludge is unmanageable, recommend you refer to the fuel supplier. **Do not mix with another fuel.**"

The properties of the bunkered fuel raised doubts and discussions between the chief engineer, the ship owner and the charterer concerning safety issues

caused by the use of substandard fuel in the main engine. Finally, the ship owner decided to make a tentative use of that fuel, knowing that this may have resulted in operating difficulties. In the port of Trinidad the ship was supplied with an emergency amount of 450 MT of RMG 380 fuel of very high quality, confirmed by Lab No. 1. It was to be used in case of difficulties with the combustion of the US-delivered fuel that did not meet the standards.

Additional information

The installation of residual fuel includes a settling tank with a capacity of 14 m^3 and service tank with a capacity of 16 m^3 fuel. The fuel for the service tank is purified by Mitsubishi SJ 50GH purifiers, equipped with a "multi-monitor" controlling the water content at the purifier outlet and the amount of sludge in the sludge space of the centrifuge drum. The main engine fuel supply installation had a primary filter KS 15 (mesh size 100 μm), automatic back-flash filter (10 μm mesh size) and safety K8FE filter (mesh size 50 μm).

Description of the failure

On July 13th, 2006 at 08.00 local time, during a sea voyage from Trinidad and Tobago to the US ports with a cargo of 43,800 MT of methanol, the ship started using fuel that had been bunkered on June 27th, 2006 in the US. The operation was carried out routinely. Because of the potential problems associated with the use of fuels with high TSP, the purifier capacity was reduced to the minimum and a second purifier was employed. All fuel filters in the ME feeding system were cleaned.

The ship worked in the unmanned engine room regime. On July 15th, at 23.00 LT the duty engineer was watching the engine room and ascertained that all the operating parameters of the main engine were correct. At that time, the ME feed system contained only "new" fuel; its daily consumption by the ME was 32–33 MT. The fuel purifiers were running smoothly, the performance of the filters in the ME fuel supply system also showed no deviation.

On July 16th, 2006 at 03.30 the engine monitoring system registered a large (over 50 degrees) deviation of the temperature of exhaust gases from cylinder No. 1. The chief engineer inspected the engine and found that the injection pump of the ME No. 1 unit did not supply fuel to the cylinder. Observation through the transparent cover of the camshaft revealed that the roller was not resting on the fuel

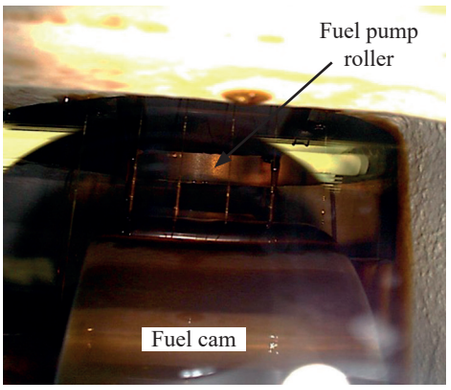

Figure 1. Suspended drive roller of the fuel pump

cam. The injection pump plunger remained in the upper position in the pump cylinder. Figure 1 presents a photo of the suspended drive roller. At 03.40 ME was stopped to replace components of the defective injection pump in ME No. 1 unit and identify the cause of pump failure. The ship was drifting. After dismantling the pump and removing the plunger and barrel from the pump body, the identified defects included plunger seizure, suspension of suction-delivery valve and overflow valve.

All internal components of the pump were covered with a layer of sediments that, under high temperature, had sustained carbonization. Figures 2 and 3 show photographs of injection pump elements after failure. Dismantling the injection pump was difficult because of hard deposits that caused seizure

Figure 2. Dismantled barrel of fuel pump, unit No. 1 after failure

Figure 3. Traces of seizure on the fuel pump plunger, No. 1 unit after failure

and jamming of the mating elements. The injection pump of the piston-crank unit was reassembled using new spare parts: a plunger-barrel unit, suction valve, overflow valve, plus a new set of sealings.

During the initial adjustment of the repaired injection pump and preparation of the main engine to resume the voyage, the crew rotated the main engine crankshaft using a turning gear.

After this operation, it was found after this operation that in six the remaining seven fuel pumps, the plungers remained in the upper position. The rollers of fuel pump drive systems were not resting on the surface of the cam surfaces of the camshaft. It was decided to overhaul the remaining six injection pumps. After dismantling, the same condition was observed in each of the pumps as had been found in the injection pump of No. 1 unit. All pumps were repaired with new spare parts: plungers and barrels, suction valves and overflow valves, plus sealings.

The overall repair operation of all injection pumps and the cleaning of fuel feed system took 32.5 hours, and by this time the ship had drifted.

After the failure

The failure of all seven of the ME injection pumps was undoubtedly caused by fuel that did not meet the ISO 8217 standards. It was therefore decided not to use the same fuel to feed the engine and to change to the fuel bunkered as "emergency" in Trinidad. For this purpose, the problematic fuel was removed from the installation, the settling and service tanks. The tanks were cleaned by the engine crew. The power system was flushed with distillate fuel and filled with "good" RMG 380 fuel. The condition of fuel filters was checked and found in good condition.

Representatives of the P&I Club insurer, fuel supplier, ship owner and B&W company arrived onboard in the first US port of methanol discharge. After inspection of the damaged parts of injection pumps, all parties agreed that the poor fuel quality had caused such serious defects. The fuel supplier agreed to cover the losses that the owner incurred in connection with the failure. At the expense of the supplier, the disputed fuel was pumped from the ship to land-based installations in the US.

Causes of the failure

Additional analysis of fuel made after the accident showed chemical contaminations (polymethacrylates) in the fuel, which, among others, were responsible for the TSP value of 0.19%. At the high temperature required to achieve the desired fuel viscosity before the fuel injectors, approximately 135°C, these compounds settled on the injection pump barrel walls, hindering heat exchange between the barrel and the plunger of the injection pump and locally raising the temperature. This process adversely affected lubrication, reducing the plunger-barrel clearance (due to different thermal expansion of the components), and caused seizures due to the coagulating sediments of hard particles.

Ship No. 2

The incident took place on a general cargo ship, driven by a four-stroke main engine 6M32C MAK from Caterpillar Motoren GmbH & Co (in-line cylinders) with a power output of 3000 kW at 600 min^{-1}. It was run on RME 180 fuel. The four-blade controllable pitch propeller Berg BCP 950 with a diameter of 3300 mm was driven by a flexible coupling Vulcan Rato-R and a reduction gear (600/187 min^{-1}).

Circumstances preceding the failure

Fuel was taken on May 22nd, 2010 in one of the ports in West Africa, and the sample was sent to Laboratory No. 2. Analysis of fuel physicochemical parameters showed a significant excess of water content in the fuel (2.05% vol. where the limit was 0.5%). The technical condition of the engine and fuel preparation did not show any defects.

Description of the failure

Disruptions in the functioning of the ME's propulsion appeared on May 22nd, 2010, immediately after introduction of the newly bunkered fuel to the engine installation during departure manoeuvres and consequently made proceeding to sea impossible.

The first symptom observed was difficulty in maintaining the required engine load. After the start of the voyage, increased exhaust gas temperatures on a couple of cylinders were observed, deviating from previously noted temperature differences between the individual cylinders. The level of noise emitted by individual cylinder units was rising. Also, injection valves produced unnatural sounds. The main engine fell into periodic vibrations. The speed governor was setting the fuel pumps in the position of maximum fuel amount, causing an overload alarm. At the same time, the turbocharger did not reach the expected rpm. The sea passage and ship manoeuvring became impossible after the control system reduced the propeller blade angle. As a result, the main engine was stopped.

The viscometer indicated high viscosity, initially 14 mm/s^2 at a temperature of 138°C, later both parameters rose to 22 mm/s^2 and 151°C. The automatic fuel filter alarm indicated a high pressure difference before and after the filter. The control system turned off the fuel purifier SA816 (Alcap system) due to high backpressure of fuel.

After stopping the main engine and checking some of its elements and the fuel supply installation, the following was identified:

1. Main engine:
   a) Significant amount of deposits on the nozzle ring of the turbocharger (turbine side), reduced cross-sectional area of flow;
   b) Worn out material on the surfaces of valve spindle and seats;
   c) Hard deposits on atomiser nozzles;
   d) High-viscosity sediments covering the surfaces of pump plungers and cylinders of fuel pumps.
2. Installation of fuel treatment:
   a) Presence of free water in the service and settling tanks;
   b) Surfaces of fuel filters blocked with thick layer of sediment of fibrous structure, presence of water;
   c) Large amounts of high viscosity sediments in the fuel centrifuge bowl;
   d) Faulty viscosity sensor surface (traces of seizure and scratching) in the fuel viscosity control system.

After the failure

In order to continue the voyage the crew decided to use a mixture containing approximately 5 to 10% of troublesome fuel and 95% of the fuel from the previous bunkering. The remaining amount of fuel needed to reach the next bunkering port was prepared in standby tanks in the 5:95% ratio. Fuel transfer pumps were used to homogenise the mixed fuel.

In the following port, fuel samples (shipborne and supplier's) were sent to lab No. 3 and new fuel was bunkered. The engine crew continued to add newly bunkered fuel in the previously defined proportions. The entire amount of fuel from the latest delivery was used after approximately five months, almost 20 MT were discharged ashore.

Table 2. Selected data from Fuel Quality Reports – ship No. 2

Characteristic	Unit	Bunker Delivery Note 22.05.10[1]	Limits 8217:2005 RME 180[2]	Lab 2	Lab 3	
				Ship's sample 03.06.2010 482562[3]	Supplier's sample 14.07.10 482573[3]	Ship's sample 26.07.10 482546[3]
Density at 15°C	g/cm^3	0.9801	**Max. 0.991**	0.9586	0.9625	0.9584
Viscosity at 50°C	mm^2/s	180	**Max. 180**	70.8	159.5	72.63
Flash Point	°C	85	**Min. 60**	> 70	> 76	88
Pour Point	°C	15	**+30**	0	0	< –3
Carbon residue	% m/m	–	**15**	8.6	10.9	8.53
Ash	% m/m	–	**0.10**	0.08	0.062	0,099
Water	% v/v	< 0.05	**Max. 0.5**	**2.05**	0.30	**1.75**
Sulphur S	% m/m	0.92	**Max. 4.5**	1.12	3.31	1.33
Al + Si	mg/kg		**Max. 80**	17	5	20
Vanadium V	mg/kg	–	**200**	48	–	63
Phosphorus P	mg/kg	–	**15**	2	< 1	3
Calcium Ca	mg/kg	–	**30**	43	8	45
Zinc Zn	mg/kg	–	**15**	2	1	3
TSP	% m/m	–	**Max. 0.1**	0.04	0.02	0.06
CCAI	–	–	**Max.**	840	–	839

[1] (BDN, 2010), [2] (ISO-8217:2005), [3] (FQR, 2010)

Over the five-month period, during routine maintenance of the engine components, it was found that all the inspected atomisers, which had operated for 1500 hours, had to be replaced, despite the nominal operating life of 3000 h.

Causes of the failure

In reports of additional tests of samples from the ship and supplier (after the failure), laboratory No. 3 did not indicate any direct cause of the accident, although excessive water content in the fuel was confirmed (Table 2).

The vast majority of failure symptoms described is characteristic of the presence of significant amounts of water in the fuel.

Nevertheless, the analysis previously performed in laboratory No. 2 was followed by these comments and recommendations:

1. The sample indicates the water content is above the specification and this level, if not removed, could cause problems with the fuel injection equipment and give poor combustion leading to deposits in cylinder and turbochargers.
2. If possible, increase the residence time of the fuel in the settling tank.
3. Operate the purifiers in parallel at the lowest possible flow rate (enough to meet daily consumption).
4. Check the settling and service tanks frequently and drain all water.

The recommendations were not known to the crew, because the fuel was used immediately after bunkering, on May 22nd, 2010, and the results of the analyses from lab No. 2 were only known on June 6th, 2010.

Ship No. 3

In 2010, on another ship belonging to the company from example I, fuel pump plungers were once again subject to seizures. This time, the fuel came from one of the major ports in Asia. Below is a set of physico-chemical characteristics of fuel, the use of which immobilised the vessel. The study of the fuel was made after the occurrence of the failure (Table 3).

The fuel was found to meet the requirements of the ISO 8217 standard. After the accident, additional analyses were carried out on the chemical composition of the fuel, going beyond the routine analysis and the ISO 8217 recommendations. The following results were found:

1. High levels of asphaltenes (method IP 143/04);

Table 3. Selected data from Fuel Quality Report – ship No. 3

Characteristic	Unit	Limits 8217:2005 RMG 380[1]	Lab 4	
			Supplier's data	Ship's sample 03.01.2011 No. S66191/ 3393003[2]
Density at 15°C	g/cm^3	**Max.0.991**	0.9895	0.9882
Viscosity at 50°C	mm^2/s	**Max. 380**	372.7	**396.6***
Flash Point	°C	**Min. 60**		>70
Pour Point	°C	**+30**		0
Carbon residue	% m/m	**18**		11.53
Ash	% m/m	**0.15**		0.04
Water	% v/v	**Max. 0.5**	0.1	0.2
Sulphur S	% m/m	**Max. 4.5**	2.4	2.48
Al + Si	mg/kg	**Max. 80**		44
Vanadium V	mg/kg	**300**		98
TSP	% m/m	**Max. 0.10**		0.02

[1] (BDN, 2010), [2] (FQR, 2011)

* Viscosity at 50°C is out of specification, but within the acceptability criteria for ISO 4259 for a single result. Acceptability Criteria for IFO 380 at 50°C ranges from 380 to 396.6 mm^2/s.

2. High value of xylene equivalent (method: BP);
3. Presence of C16 FAME.

Causes of the failure

Based on experience of, among others, the engine manufacturer and on information on the materials used, the failure was attributed to a problem in the unit injector fuel due to the presence of high value-xylene equivalents. The fuel used had a tendency to form hard coke deposits, potentially causing plunger seizure.

Summary

In the above cases, it has been possible to identify the main causes of failure of the main propulsion system. In case of ship I, the technical services of the owner decided to use the fuel, despite the result of the analysis indicating excessive TSP, a parameter essential for the operation of the engine and the engine room. In ship II, the crew decided to use the newly received fuel, before knowing the results of fuel analysis. The report from the fuel examination provided guidelines for minimizing or even avoiding the technical consequences of poor quality fuel. In case of ship III, the crew complied with all procedures for the use of fuel, and still did not prevent a major failure due to fuel properties.

Using fuel that meets all the requirements of the standard for residual fuels does not guarantee trouble-free operation of the engine and engine room.

The results of the analysis of fuel in ship III indicate compliance with the ISO 8217, but the same problem was experienced as in the case of ship I, where TSP values where clearly above the limits.

Even extended and highly specialised tests will not give complete certainty on fuel quality. The cases of ships I and III show that the same effect (plunger seizures) was due to different causes, as noted in the reports of the laboratories 1 and 4.

Cases I and II contribute to the assessment of the role of the human factor in the safety of the ship. The decisions taken, deliberately bypassing the rules and criteria for handling the fuel on board caused the loss of vessel manoeuvrability.

Although information is abundantly available on the characteristics of the single compounds present in fuels, residual fuel is a mixture of many compounds in different proportion. The ability to predict the behaviour of the mixture based on the characteristics of the individual compounds can be highly biased.

Fuel quality is a function of crude oil composition and production technology. In the opinion of "petroleum services" organizations, most uncertainties regarding the quality derive from the so-called "tank farms", where refinery by-products from dozens of tanks are blended to make fuel according to the current demand (Nair, 2014). Concerns relating to the quality of tank contents as well as proportions used in the mixtures (Nair, 2014) suggest the importance of product quality supervision in bunker stations.

Conclusions

1. The complete elimination of the main propulsion failures caused by residual fuel quality is not possible due to:
   a) current technologies of making residual fuels from crude oil;
   b) limited set of selected properties and methods for determining their value within the standards;
   c) specificity of deep-sea ship operation and fuel use cycle.
2. We can significantly reduce the risks related to navigation safety by using the existing procedures for fuel use and accepting the principle that during manoeuvres the newly bunkered fuel should not be used.
3. Monitoring the compliance with marine fuel procedures by the management staff of the ship owner should be complemented by improving and updating the competence of technical service personnel, both on shore and on board, as part of professional training.

References

1. BDN (2010) Bunker Delivery Note – ship No. 2, No. 011301, Lagos, 20.05.2010.
2. DNV (2014a) *DNV PS Bunker Alerts, 2010–2014*. Fuel Management Course, Tumba, Sweden, 13–15 May, 2014.
3. DNV (2014b) *DNV PS Newsletters, 2010–2014*. Fuel Management Course, Tumba, Sweden, 13–15 May, 2014.
4. DNV (2014c) *DNV PS Lloyd's List Articles, 2006–2009, 2010–2014*. Fuel Management Course, Tumba, Sweden, 13–15 May, 2014.
5. Fuel Quality Reports of samples: 019701, 482562, 482573, 482546, S66191/3393003.
6. ISO 8217:1996. Petroleum products – Fuels (class F) – Specifications of marine fuels.
7. ISO 8217:2005. Petroleum products – Fuels (class F) – Specifications of marine fuels.
8. Nair, S. (2014) Bunkering in Fujairah. *Asia Week* 17th April 2014. pp. 8–9. [Online] Available from: http://www.v-p-s.com/assets/news/140417_SeatradeAsiaWeek-BunkeringinFujairah.pdf [Accessed: April 29. 2016]

Scientific Journals
of the Maritime University of Szczecin

Zeszyty Naukowe
Akademii Morskiej w Szczecinie

2016, 48 (120), 22–28
ISSN 1733-8670 (Printed)
ISSN 2392-0378 (Online)
DOI: 10.17402/171

Received: 29.04.2016
Accepted: 20.09.2016
Published: 15.12.2016

Selection of a mathematical model to describe solid fuel pneumatic transport to the ship boiler

Daniel Łuszczyński, Wojciech Zeńczak

West Pomeranian University of Technology in Szczecin
41 Piastów Ave., 71-065 Szczecin, Poland
e-mail: {Daniel.Luszczynski; wojciech.zenczak}@zut.edu.pl
corresponding author

Key words: pneumatic transport, two-phase flow, mathematical model, pressure drop, transport installation, ship boiler

Abstract
This article presents an overview of the mathematical models applied for the description of the pneumatic transportation of grain materials. Thus the model that has been selected is best suited for the description of the pressure drop in the pneumatic transport installation of solid fuel for a ship boiler. The research conducted allows for verification of the hypothesis that the ship's motion is of minor importance and therefore it is possible at the design stage to apply the simplified model to determine the pressure losses in the installation.

Introduction

The most important and most frequently examined parameter in connection with the grain material pneumatic transportation is determination of the flow resistances in the installation which are significant regarding the selection of the appropriate flow machine. The laboratory stand, complete with the transport installation located on the movable platform that simulates the ship's rolling at sea, has been built in order to enable examination of the pressure drop in the shipboard pneumatic transport installation of solid fuel. The stand has been specified in detail in Łuszczyński & Zeńczak (Łuszczyński & Zeńczak, 2014). The examinations conducted are of active nature. A factor that interferes with the transport process in the laboratory conditions is the swinging movement of the platform. The obtained results of the experimental research will be applied for the validation of the mathematical model of the process.

Since multiphase mixture flows in pipelines are a complex phenomenon, and thus hard to define, in mathematical models several idealising assumptions and simplifications have been applied. In effect, numerous models can be found with various degrees of simplification, which are applied to describe the same process.

The goal of this paper is to present the most frequently encountered models and indicate that the model is reasonably simple, with determined accuracy, and possibly most useful for the description of the process of pressure drop in the solid fuel pneumatic transportation to the boiler during the interferences caused by the ship's movement on waves.

Analysis of the Pneumatic Transport Phenomenon

Introduction

Pneumatic transport is a particular example of the two-phase flow phenomenon. It is characterised by the fact that its continuous phase is gas while solids constitute the dispersed phase. The continuous phase is a carrier medium whose movement is caused by the pressure difference. The carrier medium employed while flowing past the interior

surface of the pipeline at a specified rate produces the lift force, which transports the particles of the solid object. In pneumatic transport, as opposed to hydraulic transport, a specific feature is a substantial ratio of solid phase density to the continuous phase, i.e. in the order of 103. This means that in pneumatic transport the velocity of the fluid (gas) is larger by an order of magnitude and the solid phase participation is smaller than in hydraulic transport by a volume of an order or two of magnitude (Orzechowski, 1990). Owing to the large gas velocities, the pressure losses at the transport line unit of length are significantly greater than in the case of hydraulic transport, which is why the pneumatic transport lines do not exceed several hundreds of meters in length (Dziubiński & Prywer, 2009). While this is a limitation, it is not an obstacle in the application of such installations on board ships because they do not exceed 100 m (Schroppe & Gamble, 1981).

In marine conditions horizontal and vertical segments in the transport line occur together with elbows. In each of these segments we face somewhat different phenomena. In the case of ship's rolling on waves, the particular segments will temporarily also become the segments inclined at a certain angle which offers yet another representation of the phenomenon.

The air velocity in horizontal segments should be larger than the sedimentation rate of the particles, and in the vertical segments larger than the so called choking velocity, in the other words such velocity that is accompanied by the pressure gradient that is unable to compensate for the weight of particles resulting in them falling down. The flow then becomes the plug flow. Its equivalent in the horizontal segment is so called saltation, or in other words the formation of material clusters resembling sand dunes.

Vertical Flow

In the pneumatic transport as a rule the material concentration is of low value and the mass ratio of solids to gas is lower, ranging from 10 up to 20 (Kunii & Levenspiel, 1991).

Figure 1 shows examples of the structures of flow characterised by their dependence on the gas velocity, material condensation and diameter of particles. The solid material particle movement lifted upwards by an air jet is always locally unsettled. As shown in Figure 1 the loose groups of particles mostly move in the form of smudges, streams or layers. Our own observations at the research stand as well as references from literature indicate that at particularly larger material concentrations the particle groups flow not only upwards but also downwards.

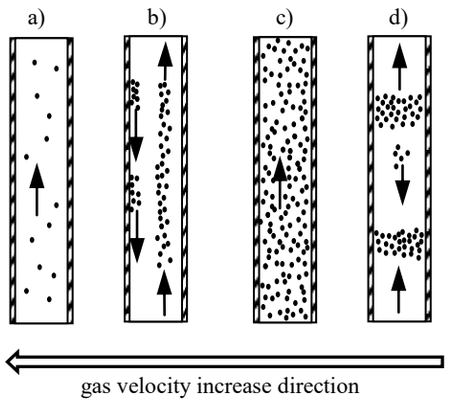

Figure 1. Structures of flow of gas/solid mixture in vertical duct: a) lifting of particles at low concentration, b) smudges, c) particle lifting in larger concentration, d) plugging (Orzechowski, 1990; Kunii & Levenspiel, 1991; Dziubiński & Prywer, 2009)

Figure 2 shows an image of the wheat grain flow structure obtained within our own means at the research stand.

Figure 2. Flow structure during vertical pneumatic transportation of wheat grains

This phenomenon occurs mostly near the pipeline wall and is caused by the friction of air and particles against the pipe wall. In effect, in the core of the duct the particles move faster than at the wall. As the air velocity decreases from the maximum value (Figure 1a), the friction reduces and thus the pressure resistances start to depend on the sum of the gas and material static height to a larger degree. Initially the joint flow resistances decrease accompanying the air velocity decrease, but after passing the characteristic bending point they start to increase again, because the concentration of the solid material increases. At that time the flow gets throttled and

the aforementioned choking occurs. Figure 3 presents the typical image of pressure changes during the vertical transportation.

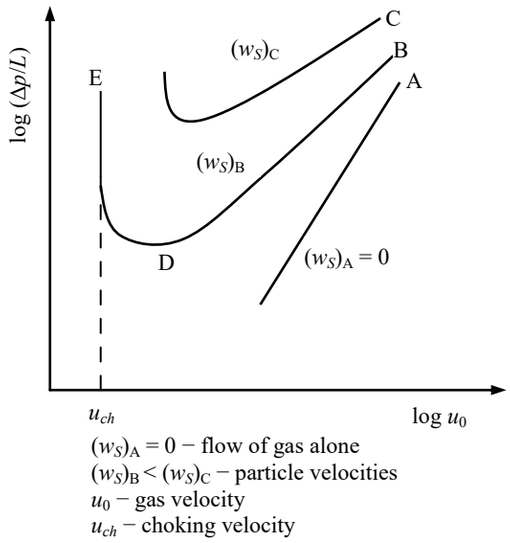

Figure 3. Picture of the changes in specific pressure losses during vertical pneumatic transport (Kunii & Levenspiel, 1991)

The phenomenon of choking itself is interesting although more attention is paid to determination of the minimum air velocities, which guarantee safe pneumatic transport.

Horizontal Flow

The picture of the flow in horizontal pipeline is more complex than in the vertical line because the movement of a single particle in the vertical duct, regardless of friction and inertia forces, depends only on the forces of gravity, displacement and resistance. In the horizontal line the particle is additionally influenced by Magnus force, related to the revolution of particles owing to the pressure gradient at the pipeline wall. This force causes lifting of the particle and momentarily keeps them suspended because in case of horizontal flow the resistance force is directed perpendicularly to the gravity force. The particles move up by jumps and fall down. The horizontal flow is possible when these forces keep the particle suspended, which is possible with an adequately large gas velocity. With the large flow rate and low concentration the particles move approximately along the straight runs which take turns in case of mutual collisions and resultantly hitting the duct wall (Orzechowski, 1990). In Figure 4 the diagram of Magnus force effect is presented in relation to the resting particle and the flow structure with large air velocity.

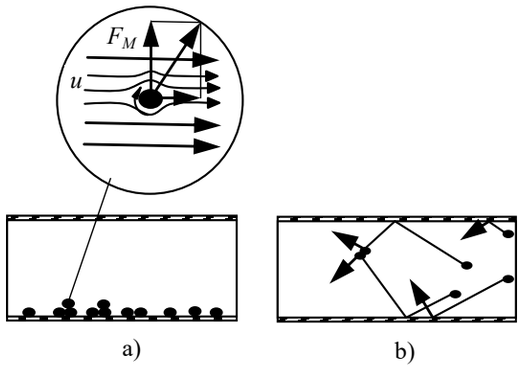

Figure 4. Diagram of Magnus force effect on resting particle (a) and the flow structure with the large air velocity (b) (Orzechowski, 1990)

While the gas flow velocity decreases, the particles start to collect in the lower part of the pipeline forming a layer that moves in a sliding motion, and which in case of continued velocity decrease forms the wandering dunes (phenomenon of saltation). Earlier small wandering waves are also formed. Similar phenomena are observed in the transport lines inclined at a certain angle to level (Kunii & Levenspiel, 1991).

Figure 5 shows the typical flow structures in horizontal pneumatic transport. On the other hand, Figure 6 shows the picture of flow structure during the horizontal pneumatic transport of wheat grains as observed at own research stand. In the pipeline lower part, the lower layer is clearly visible as it moves in a sliding manner (a) and the beginnings of saltation (b).

Figure 7 shows the picture of specific pressure changes during horizontal transport with various particle contents. Similarly as in the vertical flow it is observed that as the velocity decreases the friction decreases, thus resulting in pressure losses owing to friction, and in point D corresponding to saltation

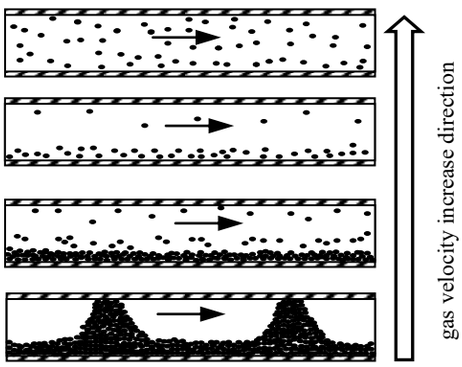

Figure 5. Flow structures in horizontal pneumatic transport (Orzechowski, 1990; Kunii & Levenspiel, 1991; Dziubiński & Prywer, 2009)

rate, the particles start to sediment in the lower part of the pipeline. In effect the duct diameter gets reduced and pressure rises abruptly as far as point E (Kunii & Levenspiel, 1991).

a)

b)

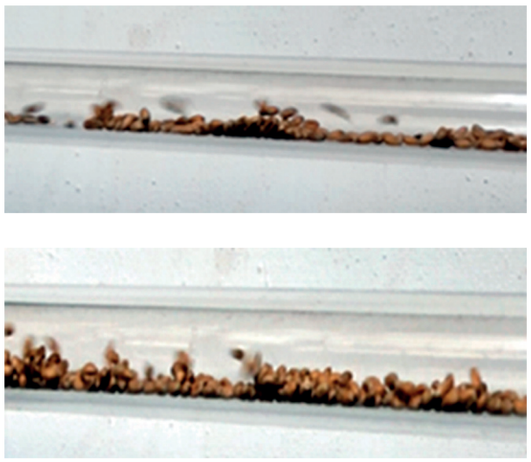

Figure 6. Image of flow structure during the horizontal pneumatic transport of wheat grains: a) layer moving by sliding b) saltation beginning

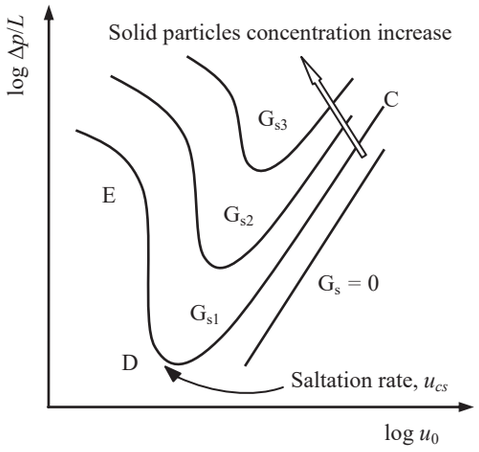

Figure 7. Specific pressure changes during horizontal transport with various particle content (Kunii & Levenspiel, 1991)

Flow in Inclined Ducts and Elbows

As already mentioned, in the pneumatic transport lines inclined at a certain angle to level, similar phenomena occur regarding the horizontal flow and they will not be further analysed in this article.

In elbows connecting various straight segments, the result of the centrifugal force is a change in the flow structure. Particles move almost along the straight-line runs, hit the elbow wall and segregate so that after collision they form a bundle of smaller diameter than the bundle consisting of the biggest elements. Just behind the elbow, in the effect of abrupt velocity reduction in that place, a significant concentration occurs. According to research, subject to the radius and diameter of the pipeline, the return to the flow conditions as they were before the elbow could occur at a maximum distance of approximately 30 diameters of the pipeline (Dziubiński & Prywer, 2009). The picture of the flow in the elbow is shown in Figure 8.

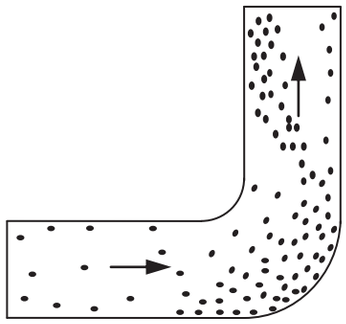

Figure 8. Solid phase flow through elbow (Dziubiński & Prywer, 2009)

The Basis of Construction of Mathematical Models Applicable in Two-Phase Flows

Mathematic modelling consists of the mathematical description of a system, process or physical phenomenon. It is a system of equations or inequalities which map the performance of a system or the course of the modelled process with specified accuracy. The mathematical models are used to conduct analyses of the performance of actual objects under the influence of various external factors. Since the changes of the phenomena observed in nature occur in time and space, they are described through the time sequences of condition variables and input variables (Tarnowski, 2004). The computer simulating models built on the basis of the mathematical model provide the possibility of simulating and observing the performance of systems both under normal operation conditions as well as in hypothetic emergency conditions without fearing their destruction.

The pneumatic models are created on the basis of the laws of physics and process observations or the observations of the performance of the examined system. The paradigms are used for that purpose, for instance the law of conservation of mass, momentum and energy and the defining equations as well as the particular models of the phenomena (Tarnowski, 2004). The starting point being the assumed search for a model that is reasonably simple in these considerations, the focus has thus been made on two-phase one-dimensional settled flows without heat and mass exchange.

A characteristic feature of the two-phase flow is the occurrence of the interface. The flow area may be regarded as an area divided by the moving boundary surface into two one-phase sub-areas. Thus the equations can be formulated for each of the phases separately as for the one-phase flow. The varied, i.e. not uniform, distribution of the dispersed phase and the moving division boundaries of shape varying in time cause it to be impossible to achieve the explicit mathematical description of these flows. This results in the necessity of looking for substitute flow models (Orzechowski, 1990; Malczewski & Piekarski, 1992; Dziubiński & Prywer, 2009).

There are two methods applicable for the description of the two-phase flow dynamics (Dziubiński & Prywer, 2009):

- phenomenological method;
- averaging method.

The phenomenological method to describe the two-phase flows does not take into account the particle or atom structure of the mixture, because it consists of the description and survey of what is given directly. Thus in this method the mixture flow is described in the macroscopic terms and refers to direct measurement of the physical figures such as: pressure, velocity/rate and temperature. The essential merits of the phenomenological description of the motion are: low degree of complexity of the calculations, universal nature of the laws and the possibility of their experimental analysing (Szargut, 2000; Wiśniewski, 2013).

In general terms, the averaging may be done in space, in time or statistically. The equations describing the two-phase dynamics, i.e. equations describing the processes in microscale inside the one-phase sub-areas, are averaged for the temporary local variables. The spatial microscale is the characteristic linear size of the irregularities, in this case the size of particles. The important advantages of averaging are: profound description of the physical laws and notions as well as the possibility of calculating the physical properties of the mixtures from the input data referring to the molecular structure and elementary particles, which in the phenomenological method should be determined empirically. If averaging by the volume is conducted simultaneously for both phases, the obtained equations are referred to as the homogenous model. In the homogenous model each of the components fills the entire volume and loses the individual traits so both phases are perfectly mixed and move with the same velocity (non-sliding model). Thus in this model the interface also disappears which presents a serious problem from the mathematical point of view. The opposite of the homogenous model is the heterogeneous model in which each phase retains its features in its separated volume which represents the component of the total volume of both phases (Orzechowski, 1990; Malczewski & Piekarski, 1992; Dziubiński & Prywer, 2009). In the modelling of flows this is referred to as flow with the division of phases. One of the features of two-phase flow thus regarded is the occurrence of different velocities of both phases. Models in which a particular stress is put not on the velocity of each phase, but on the flow velocity of one phase versus the other, belong to the class of sliding models (Dziubiński & Prywer, 2009). The following averaging methods of transport equations are commonly used (Malczewski & Piekarski, 1992):

- averaging by Euler's method;
- averaging by Lagrange's method;
- averaging by a statistical method, e.g. Boltzmann's.

While applying Euler's method (local analysis), the movements of subsequent elements of the two-phase mixture are examined as they move through the fixed point of defined coordinates. By averaging the chosen flow parameter in Euler's method the control surface is introduced, i.e. confined or an open immobile surface is established by the same fixed points in space. In Euler's method the averaging applies to a given figure, e.g. pressure, velocity/rate, temperature in time or on surface or by volume. Thus the essence of the method is the averaging in time of the variable figure observed in a given point of space (Jeżowiecka-Kabsch & Szewczyk, 2001).

Lagrange's method (Lagrangian analysis) is applied less often. By its application the selected mixture flow parameters are examined, e.g. velocity, individually for each element of the mixture moving in space, by averaging them in time. At a given time, the coordinates of the given mixture element will be dependent on the initial coordinates and time. Having the trajectory equations at disposal we can determine e.g. the average velocity of given element of the mixture (Jeżowiecka-Kabsch & Szewczyk, 2001).

In Boltzmann's method, also referred to as LBM or Lattice Boltzmann Method, the discrete variables determining the particle velocities are substituted by seven continuous variables interpreted as probabilities that the particles follow in the direction determined on the lattice. Knowing these functions we can determine the macroscopic flow parameters such as the local velocity and density of fluid. The essence of Boltzmann's method is the simple algorithm (a kind of cellular automaton) where the

evolution of the distribution function is completed in two steps: shift and collision (Matyka, Koza & Mirosław, 2016).

In these examinations owing to their specific nature, typical for the technical issues, it is proposed to adopt the method to calculate the pressure drop on the basis of the one-dimensional non-sliding model.

Homogenous Model

As already mentioned, the basic assumptions in the homogenous model are equal velocities of flow for both phases and their homogenous blending. In the one-dimensional model the changes being undergone are considered only in the direction of the z axis. Therefore in the mathematical notation, instead of partial derivatives, there will be complete derivatives to aid further simplification. Basic equations describing the model are the mass conservation equation and the momentum conservation equation which allows for determination of the flow resistances.

The mass conservation equation (flow continuity)

$$\dot{m} = \rho\, u\, A = \text{idem} \tag{1}$$

where:

$\dot{m}$ – two-phase mixture mass flow;
ρ – mixture density (determined according to mass participation);
A – sectional area of duct/pipeline cross-section;
u – mixture velocity.

The momentum conservation equation (movement equation) consists of the balance of forces acting on an isolated element (layer) of the flowing mixture. The forces acting on the isolated element of mixture are shown in Figure 9.

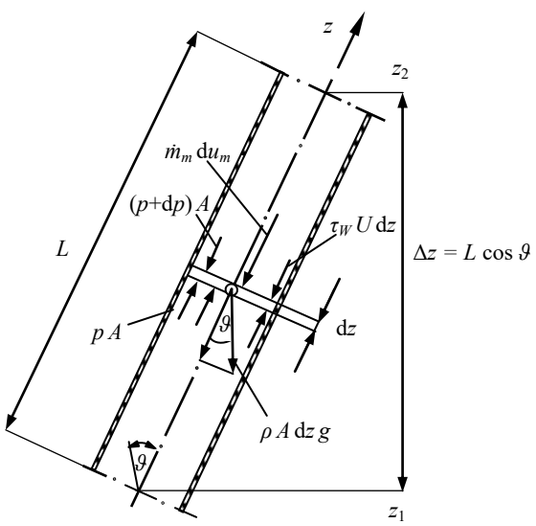

Figure 9. Forces acting on isolated element of mixture (Dziubiński & Prywer, 2009)

$$pA - (p + \mathrm{d}\,p)A = \tau_W U\,\mathrm{d}\,z + \dot{m}\,\mathrm{d}\,u + \rho A\,\mathrm{d}\,z g\cos\vartheta \tag{2}$$

where:

τ_w – average contact tension on duct/pipeline wall;
p – pressure;
U – perimeter of duct/pipeline cross section (moist perimeter).

Terms on the left side of the equation (2) represent the pressure forces while on the right side: friction force against the wall, force of inertia of lift and component of gravity force at the axis z accordingly.

Upon dividing the equation (2) by $A\mathrm{d}z$ and after transformation we obtain the equation representing the pressure drop along the duct/pipeline (Orzechowski, 1990; Zarzycki, Orzechowski & Prywer, 2001; Dziubiński & Prywer, 2009):

$$-\frac{\mathrm{d}\,p}{\mathrm{d}\,z} = \frac{U}{A}\tau_w + \frac{\dot{m}}{A}\frac{\mathrm{d}\,u}{\mathrm{d}\,z} + \rho\, g\cos\vartheta \tag{3}$$

The terms on the right side of equation (3) stand for:

$\frac{\mathrm{d}\,p_f}{\mathrm{d}\,z} = -\frac{U}{A}\tau_w$ – pressure gradient caused by friction of mixture against duct wall;

$\frac{\mathrm{d}\,p_a}{\mathrm{d}\,z} = -\frac{\dot{m}}{A}\frac{\mathrm{d}\,u}{\mathrm{d}\,z}$ – pressure gradient caused by mixture acceleration;

$\frac{\mathrm{d}\,p_h}{\mathrm{d}\,z} = -\rho\, g\cos\vartheta$ – pressure gradient resulting from the force of gravity.

The pressure gradient caused by the mixture acceleration in the case of a fixed duct/pipeline diameter is often disregarded (Dziubiński & Prywer, 2009). Thus the most significant gradient will result from the pressure losses caused by mixture friction against the duct/piping wall which would always occur. On the other hand, the gravity force component will only cause losses in the vertical or inclined segments. It is also worth noting that with the angles $\vartheta > 90$ the pressure loss component will be negative.

The relation between the contact tension τ_w and the pressure loss in the duct/pipeline of the length L and hydraulic diameter d_h is as follows (Orzechowski, 1990; Zarzycki, Orzechowski & Prywer, 2001; Dziubiński & Prywer, 2009):

$$\Delta p_f = 4\frac{L}{d_h}\tau_w \tag{4}$$

After comparing the equation (4) to the Darcy's-Weisbach's model, i.e.:

$$\Delta p_f = \lambda \frac{L}{d_h} \rho \frac{u^2}{2} \tag{5}$$

determining τ_w, pressure gradient caused by friction can be put down as:

$$\frac{\mathrm{d}\, p_f}{\mathrm{d}\, z} = -\frac{U}{A} \cdot \frac{1}{4} \lambda \rho \frac{u^2}{2} \tag{6}$$

where: λ – friction factor.

Thus finally considering that $d_h = 4A/U$ and disregarding the pressure gradient caused by mixture acceleration upon substituting in (3) the relation for the pressure drop takes the following form:

$$-\frac{\mathrm{d}\, p}{\mathrm{d}\, z} = \lambda \frac{\rho\, u^2}{2 d_h} + \rho\, g \cos \vartheta \tag{7}$$

Conclusions

The homogenous model can be particularly useful during research studies where the movement of individual particles in two-phase mixture is not analysed, and the most vital parameter which shall be determined is the value of mixture resistances. For the analysis the parameter averaged values are used which simplifies the complexity of the model itself and the calculations. The presented model is suitable most of all to determine the pressure losses in the established conditions of navigation such as, e.g. permanent ship's list, trim by the head or by the stern. In the conditions of continuous rolling it will also be necessary to consider the forces of inertia conditioned by the angular accelerations. The conducted experimental research aims to check how significant the changes in the flow resistances are during the ship's rolling in relation to sailing in calm sea. They will allow also for verification of the hypothesis that this movement is of minor significance and at the design stage it is possible to apply the aforementioned simplified model.

References

1. Dziubiński, M. & Prywer, J. (2009) *Mechanika płynów dwufazowych*. Warszawa: Wydawnictwo Naukowo-Techniczne Sp. z o.o.
2. Jeżowiecka-Kabsch, K. & Szewczyk, H. (2001) *Mechanika Płynów*. Wrocław: Oficyna Wydawnicza Politechniki Wrocławskiej.
3. Kunii, D. & Levenspiel, O. (1991) *Fluidization Engineering*. Stoneham: Butteworth-Heinemann.
4. Łuszczyński, D. & Zeńczak, W. (2014) Transport pneumatyczny paliwa stałego do kotła w warunkach morskich. *Zeszyty Naukowe Akademii Marynarki Wojennej* 4 (199). pp. 39–50.
5. Malczewski, J. & Piekarski, M. (1992) *Modele procesów transportu masy, pędu i energii*. Warszawa: Wydawnictwo Naukowe PWN.
6. Matyka, M., Koza, Z. & Mirosław, Ł. (2016) *Wydajność otwartych implementacji metody sieciowej Boltzmana na CPU i GPU*. [Online] Available from: www.ift.uni.wroc.pl [Accessed: February 07, 2016]
7. Orzechowski, Z. (1990) *Przepływy dwufazowe jednowymiarowe ustalone adiabatycznie*. Warszawa: PWN.
8. Schroppe, J.T. & Gamble, R.L. (1981) A Coal Fired Fluidized-Bed Steam Generator for Marine Application. *SNAME Transactions* 89. pp. 379–395.
9. Szargut, J. (2000) *Termodynamika*. Warszawa: Wydawnictwo Naukowe PWN.
10. Tarnowski, W. (2004) *Modelowanie systemów*. Koszalin: Wydawnictwo Uczelniane Politechniki Koszalińskiej.
11. Wiśniewski, S. (2013) *Termodynamika techniczna*. Warszawa: Wydawnictwo Naukowo-Techniczne.
12. Zarzycki, R., Orzechowski, J. & Prywer, J. (2001) *Mechanika płynów w inżynierii środowiska*. Warszawa: WNT.

Scientific Journals
of the Maritime University of Szczecin

Zeszyty Naukowe
Akademii Morskiej w Szczecinie

2016, 48 (120), 29–36
ISSN 1733-8670 (Printed)
ISSN 2392-0378 (Online)
DOI: 10.17402/172

Received: 27.05.2016
Accepted: 14.07.2016
Published: 15.12.2016

Input data selection for identification of the incremental ship's model

Anna Miller

Gdynia Maritime University, Department of Ship Automation
81–87 Morska St., 81-225 Gdynia, Poland, e-mail: a.miller@we.am.gdynia.pl

Key words: model identification, mathematical linear model, model for Model Predictive Control (MPC), selection procedure, data, parameters

Abstract

The procedure of Linear Incremental Model (LIM) identification requires input and output signal deviations as opposed to their actual values. When considering a vessel as a plant, the sequence of input signals determines the traceability of the estimated LIM. The manual input signals selection procedure is a demanding and time consuming empirical procedure. In order to increase the speed of object identification and to eliminate input-output signal sequences which give unreliable data, an incremental linear model identification algorithm was developed and is presented. Moreover, the method of parameter selection for input signal pseudo-random sequences is described in this paper. Emphasis is placed on the practical aspect of astatic objects – ship's LIM creation and input-output signal deviations selection method.

Introduction

Model Predictive Control (MPC) is a control strategy, which requires an adequate mathematical model for proper operation. This means that control signal values are computed on the basis of the previously designed model, whose structure should be adequate with respect to the controller's operational goal. This model should be as simple as possible (Camacho & Bordons, 1999, pp. 11–13) to guarantee fast computations, and therefore modelling is intimately associated with the MPC. Generally, linear state-space or transfer function models are incorporated into the controller's structure.

This paper focuses on linear incremental model (LIM) identification for future model predictive controller design. Data preparation for incremental model identification is more complicated than for an ordinary linear model. It is connected with the need to use signal deviations with respect to the operating points instead of signal values in the operating points during the identification procedure, so the incremental mathematical models are not very popular. Procedures for the linear system's LIM identification and usage are described in (Jayawardhana et al., 2007; Rajasekar & Sundaram, 2012). A model identification procedure often is based on the data sets, which were obtained during real experiments or simulations (Gelu & Toma-Leonida, 2013; Theisen et al., 2015). Moving objects like ships (Gierusz, 2016), aircraft (Armanini et al., 2016) and cars are modelled and identified on the basis of big data sets obtained during real experiments, and linearized for future control systems. The collection of data sets, containing high quality input-output signals which will give favorable results in the object's identification procedure, is a time consuming iterative process. When taking into account LIM, where output signal deviations are dependent on the input signal deviations and past input signal values, the procedure of data set composition becomes more complicated. In this work, input data selection and output data verification for the ship's incremental linear model is presented. This procedure can be adapted for other astatic objects such as planes, cars and wheeled robots.

In this paper are described the conditions under which identification of the LIM is possible, operating point selection, input signal period selection and its influence on the quality of the identification process. The influence of the input signal's deviation on the quality of obtained data was also taken into account. The research undertaken shows that it is possible to find rules for input signal for identification process selection, which give better results in a shorter time than empirical data selection. The identification process was performed with the use of the Matlab System Identification Toolbox. Simulation results were obtained using Matlab Simulink software.

Incremental Mathematical Model of Ship Dynamics

Developing a model of a system must be related to the application it is going to be used for (Ljung, 2016). The incremental linear ship's model is designed for the future Model Predictive Control (MPC) for a service ship (SS) during replenishment while underway. The identified model is the LIM of the real floating Liquid Natural Gas (LNG) Carrier 'Dorchester Lady', built to 1:24 scale. It is owned by the Foundation for Safety of Navigation and Environment Protection. It is equipped with two rotatable azipods on the stern, bow tunnel and rotatable thrusters. A ship is a highly nonlinear object, which may be linearized around the chosen operating point. A linear model does not require such large computing power as nonlinear one during MPC control signals computation, and it also maps input-output dependences in a relevant way. Therefore, the MPC controller incremental, state-space model (1), (2) was chosen.

$$\dot{x}(t) = A \cdot x(t) + B \cdot \Delta u(t) \tag{1}$$

$$\Delta y(t) = C \cdot x(t) \tag{2}$$

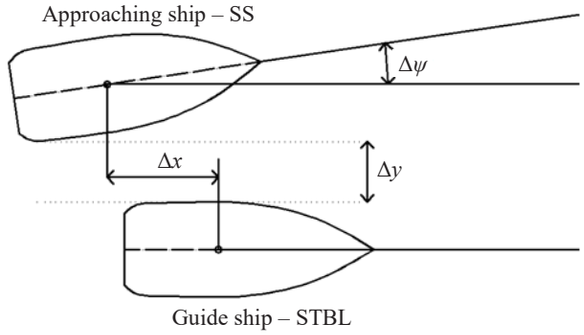

Figure 1. Ships' configuration during replenishment while underway (Gierusz & Miller, 2016)

where:

$x(t)$ – state space vector;

A, B, C – estimated dynamics, input, output (sensor) matrices;

$\Delta u(t)$ – input signal deviations vector (which consists of azipods revolution deviation, Δn, and angle of rotation deviation, $\Delta\delta$);

$\Delta y(t)$ – output signal deviations vector (which consists of longitudinal shift, Δx_p, transversal shift, Δy_p, and course deviation, $\Delta\psi_p$), as presented in Figure 1.

Linear IM Identification Procedure

Dorchester Lady is a real floating training ship, which is a highly nonlinear Multiple Input, Multiple Output (MIMO) plant. Its input and output signals are shown in Figure 2. The input signals vector [n δ] consists of thruster revolutions (n) and thruster angle of rotation (δ). The thrust allocation system computes forces and moments derived by the ship propelling and steering plants ([X_i Y_i N_i]). Output signals are: position (x, y), heading (ψ), longitudinal speed (u), transversal speed (v) and rotational speed (r).

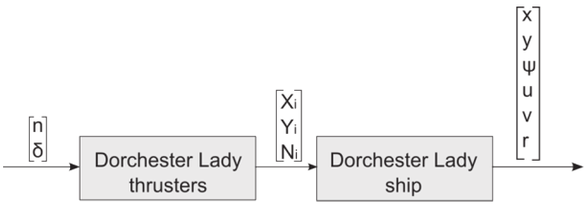

Figure 2. Input and output signals of the LNG carrier model

The linear incremental state-space model is designed to predict plant outputs and designate optimal values of the MPC control signals. Its identification requires estimation of the particular elements of the matrices A, B and C. The identification procedure was carried out with the use of Matlab System Identification Toolbox. This software enables space-state, transfer function and polynomial black-box model parameters estimation. In order to obtain the best possible model in the shortest time, the identification algorithm presented in Figure 3 was developed.

The LIM identification procedure using Matlab System Identification Toolbox is an incremental procedure. It was carried out 'experimentally' according to (Gierusz, 2004). First of all there is a need to choose which type of model is required. For the future MPC control system, the black-box state space model was chosen. This will be the simplest model and will allow for the fast computation of output signals. The LNG Carrier 'Dorchester Lady' is

a MIMO plant, so its LIM also has to be a MIMO one. Matlab System Identification Toolbox allows for MIMO black-box model identification (Ljung, 2016); there are two possible ways to do this:

- directly identify the MIMO object on the basis of all measured outputs and inputs;
- merge SIMO (Single Input Multiple Output) models obtained for each input signal.

Modelling multiple outputs as a combination of single-input models gives better control of the identified channel behavior. It also enables faster proper input signals sequence finding, because the user has to control only one input when analyzing if the shift (Δx, Δy) and heading ($\Delta\psi$) deviations have accepted values. During the LIM identification procedure, which needs very precise and careful selection of input signals and output signals verification, the second described method was chosen.

According to Figure 2, the 'Dorchester Lady' linear model incorporates thruster and ship dynamics. It has two input signals, namely azipods set point (n) and azipods angle of rotation (δ), and six output signals. The identified LIM will be used for the future Underway Replenishment (UNREP) control system, so its structure needs adjustment for this purpose. It needs azipod set point (Δn) and angle of rotation ($\Delta\delta$) deviations as input signals, and output signal deviations of position (Δx, Δy) and heading ($\Delta\psi$) deviations. Input signal deviations are counted as a difference between set point $n = 7$ and angle of rotation $\delta = 0°$, allowing for the straight motion at half ahead speed ($u = 1.1$ m/s for the model ship) and current set point. Output signal deviations are the differences between the reference position, where the ship would be at the specific time point if it proceeded with the half ahead speed from its current position. Course deviation is counted in the same way as position deviation.

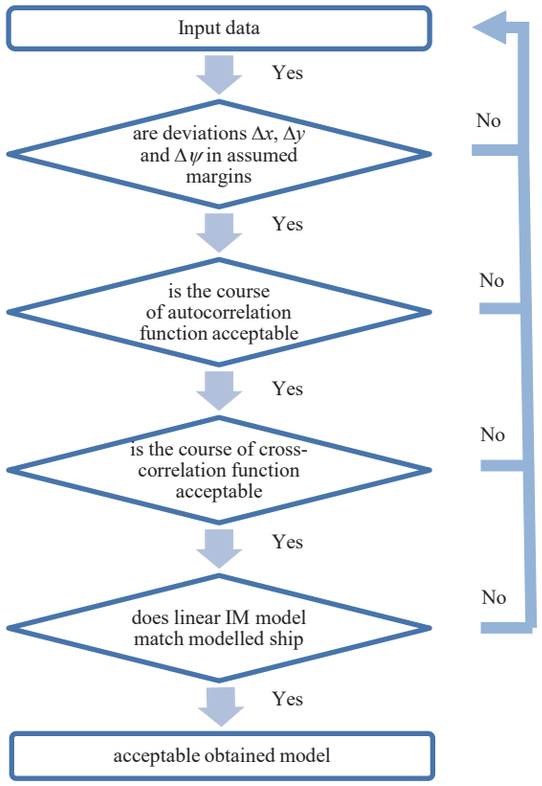

Figure 3. Incremental linear model identification algorithm

The LIM model was estimated based on the simulations of the nonlinear model. This method is more complicated than data acquisition on the real floating ship during sea trials, because it requires the creation of a nonlinear model, but it allows the analysis of wide range of input data sequences and the selection of the best quality ones for model identification. This is very important when estimating the LIM model, where input data period and sequence have a big influence on the quality of the output data. Figure 4 shows the Simulink scheme which was used during input-output data acquisition. The 'Dorchester Lady' block is the non-linear multidimensional ship's

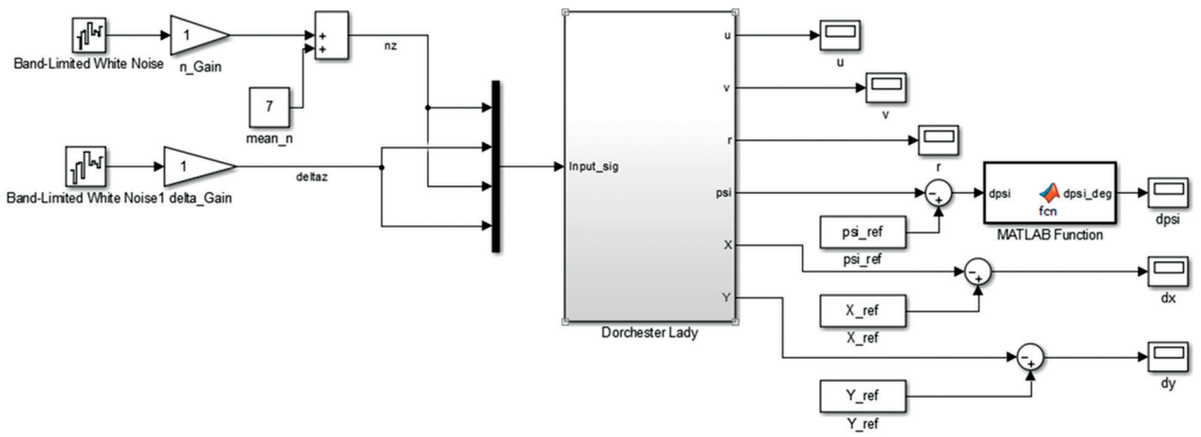

Figure 4. Matlab Simulink scheme for input-output data acquisition

model (Gierusz, 2016). Input signals were simulated by the 'Band-Limited White Noise' blocks that are normally distributed random numbers. The starting seed of the random number generator and the sample time are parameters defined by the user. The label 'nz' refers to the azipod set points and 'deltaz' are azipod angles of rotation. Their values are the same for both thrusters, because it was assumed that they will work in a coupled mode in the future control system. The blocks called 'psi_ref', 'X_ref' and 'Y_ref' are reference data used for the output signal deviations count. All output signals are shown on the scopes. During input-output data sets simulations, only those which fulfilled the first algorithm condition (Figure 3) were taken into account during the identification procedure.

The Linear IM of the LNG Carrier 'Dorchester Lady' was estimated in two separate channels, which are presented in Figure 5. In the first part of the data acquisition process, the azipods were in the straight position ($\Delta\delta = 0°$), and their set-point deviations were variable (red line in Figure 5). The second part of the data acquisition process involved constant azipod set-points ($\Delta n = 7$) and variable angle of rotation deviations (blue line in Figure 5).

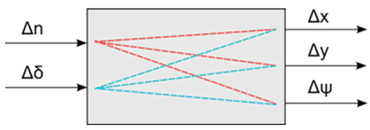

Figure 5. Linear IM identification channels

This input signals separation allowed for better output signals monitoring and disqualification of the input-output data which did not fulfil the conditions described in the next section.

Input Data Preparation

The input data sequence has a big influence on the quality of the identification process. There is a need to find signals which will allow for system dynamics mapping while preserving input/output couplings between identified channels. Therefore, special attention should be paid to the input sequence and its sampling time. This means that the period of the random signal should match plant dynamics and not be shorter than the plant's delay or much longer than its time constant.

Analysis of the Acceptable Input Signal Parameters for the LIM Identification Process

Assumptions for channel $\Delta n \rightarrow [\Delta x, \Delta y, \Delta\psi]$ identification:

- simulated and reference trajectories should not differ significantly, and Δx had to oscillate around a mean value 0 with a magnitude not bigger than 7 m or smaller than 0.5 m;
- Δy and $\Delta\psi$ also had to oscillate around 0, and their magnitude had to not to exceed 0.1 m and 0.1°, respectively;
- output signal deviations in acceptable trials were not allowed to change monotonically; their character had to be oscillatory.

At first, the LNG Carrier 'Dorchester Lady' dynamics and output signal deviations were analyzed as the response. In order to check how fast the ship reacts on the azipod set-point change, longitudinal shift deviation derivative was counted (Figure 6), because speed change has the greatest impact on this value. This changes fast during the 100 s after azipod set-points change and becomes constant after 200 s. The time delay for the 'Dorchester Lady' is about 10 s.

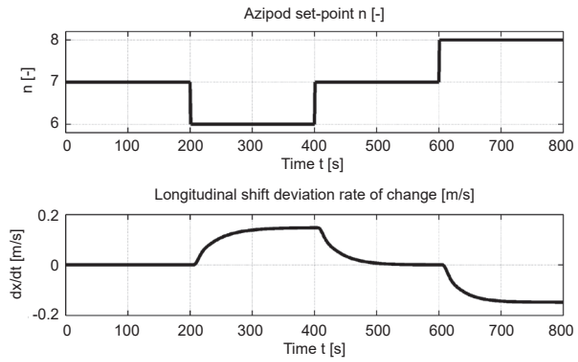

Figure 6. Longitudinal shift deviation rate of change with respect to azipod set-point

Figure 7 shows that long periods of the azipod set-points lead to large values of the longitudinal deviation (Δx), which exceed design criteria. Even in these conditions, transversal shift (Δy) and heading ($\Delta\psi$) deviations are smaller than the values declared in the assumptions. Azipod set-points should oscillate between 6 and 8, which gives speeds between 'slow ahead' and 'full ahead'. Simulations have proved that preserving the value of Δx in the predefined limits requires a change of azipod set-points from $n = 6$ to $n = 8$ after 68 seconds of motion, and after the next 92 seconds of motion the observed value crosses the limit, as shown in Figure 8.

Analysis of the simulation results showed that the azipod set-points change period should be not smaller than 10 seconds due to the plant delay, and should not exceed 68 seconds because of the Δx signal's

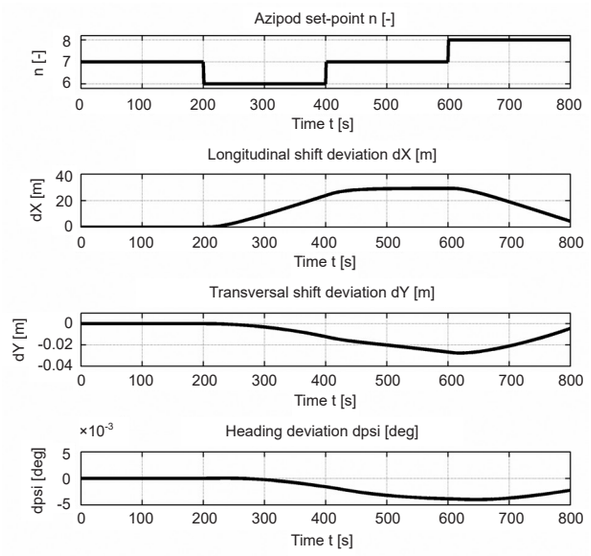

Figure 7. Longitudinal, transversal and heading deviations according to azipod set-points change

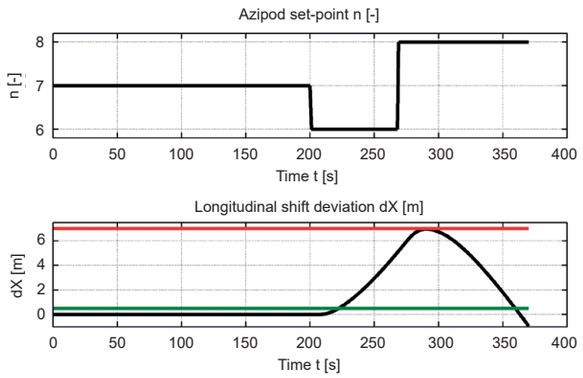

Figure 8. Longitudinal shift deviation according to azipod set-points change

value limitation, when taking into account an input signal standard deviation equal to 1.

Assumptions for channel $\Delta\delta \rightarrow [\Delta x, \Delta y, \Delta\psi]$ identification:

- simulated trajectory should oscillate around reference trajectory and training ship was not allowed to circulate during trial;
- Δx was able to change monotonically, but its magnitude was not allowed to exceed 1.5 m;
- Δy and $\Delta\delta$ also had to oscillate around 0 and their magnitude was not to exceed 9 m and 7°, or be smaller than 0.5 m and 0.5°, respectively.

As in the case of the first channel, the 'Dorchester Lady' dynamics and output signal deviations were analyzed as the response to the change in the azipod angles of rotation. In order to check how fast the ship reacts to the change of the azipod angle of rotation, a heading deviation derivative was measured (Figure 9), because this changes in the fastest way when taking into account all described above output signals.

The heading deviation derivative changes fast during the first 50 seconds after the angle of rotation change, then it becomes almost constant. The time delay does not exceed a second.

Figure 10 shows that such long periods of constant values of azipod angle of rotation lead to constantly increasing values of the longitudinal (Δx) and transversal (Δy) shift deviation. So this output signal does not fulfil the input signal selection criteria. Also the heading deviation does not oscillate around 0°. In Figure 11, it is shown that acceleration of the changes in the angle of rotation leads to minimization of the heading deviation magnitude. When taking into account the standard deviation of the angle of rotation equal to 5°, the input signal should change from 5° to –5° after 118 seconds and should not last more than 67 seconds.

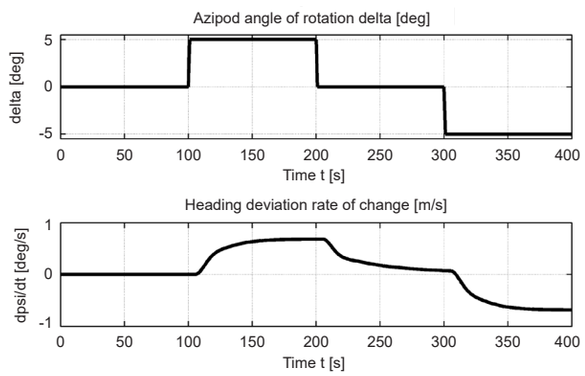

Figure 9. Heading deviation rate of change with respect to azipod angle of rotation

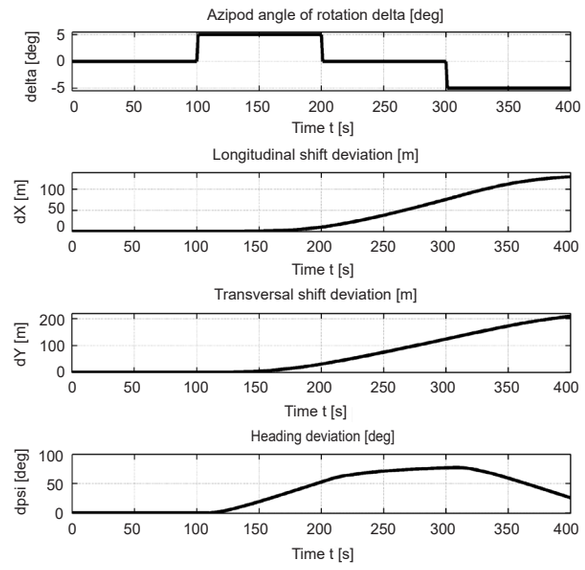

Figure 10. Longitudinal, transversal and heading deviations according to azipod angle of rotation change

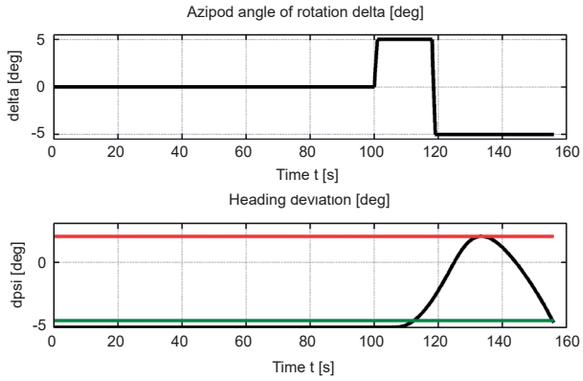

Figure 11. Heading deviation with respect to azipod angle of rotation

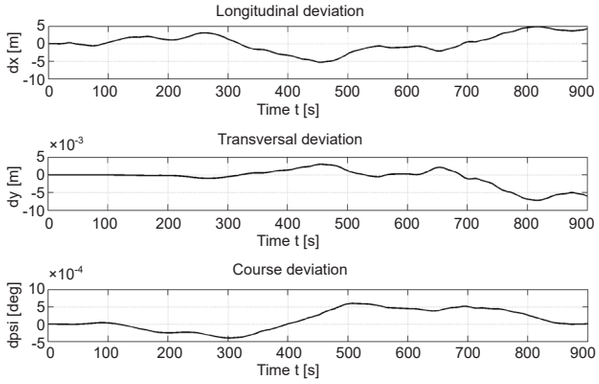

Figure 14. Exemplary acceptable output signal deviations for variable Δn and constant $\Delta\delta = 0$

Examples of the Acceptable and Unacceptable Input-Output Signal Sets for the LIM Identification

Exemplary input signals, acceptable ship's trajectory and output signal deviations for variable Δn and constant $\Delta\delta = 0$ are presented in Figures 12, 13 and 14, respectively. In all figures, δ is described as 'delta' and Δ as 'd'.

In Figure 13, the trajectory and reference trajectory coincide, so they are presented as a single line. When exemplary input signals (Figure 12) are applied to the LIM, it does not change heading, but it influences only the longitudinal speed. So the model moves with a different speed, but on the same trajectory as the ship when $n_{\text{ref}} = 7$ and $\delta_{\text{ref}} = 0$.

Exemplary acceptable ship's trajectory and output signal deviations for variable $\Delta\delta$ and constant $\Delta n = 0$ are presented in Figures 15, 16 and 17.

Furthermore, an exemplary unacceptable input signals sequence, ship's trajectory and output signal deviations for variable $\Delta\delta$ and constant $\Delta n = 0$ are presented in Figures 18, 19 and 20. In these figures it is shown that the training ship's simulated trajectory

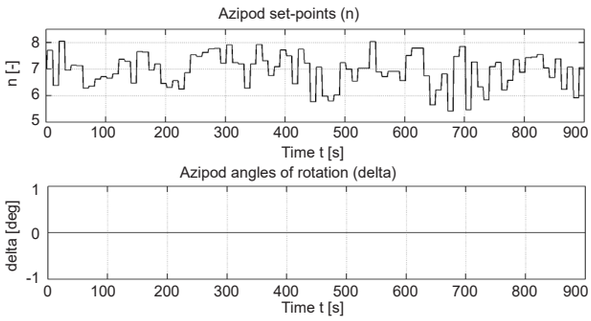

Figure 12. Exemplary acceptable input signals for model identification

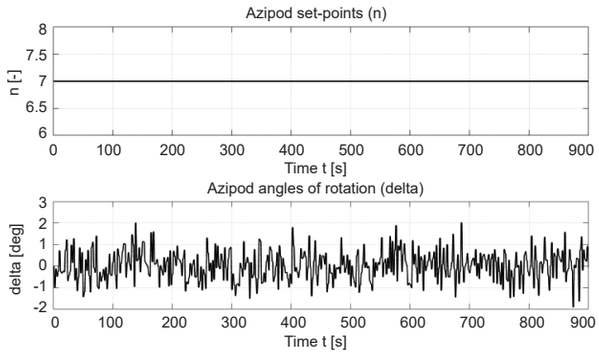

Figure 15. Exemplary acceptable input signals for model identification

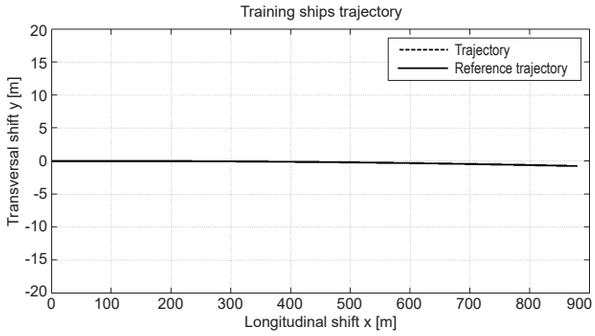

Figure 13. Exemplary acceptable ship's trajectory for variable Δn and constant $\Delta\delta = 0$

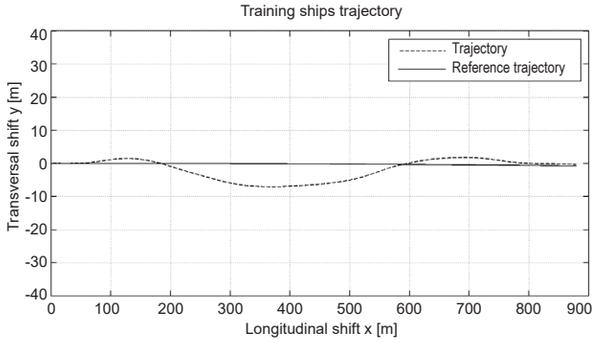

Figure 16. Exemplary acceptable ship's trajectory for variable $\Delta\delta$ and constant $\Delta n = 0$

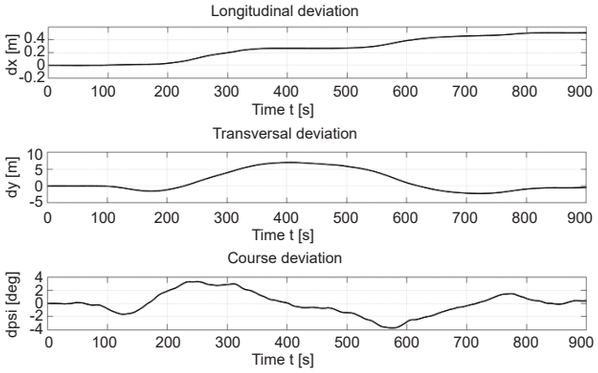

Figure 17. Exemplary acceptable output signal deviations for variable $\Delta\delta$ and constant $\Delta n = 0$

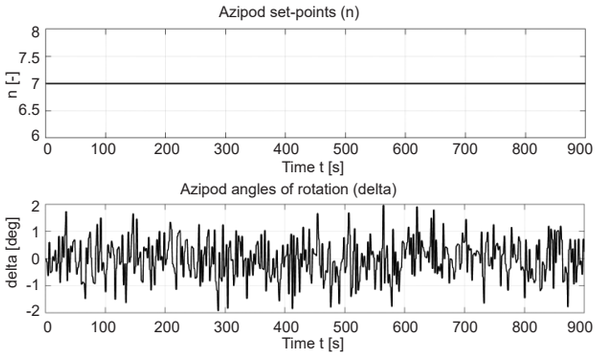

Figure 18. Exemplary unacceptable input signals for model identification

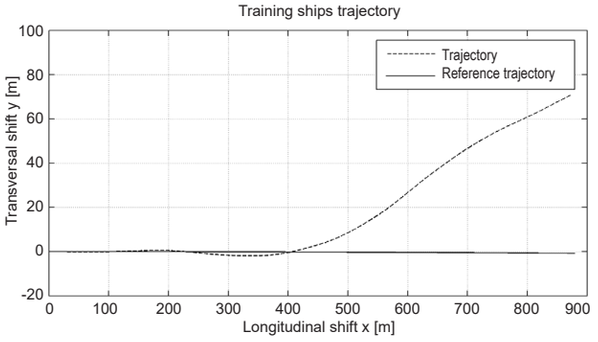

Figure 19. Exemplary unacceptable ship's trajectory for variable $\Delta\delta$ and constant $\Delta n = 0$

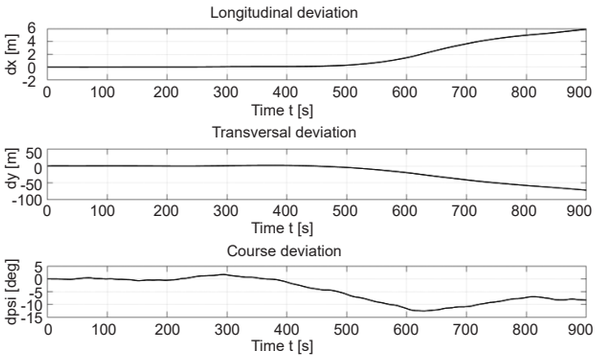

Figure 20. Exemplary unacceptable output signal deviations for variable $\Delta\delta$ and constant $\Delta n = 0$

recedes in a constant fashion. Neither longitudinal nor transversal deviations fulfill assumptions and they monotonically increase to 6 m and decrease to –60 m, respectively. Trials such as these presented in Figures 19 and 20 were rejected, and did not take part in the incremental linear model identification procedure.

The finally chosen identification signal values are presented in Table 1. Due to the expected future use of the identified model, the input signals had to change with different periods. The azipod angles of rotation $\Delta\delta$ had to change about 10 times faster than the azipod set-points to avoid ship circulation.

Table 1. Acceptable values of signal standard deviation and signal change period

Input signal	Reference value	Unit	Standard deviation	Signal change period [s]
Δn	7	[–]	0.6; 0.8; 1	10; 15; 20; 30
$\Delta\delta$	0	[deg]	1.5; 2; 5	1; 2; 5

An identified channel has to fulfill certain conditions. In order to obtain the LIM model, which in simulations will give results approximate to the plant output signals near the set point, input signal deviations should be chosen carefully. Their range of values should be chosen on the basis of the particular plant. The only way to check if the input signal sequence is suitable is to look at the object outputs after simulation. Therefore, the output signal deviations and ship's trajectory were analyzed after every trial. For each channel certain criteria had to be fulfilled, according to the algorithm presented in Figure 3.

Conclusions

This paper has proposed an incremental linear model identification algorithm, which was developed on the basis of a real floating training ship – the LNG Carrier 'Dorchester Lady'. This procedure was created based on the simulations carried out with the use of Matlab Simulink and Matlab System Identification Toolbox by Mathworks. The proposed algorithm can also be customized for the modelling of other plants.

The presented method is proven for MIMO plants and it requires model division into SIMO channels. These are identified in the separate simulations (experiments) and after successful completion of the algorithm, a MIMO linear incremental model is produced by merging two or more SIMO models.

Moreover, in this paper is described a procedure which allows for a fast input signal change period and its standard deviation selection. It involves plant dynamics analysis based on its response to the input signal deviations for each channel. Knowledge of the plant dynamics and change in set-point allows for faster input signal deviation change periods and determination of standard deviations.

The proposed input-output data selection procedure is based on empirical rules and analysis of simulation results, and requires earlier recognition of the future model destination. Therefore this method is based on the expert's knowledge.

There are several limitations of the LIM identification process. The proposed method gives a linear model, which may be used only in special applications such as model predictive control. It is not suitable for simulation of objects, because the input/output signals are chosen deviations. This method is easy to use when someone has a nonlinear mathematical plant's model at their command. Conformity of this method to the modelling on the basis of a real object (ex. floating ship) and data acquisition according to the presented scheme will require a huge amount of experimentation. This is because the presented method is iterative and its results may be proved only after a particular step of the algorithm is finished.

References

1. Armanini, S.F., de Visser, C.C., de Croon, G.C.H.E. & Mulder, M. (2016) Time-varying model identification of flapping-wing vehicle dynamics using flight data. *Journal of Guidance Control and Dynamics* 39 (3). pp. 526–541.
2. Camacho, E.F. & Bordons, C. (1999) *Model Predictive Control*. Springer.
3. Gelu, L.I. & Toma-Leonida, D. (2013) *Dynamic Models Adaptation for a 4 Inj – 2PP Common-rail Pressure System*. In: IECON 2013 – 39th Annual Conference of the IEEE. Vienna, Austria, 10–13 November 2013.
4. Gierusz, W. & Miller, A. (2016) Ship motion control system for replenishment operation. *Applied Mechanics and Materials* 817. pp. 214–222.
5. Gierusz, W. (2004) *Synteza wielowymiarowych układów sterowania precyzyjnego ruchem statku z wykorzystaniem wybranych metod projektowania układów odpornych*. Gdynia: Gdynia Maritime University (in Polish).
6. Gierusz, W. (2016) Private communication.
7. Jayawardhana, B., Ortega, R., Garcia-Canseco, E. & Castanos, F. (2007) Passivity of nonlinear incremental systems: Application to PI stabilization of nonlinear RLC circuits. *Systems & Control Letters* 56 (9). pp. 618–622.
8. Ljung, L. (2016) *System Identification Toolbox for Use with MATLAB*. [Online] The MathWorks Inc, Available from: http://cn.mathworks.com/help/pdf_doc/ident/ident_gs.pdf. [Accessed: May 10, 2016]
9. Rajasekar, N. & Sundaram, K.M. (2012) Feedback controller design for variable voltage variable speed induction motor drive via Ant Colony Optimization. *Applied Soft Computing* 12. pp. 2132–2136.
10. Theisen, L.R.S., Niemann, H.H., Santos, I.F. & Blanke, M. (2015) Modelling and identification for control of gas bearings. *Mechanical Systems and Signal Processing* 70–71. pp. 1150–1170.

Scientific Journals
of the Maritime University of Szczecin

Zeszyty Naukowe
Akademii Morskiej w Szczecinie

2016, 48 (120), 37–42
ISSN 1733-8670 (Printed)
ISSN 2392-0378 (Online)
DOI: 10.17402/173

Received: 12.09.2016
Accepted: 02.11.2016
Published: 15.12.2016

Force analysis and simulation – experimental research on the measurement of cylindrical surface profiles

Krzysztof Nozdrzykowski

Maritime University of Szczecin, Institute of Basic Technical Sciences
2–4 Willowa St., 71-650 Szczecin, Poland, e-mail: k.nozdrzykowski@am.szczecin.pl

Key words: energy converter crankshafts, measurement of geometric deviations, force analysis, practical application, simulations, experimental tests

Abstract

The results of tests presented herein can have practical applications for the adjustment of rotary speed to ensure constant contact between the measuring sensor's spindle tip and the crankshaft journal of a piston energy converter, whose roundness profile is being measured. Analytical considerations have been supported by the results of simulations as well as experimental tests. The research has also shown that an increase in rotary speed affects the obtained profile shape and the value of determined roundness deviation.

Introduction

Profiles of cylindrical surfaces are measured by either non-reference or reference methods. During such measurements, a tested object rotates and the sensor spindle makes a relative movement, or the spindle simultaneously moves axially and around the stationary object being measured. In modern measuring instruments or setups, the rotary movement of the object or sensor relative to each other takes place automatically.

To what extent the object's physical profile is reproduced depends on the distribution of forces resulting from the interaction between the measured object and the measuring sensor spindle. A loss of contact results in the zeroing of mutual forces between the measuring spindle and measured object interaction at their contact point (creating the assumption of a lack of surface deformations of the interacting elements). In practice such issues are not analyzed. It is obligatorily assumed that interaction between the spindle and measured object cannot occur. However, research shows that such a possibility does exist, especially when the measured profile is characterized by substantial irregularity and significant values of geometrical deviations (Fita, 1977; Żebrowska-Łucyk, 1997).

If we consider the mutual interaction between the sensor spindle and the measured object, we may arrive at the conclusion that their physical contact may be interrupted when:

- rotary speed is too high, which may cause the spindle to 'leap' over an irregularity, thus essential details of the profile will not be recorded;
- rotary speed is so high that the inertial mass force of the spindle will be higher than the pressure exerted on the measuring spindle.

Both of these reasons for which the spindle may lose contact with the measured object are directly linked to the rotary speed of relative motion, measuring pressure, diameter, and profile irregularity of the object (Whitehouse, 1990; 1996; Pawlus & Śmieszek, 2005; Tian et al., 2009).

Analysis of forces in the measurement system

For an analysis of forces occurring at the interaction of the measured object-sensor spindle we can use the diagram shown in Figure 1.

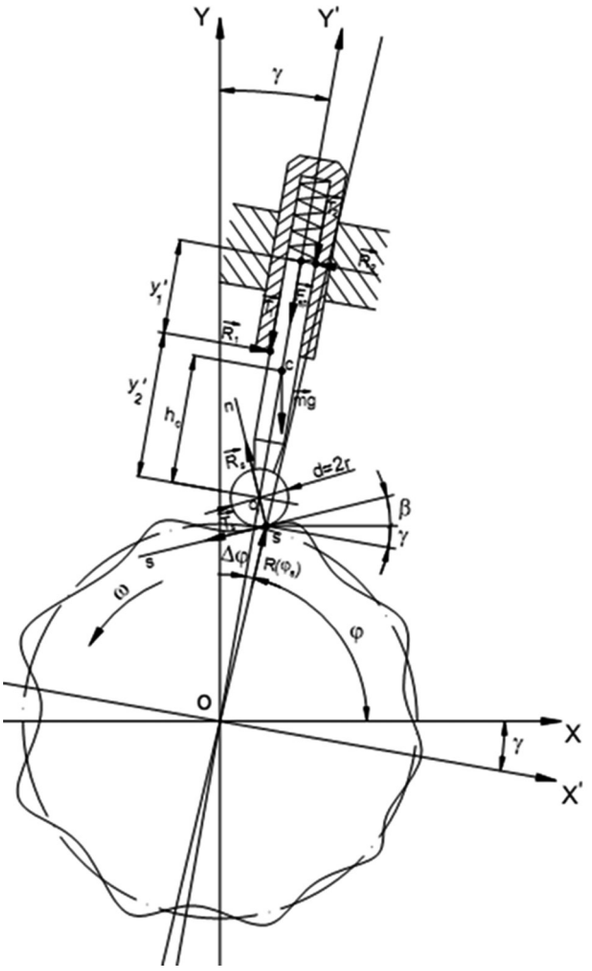

Figure 1. Distribution of forces at the measured object-spindle interaction

The diagram provides a basis for the formulation of the following relations between the forces, resulting from the kinetostatic equilibrium of the measuring tip:

$$R_1 - R_2 + mg\sin\gamma - R_s\sin(\beta+\gamma) + \\ - T_s\cos(\beta+\gamma) = 0 \tag{1}$$

$$-T_1 - T_2 - F_{sp} - mg\cos\gamma + R_s\cos(\beta+\gamma) + \\ - T_s\sin(\beta+\gamma) - ma_{O1} = 0 \tag{2}$$

$$-T_s r - mgh_c\sin\gamma - R_1 y_2' + (T_1+T_2)\frac{d_1}{2} + \\ + R_2(y_1'+y_2') = 0 \tag{3}$$

where friction forces: $T_1 = R_1\,\mu$, $T_2 = R_2\,\mu$, $T_s = R_s\,\mu$.

The condition under which the measuring tip will lose contact with the measured profile is when the normal reaction R_s is equal to zero, hence the equations describing such a state can be written as follows:

$$R_1 - R_2 + mg\sin\gamma = 0 \tag{4}$$

$$-R_1\mu - R_2\mu - k(OO_1 - OO_{10}) + \\ - mg\cos\gamma - ma_{O1} = 0 \tag{5}$$

$$R_1\left(\mu\frac{d_1}{2} - y_2'\right) + R_2\left(y_1' + y_2' - \mu\frac{d_1}{2}\right) + \\ - mgh_c\sin\gamma = 0 \tag{6}$$

After substitutions and transformations, we can determine the value of acceleration, $a_{o1,}$ of the center of the sensor's measuring tip resulting from its relative motion along the curvature of the profile:

$$a_{o1} = (\sin\gamma\,\mu - \cos\gamma) + \\ - \frac{2g\sin\gamma\,\mu}{y_1'}\cdot\left(\frac{\mu d_1}{2} - y_2' + h_c\right) - \frac{k}{m}(OO_1 - OO_{10}) \tag{7}$$

According to the commonly accepted theory of harmonic analysis of roundness profiles, any measured roundness profile $R(\varphi)$ can be written as this relation (Adamczak, Domagalski & Janecki, 1988; Adamczak, 1988; 2008; Nozdrzykowski, 2013):

$$R(\varphi) = R_o + \sum_{n=2}^{k} C_n\cdot\cos n(\varphi - \varphi_n) \tag{8}$$

where:
R_o – radius of mean circle;
C_n – amplitude of harmonic component n of the profile;
φ_n – phase shift of the harmonic component n;
φ – instantaneous angle of rotation;
n – number of harmonic component.

An instantaneous change of the sensor spindle displacement value (path of sensor displacements) depends on the measured profile, radius, r, of the measuring tip, and angle, γ, defining the direction of spindle displacements in the adopted coordinate system.

If we assume a constant value of the radius, R_o, an instantaneous change of the spindle displacement value may correspond to a change in distance, OO_1. That distance, with the relations resulting from the diagram in Figure 1, may be described by the following function:

$$OO_1 = R(\varphi)\sqrt{1 - \frac{r^2\tan^2(\beta+\gamma)}{R^2(\varphi)\left(1+\tan^2(\beta+\gamma)\right)}} + \\ + \frac{r}{\sqrt{1+\tan^2(\beta+\gamma)}} \tag{9}$$

Relation (9) determines the path of sensor spindle displacements expressed by the means of parameters

describing the measured profile, parameters of the measuring system (radius, r, and angle, γ), and an instantaneous value of angle, φ, of the measured profile presented in the polar coordinate system.

Making a double differentiation of function (9) in regards to φ and assuming that at a constant angular speed, ω, the quotient $d\omega/d\varphi = 0$, we get a relation determining the value of acceleration, a_{o1}, corresponding to the acceleration determined from the previous relation (7).

Comparing relations (7) and double differentiation (9) and assuming that $\gamma = 0$, $r = \text{const.}$, we obtain the following functional relation:

$$n_o = f(R_O, C_n, n, \varphi_n, \varphi, P_k) \tag{10}$$

Relation (10) enables us to determine a minimum rotary speed at which the contact between the sensor spindle tip and the object will be lost, depending on the object diameter and the nature of changes of the measured profile and measuring pressure $P_k = F_{sp}$.

Testing the model

Based on relation (10), an analysis was made to find out how the measured object diameter and parameters describing the measured roundness profile and acceleration, a_{o1}, affect the value of minimum rotary speed at which the spindle tip-object contact will be lost. Calculations were made for regular roundness profiles described by relation (8), for $n = (2 \div 45)$, which are the describing the harmonic profiles of the shape and $n = (60 \div 480)$ describing the profiles of waviness. The analysis involved an object with a diameter $D_o = (0 \div 300)$ mm and measuring pressure $P_k = (0 \div 0.96)$ N (measuring tip mass, $m = 4$ g). The test results are shown in charts quantitatively and qualitatively illustrating the dependence between the factors under consideration. Example charts are given in Figure 2 (a–h).

The calculations have shown that a change in diameter, D_o, does not significantly affect the minimum value of rotary speed at which the measuring tip may lose contact with the measured profile. The influence of this parameter is visible only for small diameters $D_o = (0 \div 4)$ mm. The decisive impact comes from the shape of the measured profile described by parameters C_n, n, and measuring pressure P_k.

The mean measuring pressure of inductive sensors presently used for measurements of shape deviations and profiles is $P_{ki} = 0.63$ N, which corresponds to an acceleration $a_{o1i} = 157.5$ m/s^2. The rotary speed range applied in measurements of roundness profiles should not exceed a few revolutions per minute (especially for large parameters C_n and n characterizing their profile). Inductive sensors with a movable spindle have a measuring pressure not higher than 0.5 N. In such a case, the probability of contact loss is high. The probability substantially rises for small diameters of the measured object, as illustrated in Figure 2e and f.

However, if we assume that assessment will comprise shape deviations described by harmonics in the range $n = (2 \div 45)$ and that the recommended rotary speeds should not exceed 6 rev/min in this case, then maintaining an average measuring pressure $P_k = (0.5 \div 0.65)$ N will have solid grounds to expect that the measuring tip will not lose contact with the measured profile surface.

Such a conclusion is based on the results of the model simulations of force distribution at the point of contact between the spindle tip and the measured object. The simulations were executed using the Working Model 2005 program for modelling the actual roundness profile of the measured object. The profile was obtained by measuring the roundness profiles of main journals of a crankshaft whose extreme journals were set in V-blocks. Recorded analogue signals were discretized into digital signals, allowing the data to be presented mathematically and graphically as charts in either polar or Cartesian coordinate systems. The graphical representation of the profile provided a basis for analysis of the forces acting at the contact of the measuring tip and the measured profile using the aforementioned Working Model 2005 program. In simulation tests, the varied parameters included the profile's rotary speed, measuring tip pressure and parameters of the measuring system. For the examined profile described by $n = 50$ harmonics and a roundness deviation of 48.9 μm, with the actual proportions of the measuring system parameters maintained, the standard measuring tip pressure, and the rotary speed ranging from 0 to 8 rev/min, the forces at the measuring tip-measured profile contact point were found not to compensate each other to zero.

The analytical-simulation tests were followed by experiments. These included measurements of shaft external surface profiles with repeated irregularities. A specimen specifically prepared for this purpose was a shaft section with a 300 mm diameter whose external central part had a series of grooves made at regular intervals and with blunt edges. There were 360 grooves of 150 μm deep symmetrically distributed on the shaft circumference. Cross-sections were measured on the shaft while its external

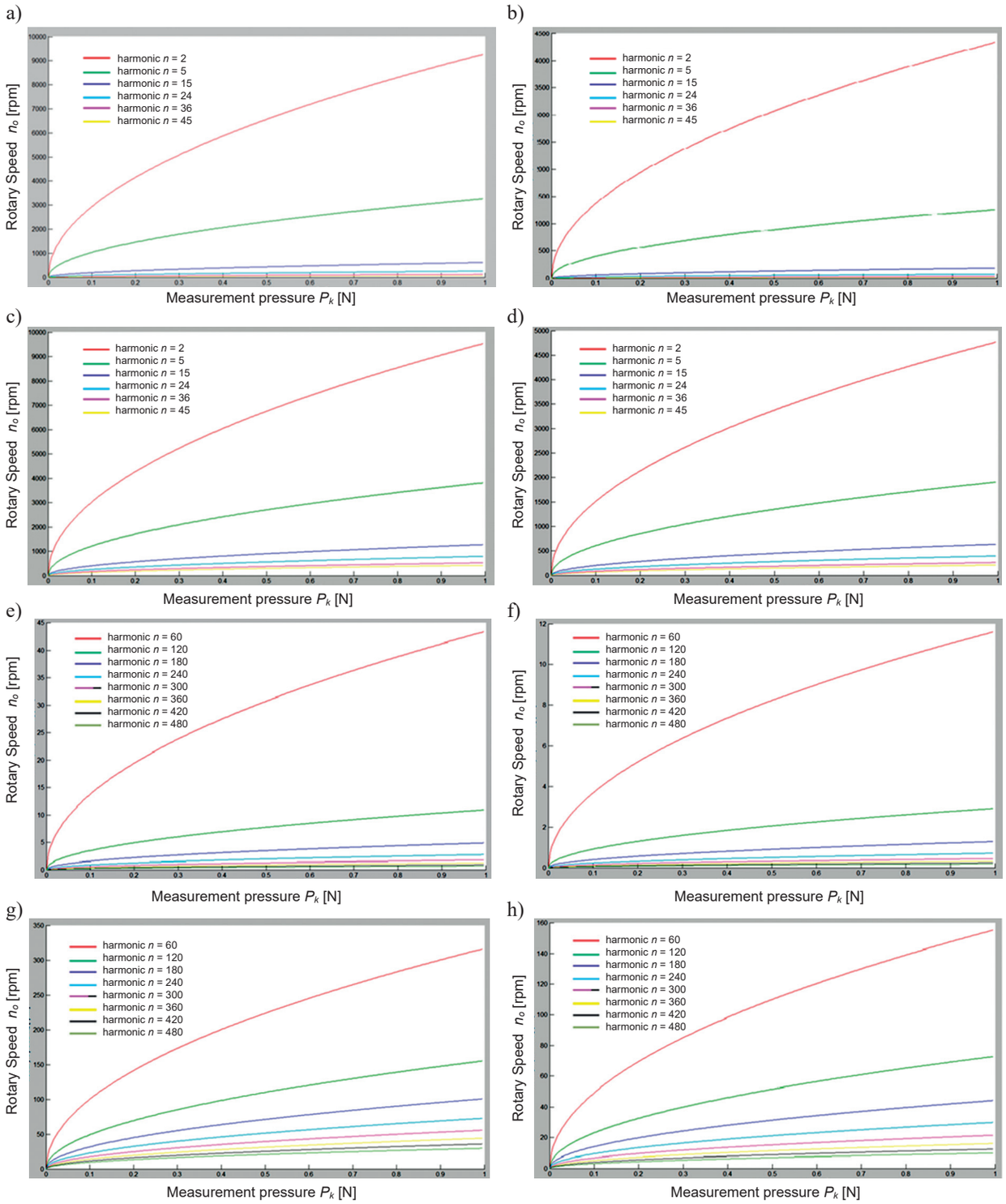

Figure 2. Graphic interpretation of relation $n_o = f(P_k)$ for: a) C_n = 50 µm, R_o = 2 mm, n = ⟨2÷45⟩, b) C_n = 200 µm, R_o = 2 mm, n = ⟨2÷45⟩, c) C_n = 50 µm, R_o = 150 mm, n = ⟨2÷45⟩, d) C_n = 200 µm, R_o = 150 mm, n = ⟨2÷45⟩, e) C_n = 50 µm, R_o = 2 mm, n = ⟨60÷480⟩, f) C_n = 200 µm, R_o = 2 mm, n = ⟨60÷480⟩, g) C_n = 50 µm, R_o = 150 mm, n = ⟨60÷480⟩, h) C_n = 200 µm, R_o = 150 mm, n = ⟨60÷480⟩

end surfaces were mounted in center points. The measurements were made by changing the rotary speed of the shaft and the pressure of the measuring tip. During these measurements, the shaft speed was varied smoothly, while the measuring spindle axis ran horizontally. In this way, the weight of the spindle did not affect changes of the measuring tip pressure.

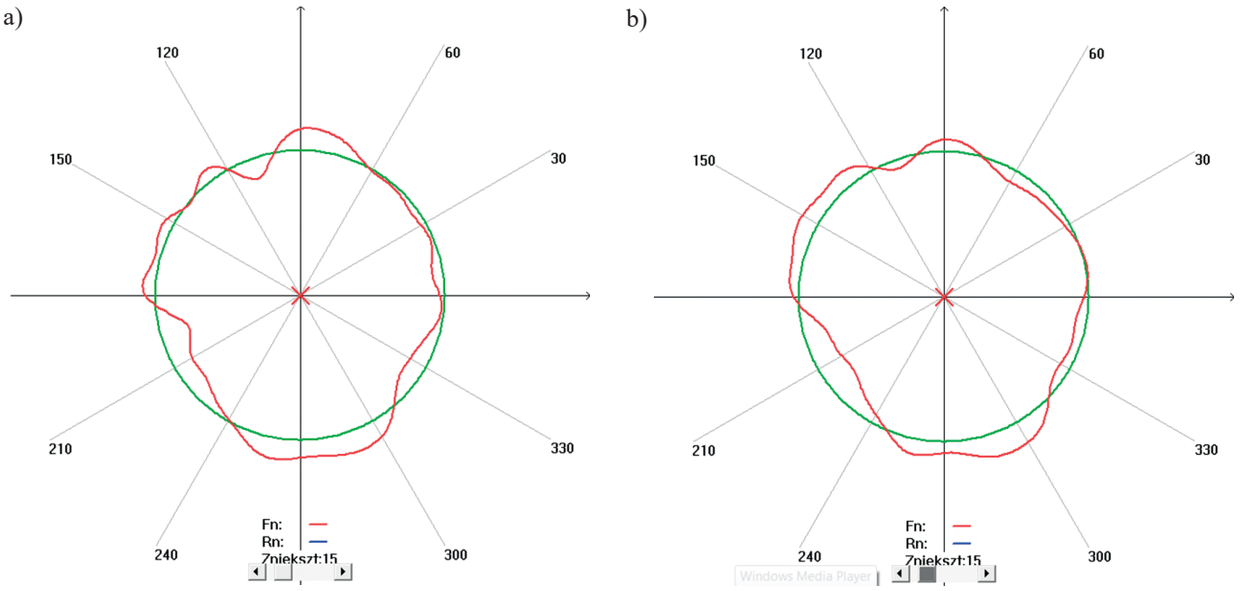

Figure 3. a) Measured roundness profiles for measuring pressure 0.5 N and rotary speed 6 rev/min, and b) measuring pressure 0.5 N and rotary speed 12 rev/min

The assessment was made by comparing specimen profile measurements obtained for various rotary speeds. The results confirmed previous observations that there is no risk of losing contact between the measuring tip and the measured profile at low rotary speeds. However, an increase in the rotary speed at a minimum tip pressure leads to a gradual rise in the amplitudes of spindle displacements, yielding essential changes in the shape of the measured profile. A similar conclusion can be drawn from results of measurements of actually irregular roundness profiles encountered in practice. In this case the measured item was a set of marine engine crankshaft journals. Example measurement results of roundness profiles of journal No. 3 obtained for varied rotary speeds and constant measuring tip pressure 0.5 N are shown in Figure 3a and b. The measured profile was characterized by significant irregularities, and as a result, at n_o = 12 rev/min essential changes were observed in the shape of the profile and there was a consequent increase in the roundness of deviation.

Conclusions

The presented test results indicate that in measurements of cylindrical surface roundness profiles and deviations the rotary speed of the measured object should not exceed 10 rev/min. This conclusion is based on theoretical considerations, simulation tests and experiments. The results of these tests have also shown that an increase in rotary speed directly affects the shape of the obtained profile and the determined value of roundness deviation. Whether contact will be lost between the measuring tip and the object depends largely on the actual shape and character of irregularities of the measured profile. Therefore, the rotary speed should be adjusted to the roundness profile being measured, and such adjustment may be based on analytical relations between the object rotary speed and parameters describing the shape of the measured profile.

References

1. Adamczak, S. (1988) *Odniesieniowe metody pomiaru zarysów okrągłości części maszyn*. Monografie, Studia, Rozprawy. Kielce: Politechnika Świętokrzyska.
2. Adamczak, S. (2008) *Pomiary geometryczne powierzchni zarysy kształtu falistości i chropowatości*. Warszawa: Wydawnictwa Naukowo-Techniczne.
3. Adamczak, S., Domagalski, R. & Janecki, D. (1988) *Experimental research into the significance of determination of harmonic roundness profiles and surface waviness*. 9th DAAAM International Symposium, Technical University Cluj-Napoco, Romania.
4. Fita, S. (1977) *Analiza błędów metod pomiaru kształtu przedmiotu o przekroju kołowym*. Rozprawa doktorska. Politechnika Wrocławska.
5. Nozdrzykowski, K. (2013) *Metodyka pomiarów geometrycznych odchyłek powierzchni walcowych wielkogabarytowych elementów maszyn na przykładzie wałów korbowych silników okrętowych*. Szczecin: Wydawnictwo Naukowe Akademii Morskiej w Szczecinie.
6. Pawlus, P. & Śmieszek, M. (2005) The influence of stylus flight on change of surface topography parameters. *Precision Engineering* 29. pp. 272–280.

7. Tian, Y., Liu, X., Zhang, D.G. & Chetwynd, D.G. (2009) Dynamic modeling of the fidelity random surface measurement by the stylus method. *Wear* 266, 5–6. March.
8. Whitehouse, D.J. (1990) Dynamic aspects of scanning surface instruments and microscopes. *Nanotechnology* 1. pp. 93–102.
9. Whitehouse, D.J. (1996) Enhancement of instrument and machine capabilities. *Nanotechnology* 7. pp. 45–51.
10. Żebrowska-Łucyk, S. (1997) *Wpływ nacisku pomiarowego czujników okrągłościomierzy na dokładność odwzorowania kształtu zarysów*. VII Konferencja Naukowo-Techniczna – Metrologia w Technikach Wytwarzania Maszyn, Kielce 97, Zeszyty Naukowe Politechniki Świętokrzyskiej w Kielcach tom II, Kielce.

Scientific Journals
of the Maritime University of Szczecin

Zeszyty Naukowe
Akademii Morskiej w Szczecinie

2016, 48 (120), 43–50
ISSN 1733-8670 (Printed)
ISSN 2392-0378 (Online)
DOI: 10.17402/174

Received: 29.04.2016
Accepted: 15.11.2016
Published: 15.12.2016

Ship service speeds and sea margins

Tadeusz Szelangiewicz, Katarzyna Żelazny

Maritime University of Szczecin, Faculty of Navigation
1–2 Wały Chrobrego St., 70-500 Szczecin, Poland
e-mail: {tadeusz.szelangiewicz; k.zelazny}@am.szczecin.pl
corresponding author

Key words: design of transport vessels, contractual and service speed, sea margin, seasonal weather conditions, design parameters, decision-making

Abstract

When designing a transport vessel, one of the most important parameters assumed by the owner is the service speed of the ship. Service speed and motor power are calculated as an approximation of the ship's speed in calm water (i.e., the contract speed) with the addition of the sea margin (SM). In current design practice, the addition of SM is not dependent on weather parameters occurring in liner shipping. This paper proposes a new method for establishing the value of SM depending on the type and size of the vessel and the average statistical weather parameters occurring on various shipping lines. The results presented in this paper clearly demonstrate that further research is needed to determine the precise relationship between the shipping and vessel type and the weather parameters on a shipping line.

Preliminary design of the ship

Designing vessels is reduced in the first instance to determining the basic dimensions (length, beam, draft, side depth), displacement, and block coefficient, and on the basis of fixed dimensions, the theoretical lines of the ship's hull. Then the propulsion power, the volume and surface of the hull, stability, freeboard, damage stability, sea keeping, range and autonomy, and the cost of the ship's construction are determined. All subsequent parameters of the designed ship and its properties depend on the main dimensions, which are determined in the preliminary design phase. The design process is performed iteratively, and thus it is divided into respective stages. Of the all of the design stages, the preliminary design phase (which includes analysis of the assumptions of the owner, development of the basic dimensions of the main development of the concept and preliminary design) is the most important initial stage, because at this stage (Figure 1), the designer has the greatest possible freedom in decision-making. However, at this point, knowledge of the planned ship is the least complete, and although it is the lowest cost phase to implement, errors generated at this stage have the greatest consequences.

Therefore, in order to, on the one hand, reduce the number of iterations leading to the optimal solution, and on the other, reduce the possibility of errors in the operating project, mathematical models have been developed that are functions of certain properties or parameters of the designed ship dependent only on these basic dimensions and, most recently, on the environmental conditions in which the designed ship will be operated.

During design, the designer seeks an optimal solution to meet the assumptions (requirements) of the owner, which are mainly concerned with the operating speed and load capacity of the ship and meeting technical criteria (contained in certain regulations) such as buoyancy, stability, and subdivision.

One of the major tasks carried out at the preliminary design stage is determining the propulsion power for the assumed service speed at which the ship will be sailed by the owner. Propulsion power, in addition to the predetermined speed, has a crucial

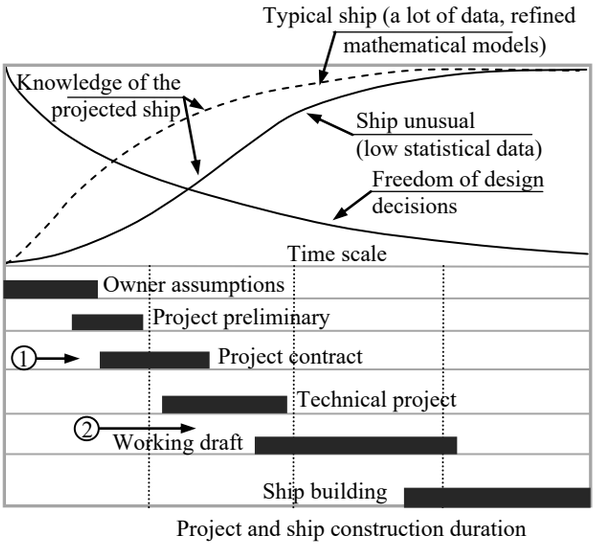

Figure 1. The importance of the next stages of the design for knowledge of the planned ship [own study based on (Chądzyński, 2001)]; ① – at this stage dimensions of the vessel and the propulsion for the established service speed should be defined, ② – in the current design process, ship resistance and propulsion power are determined after signing the contract, based on model tests of these studies and the attached sea margin (SM) is calculated service speed

impact on the shape of the ship's hull and the parameters of its propeller – the geometry of the ship's hull and propeller also impact the overall efficiency, which should be maximized.

The aim of the design process is therefore to choose the design parameters (e.g., the basic dimensions of the main ship) to achieve the desired result, which is a ship project guaranteed to achieve the assumed speed at the assumed capacity with the least propulsion power and the lowest ship construction costs. The owner can then expect to profitably operate the designed ship.

The solution thus defined the design task using mathematical models containing compounds between the geometry of the hull and the propeller and service speed, power propulsion and weather conditions occurring on the shipping line on which is the ship is operated.

The speed and power propulsion in the process of ship design

When designing a vessel to be used for maritime transport, another important consideration is that the ship owner expects to profit from its operation. Thus in addition to technical criteria, the design process includes additional economic criteria (Stopford, 2003). In order to determine whether the vessel will meet the expectations of the owner, economic measures in particular serve to assess the design excellence of the ship. The most commonly used evaluation measures are

- efficiency of transport (Gabrielli & Karman, 1950; Yong et al., 2005; Harries, Heimann & Hochkirch, 2006);
- the design energy efficiency index (EEDI) IMO (in force since 01.01.2013) (GHG-WG, 2009; MEPC.1/Circ.681, 2009; Ozaki et al., 2010);
- economic indicators (Abramowski, 2011).

In all these assessment measures, design excellence is judged by the ship's speed and drive power. This means that the speed of the ship, assumed by the ship's owner as a result of the propulsion power, is one of the most important design parameters. The ship's speed and propulsion power affect fuel (which has an impact on the operating costs of the ship and the owner's profits), emissions (including CO_2 and NO_x), cruise time, and – taking into account the vessel's safety – the shipping route. The ship speed is so important that it is specified in the ship's construction contract. If the ship is operated in calm water with no waves or wind, developing a mathematical model to calculate the speed and propulsion power as a function of the basic geometric parameters of the ship's hull does not constitute a problem. However, if the ship is operating on various shipping lines, which are variable, random parameters characterize the effects of waves and wind. Hence, developing a model of the service speed (and propulsion power) that the ship can attain in real weather conditions is a serious problem.

In current design practice, during the preliminary design phase, propulsion power is determined for the design speed in calm water using very rough dependence (this is equivalent to contract speed) (Figure 1). Only after the project contract has been established and signed (Figure 1) are basin model tests of resistance and propulsion power conducted in calm water (curve 1 in Figure 2). Then, taking into account the sea margin (SM) (standard 10–15%), the nominal engine power N_n and for the projected service speed V_E (Figure 2) is calculated. The SM value does not allow either the precise actual service speed in real weather conditions occurring in the shipping line or determine the propulsion power to guarantee that the assumed service speed will be achieved.

The method of estimating service speed based on ship basin model tests of resistance and drive power shown in Figure 2, is widely used for transport vessels, even though the actual operation of ships that

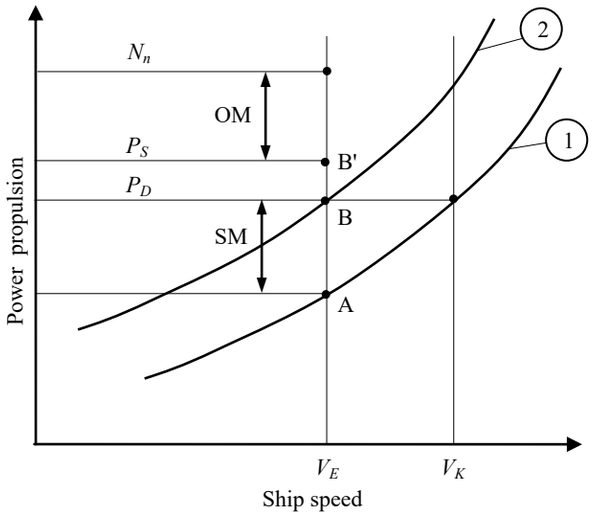

Figure 2. Determination of propulsion power and ship service speed V_E based on model tests of resistance and sea margin (SM). Explanations: N_n – nominal engine power, P_S – power to the shaft line (point B'), P_D – power delivered to the propeller, OM – assumed power reserve (standard 10%), SM – the sea margin (standard 10–15%), B'B – losses resulting from the performance shafting, B – design operating point of the propeller, A – the operating point of the propeller on the calm water, clean hull, V_K – speed contract, V_E – projected service speed, ① – the characteristics of the power propulsion in calm water, clean hull, ② – the characteristics of the power propulsion with the sea margin

reached service speed on different shipping lines does not correspond to the service speed presumed by the ship owner (Figure 3). This means additional shipping taken on some shipping lines is too small and others may be too large (Żelazny, 2005), which means that the power of the drive is either too strong or too weak.

To improve the accuracy of determining ship service speed, the method shown in Figure 2 shows the value SM is dependent on the shipping line, on which there are certain statistical averages weather conditions (i.e., seasonal parameters).

The sea margin for shipping lines

The sea margin it is defined as

$$\mathrm{SM} = 1 - \frac{R_{TS\mathrm{serv.}}}{R_{TS\mathrm{trials}}} = \frac{\Delta R}{R_{TS\mathrm{trials}}} \tag{1}$$

where:

SM – the sea margin (SM < 1);

$R_{TS\mathrm{trials}}$ – the total resistance of the vessel during tests in calm water;

$R_{TS\mathrm{serv.}}$ – the total resistance of the vessel operating in actual weather conditions.

Therefore, in order to determine what the SM should be, we must know the total resistance of the vessel when it is travelling on a given shipping route, for which there are statistical averages available for (seasonal) weather conditions.

The ship can sail on different shipping lines that run through various reservoirs. In these areas there are weather events, mainly wind and waves (Figure 4), for which numerical values of the parameters of waves and wind occur with varying probability. Waves and wind are also likely to vary depending on the season. Therefore, the total resistance of the vessel will be a random statistical average value of the assumed probability of exceeding.

The total resistance of the ship in real weather conditions is equal to

$$R_{TS\mathrm{serv.}} = R_{TS\mathrm{trials}} + \Delta R \tag{2}$$

where

$R_{TS\mathrm{trials}}$ – resistance of a ship in calm water;

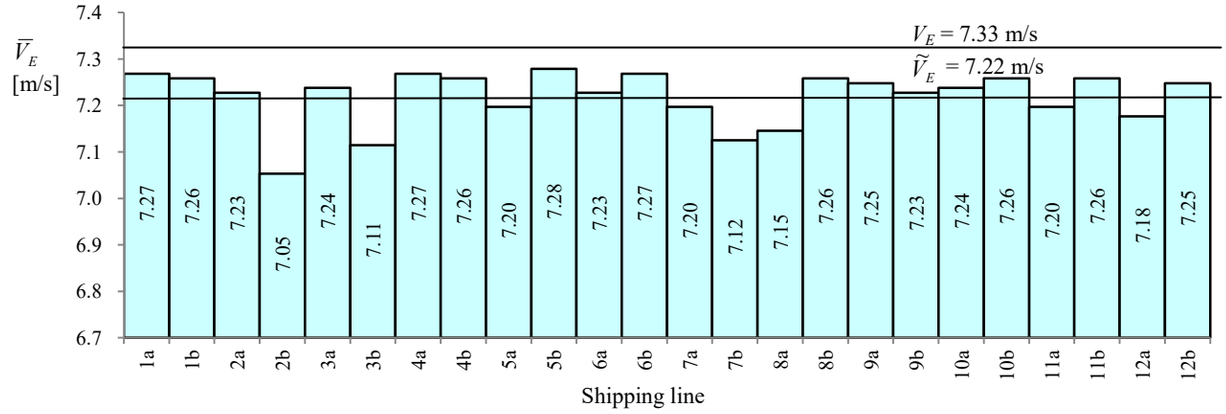

Figure 3. Average long-term service speed $\overline{V_E}$ calculated by (Żelazny, 2005) in liner shipping for bulk carrier M1, VE = 7.33 m/s – assumed by the ship owner service speed for the sea margin SM = 10% ($\widetilde{V_E}$ – average service speed for all routes)

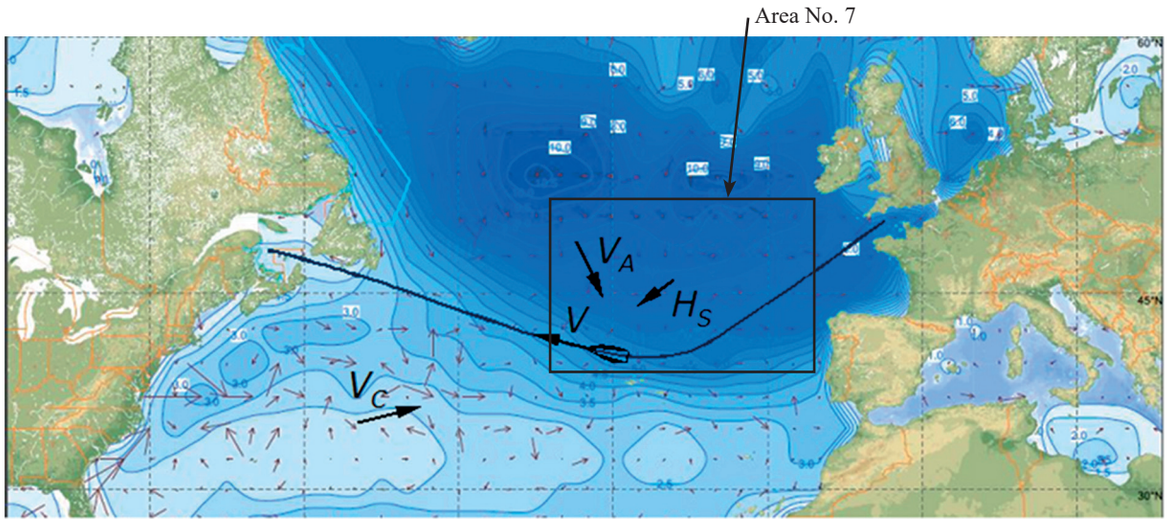

Figure 4. Example of shipping route and directions of impact on the marine environment of the ship

Table 1. The number of wave height H_S and the period T_1 for the $\mu = 0°$ on the area 7 (Figure 4) for the whole year

H_S [m]	T_1 [s]									
	calm	< 5	6–7	8–9	10–11	12–13	14–15	16–17	18–19	20–21	> 21
0.25		70	1	1	1			1			7
0.5		217	29	7	2						13
1.0		542	225	44	18	6	3	3		2	6
1.5		276	501	143	41	8	4	1			3
2.0		61	334	229	55	18	4				
2.5		25	164	143	76	14	2	2	1		
3.0		3	87	136	61	18	4				
3.5		6	35	96	49	22	8	1	1		
4.0		2	24	41	47	17	7		1		
4.5		3	14	31	27	17	2	2			1
5.0		2	3	4	4	6	1	1			
5.5		3	2	4	8	2	1				
6.0			4	6	6	3	2				
6.5			7	3	6	6		2			
7.0			1	7	1	2					
7.5				2	1		1	2			
8.0			1	4	5	4		2			
8.5				2	1	4	1				
9.0			5	2	1		1	1			1
9.5			2	1	4	1	1				

ΔR – additional ship resistance due to the impact of wind and wave and steering devices

$$\Delta R = R_{xA} + R_{xC} + R_{xW} + R_{xR} \tag{3}$$

R_{xA} – additional resistance from the wind;
R_{xC} – additional resistance from the sea surface currents;
R_{xW} – additional resistance from the waves;
R_{xR} – additional resistance from factors such as steering gear on a given course (interference of the course is also caused by the impact of wind and waves).

Shipping lines run through waters in which the average statistical parameters of waves and wind have been measured and are these are available in weather atlases such as (Hogben, Dacunha & Olliver, 1986; Hogben & Lumb, 1967). Average statistical parameters of waves for the entire year on the waters of the lines in Table 2 are presented in Table 1. In calculating total resistance $R_{TS\text{serv.}}$ for all parameters of waves, including their likelihood of occurring on a given shipping route, a statistical mean value of the total resistance $\overline{R}_{TS\text{serv.}}$ can be calculated for the shipping line. The algorithm for

Table 2. Basic technical parameters investigated ships

Parameter	Bulk carriers				Container ships		
	M1	M2	M3	M4	K1	K2	K3
Length of the vessel L [m]	138.0	185.0	175.4	240.0	140.14	171.94	210.2
Ship breadth B [m]	23.0	25.3	32.2	32.2	22.3	25.3	32.24
Draught T [m]	8.5	10.6	12.0	11.6	8.25	9.85	10.5
Block coefficient C_B [–]	0.804	0.820	0.805	0.815	0.641	0.698	0.646
Waterplane coefficient C_{WP} [–]	0.892	0.854	0.873	0.872	0.809	0.828	0.807
Displacement ∇ [m^3]	21 441	40 831	56 396	73 910	17 290	29 900	47 250
Assumed service speed of the ship V_E [m/s]	7.33	7.72	8.20	8.28	8.44	9.62	10.50

calculating the statistical mean value of total resistance of the ship on the shipping line is presented in (Żelazny, 2005).

The results of calculations for the sea margin shipping

Calculations of average statistical sea margins (SM) of two types of vessels (bulk carriers and container ships) whose parameters are shown in Table 2 for the twelve shipping lines listed in Table 3 (appendix shipping was calculated for a cruise ship on the shipping line on one side (a) and on the return side (b)).

Table 3. List of shipping lines used to calculate the supplement shipping

No. shipping line	Name
1	South America – Western Europe
2	USA East – Western Europe
3	USA East – Gulf of Mexico – Western Europe
4	USA East – Mediterranean Sea – Western Europe
5	Indonesia – Japan
6	Persian Gulf – Japan
7	North Africa – Western Europe
8	North Africa – USA East
9	Persian Gulf – Africa – Western Europe
10	Western Europe – Mediterranean Sea – Persian Gulf – Japan
11	Western Europe – Panama Canal – USA West
12	Western Europe – Latin America

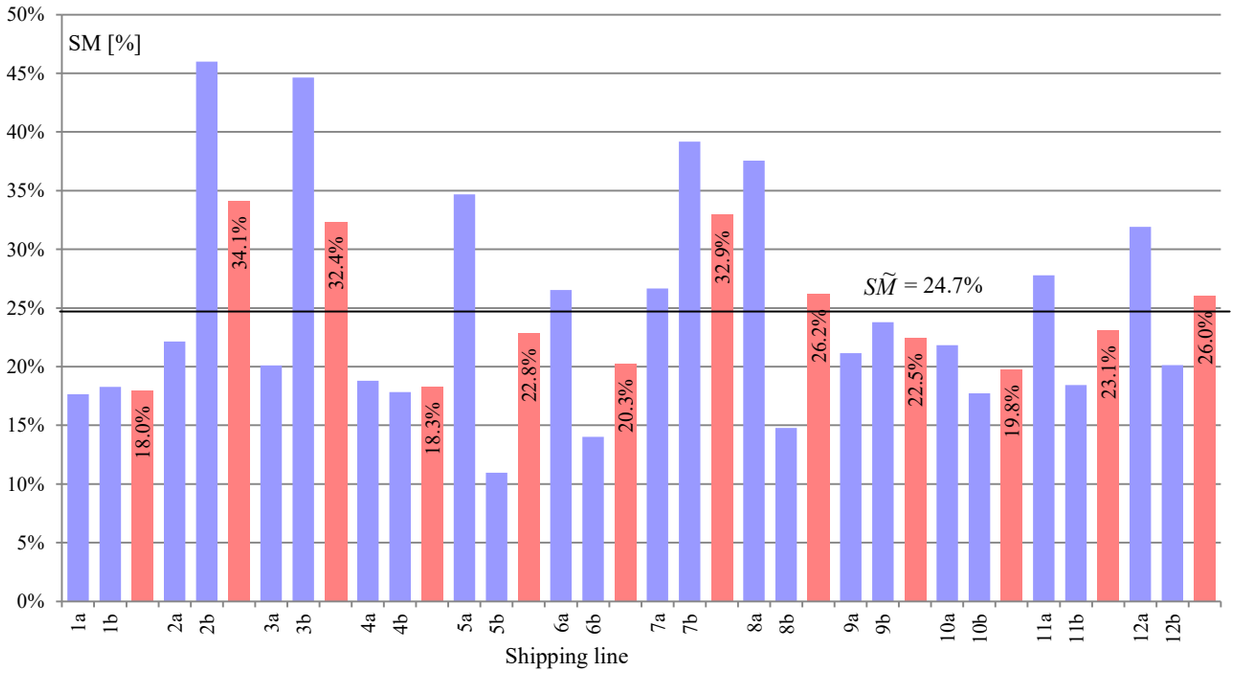

Figure 5. The calculated value of sea margin for a container K1 on different shipping lines

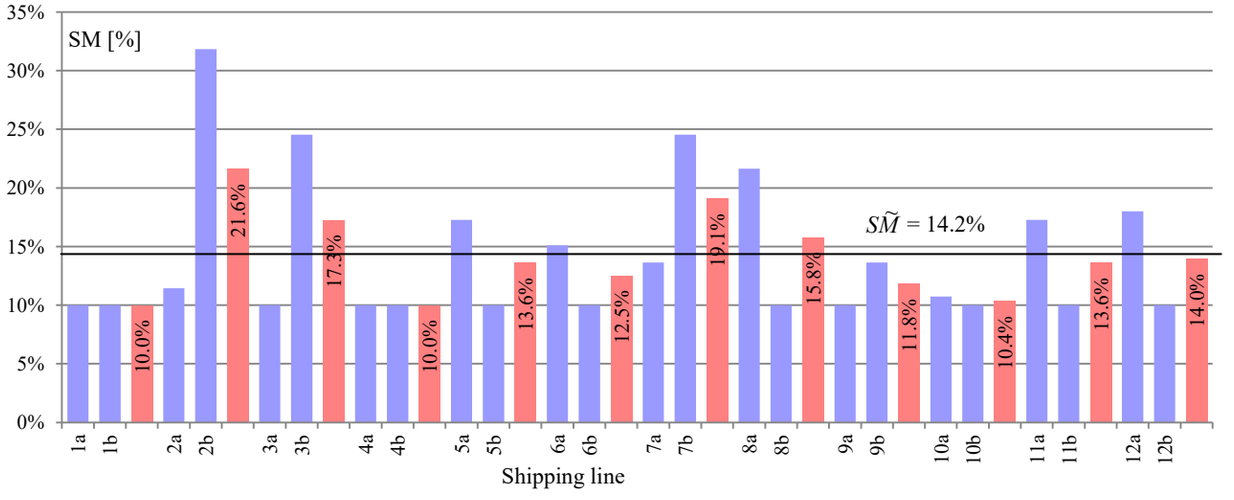

Figure 6. The calculated value of sea margin for a container K2 on different lines shipping

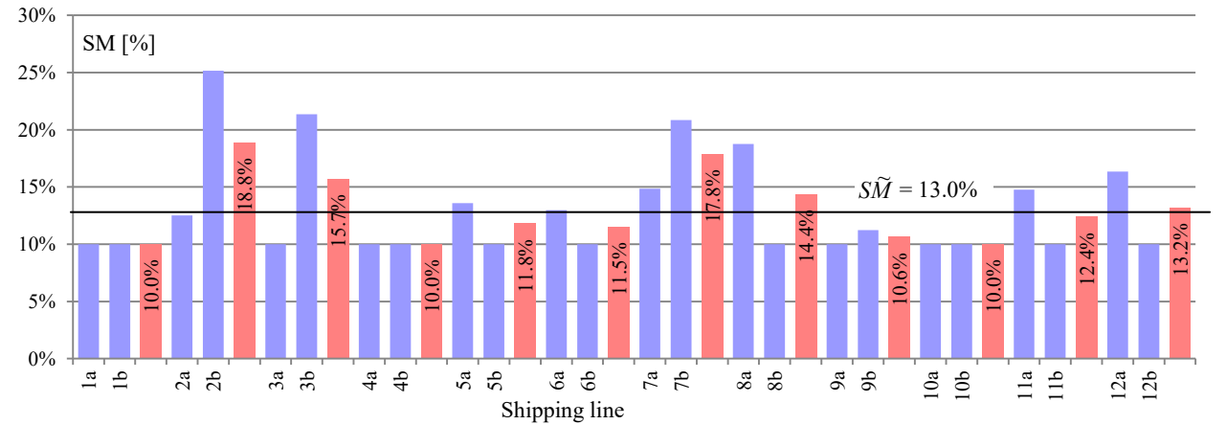

Figure 7. The calculated value of sea margin for a container K3 on different shipping lines

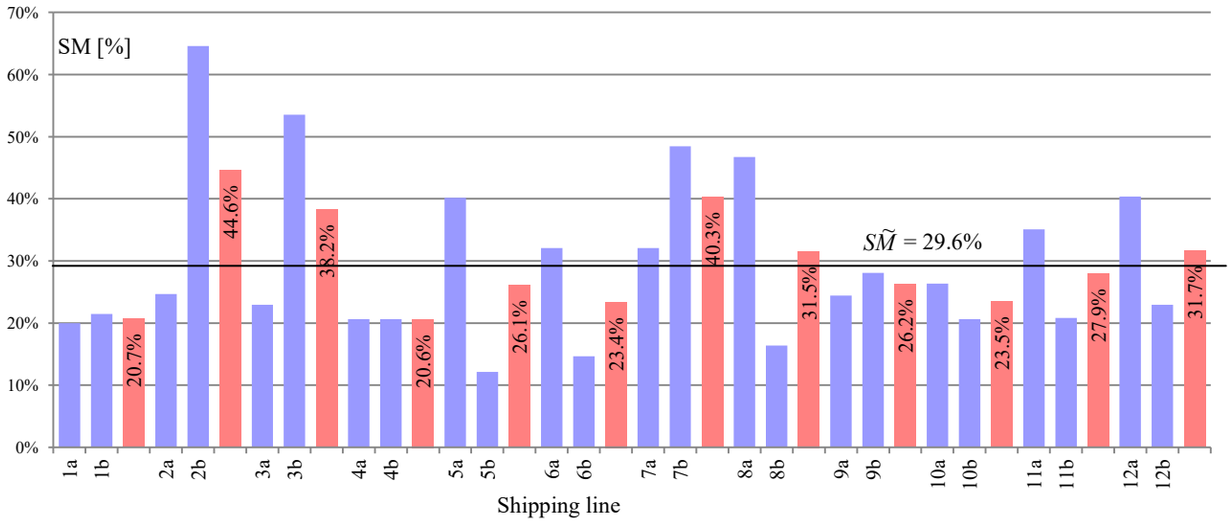

Figure 8. The calculated value of sea margin for a bulk carrier M1 on different shipping lines

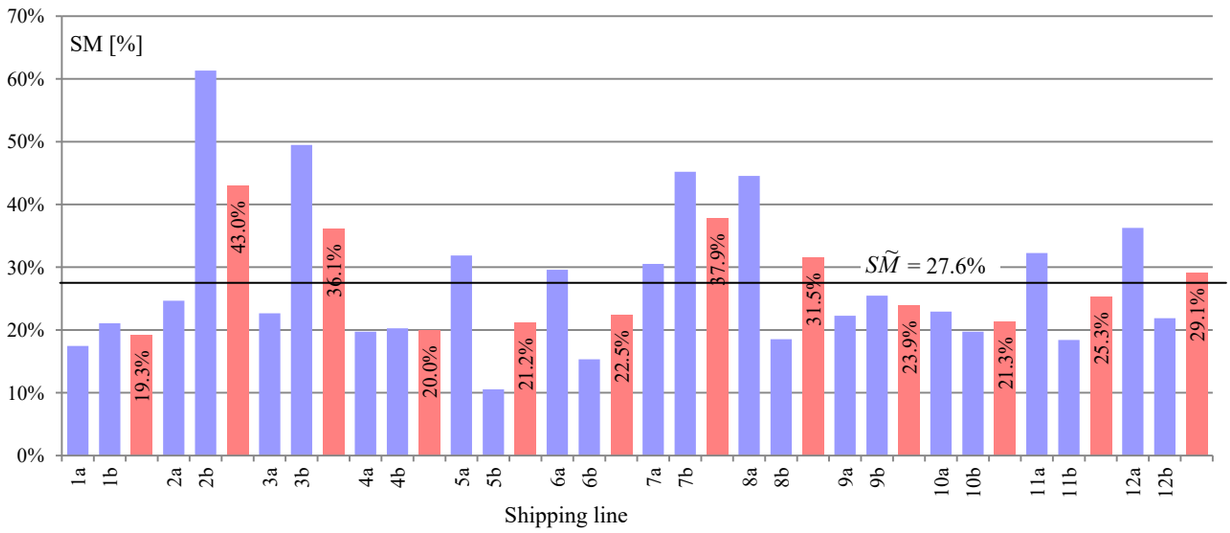

Figure 9. The calculated value sea of margin for a bulk carrier M2 on different shipping lines

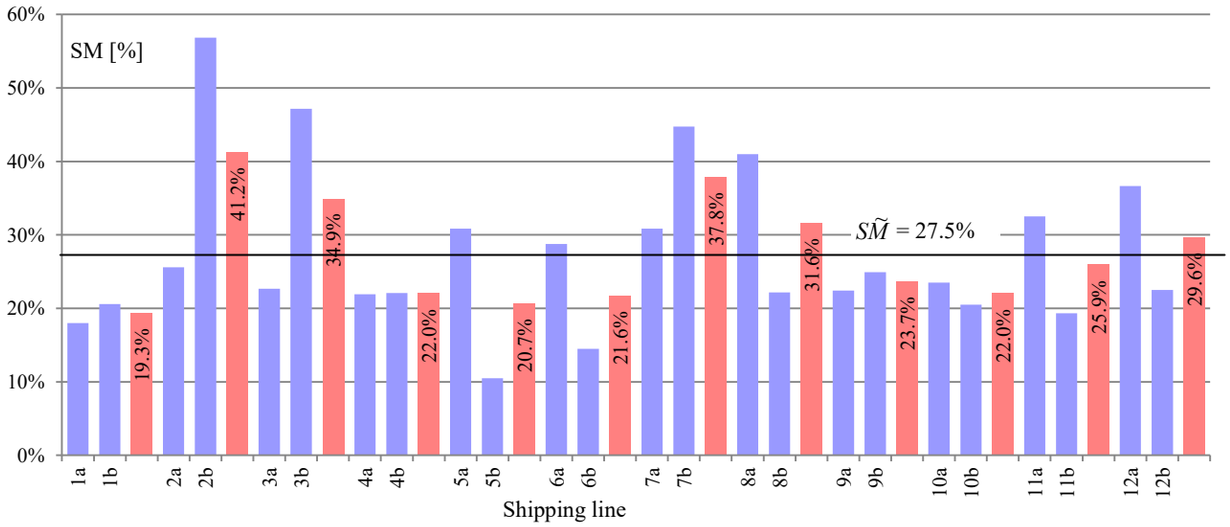

Figure 10. The calculated value of sea margin for a bulk carrier M3 on different shipping lines

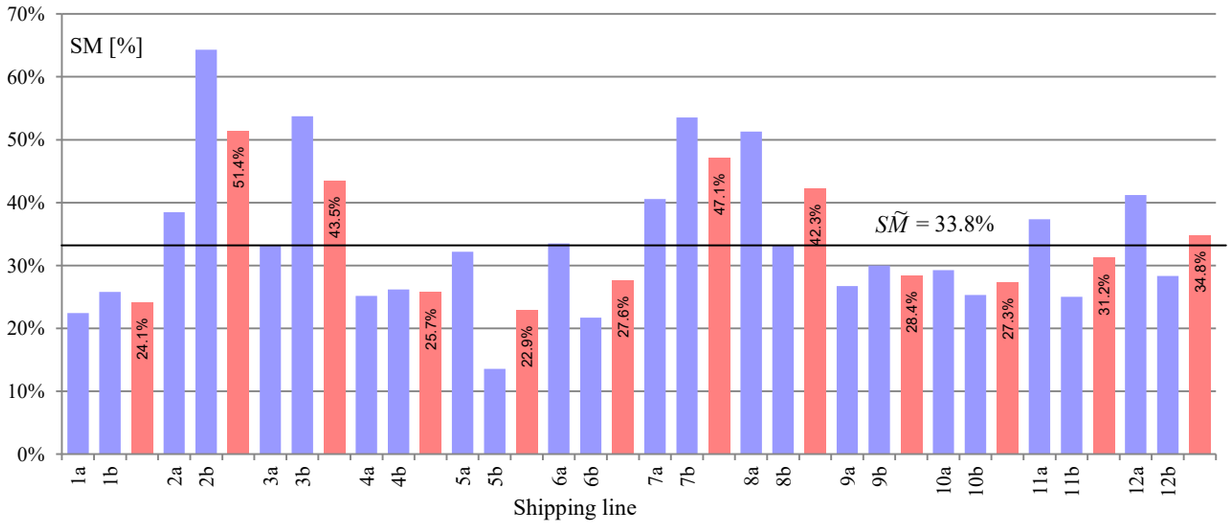

Figure 11. The calculated value of sea margin for a bulk carrier M4 on different shipping lines

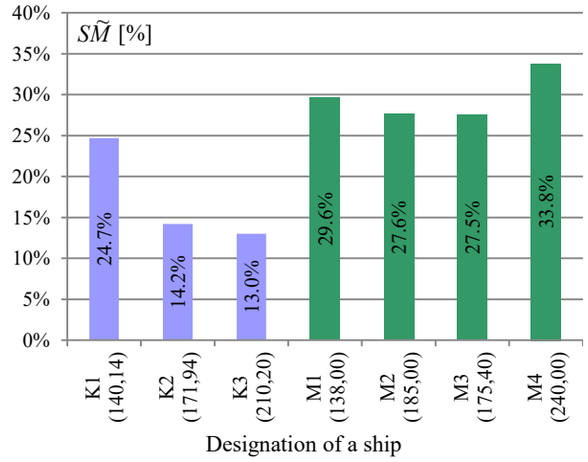

Figure 12. The average value addition shipping lines for selected ships

The calculated values for each additional shipping vessel on various shipping lines are shown in Figure 5–12 (red color – the average value of the SM for the route in both directions).

Conclusions

The sea margin (SM) for each vessel (Table 2) was calculated based on the assumption that the expected service speed would be maintained on each shipping line (Table 3) with probability $P_{VE} = 0.95$.

For the calculation of total resistance to shipping, accepted long-term statistical average parameters (i.e., annual seasonal values) for wind and waves were used (Hogben, Dacunha & Olliver, 1986).

For each vessel the calculated average sea margin was $\widetilde{SM}$ on all shipping lines. If the ship sailed on only one specific shipping line, the calculated sea margin (SM) (and propulsion power) would guarantee that the assumed service speed would be achieved with a certain probability of its maintenance.

The results presented here are preliminary, and calculating sea margins for particular types of ships and shipping lines requires further study. However, these calculations show that it was easier to maintain the assumed service speed for containers than for bulk carriers.

References

1. Abramowski, T. (2011) *Elements of multidisciplinary optimization of technical and economic indices in preliminary concurrent design of transport ships* (in Polish). Szczecin: Publishing House of West Pomeranian University of Technology in Szczecin.
2. Chądzyński, W. (2001) *Elementy współczesnej metodyki projektowania obiektów pływających*. Prace naukowe Politechniki Szczecińskiej. Szczecin: Wydawnictwo Uczelniane Politechniki Szczecińskiej.
3. GHG-WG (2009) Consideration of the energy efficiency design index for new ships, GHG-WG 2/2/7.
4. Gabrielli, G. & Karman, T.V. (1950) What Price Speed. *Mechanical Engineering* 72 (10). pp. 775–781.
5. Harries, S., Heimann, J. & Hochkirch, K. (2006) *Advanced Design of Container Carriers for Improved Transport Efficiency*. RINA Conf. Design & Operation of Container Ships, London.
6. Hogben, N., Dacunha, N.M.C. & Olliver, G.F. (1986) *Global Wave Statistics*. BMT.
7. Hogben, N. & Lumb, F.E. (1967) *Ocean Wave Statistics*. National Physical Laboratory, London.
8. MEPC.1/Circ.681 (2009) Interim Guidelines on the Method of Calculation of the Energy Efficiency Design Index for New Ship's.
9. Ozaki, Y., Larkin, J., Tikka, K. & Michel, K. (2010) *An Evaluation of the Energy Efficiency Design Index (EEDI) Baseline for Tankers, Containership and LNG Carriers*. ABS.
10. Stopford, M. (2003) *Maritime Economics*. Taylor & Francis e-Library.
11. Yong, J., Smith, R.A., Hillmansen, S. & Hatano, L. (2005) What Price Speed – Revisited. The Railway Research Group, Imperial College, Ingenia Issue 22. pp. 46–51.
12. Żelazny, K. (2005) *Numeryczne prognozowanie średniej długoterminowej prędkości eksploatacyjnej statku transportowego*. Rozprawa doktorska. Szczecin: Politechnika Szczecińska.

Scientific Journals
of the Maritime University of Szczecin

Zeszyty Naukowe
Akademii Morskiej w Szczecinie

2016, 48 (120), 51–57
ISSN 1733-8670 (Printed)
ISSN 2392-0378 (Online)
DOI: 10.17402/175

Received: 15.06.2016
Accepted: 30.08.2016
Published: 15.12.2016

Engine rooms fire safety – fire-extinguishing system requirements

Agnieszka Ubowska[1], Marcin Szczepanek[2]

[1] West Pomeranian University of Technology, Faculty of Maritime Technology and Transport
Department of Safety Engineering and Energy
71-131 Szczecin, al. Piastów 19, e-mail: agnieszka.ubowska@zut.edu.pl
[2] Maritime University of Szczecin, Mechanical Faculty
Institute of Marine Propulsion Plants Operation
1–2 Wały Chrobrego St., 70-500 Szczecin, Poland, e-mail: m.szczepanek@am.szczecin
corresponding author

Key words: fire-extinguishing systems, suppression systems, engine room, safety, pressure water spraying, requirements

Abstract
This article discusses requirements for the extinguishing systems in the engine room. The sources of fire hazards in engine rooms were characterized. The causes and consequences of selected engine room fires that occurred within the last five years were presented. The basic requirements for the fire-extinguishing systems installed in engine rooms were scrutinized. The most commonly used fire-extinguishing systems in engine rooms are the ones containing a gaseous extinguishing agent. Their main advantages are short response time after agent release and the ability to supply an extinguishing medium to areas that are hard to access. The agent used in such systems does not cause damage and there is no need to remove its residues after fighting the fire, as in the case of other agents such as foams. As an example, a CO_2 system was characterized, as it is the most frequently used in engine rooms.

Introduction

Engine rooms are particularly vulnerable to fire, due to numerous flammable materials and fire sources located in a relatively small area. The occurrence of such a situation in an engine room may disable the ship as the loss of steering ability and stability may result in contact, collision, grounding, capsizing or foundering. Therefore, fire-extinguishing systems are of paramount importance. They should be designed in a way to allow fire-extinguishing within the shortest time possible, limiting damages to a minimum. This article highlights the aspects associated with fire safety in engine rooms. It briefly describes source of fires in machinery space and exemplifies the damage that may be caused through the analysis of selected cases of fire incidents. The main part of the article reports the regulations concerning fire-extinguishing systems in engine rooms. Applicable regulations provide for fitting engine rooms with a fixed gas fire-extinguishing system, a fixed foam fire-extinguishing system, water supply systems, fixed pressure water-spraying and water-mist fire-extinguishing systems as well as placing portable fire-extinguishing appliances. The most common systems used in engine rooms are gaseous fire suppression systems. Their advantages include very short response time after agent release and the ability to supply an extinguishing medium to areas difficult to access. The agent applied in such systems does not cause damage and does not require removal of residues once the fire-fighting action is completed.

Fire in engine room

Most fires on ships start in the engine room (Figure 1).

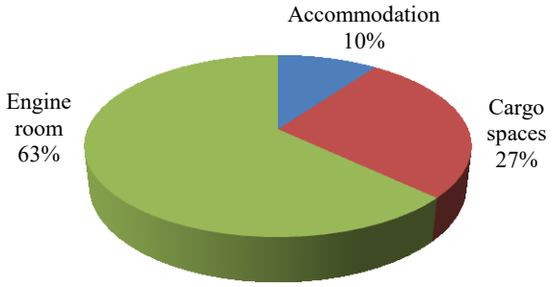

Figure 1. Causes of fire (DNV, 2010)

There are more than 130 types of machines and devices in an engine room (internal-combustion engines, flue gas turbines or steam turbines, fuel purifiers and other) that may constitute a fire hazard. Engine rooms also contain numerous tanks for fuel oil, lubricant oils, diesel, grease and chemicals, since a medium-sized ship uses approximately 40 tons of fuel per day. In addition, the heating temperature of marine residual fuels is high, in the range of 120–150°C. The combination of these fire hazards with heat sources, such as hot surfaces (e.g. exhaust systems), and potential sparking from faulty electrical systems enhances the probability of occurrence of fire. The share of individual sources of fire in the engine room is shown in Figure 2.

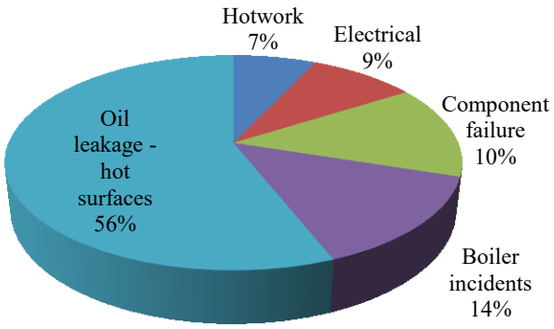

Figure 2. Sources of fire (DNV, 2010)

The most probable fire scenario involving machinery is the contact of leakage oil with a hot surface. Although it is to completely avoid oil leakage in such a particular space, methods to reduce leaks exist and include double piping on high-pressure fuel lines, and valves in fuel oil supply lines fitted with remote controls and operated from a location outside the engine room. To avoid hot surfaces, SOLAS requires maximum surface temperatures to be below 220°C (SOLAS, 2009).

The fire in the engine room may disable the ship, which may lose steering ability and stability, and consequently risk capsizing, foundering or throwing ashore. A fire occurring in the engine room is also hazardous for the adjacent spaces. Fire protection for the location is a difficult task due to the complicated construction of engine room (Kukuła, Getka & Żyłkowski, 1981). Therefore, it is extremely important to select proper fire-extinguishing systems as a means of fire protection. The effectiveness of a system determines damages and losses in the "ship's heart" during the fire.

The examples of occurrences of fires starting in the engine room of ships are presented below:

- On 11th February, 2015 an explosion took place aboard the FPSO *Cidade de São Mateus* due to a gas leak in one of the engine compartments: at least 5 deaths were reported;
- On 25th January, 2015 a fire broke out in the engine room of the luxury cruise ship m/v *Bouddica*; all engines stopped, due to the loss of power and the ship lost steering ability and started to drift;
- On 12th February, 2015 the engine room of the chemical tanker *Amaranth*, docked in Szczecin, burst into flames; the cause of ignition was oil leaking from a broken pipe which eventually flooded the engine collector;
- On 14th June, 2014 there was a fire abroad the LNGRV *Explorer*; the fire was extinguished using portable extinguishing equipment, but the vessel required towing;
- On May 20th, 2013 the fishing vessel *Arctic Storm* experienced an engine room fire; the cause of the fire was damage to the diesel vent valve, located by the main engine, which resulted in diesel spraying on the hot engine surface; the losses were estimated at $ 5mln;
- On March 10th, 2010 the fire spread all over the engine room of the trawler *American Dynasty* (Figure 3); it was suppressed after three hours.

Figure 3. Part of an engine room after a fire (U.S. Coast Guard Newsroom, 2015)

Fire protection requirements

Regulations referring to the fire protection of engine compartments have been included in the International Convention for the Safety of Life at Sea (SOLAS) of 1974. The last consolidated edition of the Convention was issued in 2014 (IMO, 2014). The requirements regarding the fire-extinguishing systems are included in Part C: Suppression of fire, Regulation 10.5 Fire-extinguishing installations in machinery spaces, SOLAS 1974 II-2/10.5.

The provisions concerning fire-extinguishing systems and fire-extinguishing appliances that are on board (to which the Convention provisions refer to) have been incorporated into the International Code for Fire Safety Systems (FSS Code) developed by IMO.

Training

When the fire occurs at sea, initial fire-fighting task will have to be met by the crew. Adequate training for the situation is therefore important. The International Convention on Standards of Training, Certification and Watchkeeping for Seafarers was adopted on 7 July 1978 in London (STCW, 2010). It specifies minimum standards relating to theoretical and practical knowledge and skills and required certification and licenses to perform duties at particular positions. One of such certificates is the "Certificate of Basic Safety Training in Personal Survival Techniques" under Regulation VI/1 of the STCWW Convention (basic level) and the "Certificate of Training in Advanced Fire Fighting" under Regulation VI/3 of the STCW Convention. During the training, participants acquire knowledge on fire protection issues.

Fire-extinguishing systems in engine rooms

Machine compartments require special fire protection. The spaces are subject to high risk of fire due to heat generated by devices and highly flammable liquids. Minor faults or leaks in engine rooms may cause severe fire, as proven by the above-mentioned examples. In order to adjust to the size and power of engines, engine rooms are also becoming larger. Consequently, their protection has become a more difficult task and the time to evacuate crew has extended. All these aspects highlight the importance of fire-extinguishing. Their effective performance affects the crew safety and determines the value of material damage and loss. A proper selection, installation and operation of fire-extinguishing system may significantly limit and minimize the damage.

Machinery spaces, in which oil-fired boilers or oil-fuel units are placed, should be equipped with one of the following fixed fire-extinguishing systems:

- a fixed gas fire-extinguishing system, complying with the provisions of the Fire Safety Systems Code;
- a fixed foam fire-extinguishing system, complying with the provisions of the Fire Safety Systems Code;
- a fixed pressure water-spraying fire-extinguishing system, complying with the provisions of the Fire Safety Systems Code; and
- fixed aerosol fire-extinguishing systems equivalent to fixed gas fire-extinguishing systems required by SOLAS (IMO, 2001a).

If the engine and boiler rooms are not entirely separate, or if fuel oil can drain from the boiler room into the engine room, the combined engine and boiler rooms shall be considered as one compartment. Additionally, there shall be in each boiler room, or at an entrance outside of the boiler room, at least one portable foam applicator unit complying with the provisions of the Fire Safety Systems Code. There shall be at least two portable foam extinguishers or equivalent in each firing space, in each boiler room, and in each space in which a part of the oil fuel installation is situated. There shall be no less than one approved foam-type extinguisher of at least 135 l capacity, or equivalent, in each boiler room. These extinguishers shall be provided with hoses on reels, suitable for reaching any part of the boiler room. In the case of domestic boilers of less than 175 kW, an approved foam-type extinguisher of at least 135 l capacity is not required. In each firing space or boiler room there shall be a receptacle containing at least 0.1 m^3 of sand, sawdust impregnated with soda, or other approved dry material, along with a suitable shovel for spreading the material. An approved portable extinguisher may be substituted as an alternative (SOLAS, 2009).

Machinery spaces containing internal combustion engines, oil-fired boilers, or oil-fuel units shall be provided with one of the fixed fire-extinguishing systems. Moreover, there shall be at least one portable foam applicator unit complying with the provisions of the Fire Safety Systems Code. Each one of these spaces shall be equipped with approved foam-type fire-extinguishers (mobile) having at least a 45 l capacity or equivalent each and sufficient in number to enable foam or its equivalent to be directed

to any part of the fuel and lubricating oil pressure systems, gearing and other fire hazards. In addition, a sufficient number of portable foam extinguishers or equivalent shall be provided in locations such that the maximum walking distance from any point in the room to the extinguisher is 10 m. In any case, at least two extinguishers must be present in each one of these rooms (SOLAS, 2009).

In machinery spaces containing steam turbines or enclosed steam engines, one of the fire-extinguishing systems specified above shall be provided. Additionally, there shall be approved foam fire-extinguishers (mobile), each of at least 45 l capacity or equivalent, sufficient in number to enable foam or its equivalent to be directed to any part of the pressure lubrication system, on to any part of the casings enclosing pressure lubricated parts of the turbines, engines or associated gearing, and any other fire hazards. Such extinguishers are not required if protection is provided by a fixed fire-extinguishing system. There shall be a sufficient number of portable foam extinguishers or equivalent, which shall be so located that no point in the space is at a walking distance of more than 10 m from an extinguisher. In any case, at least two extinguishers must be present in each one of these rooms (SOLAS, 2009).

Additional requirements have been adopted for engine rooms on passenger ships. In the case of passenger ships carrying more than 36 passengers, each machinery space of category A shall be provided with at least two suitable water fog applicators (a water fog applicator shall consist in an L-shape metal pipe, with the longer section having a length of 2 m, that may be connected to a fire hose, and with a shorter section, 250 mm long, fitted with fixed fog nozzle or other device appropriate for the connection to a water spray nozzle).

The following requirements refer to the fixed fire-extinguishing systems for passenger ships of 500 gross tonnage and above and cargo ships of 2000 gross tonnage and above. In these ships, machinery spaces above 500 m^3 in volume shall be additionally protected by an approved type of fixed water-based, or equivalent, local application fire-fighting system, based on the guidelines developed by the Organization (IMO, 1999; 2003). In the case of periodically unattended machinery spaces, the fire-fighting system shall have both automatic and manual release capabilities. In the case of continuously manned machinery spaces, the fire-fighting system is only required to have a manual release capability. Fixed local application fire-extinguishing systems are to protect areas such as the following without the necessity of engine shutdown, personnel evacuation, or sealing of the spaces:

- the fire hazard portions of internal combustion machinery;
- boiler fronts;
- the fire hazard portions of incinerators;
- purifiers for heated fuel oil.

Activation of any local fire-extinguishing system shall give a visual and distinct audible alarm in the protected space and at continuously manned stations. The alarm shall indicate the specific system that has been activated (SOLAS, 2009).

Fixed gas fire-extinguishing systems

Gas fire-extinguishing systems are most commonly used. Generally, requirements for gaseous fire-fighting systems are included in the ISO 13702 standard. Basic requirements for gaseous fire-fighting systems are as follows:

- gaseous agents not harmful to humans are preferred; if noxious and poisonous gaseous systems (e.g. CO_2) are used, it shall only be used for locked off rooms;
- the room where the gaseous agent is released shall be sufficiently tight to maintain the prescribed concentration for the pre-determined time period of minimum 10 min;
- the extinguishing agent cylinders shall be located outside of the protected room.

Where the quantity of the fire-extinguishing medium is required to protect more than one space, the quantity of medium available need not be more than the largest quantity required for any one space. The volume of starting air receivers, converted to free air volume, shall be added to the gross volume of the machinery space when calculating the necessary quantity of fire-extinguishing medium. Means shall be provided for the crew to safely check the quantity of the fire-extinguishing medium in the containers (SOLAS, 2009). The piping for the distribution of fire-extinguishing medium shall be arranged and discharge nozzles positioned so that a uniform distribution of the medium is obtained. Pressure containers required for the storage of the fire-extinguishing medium, other than steam, shall be located outside the protected spaces, and spare parts for the system shall be stored on board and be to the satisfaction of the Administration. The means of control of any fixed gas fire-extinguishing system shall be simple to operate and shall be grouped together in as few locations as possible at positions not likely to be cut off by a fire in a protected space (IMO, 2001b).

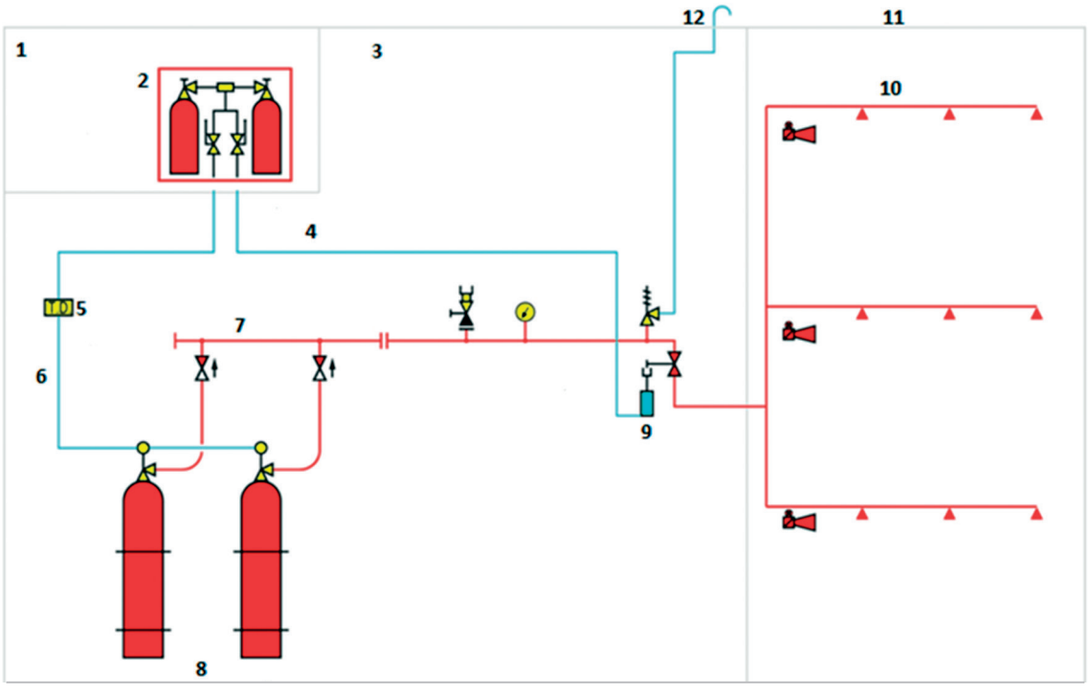

Figure 4. Diagram of gas fire-extinguishing system (CO_2): 1 – control station, 2 –release cabinet, 3 – CO_2 cylinder compartment, 4 – release line – distribution valve, 5 – time delay unit, 6 – release line – cylinders, 7 – manifold, 8 – CO_2 cylinder bank, 9 – distribution valve, 10 – distribution pipelines with nozzles, 11 – protected space, 12 – to free air (Wilhelmsen Technical Solution, 2014)

CO_2, mixtures of N_2 and Ar, or CO_2 and chemical replacements of halons are used in these systems as extinguishing agents. Still, the most common gas applied in fixed gas fire-extinguishing systems for engine room is carbon dioxide (CO_2). Figure 4 presents a diagram of a gas fire-extinguishing system (CO_2).

Fire-extinguishing, and actually suppression, by carbon dioxide causes oxygen dilution or oxygen displacement in the atmosphere. In order to obtain extinguishing effect, the protected space should theoretically have a CO_2 content of 25%. However, allowing door, skylights or vent ducts leakage, it is assumed that 40% of such a space should be filled with CO_2. According to the FSS Code for machinery spaces, the quantity of CO_2 carried shall be sufficient to give a minimum volume of free gas equal to the larger of the following volumes: (i) 40% of the gross volume of the largest machinery space so protected, the volume excludes the part of the casing lying above the level at which the horizontal area of the casing is 40% or less of the horizontal area of the space concerned, taken midway between the tank top and the lowest part of the casing; (ii) 35% of the gross volume of the largest machinery space protected, including the casing. The fixed piping system shall be such that 85% of the gas can be discharged into the space within 2 min (IMO, 2001b).

Carbon dioxide is a fire-extinguishing agent used for the suppression of fires involving flammable liquids and gases as well as electrical equipment. It is a colorless, odorless, non-toxic, and nonconductive gas. Carbon dioxide is relatively inexpensive and easily available. It does not cause corrosion, but it is an asphyxiator for humans. In extinguishing concentrations, CO_2 is lethal to humans. Therefore, the systems using CO_2 as an extinguishing agent must be equipped with devices signaling and warning the intention of its use by the crew. In spaces where a crew member is present, its concentration shall not exceed 1%, since higher content may be dangerous to human life and health (Table 1) (Kukuła, Getka & Żyłkowski, 1981; Żelichowski & Korzeniewski, 1992).

Table 1. CO_2 impact on humans (Żelichowski & Korzeniewski, 1992)

CO_2 content in the air [% of volume]	Impact to human body
2–4	Minor respiratory problems without harmful consequences
5–7	Harmful to dangerous
10	Major respiratory problems
15	After a short period – loss of consciousness
25–30	Immediate death

The IMO has developed detailed requirements concerning the construction and use of fire-extinguishing CO_2 systems, particularly in terms of protection against accidental operation, including two separate and interlocked controls, pre-discharge alarms and time-delays to protect personnel in the engine room. In any case, between detecting a fire and releasing the gas, time is needed to protect the crew and such a delay in running the fire-extinguishing system may result in an escalation of the fire.

The fixed carbon dioxide fire-extinguishing system must be maintained and controlled in order to ensure its safe and proper functioning. Guidelines developed by the IMO for the maintenance and inspections of fixed carbon dioxide fire-extinguishing systems are presented in document MSC.1/Circ.1318. There are two types of inspection: monthly and annual. Visual inspections should be carried out the overall conditions of the system, identifying obvious signs of damage. Monthly inspections include the verification that:

- all stop valves are in the closed position;
- all releasing controls are in the proper position and readily accessible for immediate use;
- all discharge piping and pneumatic tubing is intact and has not been damaged;
- all high pressure cylinders are in place and properly secured;
- the alarm devices are in place and do not appear damaged.

Additionally, on low pressure systems the inspections should verify that:

- the pressure gauge is indicating a value in the normal range;
- the liquid level indicator is indicating a value within the proper range;
- the manually operated storage tank main service valve is secured in the open position;
- the vapor supply line valve is secured in the open position.

During the annual inspection:

- the boundaries of the protected space should be visually inspected to confirm that no modifications have been made to the enclosure that not opening that would render the system ineffective have been created;
- all storage containers should be visually inspected for any signs of damage, rust or loose mounting hardware. Cylinders that are leaking, corroded, dented or bulging should be hydrostatically retested or replaced;
- system piping should be visually inspected to check for damage, loose supports and corrosion. Nozzles should be inspected to ensure they have not been obstructed by the storage of spare parts or a new installation of structure or machinery;
- the manifold should be inspected to verify that all flexible discharge hoses and fittings are properly tightened;
- all entrance doors to the protected space should close properly and should have warning signs, which indicate that the space is protected by a fixed carbon dioxide system and that personnel should evacuate immediately if the alarms sound. All remote releasing controls should be checked for clear operating instructions and indication as to the space served (IMO, 2009).

As mentioned, the equivalent fixed gas fire-extinguishing systems for machinery spaces can be used. The requirements for these systems were included in MSC/Circ. 848 – "Revised Guidelines for the Approval of Equivalent Fixed Gas Fire-Extinguishing Systems, as referred to in SOLAS 74, for Machinery Spaces and Cargo Pump-Rooms", MSC/Circ. 1267, MSC/Circ. 1316 and MSC/Circ. 1317. The agents used are clean halocarbon agents (halon replacements) and inert gases other than CO_2. Clean halocarbon agents break down the chemical reaction in the fire. Some of these agents are: FM 200 (CF_3CHFCF_3), NOVEC 1230 ($CF_3CF_2C(O)CF(CF_3)_2$), Halotron IIB – HFC 3-4-9 C2, FE 13 – CHF_3 and only need to be used in concentrations ranging between 5 and 12%. Inert gases work by reducing oxygen levels and typically require concentrations of 35–50% to work. They include: Argonite [Nitrogen (50%) + Argon (50%)] and Inergen [Nitrogen (52%) + Argon (40%) + Carbon dioxide (8%)] (IMO, 1998).

Other fire-extinguishing systems

Fixed foam fire-extinguishing systems shall be capable of generating foam suitable for extinguishing oil fires. Any required fixed high-expansion foam system in machinery spaces shall be capable of rapidly discharging a quantity of foam sufficient to fill the greatest space to be protected at a rate of at least 1 m in depth per minute. The quantity of foam-forming liquid available shall be sufficient to produce a volume of foam equal to five times the volume of the largest space to be protected. The expansion ratio of the foam shall not exceed 1,000 to 1 (SOLAS, 2009).

Fixed pressure water-spraying fire-extinguishing in machinery spaces shall be provided with approved spraying nozzles. The number and arrangement of

the nozzles shall be to the satisfaction of the Administration and shall be such as to ensure an effective average distribution of water of at least 5 l/m^2/min in the spaces to be protected. The system may be divided into sections, the distribution valves of which shall be operated from easily accessible positions outside the spaces to be protected so as to not be rapidly cut off by a fire in the protected space. The pump and its controls shall be installed outside the space, or spaces, to be protected (SOLAS, 2009).

Fixed aerosol fire-extinguishing systems for machinery spaces should have the same reliability that has been identified as significant for the performance of fixed gas fire-extinguishing systems approved under the requirements of the FSS Code. Aerosol fire-extinguishing systems involve the release of a chemical agent to extinguish a fire by interruption of the process of the fire. The system discharge time should not exceed 120 s. The quantity of extinguishing agent for the protected space should be calculated at the minimum expected ambient temperature using the design density based on the net volume of the protected space, including the casing (IMO, 2001a).

Conclusions

Fire is one of the basic hazards to a ship. According to DNV, nearly 2/3 of the fires on ships have their source in the engine room. Due to the characteristics of a space such as an engine room, the risk of fire is always high. Therefore, it is worth paying attention to fire prevention. Every seafarer is trained in fire prevention. The ability to identify a potential fire hazard is significant as well as being aware of the risk entailed by fire at sea. Contrarily to situations onshore, the crew have to fight the fire on their own. Therefore, fire-extinguishing systems on board are one of the most important elements of any ship. In case of fire, they are the main mean to fight it. Due to the fact that the engine room contains the most important operating systems and devices, it is extremely important to provide its protection. In case of failure of any of these components, the operation of the entire ship is compromised.

References

1. DNV (2010) *Fire Safety*. [Online] Available from: https://exchange.dnv.com/Documentation/Maritime/FireSafety/FIRE%20mappe%202.qxd.pdf [Accessed: June 08, 2015]
2. IMO (1998) Revised Guidelines for the Approval of Equivalent Fixed Gas Fire-Extinguishing Systems, as referred to in SOLAS 74, for Machinery Spaces and Cargo Pump-Rooms, MSC/Circ. 848, International Maritime Organization.
3. IMO (1999) Guidelines for the approval of fixed water-based local application fire-fighting systems for use in category A machinery spaces, MSC/Circ.913, International Maritime Organization.
4. IMO (2001a) Guidelines for the approval of fixed aerosol fire-extinguishing systems equivalent to fixed gas fire-extinguishing systems equivalent to fixed gas fire-extinguishing systems, as referred to in SOLAS 74, for machinery spaces, MSC/Circ.1007, International Maritime Organization.
5. IMO (2001b) International Code for Fire Safety Systems, FSS Code, International Maritime Organization.
6. IMO (2003) Unified interpretations of the Guidelines for the approval of fixed water based local application fire-fighting systems, MSC/Circ.1082, International Maritime Organization.
7. IMO (2009) Guidelines for the maintenance and inspections of fixed carbon dioxide fire-extinguishing systems, MSC.1/Circ.1318, International Maritime Organization.
8. IMO (2014) SOLAS [Online] Available from: www.imo.org SOLAS Consolidated Edition 2014 [Accessed: June 08, 2015]
9. Kukuła, T., Getka, R. & Żyłkowski, O. (1981) *Techniczne zabezpieczenie przeciwpożarowe i przeciwwybuchowe statków*. Gdańsk: Wydawnictwo Morskie.
10. SOLAS (2009) International Convention for the Safety of Life at Sea (SOLAS).
11. STCW (2010) International Convention on Standards of Training, Certification and Watchkeeping for Seafarers.
12. U.S. Coast Guard Newsroom (2015) [Online] Available from: www.uscgnews.com [Accessed: June 30, 2015]
13. Wilhelmsen Technical Solution (2014) High pressure CO_2 fire extinguishing system.
14. Żelichowski, K. & Korzeniewski, L. (1992) *Ratownictwo morskie – środki i techniki gaszenia pożarów na statkach*. Szczecin: WSM.

Scientific Journals
of the Maritime University of Szczecin

Zeszyty Naukowe
Akademii Morskiej w Szczecinie

2016, 48 (120), 58–62
ISSN 1733-8670 (Printed)
ISSN 2392-0378 (Online)
DOI: 10.17402/176

Received: 29.04.2016
Accepted: 07.12.2016
Published: 15.12.2016

Convex optimization of thrust allocation in a dynamic positioning simulation system

Paweł Zalewski

Maritime University of Szczecin, Faculty of Navigation
Centre of Marine Traffic Engineering
1–2 Wały Chrobrego St., 70-500 Szczecin, Poland
e-mail: p.zalewski@am.szczecin.pl

Key words: dynamic positioning, thrust allocation, convex optimization, configurations, programming, simulator

Abstract

Vessels conducting dynamic positioning (DP) operations are usually equipped with thruster configurations that enable the generation of resultant force and moment in any direction. These configurations are deliberately redundant in order to reduce the consequences of thruster failures and increase the safety. On such vessels a thrust allocation system must be used to distribute the control actions determined by the DP controller among the thrusters. The optimal allocation of thrusters' settings in DP systems is a problem that can be solved by several convex optimization methods depending on criteria and constraints used. The paper presents linear programming (LP) and quadratic programming (QP) methods adopted in the DP control model which is being developed at the Maritime University of Szczecin for ship simulation purposes.

Introduction

A convex optimization problem is one of the form (Boyd & Vandenberghe, 2009):

$$\begin{aligned} &\text{minimize} \quad f_0(x) \\ &\text{subject to} \quad f_i(x) \le b_i,\ i = 1,\ldots,m \end{aligned} \tag{1}$$

where the functions $f_0,\ldots,f_m : \mathbb{R}^n \to \mathbb{R}$ are convex, i.e., satisfy:

$$f_i(\alpha x + \beta y) \le \alpha f_i(x) + \beta f_i(y)$$

for all $x, y \in \mathbb{R}^n$ and all $\alpha, \beta \in \mathbb{R}$ with $\alpha + \beta = 1$, $\alpha \ge 0$, $\beta \ge 0$. In general, there is no analytical formula for the solution of convex optimization problems, but there are very effective methods for solving them, such as: the least-squares in quadratic programming (QP), linear programming (LP) or interior-point methods that are used in second-order cone programming (SOCP) or geometric programming (GP) (Boyd & Vandenberghe, 2009).

Dynamic Positioning (DP) system can be defined as a system that automatically controls a vessel, by the influence of external excitations, to maintain her position and headed exclusively by means of active thrust. The DP system divides forces among a ship's thrusters to achieve a resultant force and momentum equal to the one set by the control system. Optimization of thrust allocation is based on minimization of energy usage (need for power or fuel if feasible), additionally taking into account limitations like forbidden zones for thrusters' settings (individual and relative to each other – for instance in the case of opposing thruster pairs).

The optimal allocation of forces generated by thrusters in DP systems is a problem that can be solved by several convex optimization methods depending on the criteria and constraints used. A survey of these methods, including direct allocation by QP, has been presented by Johansen and Fossen (Johansen & Fossen, 2013). This paper presents linear programming (LP) and quadratic programming (QP) methods adopted in a DP control model developed at the Maritime University of Szczecin for ship simulation purposes.

Generation of Forces with Thrusters

For a DP control, similar to ship simulation, a ship's hull can be treated as a rigid body with the center of mass at the origin $p = 0 \in \mathbb{R}^2$. Measurements of the position of the vessel are then compared with the required position. The difference is fed into an Extended Kalman Filter (EKF) and PID-controller to convert this to the resultant force and momentum required to correct the position. The allocation unit controls the thrusters, which must generate the component forces of the resultant one. Therefore the model of thrust allocation used for a vessel with i^{th}-number of azimuth thrusters can be built according to the geometrical relations presented in Figure 1.

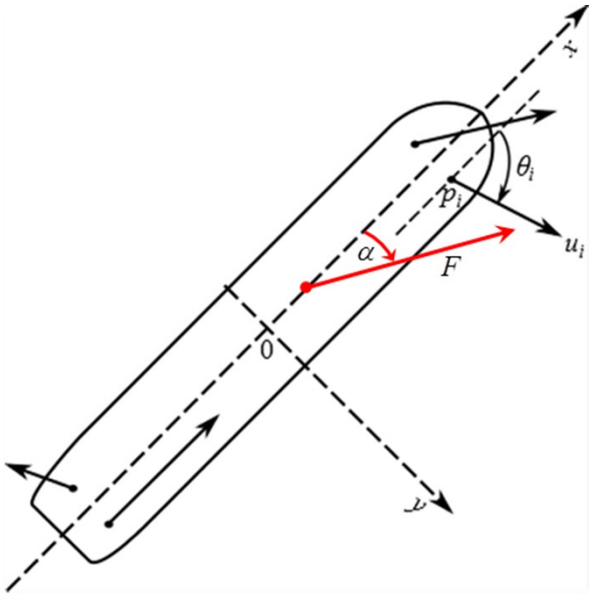

Figure 1. Thrust forces acting on a vessel with i^{th} number of azimuth thrusters

The assumptions of the model are:

- The vessel's position is stabilized at low speed (less than 2 knots or 1 m/s), and the center of mass (force reference origin) is the fixed rotation center.
- There are n component forces with magnitude u_i [kN] or [tf], acting at $p_i = (p_{ix}, p_{iy})$ [m, m], in direction θ_i [deg], $i = 1,2,\ldots,n$.
- The resultant force [kN] or [tf]:

$$F = \sqrt{F_x^2 + F_y^2} \tag{2}$$

- The resultant longitudinal force (horizontal in ship-body frame) [kN] or [tf]:

$$F_x = \sum_{i=1}^{n} u_i \cos\theta_i \tag{3}$$

- The resultant transverse force (vertical in ship-body frame) [kN] or [tf]:

$$F_y = \sum_{i=1}^{n} u_i \sin\theta_i \tag{4}$$

- The resultant torque (moment of the resultant force) [kNm] or [tfm]:

$$M_z = \sum_{i=1}^{n} (p_{iy} u_i \cos\theta_i - p_{ix} u_i \sin\theta_i) \tag{5}$$

- The force limits [kN] or [tf]:

$$0 \le u_i \le u_{\max} \tag{6}$$

- The thruster angle limits [rad] or [deg]:

$$\pi < \theta_i \le 2\pi \tag{7}$$

- The energy or fuel usage is strictly dependent on u_i and in the case of the same type of thrusters, the total energy is assumed to be linearly correlated to:

$$\sum_{i=1}^{n} u_i = u_1 + u_2 + \ldots + u_n \tag{8}$$

The problem to solve is as follows: find the appropriate values for u_i and θ_i that yield the desired resultant force and moment while minimizing the fuel or energy usage. Note that the problem is considered to be 3-DOF (degrees of freedom) or solved in 2-dimensional space. In fact, any movement in the z-direction (up/down) or around the x- and y-axis is ignored because common actuators in offshore vessels do not have the ability to produce thrust in these directions. This clearly reduces the complexity of the problem.

LP problem solution

The standard form of constrained LP can be given in matrix notation as:

$$\begin{aligned} &\underset{x}{\text{minimize}} \quad c^T x \\ &\text{subject to} \quad Ax = b,\ x \ge 0 \end{aligned} \tag{9}$$

where: $A \in \mathrm{P}^{m \times n}$; $x, c \in \mathrm{P}^n$; $b \in \mathrm{P}^m$.

For the thruster allocation problem with variables u_i and θ_i the formulation of the objective function and constraints is:

$$\begin{aligned} &\text{minimize} \quad \mathbf{1}^T u \\ &\text{subject to} \quad f u^T = F^T \\ &\qquad 0 \le u_i \le u_{\max},\ 0 \le \theta_i < 2\pi,\ i = 1,\ldots,n \end{aligned} \tag{10}$$

where:
$\mathbf{1} = [1,1,1,\ldots,u_n]$ of size n;
$u = [u_1, u_2,\ldots,u_n]$;

$$f = \begin{bmatrix} \cos\theta_1 & \dots & \cos\theta_n \\ \sin\theta_1 & \dots & \sin\theta_n \\ p_{1y}\cos\theta_1 - p_{1x}\sin\theta_1 & \dots & p_{ny}\cos\theta_n - p_{nx}\sin\theta_n \end{bmatrix} \tag{11}$$

$F = [F_x, F_y, M_z]$;
F_x, F_y, M – designated longitudinal, transverse forces, and moment.

QP problem solution

The standard form of constrained QP can be given in matrix notation as:

$$\begin{aligned} &\underset{x}{\text{minimize}} \quad x^T P x + q^T x + r \\ &\text{subject to} \quad Gx \preceq h \\ &\qquad\qquad Ax = b \end{aligned} \tag{12}$$

where:

$P \in \Sigma_+^n$; $G \in \mathrm{P}^{m \times n}$; $A \in \mathrm{P}^{o \times n}$; $x, q, r \in \mathrm{P}^n$; $h \in \mathrm{P}^m$; $b \in \mathrm{P}^o$;
Σ_+^n is the set of symmetric, positive semidefinite, $n \times n$ matrices.

For the thruster allocation problem with variables u_i and θ_i transformed to f_{xi} and f_{yi} (longitudinal and transverse components of forces u_i), the formulation of the objective function and constraints is:

$$\begin{aligned} &\text{minimize} \quad \mathbf{1}^T\left(f_x^2 + f_y^2\right) \\ &\text{subject to} \quad F_x = \mathbf{1}^T f_x \\ &\qquad\qquad F_y = \mathbf{1}^T f_y \\ &\qquad\qquad M_z = \mathbf{1}^T\left(p_x \bullet f_y - p_y \bullet f_x\right) \\ &\qquad\qquad \max\left(f_x^2 + f_y^2\right) \le f_{\max}^2 \end{aligned} \tag{13}$$

where:

$$\begin{aligned} f_x &= [f_{x1}, f_{x2}, \dots, f_{xn}] \\ f_y &= [f_{y1}, f_{y2}, \dots, f_{yn}] \end{aligned} \tag{14}$$

$$\begin{aligned} f_{xi} &= u_i \cos\theta_i \\ f_{yi} &= u_i \sin\theta_i \\ u_i^2 &= f_{xi}^2 + f_{yi}^2 \end{aligned} \tag{15}$$

and F_x, F_y, M_z are the designated longitudinal, transverse forces, and moment constraints analogous to the LP problem. If the final constraints worked out by EKF and PID are in the form of (see Figure 1):
F – resultant force;
α – orientation of the resultant force;
M_z – resultant momentum;
$f_{\max}$ – maximum individual thruster force
then:

$$\begin{aligned} F_x &= F\cos\alpha \\ F_y &= F\sin\alpha \end{aligned} \tag{16}$$

The formula (13) can be further extended by additional constraints on the thrusters' work sectors (limits of θ_i or ratio f_{yi}/f_{xi}).

Implementation in DP Simulation System

The algorithms, which solve (10) and (13) by applying Newton's method to a sequence of equality constrained problems, have been developed in Matlab with either Optimization or the CVX Toolbox (Boyd & Vandenberghe, 2009) and afterwards translated to C#. The tests proved that though generally, the solution efficiency of LP is better than the efficiency of QP (which formally is a further generalization of LP), while in the case of the thruster allocation algorithm QP was more robust and faster. The main reasons of this have been nonlinearities in constraints (11) where trigonometric functions are directly applied. The problem elaborated as (13) avoids non-convexity as all constraints are strictly convex, and it can be classified into a linearly constrained QP. Because f_x^2 and f_y^2 are convex functions, their point wise maximum $f_{\max}^2$ is also convex and can be re-expressed as two separate inequalities using a standard LP formulation. The route of QP is also followed by most of the authors dealing with thrust allocation in ship borne DP systems (Lindfors, 1993; Gierusz & Tomera, 2006; Ruth, 2008; Wit, 2009; Daalen et al., 2011; Rindarøy, 2013).

The examples of thrust allocation to four azimuth thrusters, calculated by the model adopted in the DP simulation system established by the Maritime University of Szczecin, with the resultant force in various four quadrants of ship-body fixed co-ordinate system (360° clockwise), are presented in the Figures 2, 3, 4, 5.

The co-ordinates p_{xi} [m] and p_{yi} [m] of azimuth thrusters in the figures 2, 3, 4 and 5 have been set for visualization purposes as: p_x = [5;5;–5;–5], p_y = [5;–5;–5;5] and $f_{\max}$ = 5 tf.

It must be stressed that the developed model focuses on the allocation part of the full closed loop control system which is used to keep the vessel in a stationary position. The allocation unit receives the required total force and momentum from the PID controller and generates the appropriate control signals to the available thrusters of the vessel.

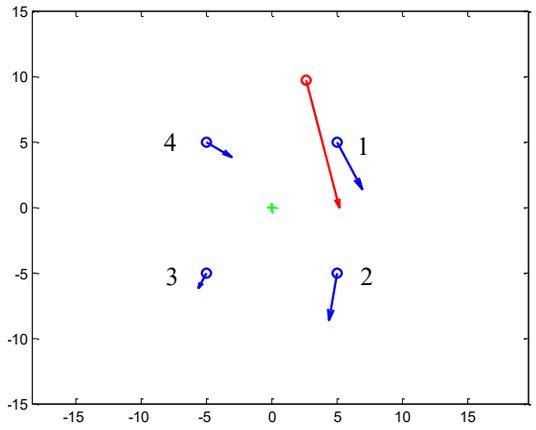

F [tf]	α [deg]	M_z [tfm]
10.00	165.0	50.00
i	u_i	θ_i
1	4.12	152.63
2	3.71	189.34
3	1.31	207.37
4	2.23	121.55

Figure 2. Example of thrust forces allocation with the resultant force in the 1st quadrant of a ship-body fixed co-ordinate system

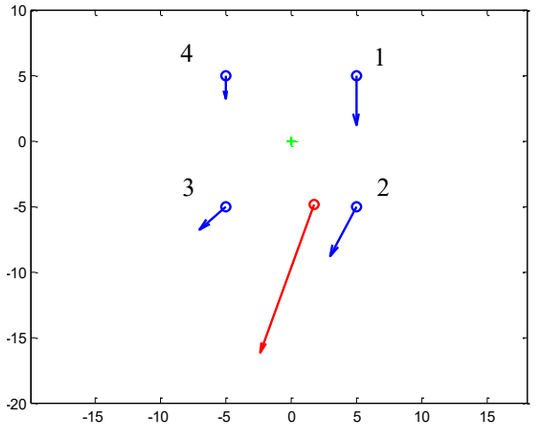

F [tf]	α [deg]	M_z [tfm]
12.00	200.0	40.00
i	u_i	θ_i
1	3.82	180.39
2	4.32	207.95
3	2.72	228.08
4	1.82	180.82

Figure 3. Example of thrust forces allocation with the resultant force in the 2nd quadrant of a ship-body fixed co-ordinate system

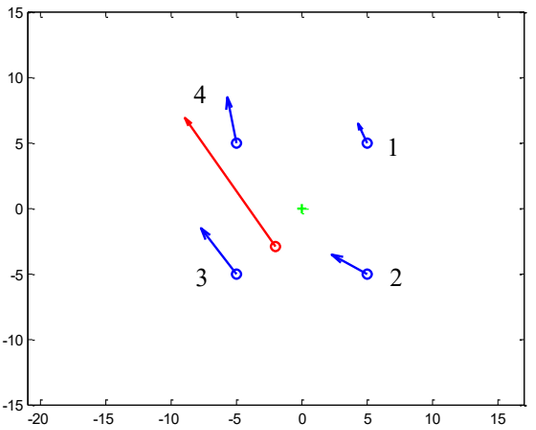

F [tf]	α [deg]	M_z [tfm]
12.00	325.0	40.00
i	u_i	θ_i
1	1.63	333.69
2	3.09	298.18
3	4.40	321.80
4	3.53	348.22

Figure 4. Example of thrust forces allocation with the resultant force in the 3rd quadrant of a ship-body fixed co-ordinate system

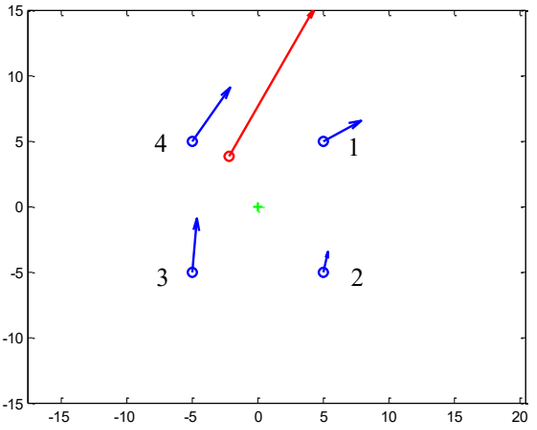

F [tf]	α [deg]	M_z [tfm]
13.00	30.0	50.00
i	u_i	θ_i
1	3.27	61.45
2	1.61	13.48
3	4.08	5.27
4	4.98	35.27

Figure 5. Example of thrust forces allocation with the resultant force in the 4th quadrant of a ship-body fixed co-ordinate system

Note that the problem is simplified by considering it to be 2-dimensional. In fact, any movement in the up/down direction is ignored due to its periodic behavior and no necessity, and no ability to control it. In addition, the presented algorithm is limited to the azimuth thrusters, which are able to direct their thrust in 360 degrees around the z-axis.

As a numerical method, the established model solves the optimization almost in real time: the computation can be treated as instantaneous compared to

the typical timescales of the vessels dynamics, as it takes less than 0.5 s to calculate the results.

Nevertheless it should also be noted that optimizing only the allocation system might not be ideal. A model-predictive approach that combines the Extended Kalman Filter (EKF), PID, and allocation unit might lead to even better results. Another important aspect of this approach would be the concept of time horizon: the power can be minimized over a given period, for example the next minute. However, this would require a full model of the vessel, together with models of the wind, current, and the waves to be implemented.

Conclusions

A thrust allocation system must be used to distribute the control actions determined by the DP controller among the thrusters. The allocation problem can be translated to a constrained optimization problem. The quadratic programming (QP) method has been developed for this purpose in the DP ship simulation model. The tests proved that the optimization algorithm translated into C# programming language worked efficiently using interior-point methods (Boyd & Vandenberghe, 2009) to solve the problem by applying Newton's method to a sequence of equality constrained problems. The further development including extra constraints like limits to the thrusters' work sector (forbidden zones) and non-azimuth thrusters, or model predictive approach will continue in the future.

References

1. Boyd, S. & Vandenberghe, L. (2009) *Convex Optimization*. New York: Cambridge University Press.
2. Daalen, E.F.G. van, Cozijn, J.L., Loussouarn, C. & Hemker, P.W. (2011) *A Generic Optimization Algorithm for the Allocation of DP Actuators*. Proceedings of the ASME 30th International Conference on Ocean, Offshore and Arctic Engineering, Rotterdam, The Netherlands, June 19–24, 2011. pp. 87–94.
3. Gierusz, W. & Tomera, M. (2006) Logic thrust allocation applied to multivariable control of the training ship. *Control Engineering Practice* 14. pp. 511–524.
4. Johansen, T.A. & Fossen, T.I. (2013) Control allocation – A survey. *Automatica* 49. pp. 1087–1103.
5. Lindfors, I. (1993) *Thrust allocation method for the dynamic positioning system*. In 10th International Ship Control Systems Symposium. pp. 3.93–3.106, Ottawa, Canada.
6. Rindarøy, M. (2013) *Fuel Optimal Thrust Allocation in Dynamic Positioning*. NTNU Norwegian University of Science and Technology. M.Sc. Thesis.
7. Ruth, E. (2008) *Propulsion control and thrust allocation on marine vessels*. Doctoral Theses at NTNU, 2008:203, NTNU Norwegian University of Science and Technology.
8. Wit, C.D. (2009) *Optimal Thrust Allocation Methods for Dynamic Positioning of Ships*. Delft University of Technology, Netherlands. M.Sc. Thesis.

Navigation
and Maritime Transport

Scientific Journals
of the Maritime University of Szczecin

Zeszyty Naukowe
Akademii Morskiej w Szczecinie

2016, 48 (120), 65–70
ISSN 1733-8670 (Printed)
ISSN 2392-0378 (Online)
DOI: 10.17402/177

Received: 29.04.2016
Accepted: 02.12.2016
Published: 15.12.2016

Vessel route optimization to avoid risk of collision between carriers of dangerous goods and passenger vessels

Renata Boć✉, Krzysztof Marcjan, Marcin Przywarty, Lucjan Gucma

Maritime University of Szczecin, Institute of Marine Traffic Engineering
1–2 Wały Chrobrego St., 70-500 Szczecin, Poland
e-mail: {r.boc; k.marcjan; m.przywarty; l.gucma}@am.szczecin.pl
✉ corresponding author

Key words: carriage of dangerous goods, risk of collision, passenger ships, chemical tankers, optimization of ship routes, algorithm

Abstract
This article presents the underlying concepts of a mathematical model optimizing the routes of vessels carrying dangerous goods proceeding in the vicinity of passenger ferries. The method is based on the estimated risk of collision between a chemical tanker and a passenger vessel. Risk assessment was performed using three models. The first model determines the distance of the passing ships on the selected area on the basis of the AIS data. The second one is a stochastic model of navigational safety assessment, which provides statistical data on the probability of collision between the two chosen types of vessels. The third model determines the consequences of collisions between passenger ships and chemical tankers. The study defines the scope of the parameters affecting the objective function of vessel route optimization and their importance in the optimization problem.

Introduction

Maritime transport fulfills a particularly important function in the transport of cargo over long distances. A large amount of carried goods are hazardous substances, which could cause serious ecological disaster if they were dispersed in the ecosystem. The transportation of chemical cargo, even though quantitatively small relatively to crude oil and petroleum products transportation, is subject to the risk of leakage and the related consequences may be much larger than those of an oil spill (Sormunen et al., 2015). Chemical tankers can often carry more than one dangerous and harmful substance, which is an additional complication in case of failure due to possible formation of dangerous mixtures. Even small amounts of chemicals may pose a risk, for example aluminum phosphide in contact with water forms phosphine (PH3) – a toxic gas (Boć & Gucma, 2015).

Transport statistics for the Baltic Sea confirm that the carriage of goods has grown rapidly in recent years. Considering only the most dangerous liquid chemicals, their freight reached 11 million tons in 2010, compared to only 4.9 million tons in 2002 (Posti & Häkkinen, 2012). The increasing amount of sea freight results in more frequent meetings of ships at sea and thus increases the likelihood of collisions. The specificity of maritime transport makes it difficult to compare the consequences of ship collisions to similar accidents on land. Loss recovery of a disaster at sea is much more difficult and the consequences are higher. Thus, even a seemingly low probability of a collision at sea should be treated with greater precaution than in the case of a similarly low probability of land collision between cars. Competition among specialized freight forwarders in minimizing transport costs and reducing the time of transport do not go hand in hand with maximizing the transport safety. In the eyes of ship owners, the conventions and regulations aimed at improving safety at sea are too numerous and too restrictive. Therefore, the introduction of additional directives

aiming to improve maritime safety should be made in a very cautious way. In land traffic it is possible to plan routes in such a way that the carriage of dangerous goods avoids potential collision areas, such as large agglomerations or crowded routes. In maritime transport, there is no such possibility. Traffic routes of chemical tankers cross other ships routes. For instance, ships navigating from ports of the Eastern Baltic Sea and proceeding to the North Sea have to cross the route of ferries proceeding from Świnoujście to Ystad.

Optimal route planning for ships with HazMat (Hazardous Materials) aims at minimizing the risks and costs incurred in the event of a collision or an accident, and should also be an important tool to support decisions in planning transportation routes. The priority will be objective economic criteria, such as minimum travel time, fuel consumption, damage to the ship and punctual arrival at the port (Jurdziński, 2014). On the other hand, the safety of shipping is mainly influenced by objective parameters like meteorological data, vessel specifications and risks of collision. Decision making, both during the planning phase of a trip and during en-route implementation of adjustments, should give the priority to objective factors at a fixed acceptable level of risk.

Assumptions for building a model of route optimization of ships carrying dangerous goods

In the planning of transport routes economic factors are primarily taken into consideration. In most cases, any course alteration made to increase the safety affects the competitiveness of freight. Therefore, it is reasonable to define the areas in which such action is necessary. Optimization based on the probability of collisions must be undertaken primarily for areas with high levels of risk, which are mainly represented by traffic intersections.

The ultimate goal of this optimization is the determination of routes for vessels carrying HazMat in order to minimize the probability of collision with passenger vessels, taking into account the acceptable level of risk of collision, objective criteria affecting the organization of maritime transport, the degree of danger posed to the carried cargo. At the same time, the negative impact of such optimization on the economic parameters of transport should be minimized.

The vector of defined objective functions includes parameters defining the criteria for assessing the risk associated with the dangerous cargo, the risk of collision, objective parameters and economic parameters.

$$F(x) = (f_{\text{cargo}}, f_{\text{risk}}, f_{\text{corr}}, f_{\text{ob}}, f_{\text{econ}}) \quad (1)$$

where:

f_{cargo} – class of danger of the transported cargo;
f_{risk} – class of risk of collision for intersecting routes;
f_{corr} – number of areas where a correction is needed;
f_{ob} – objective criteria;
f_{econ} – economic criteria.

The essential parameters and criteria considered when defining the objective function are discussed in detail later in this work.

Optimization restrictions

The theoretical model puts very strict standards on optimization. The restrictions that must be imposed on the adopted theoretical model parameters should take into account the actual conditions of carriage and, above all, minimize the cost of implementing the optimization results with the following limitations:

- Route optimization is carried out on the basis of economic criteria, with the exception of high-risk areas.
- The imposition of course alteration to prevent excessive proximity between passing vessels takes place only in areas with a high level of risk of collision.
- It is necessary to designate the areas with a high level of risk of collision and take into account the given objective parameters to determine whether a vessel with HazMat should procced through a relatively narrow traffic lane set within the recommended zone.

To determine the effect of various parameters on the objective function, it is significant to characterize parameters which are important when deciding on the route of the ship. Assessment of the danger consists in assigning to each function parameter. Another important task is to separate, on the basis of empirical data derived from AIS, the areas with increased risk of collision.

Description of parameters affecting the optimal route of ships carrying dangerous cargo

Economic parameters of route planning

These parameters are not specific to the transport of dangerous goods, but rather are taking a significant share of optimization procedure for all transport. For economic reasons, the goal of each

company is to save time and fuel. Both of these factors allow to save money, and therefore to increase the profits. Owners seek to minimize costs through efficient economic operation of ships. The impact on the decisions taken by the ships' captains is difficult to estimate.

Hazard class of substances transported by vessels

The International Maritime Organization (IMO) has unified rules on the transport of dangerous goods by sea by releasing the IMDG code (International Maritime Dangerous Goods). In this code, dangerous goods are divided into nine classes according to their threat. The IMDG code also includes guidelines for transport, labeling and securing of dangerous goods. First of all, for further optimization measures it is necessary to build an additional classification of hazardous cargo that is based on the IMDG code but also takes into account the volume of transport, composition and other factors. This would be the first criterion influencing the optimization of transport routes.

According to the report presenting transportation of cargo in the Baltic Sea (Posti & Häkkinen, 2012) almost 730 million tons of international cargo was handled in the Baltic Sea Ports. Around 42% of this was liquid bulk. Oil and oil products are the most common type of liquid bulk cargo (with a 95% share), the liquid chemicals share is 3.5% and the rest is other liquid bulk cargo. Courtiers with the biggest share of liquid chemicals handling are: Finland (57%), Estonia (11%), Sweden (8%) and Poland (7%). The report (Posti & Häkkinen, 2012) states that in case of Swedish ports, the real volume of liquid chemicals is higher than reported and the estimated volume of handled chemicals is supposedly over 2 million tons. It also states that German ports situated in the Baltic Sea handle liquid chemicals in large quantities, but exact amounts are unknown. According to Posti & Häkkinen (Posti & Häkkinen, 2012), the most abundant chemicals handled in the Baltic Sea area are methanol, sodium hydroxide solution, ammonia, sulfuric and phosphoric acid, pentanes, aromatic free solvents, xylenes, methyl ter-butyl ether (MTBE), and ethanol and ethanol solutions.

A method of determining and classifying particularly dangerous intersections of cargo and passenger ship routes on the basis of a simulation

Areas where routes running from north to south intersect routes running from west to east of the Baltic Sea are particularly vulnerable to collisions. Hence the need for thorough look at these zones. The specificity of maritime shipping route intersections does not allow the possibility of avoiding them; however, they can be precisely traced and treated as the areas of increased risk of collisions.

The designation of suggested shipping lanes and traffic separation schemes (late nineteenth century) replaced the so-called "freedom of navigation" and forced to proceed along specified routes. This helped significantly reduce the number of collisions in those areas where such restrictions were applied (e.g. English Channel 1967 years).

Ordering the traffic of vessels in the Baltic Sea is systematically implemented and there is no turning back from these decisions if one thinks of maintaining the safety in the maritime transport while increasing the volume of goods being transported.

Planning the route between the port of departure and the destination port is one of the tasks of the vessel's crew. The concept of route optimization taking into account safety aspects should be based on obligatory course alterations only in areas of heightened risk of collision. In these areas, HazMat vessels would proceed into a separated narrow route, which would be represented as a zone where increased precautions must be taken. The ship approaching such an area should optimize its navigational decisions depending on navigation conditions and knowledge about potential threats.

Initially, the location of particularly sensitive areas should prevent from close quarters situations between chemical tankers and passenger vessels. In addition, it should then prevent vessels from approaching areas of high traffic density intersections. The optimization should be made on the basis of AIS data and also on historical statistical data.

The AIS data is increasingly being used in research on maritime safety as a valuable source of information about the movement of ships. AIS identifies each vessel fitted with an AIS transmitter and transmits static data (IMO number, destination, cargo, etc.) and information about the ship's position, speed and course. AIS information databases are used, for example to create advanced methods for detecting possible near miss collisions (Zhang, 2013).

It was assumed that a model of navigational safety assessment could be used to evaluate the risk of collision while planning the optimal routes for vessels carrying dangerous goods. In the present study, the model developed by the Institute of Marine Traffic Engineering in Maritime University of Szczecin

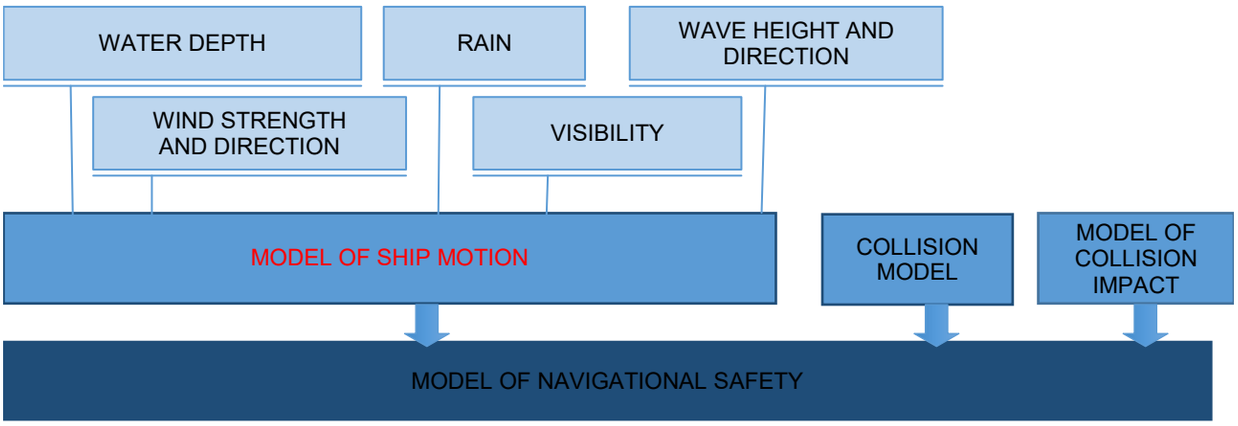

Figure 1. Scheme of navigational safety assessment model

was used. Construction of this model uses sub-models developed mainly on the basis of statistical data. The ship traffic model is developed on the basis of AIS data and navigational charts; the model of external conditions is based on data from hydro-meteorological stations and navigational publications. Detailed specification of this model can be found in (Przywarty, 2012) and conference papers (Przywarty et al., 2015). The scheme of the navigational safety assessment model is shown in Figure 1.

Computer simulations developed on the basis of this model and on collected statistical data allow to carry out simulation experiments for chemicals tankers. The simulation identifies and classifies the intersections of merchant vessel routes with routes of passenger ferries.

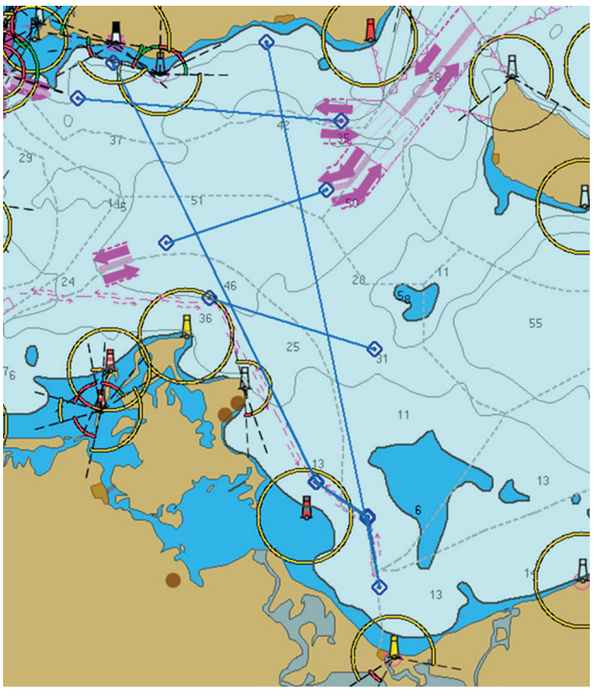

Figure 2. Shipping routes designated on the basis of AIS data

The model works in accelerated time, enabling the analysis of a large number of scenarios and providing stable statistical results. To pre-determine the critical zone for navigation in the study area of the Baltic Sea, the AIS data of highest vessel traffic density in the two summer months (June and July) of 2011 was used. Analysis of the data from this system also allows to determine the parameters of shipping routes that are presented in Figure 2, marked with blue lines.

After gathering and implementing all the required statistical data, a simulation trial was conducted in order to identify the number of incidents and accidents. Details allowing classification of intersections are shown in Table 1, and the simulation results show places with the largest number of encounters between passenger ships and chemical tankers Figure 3.

Table 1. Encounters between passenger vessels and chemical tankers

Intersection	Number of encounters	Number of iterations	Encounters frequency [1/month]	A mean time between encounters [months]
I	358	100	1.8	0.6
II	342	100	1.7	0.6
III	214	100	1.1	0.9
IV	549	100	2.8	0.4
V	664	100	3.3	0.3
VI	90	100	0.5	2.2
VII	122	100	0.6	1.6
VIII	74	100	0.4	2.7

The results of computer simulations allow to distinguish eight areas with different frequencies of encounters between passenger ships and chemical

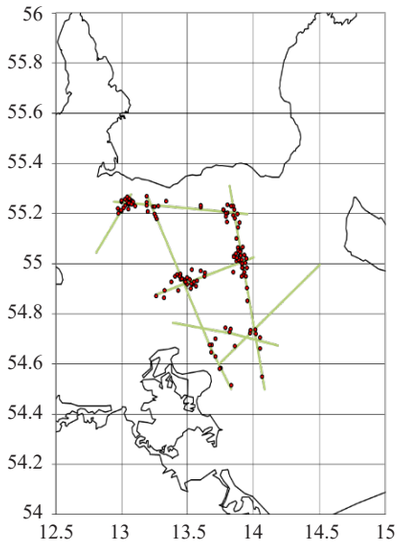

Figure 3. Positions of simulated encounters between passenger ships and chemical tankers in the study area (the two-month iterations)

tankers. The areas have different encounter densities, allowing the assignment of different weights that would affect the role of the parameter describing the risk of an encounter. In areas I, IV, V the highest priority should be assigned, whereas the lowest priority should be assigned to area VIII.

Route planning objective parameters

Unlike the other classes affecting the assessment of the risk of collision between a passenger ship and a ship carrying dangerous goods, these parameters are completely objective and have a decisive influence on the process of route optimization. These parameters include meteorological and navigational conditions as well as technical parameters of the ship. Unlike the other parameters, these can be objectively defined and measured.

When building a target function for individual subjects in this class of parameters the following should be considered:

- weather conditions – wind strength and direction, wave height and direction, occurrence of haze or rain;
- navigational conditions – water depth, shoals;
- parameters of the ship – deadweight tonnage, current % of loading, maximum speed, maneuverability.

Especially in the decision-making process of the optimal route selection, the main factor to be considered is the weather condition, since it affects the duration of the voyage. Along with the accepted risk of collision, weather conditions will be the basis of route optimization.

Determination of the effect of various parameters on the risk of collision is a major problem that must be entered as input data and that will have a decisive impact on the optimization of the route. Conducting research on the influence of parameters on the level of collision risk of a vessel carrying dangerous goods is a key issue to create a mathematical model.

An algorithm selecting a method optimizing the route of dangerous goods in maritime transportation

The next step after creating a mathematical model, whose task is to define and calculate the values of factors affecting the optimization of routes of ships carrying dangerous cargoes, is to create an algorithm of computer application to verify the obtained results. An example of this algorithm is shown in Figure 4.

After dividing the route into smaller sections, the algorithm determines the procedure for each segment based on the answers to questions. After loading new data, the algorithm checks if the cargo carried by the vessel is DG cargo type. If the answer is negative, the calculation block chooses the economic criterion and ends operations. If the vessel is carrying dangerous goods the algorithm checks whether the vessel is already in its port of destination. If the vessel is still underway, vessels rout is checked in the following steps and, if it is planned to enter an area of increased risk, vessel parameters and weather conditions are calculated. After taking into consideration these parameters, a calculation block determines whether the vessel's course is safe or whether it should be changed. Once more, the weather conditions and whether the ship had already left the area of increased risk are checked. When the vessel is already outside the area of increased risk, the algorithm is completed. For the purposes of this algorithm, objectified weight should be assigned for each parameter of the ship navigational and meteorological conditions that would lead to a final "yes" or "no" decision. The created algorithm identifies areas of increased risk, calculates the vessel's parameters and checks the weather conditions to allow correction of the vessel's course and safe way of leaving the increased risk area. The algorithm is an introduction to create a model for the route optimization of ships carrying dangerous.

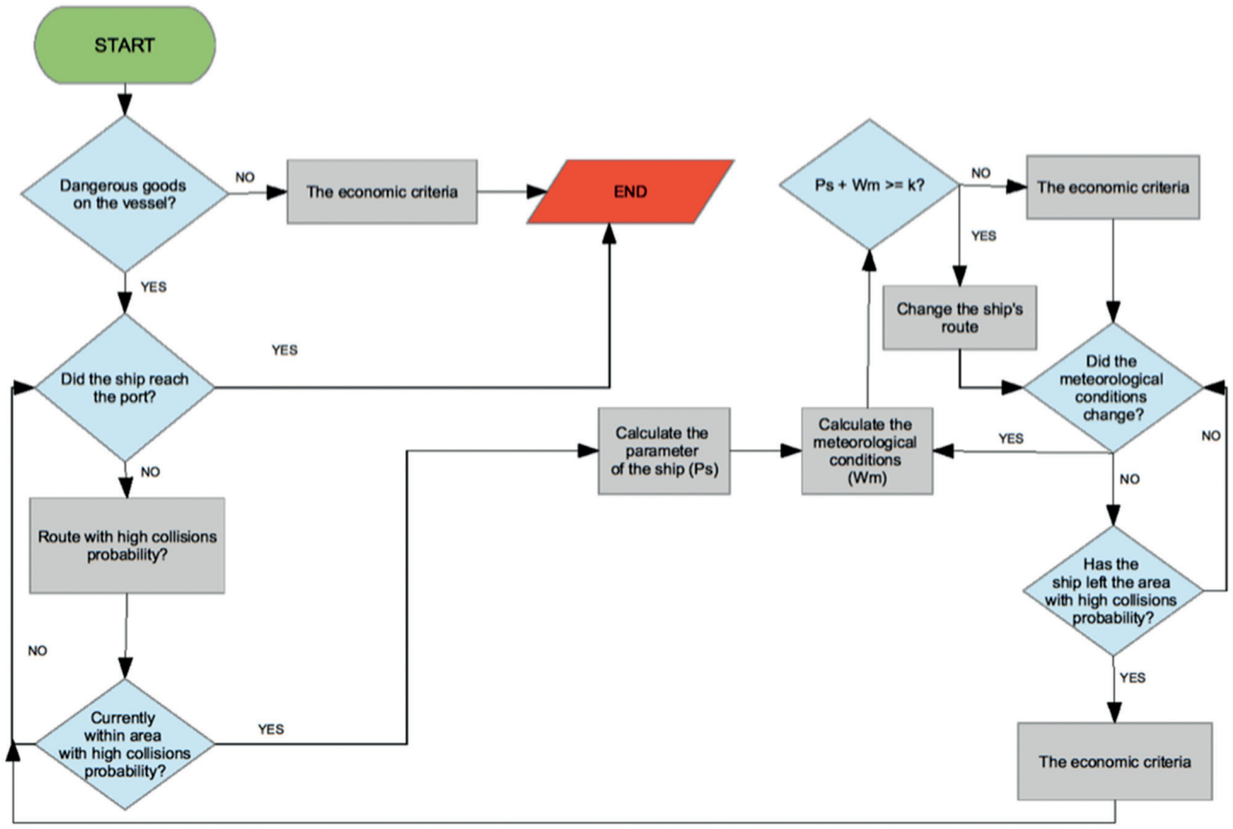

Figure 4. Algorithm for optimal route selection

Conclusions

Because of the complexity of the problem, construction of a mathematical model to optimize routes of vessels carrying dangerous goods requires firstly the determination of a domain for each parameter affecting the target function. The importance of the different parameters on the optimization problem should then be quantified.

In this paper, auxiliary issues that are necessary to build the mathematical model are indicated. Finally, the ways of determining the critical areas of navigation based on data from AIS are described. In order to create a computer application that will allow to verify the obtained results, some additional parameters still need to be systematized, classified and assigned with factors determining their impact on the navigational safety.

Acknowledgments

This research outcome has been achieved under the research project No. 1/S/CIRM/16 financed from a subsidy of the Ministry of Science and Higher Education for statutory activities of Maritime University of Szczecin.

References

1. Boć, R. & Gucma, L. (2016) Analysis of the traffic of chemical tankers in the Szczecin and Świnoujście seaports. *Scientific Journals of the Maritime University of Szczecin* 46 (118). pp. 122–128.
2. Jurdziński, M. (2014) Wybrane warianty planowania podróży statku w żegludze oceanicznej. *Zeszyty Naukowe Akademii Morskiej w Gdyni* 87. pp. 14–21.
3. Posti, A. & Häkkinen, J. (2012) *Survey of Transportation of Liquid Bulk Chemicals in the Baltic Sea*. Turku: University of Turku.
4. Przywarty, M. (2012) *Stochastyczny model oceny bezpieczeństwa nawigacyjnego na akwenach otwartych*. Dsc. Thesis. Maritime University of Szczecin.
5. Przywarty, M., Gucma, L., Marcjan, K. & Bąk, A. (2015) Risk analysis of collision between passenger ferry and chemical tanker in the western zone of the Baltic Sea. *Polish Maritime Research* 2(86), vol. 22. pp. 3–8.
6. Sormunen, O.-V.E., Goerlandt, F., Häkkinen, J., Posti, A., Hänninen, M., Montewka, J., Ståhlberg, K. & Kujala, P. (2015) Uncertainty in maritime risk analysis: Extended case-study on chemical tanker collisions. *Proceedings of the Institution of Mechanical Engineers, Part M: Journal of Engineering for the Maritime Environment* 229 (3). pp. 303–320, first published on January 30, 2014.
7. Zhang, W., Goerlandt, F., Kujala, P. & Wang, Y. (2016) An advanced method for detecting possible near miss ship collisions from AIS data. *Ocean Engineering* 124. pp. 141–156.

Scientific Journals
of the Maritime University of Szczecin

Zeszyty Naukowe
Akademii Morskiej w Szczecinie

2016, 48 (120), 71–74
ISSN 1733-8670 (Printed)
ISSN 2392-0378 (Online)
DOI: 10.17402/178

Received: 29.04.2016
Accepted: 18.09.2016
Published: 15.12.2016

Using the Monte Carlo method to create probability maps for search and rescue operations at sea

Grzegorz Bugajski

Maritime University of Szczecin
1–2 Wały Chrobrego St., 70-500 Szczecin, Poland, e-mail: g.bugajski@am.szczecin.pl

Key words: Monte Carlo, probability map, rescue operation, shipwrecked, probability distribution, probability model

Abstract

In this article we proposed a probability map that allows for location of the position of survivors. We used a probability model of a survivor drift to create the map. The model is based on the provisions of IAMSAR containing factors like leeway and wind current. Our proposal of utilizing a probability map differs from that shown in the IAMSAR by using other probabilistic methods. We performed analysis of a drifting raft using the Monte Carlo method. The map is closer to reality, since it is asymmetrical and generated by the simulation. However, preparing probability maps might be helpful in SAR action planning.

Introduction

The effectiveness of the rescue operation is dependent on the probability of finding a survivor in the search area. It will take a few hours before the arrival of the unit of the emergency rescue or other vessel designated to start looking. If we know how much time expires between the SOS signal and the beginning of search operation, we could calculate the trajectory of a drifting object and sail to the point where we it should be located. In practice, the calculation and hydrometeorological data are inaccurate. We want to look for a place where you will find the missing object after the elapsed time, starting from the moment of giving the last position. As a result of calculation errors, we will not seek a point, but the area where the missing object can be located. If we add to this area probability density function then we obtain probability map, which will be a much better tool than simply one geographic point.

Determination of the datum point

The starting point of the search and rescue operation is called a datum point, which is drifting away in time (Kasyk & Pleskacz, 2015). Setting a datum point depends on the search unit, hydrological data and the span of time. According to IAMSAR regulations we can calculate the direction of a drift based on a scheme placed in the book IAMSAR vol. II (IMO, 2013). By knowing the maximum speed of the unit that is a crossing point of both the drifting survivor's and search crew's trajectory, we are given the starting point of the search and rescue.

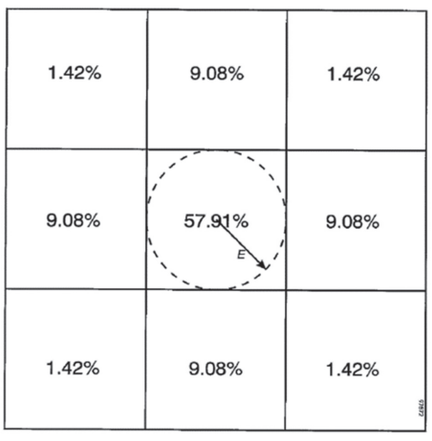

Figure 1. Probability map for a point datum (IMO, 2013)

IAMSAR also reports an error that is made while the calculations are performed. It depends on a few factors, including: determining the speed of wind and determining the influence of the wind current upon speed of wind. As the result, we are given a total probable error of the survivor's position E. Then we are able to create an entry map of probability. This is a map that uses a two dimensional normal distribution where the expected value for the datum point and standard deviation equals E for both coordinates Figure 1). The total probable error of position is used to create this value.

The concept of probability map

A map with the frequency of a given phenomenon has use in many fields. Determining the location of weather phenomena depends on many factors including the accuracy of measurements or lack of it. To determine this, probability calculus and statistic methods are used. We can use prognosis wind direction as an example. This value will be restricted to a selection of the cardinal points on a compass rose (Figure 2). If we assume that the predicted wind direction of 90° = E on the cardinal points scale, the direction is going to belong in the (78°45', 101°15') interval. Because of that, we can calculate the coordinates of the survivor after a given time. Calculating the datum point is only limited to the adoption averaged values. As an outcome, we have optimized the point to start search and rescue, which does not mean that the survivor is precisely there.

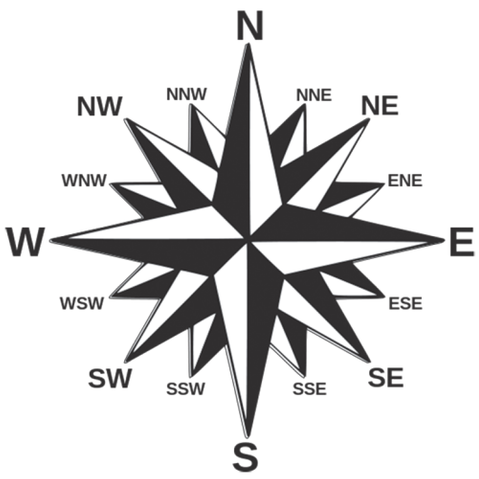

Figure 2. A 16-point compass rose (Wikipedia, 2016)

If we know the hydro metrological conditions, it is good to propose additional analysis regarding this data. In addition to calculating the datum point, we are going to look for the area where the survivor might be located. Next, this area can be divided into smaller sectors and corresponding probability values can be ascribed to them.

Model of survivor displacement

The main tool needed to create a map of probability is probability distributions. All the uncertainties such as the accuracy of measurement, relation between measurable hydrometeorological factors, and the drift of the object will be replaced with probability distributions. For the purpose of this article, we will introduce chosen factors, which will allow creation of the map of probability.

We input the factor of wind, which will affect the drift of the object in two ways. We assume that the wind blows in a specified direction α with a certain velocity V. The direction of the wind will be described using a normal distribution with an expected value α and a standard deviation with a value of half of the cardinal point 11°15'. The wind velocity will also be described using a normal distribution. This wind will generate the wind current and according to the Coriolis force, his direction will be deviated 45° right on the northern hemisphere or left of the southern hemisphere. The speed of the wind current can be calculated from the linear dependency model (Figure 3).

Due to the fact that it is a subject of the lateral drift caused by the wind, the vessel is not moving exactly with the direction of the wind. The velocity of this component of the drift can be calculated using available tables (IMO, 2013) and displayed using a normal distribution. A model of the displacement of the object can then be presented as the assembly

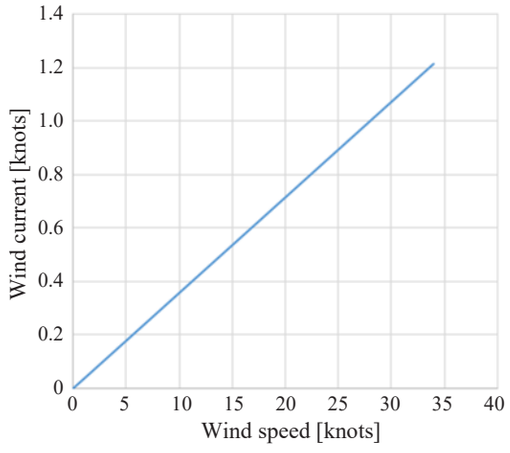

Figure 3. Local wind current graph

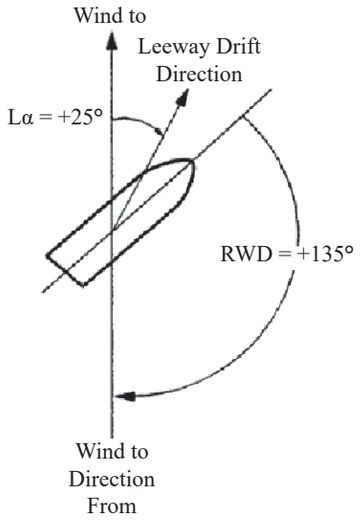

Figure 4. Relationship between Relative Wind Direction (RWD) and Leeway angle (L alpha) (Allen, 2005)

of two vectors. Thus, the vector of displacement is the sum of the wind current vector and direction of the wind vector (Figure 4).

Creating a distribution of probability using the Monte Carlo method

Let's assume that we know details of components describing the wind, which are its direction and velocity. We also know the kind of vessel being searched for, and the amount of time which has passed since the moment that the last known position of the survivor was broadcasted. We will calculate the distribution of probability of the coordinates where the survivor can be at given moment in time. To achieve that, we will apply the Monte Carlo method. Having the model of survivor's movement, we can generate the following. According to the distributions we assumed, we generate the direction of the wind and its velocity. Based on this data we can calculate the lateral and surface drift, which will provide us with a resultant direction of drift and its velocity. We move the starting position with translation by the vector with a direction compatible to the one last received, and a length equal to the product of time that has passed since the broadcast of the last known location and drift speed. All that gives us is a point where the survivor might appear, taking all the predicates into account. We repeat this activity as many times as we want. Having done all that, we created a map consisting of points that created a discrete distribution of the probability of the position of the ship. The more points we generate, the better projection we will get.

Construction of the map of probability

To create a map of probability we need to obtain a distribution of probability of the survivor's position. Thanks to the Monte Carlo method we obtain a discrete distribution, which is why the construction of a probability map will be based on counting the points on it. The first step will be to mark an area that we wish to search. It will be a rectangle covering almost 100% of the distribution of probability. We cannot assume that the probability of containment of a survivor in certain area can be 100%, because with the increase in the number of points, using the Monte Carlo method makes the area of the search grow. That's why we'll apply the three-sigma rule, in accordance with the concept of map creation from IAMSAR. On the basis of randomly selected points, we calculate the expected value and standard deviation. Then we exclude the points that are farther from the middle than the value of three standard deviations. That leaves us with a collection of points in which every single one belongs in the rectangle, in which the sides of the shape are passing through the extreme points of each of the sides. The next step involves the division of the rectangles into parts, which are smaller rectangles of equal dimensions. In each part we calculate the number of the generated points and then divide it by the total number of points. This way we obtain a probability for a survivor to be in each rectangle in a given moment of time.

Example – raft drift

Without decreasing the applicability of the general model, we assume that our survivor is located at the northern hemisphere, and as a point of reference we'll take the starting position (ONM, ONM). Every other point is equivalent with the vector of displacement of the survivor in time. The raft is not equipped with a drogue anchor. We assume that the wind is blowing in direction 0° with a velocity of 20 knots. The average velocity of wind current is $0.714w$, and its average direction is 315°. The second factor is lateral drift, and in this example the direction of the drift is deviated by 25° in relation to the wind current and has an average velocity of $1.34w$. We assume that the standard deviation of this velocity equals $0.25w$ and the time of drift is 1 hour. Then, we randomly select 1000 different sets of data compatible with the model of survivor displacement. Subsequently, we calculate points in which raft will find itself after 1 hour.

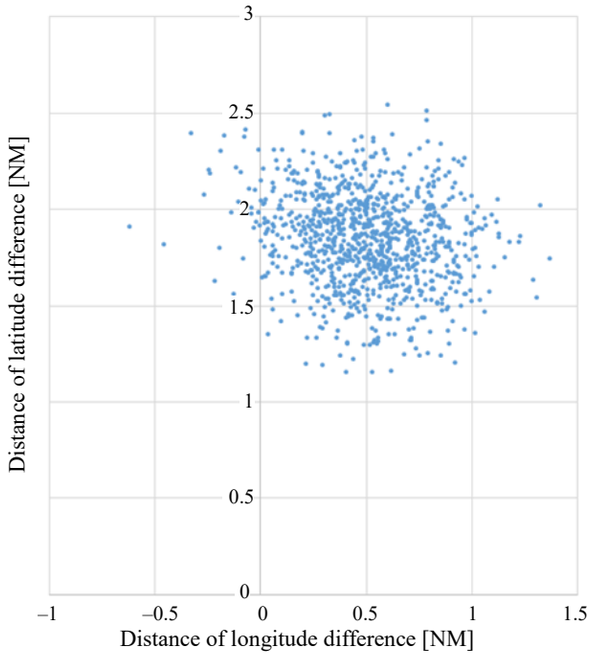

Figure 5. Changing the position of the raft after one hour drift

The Figure 5 shows a distribution of probability of a ships position in relation to the starting point. In accordance with the accepted three-sigma rule, we remove the points located on the extremes. Then we create a rectangle covering all the points save for those removed, and finally divide the rectangle into a grid of smaller rectangles 5 by 5. For every one of those we attribute the quotient of the numbers included in it and sum of all elements on the map.

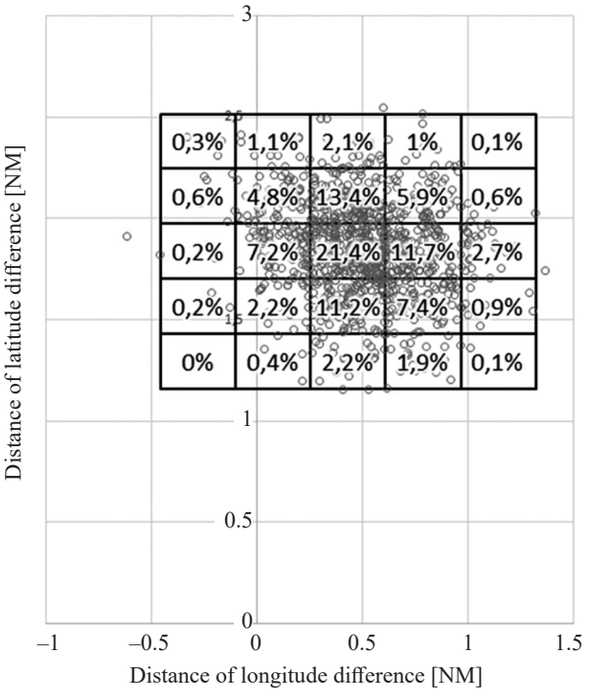

Figure 6. Probability map after one hour drift

As a result, we get a map of the probability of positions of a raft being adrift after 1 hour passes (Figure 6). The dimensions of the map and the passage of time from the starting position were chosen specifically for the requirement of presentation of the map.

Conclusions

The most important aspect of search and rescue operations is their rate capability. Success of those actions depends on many factors (Turner et al., 2007). One critical aspect is very good organization. In order to mount a rescue quickly, one must determine both the place and method of extraction, and for that one needs the proper tools to verify the plan of the SAR operation. There are certain prescriptions on how to proceed when hydrometeorological conditions are adverse, including certain major changes. One must facilitate a starting point for an action and pattern of movement for an object, which is adrift. Having a map of the probability of the potential location of the searched object in question can contribute to having a better planned rescue. That's why it is worth knowing where the probability of finding said survivor is slim to none, and where it is really high. Mounting a rescue whilst using a map of probability can significantly narrow down the area in which we won't find anything. Thus, saved time and resources can be used to search an entirely different area. The proposed map of probability must be developed in many aspects. Specifically, the model of drift included in this article encompasses the important influence of wind. In the next stages, there is a great need to perfect the model, by adding other necessary variables. Further, the shape of the map of probability should also be verified in the future.

References

1. Allen, A.A. (2005) Leeway Divergence. Final Report. U.S. Coast Guard Research and Development Center.
2. IMO (2013) *IAMSAR manual*. Vol. II. London: IMO.
3. Kasyk, L. & Pleskacz, K. (2015) An Adaptation of an Algorithm of Search and Rescue Operations to ship Manoeuvrability. *TransNav, the International Journal on Marine Navigation and Safety of Sea Transportation* 9 (2). pp. 265–268.
4. Turner, C., Lewandowski, S., Lester, D., Mack, E., Howlett, M., Spaulding, E. & Comerma, M. (2007) Evaluation of Environmental Information Products for Search and Rescue Optimal Planning System (SAROPS).
5. Wikipedia (2016) [Online] Available from: https://upload.wikimedia.org/wikipedia/commons/thumb/e/e0/Compass-Rose16A.svg/550px-CompassRose16A.svg.png [Accessed: April 28, 2016

Scientific Journals
of the Maritime University of Szczecin

Zeszyty Naukowe
Akademii Morskiej w Szczecinie

2016, 48 (120), 75–80
ISSN 1733-8670 (Printed)
ISSN 2392-0378 (Online)
DOI: 10.17402/179

Received: 29.04.2016
Accepted: 15.09.2016
Published: 15.12.2016

Wind shear detection based on direct measurements, remote sensing and numerical models

Dariusz Chaładyniak✉, Janusz Jasiński, Sławomir Pietrek, Karolina Krawczyk

Military University of Technology, Faculty of Civil Engineering and Geodesy
Institute of Geodesy, Department of Geographic Information Systems
2 Kaliskiego St., 00-908 Warsaw 49, Poland
e-mail: {dariusz.chaladyniak; janusz.jasinski; slawomir.pietrek; karolina.krawczyk}@wat.edu.pl
✉ corresponding author

Key words: wind shear, vertical air currents, omega equation, sonars, radars, wind profilers, WRF model

Abstract
Wind has huge influence on take-off, landing and cruising of aircraft. Therefore measuring wind direction and speed as well as evaluating its structure are the most important tasks in meteorological support of flights. Wind shear, which is characterized by rapid changes of speed and/or direction, is one of the most hazardous phenomena for aviation. This phenomenon exists mostly in low tropospheric jet streams, areas of active atmospheric fronts, near convective clouds and strong temperature inversions. The paper proves that wind shear is mainly dependent on non-uniform layout of ascending and descending air currents and shows that this phenomenon can be detected by using ground sensors (ultrasonic anemometers), remote sensing methods (sodars, radars, wind profilers) and data from numerical mesoscale models.

Introduction

Scientists of various areas have always been interested in the research of the boundary layer of the atmosphere. Its processes, structure and principal parameters are at the basis of physics of the atmosphere. Theoretical and experimental work has resulted in credible forecasts of atmospheric evolution, making it possible to predict the values of meteorological elements as well as particular types of atmospheric phenomena. This is crucially important when wind structure of its lowest levels is analyzed, especially when wind shear – hazardous for aviation – needs to be detected. Thanks to dynamically developing aviation technology, safer aircraft flights are becoming possible. At the same time, current reports about aviation disasters confirm the great influence of unfavorable weather conditions on take-off and landing, especially as planes have low lift-to-drag ratios.

Vertical air currents

The vertical currents field is one of the most important variables describing the state of the atmosphere. Numerous weather phenomena are caused by ascending or descending air currents. Vertical currents are very important for the development and evolution of pressure systems and frontal zones as well as the formation of cloud systems and precipitation. They are a crucial element of analysis and forecast of the dynamics of pressure systems (Chaładyniak & Jasiński, 2008). The vertical component of the wind field analyzed in the synoptic scale is of the order of a few centimeters per second. Standard meteorological measurements are made with accuracy of 1 m/s. Hence, it is difficult to make direct measurements of vertical currents. This quantity is determined indirectly using wind fields that are measured regularly. Two methods are commonly used to compute vertical currents: kinetic – based on

the continuity equation – and adiabatic – based on the thermodynamic energy equation. Both methods are referenced to an isobaric coordinate system, in which the $\omega(p)$ function is computed according to the following formula:

$$\omega = \frac{Dp}{Dt} = \frac{\partial p}{\partial t} + \mathbf{V} \cdot \nabla p + w\left(\frac{\partial p}{\partial z}\right) \tag{1}$$

written in the (x, y, z) coordinate system.

In large scale atmospheric flows, the horizontal wind is, in first approximation, considered to be geostrophic. We can therefore write that: $\mathbf{V} = \mathbf{V}_g + \mathbf{V}_a$ but $\mathbf{V}_g = (\rho f)^{-1}\mathbf{k}\times\nabla p$, which means that: $\mathbf{V}_g \cdot \nabla p = 0$. We can convert equation (1), using the equation of statics, to obtain:

$$\omega = \frac{\partial p}{\partial t} + \mathbf{V}_a \cdot \nabla p - g\rho w \tag{2}$$

Analyzing the order of the components of the right hand side of equation (2) for large scale atmospheric flows we obtain that the pressure changes during one day are as follows:

$$\partial p/\partial t \sim 10 \text{ hPa}$$

$$\mathbf{V}_a \cdot \nabla p \sim 1 \text{ hPa}$$

$$g\rho w \sim 100 \text{ hPa}$$

Therefore we can use the following approximating relation:

$$\omega = -g\rho w \tag{3}$$

Since geostrophic vorticity, ζ_g, and wind, $\mathbf{V}_g$, can be expressed using only the geopotential, Φ, the following equation:

$$\frac{\partial \zeta_g}{\partial t} = -\mathbf{V}_g \cdot \nabla\left(\zeta_g + f\right) + f_0 \frac{\partial \omega}{\partial p} \tag{4}$$

can be used to analyze vertical currents fields, ω, when the Φ and $\partial\Phi/\partial t$ fields are available. Geopotential tendency, $\chi = \partial\Phi/\partial t$, is a basic forecast field used operationally in weather services. Despite the fact that upper air levels analyses are available only twice a day, the tendency approximation based on observations of geopotential at 12-hour intervals provides more accurate forecasts than other methods in use. This paper presents an alternative method based on vorticity and thermodynamic equations.

Omega equation

The omega equation was first presented by J.G. Charney in 1947. It enables to determine vertical currents fields, ω, exclusively on the basis of the spatial distribution of geopotential. To derive the omega equation we can use the mathematical definition of the baroclinic model (Charney, 1947):

$$\frac{\partial \chi}{\partial p} = -\mathbf{V}_g \cdot \nabla\left(\frac{\partial \Phi}{\partial p}\right) - \sigma\omega \tag{5}$$

where σ is the parameter of the static stability of the atmosphere in the quasi-geostrophic approximation:

$$\nabla^2 \chi = -f_0 \mathbf{V}_g \cdot \nabla\left(\frac{1}{f_0}\nabla^2\Phi + f\right) + f_0^2 \frac{\partial \omega}{\partial p} \tag{6}$$

The procedure proposed in the paper consists in eliminating the geopotential tendency χ from the above system of functions. To achieve this, we apply the ∇^2 operator to equation (5):

$$\nabla^2\left(\frac{\partial \chi}{\partial p}\right) = -\nabla^2\left[\mathbf{V}_g \cdot \nabla\left(\frac{\partial \Phi}{\partial p}\right)\right] - \sigma\nabla^2\omega \tag{7}$$

and we differentiate equation (6) against pressure, p:

$$\frac{\partial}{\partial p}\left(\nabla^2 \chi\right) = -f_0 \frac{\partial}{\partial p}\left[\mathbf{V}_g \cdot \nabla\left(\frac{1}{f_0}\nabla^2\Phi + f\right)\right] + f_0^2 \frac{\partial^2 \omega}{\partial p^2} \tag{8}$$

Since $$\nabla^2\left(\frac{\partial \chi}{\partial p}\right) = \frac{\partial}{\partial p}\left(\nabla^2 \chi\right)$$

the differential operators on the right side of equations (7) and (8) are equal, that the term $\nabla^2(\partial\chi/\partial p)$ can be eliminated, resulting in:

$$\underbrace{\left(\nabla^2 + \frac{f_0^2}{\sigma}\frac{\partial^2}{\partial p^2}\right)\omega}_{\text{A}} = \underbrace{\frac{f_0}{\sigma}\frac{\partial}{\partial p}\left[\mathbf{V}_g \cdot \nabla\left(\frac{1}{f_0}\nabla^2\Phi + f\right)\right]}_{\text{B}} + \underbrace{\frac{1}{\sigma}\nabla^2\left[\mathbf{V}_g \cdot \nabla\left(-\frac{\partial \Phi}{\partial p}\right)\right]}_{\text{C}} \tag{9}$$

Equation (9) is the so-called classical omega equation and it only contains derivatives with respect to the spatial variables. This equation defines a method of determining the ω function that, unlike the continuity equation, is independent of the ageostrophic component of the wind field:

$$\nabla \cdot \mathbf{V}_a + \frac{\partial \omega}{\partial p} = 0 \tag{10}$$

By integrating equation (10) with respect to pressure we obtain:

$$\omega(p) - \omega(p_s) = \int_{p_s}^{p}\left(\frac{\partial u_a}{\partial x} + \frac{\partial v_a}{\partial y}\right)\mathrm{d}\,p \tag{11}$$

where p_s is the reference pressure (e.g. 1000 hPa or surface pressure) and p is the pressure at a selected level.

Hence, direct measurements of wind are not necessary. Equation (9) does not require information on the distribution of vorticity tendency. This means that in order to determine the ω field, it is sufficient to know the distribution of geopotential for a single observation time. On the other hand, the analyzed equation includes second order derivatives with respect to the vertical coordinate. The precise assessment of the specific expressions through measurement data characterized by noise may be a very difficult task. The left side of equation (9) is not a classical Laplace operator and the σ coefficient that appears at the vertical coordinate is dependent on static stability of the atmosphere. Analysis of components in the omega equation (9) shows that the differential operator defined as A (with the assumption that σ = const.) corresponds to operator A in the geopotential tendency equation (Hoskins, Draghici & Davis, 1978):

$$\underbrace{\left[\nabla^2+\frac{\partial}{\partial p}\left(\frac{f_0^2}{\sigma}\frac{\partial}{\partial p}\right)\right]}_{\text{A}}\chi=\underbrace{-f_0\mathbf{V}_g\cdot\nabla\left(\frac{1}{f_0}\nabla^2\Phi+f\right)}_{\text{B}}+\underbrace{-\frac{\partial}{\partial p}\left[-\frac{f_0^2}{\sigma}\mathbf{V}_g\cdot\nabla\left(-\frac{\partial\Phi}{\partial p}\right)\right]}_{\text{C}} \tag{12}$$

i.e.: $\nabla^2+\frac{\partial}{\partial p}\left(\frac{f_0^2}{\sigma}\frac{\partial}{\partial p}\right)=\nabla^2+\frac{f_0^2}{\sigma}\frac{\partial^2}{\partial p^2}$.

Since the forces defined on the right hand side of equation (9) have their maxima in the middle of the troposphere and the ω function equals zero at the lower and upper boundaries of the atmosphere, it is possible to assume that ω has sinusoidal courses both in the horizontal plane and along the vertical axis:

$$\omega=W_0\sin\left(\pi p/p_0\right)\sin kx\sin ly \tag{13}$$

Introducing solution (13) to equation (9) gives:

$$\left(\nabla^2+\frac{f_0^2}{\sigma}\frac{\partial^2}{\partial p^2}\right)\omega\approx-\left[k^2+l^2+\frac{1}{\sigma}\left(\frac{f_0\pi}{p_0}\right)^2\right]\omega \tag{14}$$

Expression A is thus proportional to $-\omega$. Having in mind that ω is proportional to $-\omega$ (see equation (5)), we conclude that $\omega < 0$ results in ascending air currents and consequently A is proportional to vertical velocity. This means that positive values of the sum of B and C result in ascending air currents, while negative values result in descending currents. Expression B in equation (12) is called total vorticity advection. Expression B in equation (9) is proportional to the value of the increase of the total vorticity advection with altitude and it is sometimes called differential vorticity. Figure 1 illustrates that:

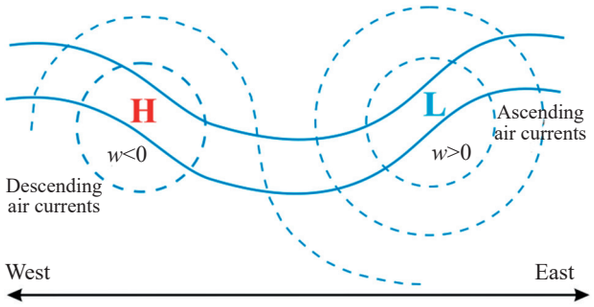

Figure 1. Geopotential of the 500 hPa (solid line) and the 1000 hPa (dashed line) level surfaces presenting areas of strong vertical movements caused by total vorticity advection. H – high pressure area, L – low pressure area (Holton, 1992)

$$w\propto\left\{\frac{\partial}{\partial z}\left[-\mathbf{V}_g\cdot\nabla\left(\zeta_g+f\right)\right]\right.$$

< 0 over a high pressure area H

> 0 over a high pressure area L (15)

The total vorticity advection therefore corresponds to ascending air currents over ground low pressure areas and descending air currents over ground high pressure areas. Expression C in equation (12) is the horizontal Laplace function of the specific volume advection. The vertical velocity value due to this component can be determined by means of the following formula:

$$w\propto\nabla^2\left[\mathbf{V}_g\cdot\nabla\left(-\frac{\partial\Phi}{\partial p}\right)\right]\propto-\mathbf{V}_g\cdot\nabla\left(-\frac{\partial\Phi}{\partial p}\right) \tag{16}$$

In case of warm air advection, expression C is positive. Hence, for very weak or inexistent total vorticity advection, the vertical velocity, ω, is also positive. For cold air advection, expression C is negative. Hence, for very weak or inexistent total vorticity advection, the vertical velocity, ω, is also negative.

Figure 2 illustrates ascending currents occur on the eastern side of a ground low pressure system in the area of the warm front while descending currents occur behind the cold front on the western side of the ground low pressure system. Further analysis indicates that the vertical currents and temperature advection sustain the geostrophic character of the

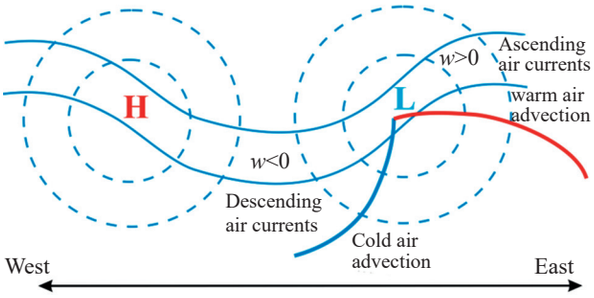

Figure 2. Geopotential of the 500 hPa (solid line) and the 1000 hPa (dashed line) level surfaces presenting areas of strong vertical movements caused by temperature advection. H – high pressure area, L – low pressure area (Holton, 1992)

upper vorticity field. Warm air advection increases the thickness of the 500/1000 hPa layer in the area of an upper ridge at the 500 hPa surface. The geopotential increases and anti-cyclonic vorticity in the region of the ridge guarantee the preservation of geostrophic balance. Since vorticity advection cannot increase the anti-cyclonic vorticity in the upper ridge, the horizontal divergence has to balance the negative tendency of vorticity. According to mass conservation, divergence of the upper vorticity field is compensated by ascending air currents. Descending currents occur in the area of the trough at the 500 hPa surface (cold air advection region).

Wind shear

Wind shear poses the greatest threat to aircraft during take-off and landing. Wind shear may result in changing flight path or throwing off aerodynamic balance. According to ICAO, among all accidents occurring during landing, wind shear is responsible for over 20% of cases in which the aircrafts drive off the runway and 10% of short landings. This information itself shows how important wind shear detection is for direct meteorological support. Airport systems are required to provide credible information about the threat of wind shear occurrence so that decisions about continuing or breaking the take-off or landing procedures can be made. The detection of wind shear using only ground sensors is extremely difficult because of its limited space and short time of occurrence, justifying the efforts of meteorologists to find more credible methods for wind shear detection. Several observations have allowed to conclude that a strong stream of descending air is formed near convective clouds, and its speed can be as high as 75–110 km/h or even 135 km/h. When the stream reaches the ground it flows horizontally in all directions, creating strong whirls of air within 2–5 km radius of the center of the descending stream and up to 600 meters above the ground. The maximum speed of the flowing air is estimated at 100 km/h (Djurić, 1994). The mechanism of wind shear creation and flying in such conditions are presented in the Figures 3 and 4.

We now move on to analyze the case of wind speed increase with height. During landing, the plane travelling into wind enters into the lower layers with weaker head wind, therefore its lift decreases gradually. As a result, the plane's actual line of flight runs below the assumed approach path, the aircraft gets mushing and despite increased drag the landing may

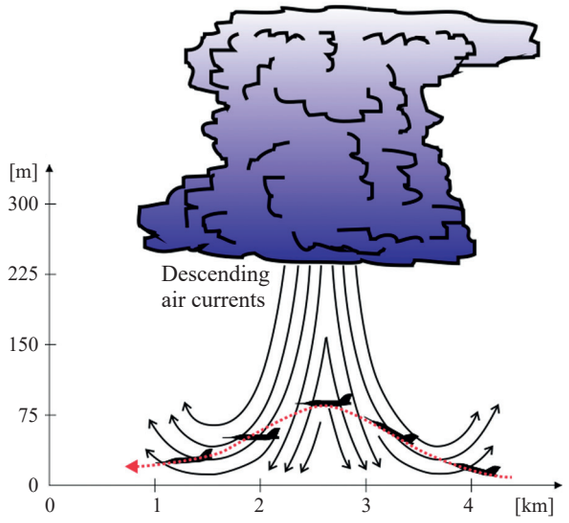

Figure 3. Influence of strong descending air currents on a flying aircraft

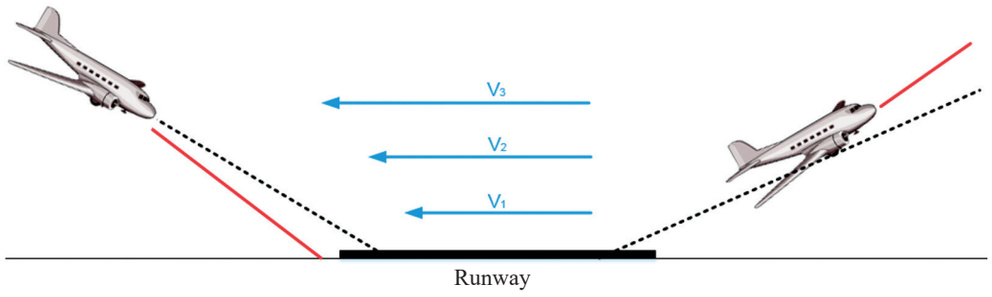

Figure 4. Influence of wind shear on take-off and landing. Expected (dashed line) and actual (solid line) flight path

be short. During take-off, the ascending aircraft gets into layers with stronger head wind and it is affected by stronger lift than in lower layers. Therefore its actual take-off path angle is higher than expected. This may result in exceeding the stalling angle and mushing of the aircraft.

During take-off and landing the speed of an aircraft fluctuates between 200 and 280 km/h. When the aircraft is flying through descending air currents it is subjected to winds of different speeds and directions. Sudden short-term changes in airspeed of the plane result in rapid increase and decrease of lift, which are especially dangerous at low altitudes and at low speed.

Wind shear detection

A few methods of detecting wind shear exist. The following are some examples of equipment used to acquire data for assessing the wind conditions favorable for the phenomenon (Figures 5–8).

Figure 5. Ultrasonic anemometer

Figure 6. Sodar (Schwechat airport)

Figure 7. Radar wind profiler (White Sands, USAF)

Figure 8. Radar (Brzuchania)

Vertical air current field layouts acquired from the WRF (Weather Research and Forecasting) numerical mesoscale model are presented in the Figures 9–11.

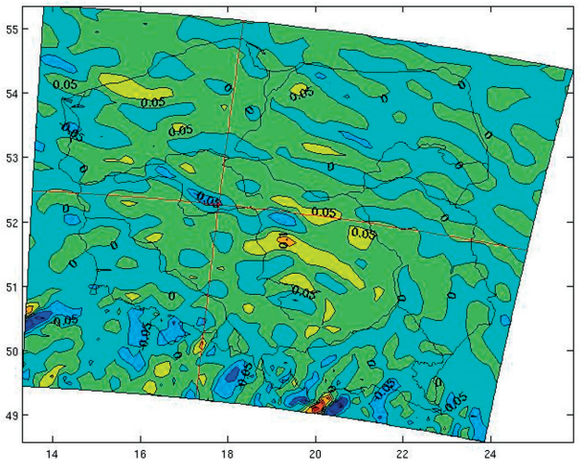

Figure 9. Field of the vertical component of wind speed at the 10th computational surface of the WRF model

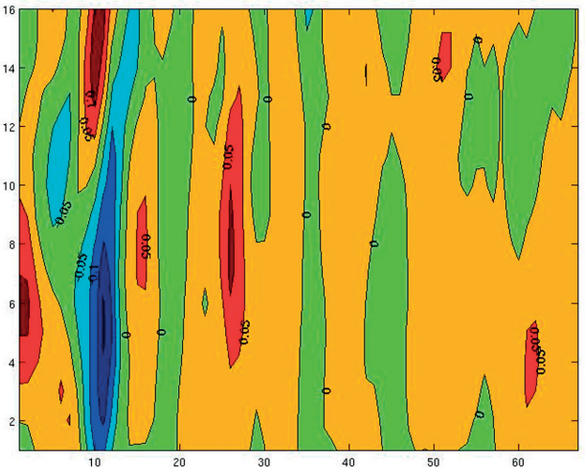

Figure 10. Vertical component of wind speed profile along a meridional line

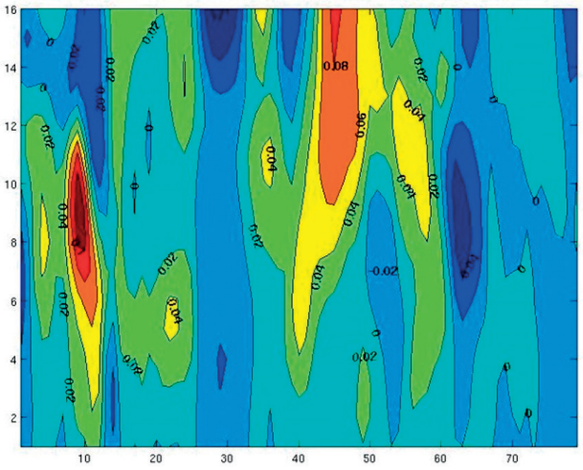

Figure 11. Vertical component of wind speed profile along a latitudinal line

Conclusions

The information provided here shows how important wind shear detection is for direct meteorological support. Airport meteorological measurement systems are required to provide credible information on the probability of occurrence of wind shear so that decisions on continuing or aborting take-off or landing can be made. The wind shear phenomenon is almost impossible to detect by using only ground sensors (ultrasonic anemometers) due to its limited range and brief occurrence. Therefore, one can understand the meteorologists' efforts to find credible wind shear detection methods. In cases where direct measuring is technically problematic or impossible because of the area size, remote sensing methods (sodars, radars, wind profilers) become especially important. Effective and credible detection of wind shear is also possible based on detailed analysis of vertical air current fields available from numerical weather prediction models.

Acknowledgments

The research was conducted and the paper was prepared by the personnel of the Department of Geographic Information Systems within Research project No. 23-933.

References

1. Chaładyniak, D. & Jasiński, J. (2008) Vertical air currents assessment for meteorological support of airborne missions of data acquisition for GIS. *Polish Journal of Environmental Studies*, *Hard Olsztyn* 17, 1C. pp. 19–22.
2. Charney, J.G. (1947) The dynamics of long waves in baroclinic westerly current. *J. Meteor*. 4, 5. pp. 135–162.
3. Djurić, D. (1994) *Weather analysis*. New Jersey: Prentice Hall, Englewood Cliffs.
4. Holton, J.R. (1992) *An introduction to dynamic meteorology*. Third edition. San Diego: Academic Press.
5. Hoskins, B.J., Draghici, I. & Davies, H.C. (1978) A new look at the ω-equation. *Quart. J. Roy. Meteorol. Soc*. 104. pp. 31–38.

Scientific Journals
of the Maritime University of Szczecin

Zeszyty Naukowe
Akademii Morskiej w Szczecinie

2016, 48 (120), 81–87
ISSN 1733-8670 (Printed)
ISSN 2392-0378 (Online)
DOI: 10.17402/180

Received: 29.04.2016
Accepted: 15.09.2016
Published: 15.12.2016

A study of coastal convective clouds using meteorological radar data

Sławomir Pietrek✉, Janusz Jasiński, Dariusz Chaładyniak, Karolina Krawczyk

Military University of Technology, Faculty of Civil Engineering and Geodesy
Institute of Geodesy, Department of Geographic Information Systems
2 Kaliskiego St., 00-908 Warsaw 49, Poland,
e-mail: {slawomir.pietrek; janusz.jasinski; dariusz.chaladyniak; karolina.krawczyk}@wat.edu.pl
✉ corresponding author

Key words: meteorological radar, radiolocation reflectivity, convective clouds, storm, hail, upper air sounding

Abstract

The paper presents the results of study of convective cloud development over land and sea. The study was based on data from the Gdańsk-Rębiechowo radar and upper air sounding from the Łeba aerological station. Radar data from the classical channel were analyzed for the atmosphere scanned at 6 elevation angles of the antenna beam. Vertical profiles of the atmosphere along selected paths presenting radiolocation reflectivity in the detected cloud structures were produced using the recorded radiolocation reflectivity. Conclusions concerning the cloud structure, the physical state of water in the clouds and the thermodynamic state of the atmosphere were formulated as the results of comprehensive analysis of the radar and upper air sounding data. The obtained values of selected parameters and indices were used to quantitatively describe selected physical processes and to formulate forecasts concerning weather phenomena that might pose threats to land, air and sea transport as well as for some industrial and agricultural branches. The developed method of radar and aerological data processing will be applied to further studies of convective clouds in other regions. It will also enable to assess the impact of environmental conditions on the development of convective processes.

Introduction

Contemporary meteorological radars, in addition to classic radars, are employed to detect areas of clouds and precipitation and to enable the study of wind fields. Radars emit horizontal and vertical electromagnetic impulses in beams of 1° width. The power of the radar echo is measured in the classic channel, which is the basis for determining the radiolocation reflectivity of meteorological objects (hydrometeors). The Doppler channel data are analyzed with respect to frequency and the results enable to quantitatively describe the wind field using the derived Doppler frequency shift of the radar echo with respect to the initial frequency of the emitted electromagnetic impulse.

Information systems adopted to process the radar data include computational procedures that utilize empirical relations developed on the basis of measurements conducted during numerous field research experiments.

As for any other atmospheric remote sensing data, the radar data interpretation should take into account the limitations resulting from the technical properties of the radar itself (e.g. antenna beam width, impulse length, receiver threshold sensitivity etc.) and the properties of the studied objects, e.g. heterogeneity of the cloud's structure (extended spectrum of the particles' sizes, various states of water, turbulence, etc.).

The impact of the environmental conditions on the development of convective clouds is an important issue to be taken into account. The type of underlying surface (sea, land) and its orography, and in some cases the infrastructure, are of special importance.

The analysis of results was based on retrieved upper air sounding data since there was no possibility to conduct a comprehensive study of the atmosphere in which the radar data might be verified using direct measurements. Therefore, the study of convective clouds had to be carried out in situations (region and time) in which the upper air soundings were truly representative.

The results of a comprehensive analysis of radar and upper air sounding data may be used to detect and monitor hazardous weather phenomena related with convective clouds (storms, heavy precipitation, hail), as well as gusty wind zones, meso-cyclones and meso-anticyclones, and convergence and divergence areas in the wind fields.

These weather phenomena induce conditions that may pose threats to many fields of human activity, with special impact on land, air and sea transport as well as for some industrial and agricultural branches.

Basics of radar data application to atmospheric studies

The scattering of electromagnetic waves, having wavelength λ, due to clouds and precipitation particles of the diameter D_i depends on the effective scatter surface, σ_i, of a single spherical particle:

$$\sigma_i = \frac{\pi^5}{\lambda^4}|K|^2 D_i^6 \tag{1}$$

where K is a function of the complex refraction coefficient of the material (water, ice or mixture).

The value of $|K|^2$ in normal conditions was established for water droplets (0.93) and ice crystals (0.197) using results of measurements conducted during numerous field experiments.

The effective scatter surface of a volume unit of a meteorological object is the sum of the effective scatter surfaces of all particles within the volume. For a homogenous cloud (consisting of only water droplets or only ice crystals) the value of $|K|^2$ is constant and the effective scatter surface of a volume unit, $\sigma_{\text{vol. unit}}$, is given by:

$$\sigma_{\text{vol.unit}} = \frac{\pi^5}{\lambda^4}|K|^2 \sum_{i,\text{vol.unit}} D_i^6 \tag{2}$$

The last element of equation (2) is the radiolocation reflectivity, Z, of a meteorological object. Its value depends on the object's size and contents, as well as on its microstructure, i.e. on the spectrum of particles' sizes and their concentration in the object (e.g. in a cloud or precipitation):

$$Z = \sum_{i,\text{vol.unit}} D_i^6 \ [\text{mm}^6/\text{m}^3] \tag{3}$$

Relation (3) is valid for cloud or precipitation particles that comply with the Rayleigh approximation, i.e.:

- they are spherical and of diameters significantly smaller than the emitted radar wavelength;
- they are of the same state of matter;
- they fill the entire space of the emitted radar beam.

The range of Z values for clouds or precipitation is very wide (e.g. for developed convective clouds it may vary between 10^4 and 10^7 mm^6/m^3) (Geçer, 2005), therefore, it is convenient to apply the logarithmic scale and express the values in the so called decibels of the radiolocation reflectivity, dBZ, calculated according to:

$$Z_e[\text{dBZ}] = 10 \log Z \tag{4}$$

where Z_e is the effective radiolocation reflectivity, i.e. the radiolocation reflectivity of a virtual cloud composed of water droplets for which the radar echo has a power, P_r, equal to the radar echo of the real cloud.

The radar equation for a meteorological object located at a distance R from the radar has the following form:

$$P_r = C_r \frac{Z_e}{R^2} \tag{5}$$

where C_r is the radar constant (the meteorological potential of the radar), whose value depends on technical parameters of the radar (Büyükbas et al., 2005).

Convective cloud phenomena recognition using radar data

Hail and storm may be recognized by means of an analysis of the vertical profile of radiolocation reflectivity. The radar echo measures the maximum height of a convective cloud. The value of the maximum radiolocation reflectivity and its height indicate the intensity of the phenomena related with the cloud. It may be assumed that when the maximum radiolocation reflectivity in an area exceeds the value of 40 dBZ, and the height of the radar echo exceeds the value of 5 km, then it is highly probable that the radar echo is related to a cloud accompanied by a storm (or at least to a cloud with strong convection).

Storms are often recognized using an algorithm based on radar echo heights (with minimum radiolocation reflectivity of 4 dBZ) – H_m [km] and maximum radiolocation reflectivity Z_m [dBZ].

Its parameter value Y is calculated according to the following formula:

$$Y = H_m \frac{Z_m - 18}{10} \tag{6}$$

The range of the parameter values indicating storm is determined individually for specific regions. In the area of Poland, the radar echo is related to a storm when $Y > 30$ (Szturc, 2004).

The procedure for hail detection (ZHAIL) uses data of radiolocation reflectivity concerning cloud layers above the 0°C isotherm (freezing level). The altitude of the freezing level may be determined using the results of an upper air sounding. Development of the ZHAIL algorithm was based on the Waldvogel algorithm. The hail occurrence criterion is fulfilled if the H_{45} altitude from which the radiolocation reflectivity value exceeds 45 dBZ and the H_o altitude of the 0°C isotherm are related as follows:

$$H_{45} > H_o + 1.4 \text{ km} \tag{7}$$

In practice, the Waldvogel criterion issues "false alerts" quite often.

The results of the ZHAIL algorithm calculations enable to determine, depending on the $H_{\max}$ altitude of the maximum radiolocation reflectivity, various levels of hail alerts. For the commonly applied radiolocation reflectivity threshold of 45 dBZ, the alert levels are defined as (Moszkowicz & Tuszyńska, 2006; Tuszyńska, 2011):

$H_{\max} > H_{45}$ – light hail;
$H_{\max} > H_{45+5\text{ dBZ}}$ – moderate hail;
$H_{\max} > H_{45+10\text{ dBZ}}$ – heavy hail.

Synoptic situation in the southern region of the Baltic Sea on July 7th, 2014

On July 7th, 2014 the weather over the southern part of the Baltic Sea and its eastern coast was determined by a ridge related with a vast high-pressure area from Scandinavia. A cold front with developing waves influenced the western part of the area (Figure 1).

The analysis concerned a cloud development observed around noon in the coastal area of the Łeba region. At 12 UTC the upper air sounding data from the Łeba aerological station indicated that the air mass advection from the ground to the altitude of about 700 m was arriving from the east and veering from southeast to west-east and upwards, becoming westerly at the altitude of about 6 km. The advection speed was about 10–15 km/h. At altitudes of 10 to 11.2 km it increased to 30–35 km/h.

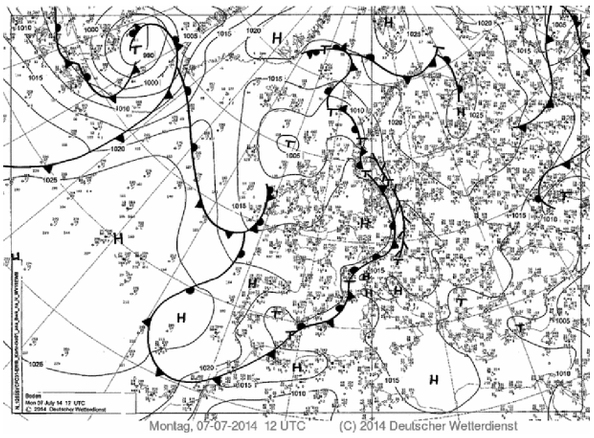

Figure 1. Surface weather chart with synoptic situation on July 07, 2014 at 12 UTC (wetter3, 2014)

Study of convective cloud development in coastal regions using radar data

Convective cloud development in a coastal region was analyzed using data from the Gdańsk–Rębiechowo airport radar. Radar data from the classic channel, acquired by scanning the atmosphere at the antenna beam elevation angles of 0.5°, 1.4°, 2.4°, 3.4°, 5.3° and 7.7°, were used in the research. The radar data and processing software (RAPOK) were acquired from the Institute of Meteorology and Water Management.

The cloud development study was initiated with analyses of the data of July 7th, 2014 at 11.40 UTC. The analysis of the radar data obtained by scanning the atmosphere at the lowest elevation angle of 0.5° indicated that there were two convective cells in the region of Łeba (Figure 2). The cloud further away from the radar developed over the sea, while the closer one developed over land.

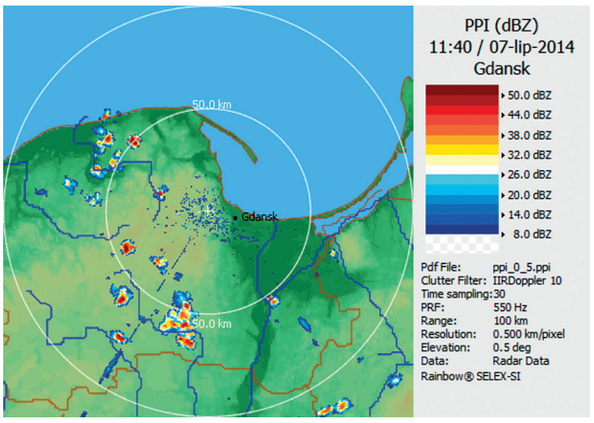

Figure 2. Radar image of horizontal distribution of maximum radiolocation reflectivity recorded for the scanning elevation angle of 0.5° by the Gdańsk-Rębiechowo radar on July 07, 2014 at 11.40 UTC

The maximum height of both clouds (8 and 6 km, respectively), their horizontal dimensions at the altitude of about 3 km (about 5 and 2 km, respectively) and the maximum values of radiolocation reflectivity (42 dBZ and 27 dBZ, respectively) were determined using vertical cross-sections of the radar echoes (Figure 3).

At 12.00 UTC the analyzed clouds merged into one convective cell with the radar echo height at about 11 km, a horizontal dimension of about 10 km and a maximum value of radiolocation reflectivity of 50 dBZ (Figure 4).

The maximum development of the convective cloud was observed at about 12.30 UTC. The cloud top reached the lower part of the tropopause (12 km) and the cloud developed a clearly visible incus

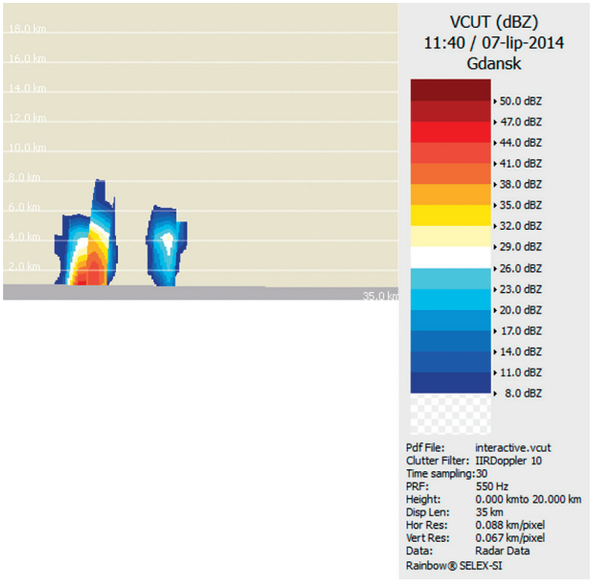

Figure 3. Vertical cross-section of the radar echoes recorded by the Gdańsk-Rębiechowo radar on July 07, 2014 at 11.40 UTC

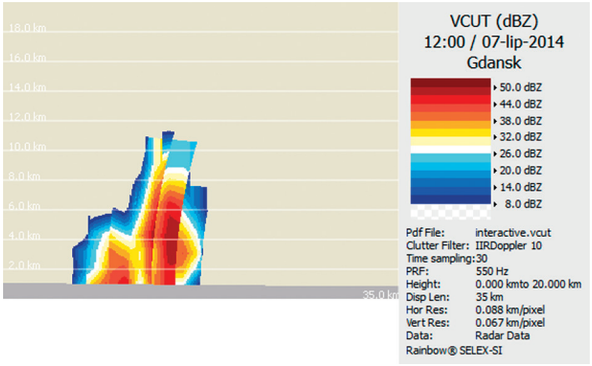

Figure 4. Vertical cross-section of the radar echoes recorded by the Gdańsk-Rębiechowo radar on July 07, 2014 at 12.00 UTC

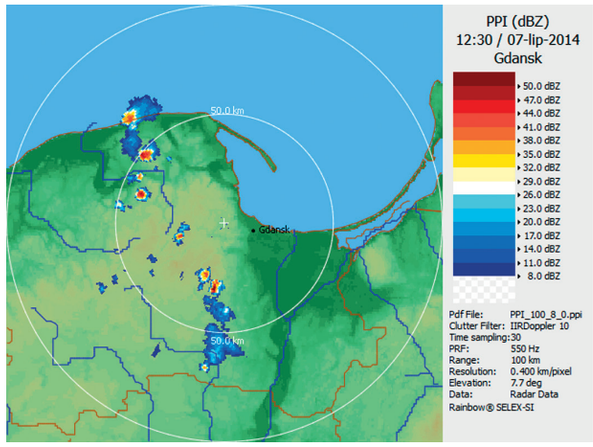

Figure 5. Radar image of horizontal distribution of maximum radiolocation reflectivity recorded for the scanning elevation angle of 7.7° by the Gdańsk-Rębiechowo radar on July 07, 2014 at 12.30 UTC

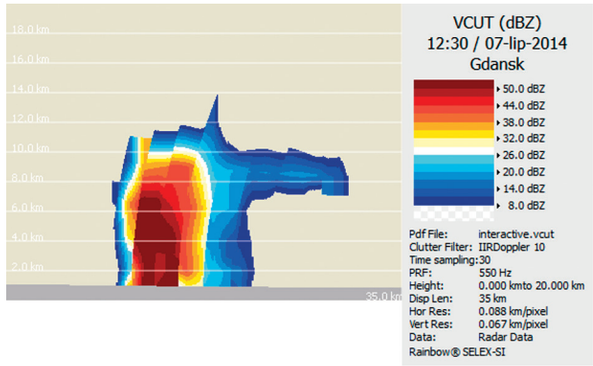

Figure 6. Vertical cross-section of the radar echoes recorded by the Gdańsk-Rębiechowo radar on July 07, 2014 at 12.30 UTC

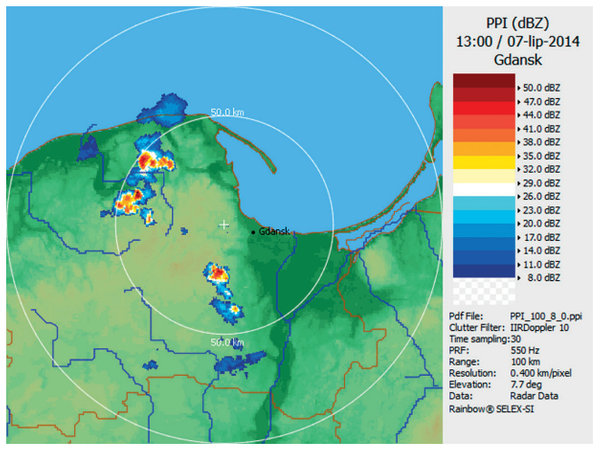

Figure 7. Radar image of horizontal distribution of maximum radiolocation reflectivity recorded for the scanning elevation angle of 7.7° by the Gdańsk-Rębiechowo radar on July 07, 2014 at 13.00 UTC

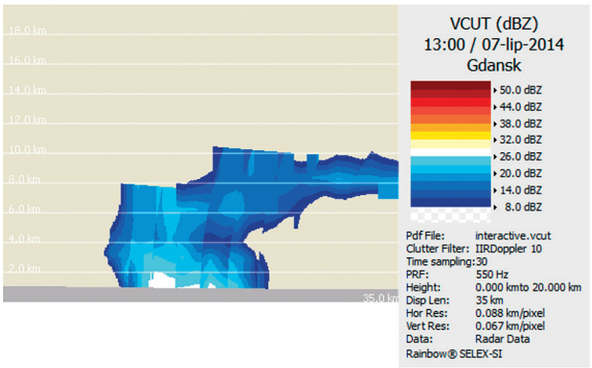

Figure 8. Vertical cross-section of the radar echoes recorded by the Gdańsk-Rębiechowo radar on July 07, 2014 at 13.00 UTC

(in the layer between 7 and 10 km) (Figure 6). The diameter of the incus cloud under the tropopause exceeded 20 km (Figure 5).

Analysis of the radar data at 13.00 UTC indicated that the studied cloud started to decay. The radar image acquired by scanning the atmosphere at the antenna beam elevation angle of 7.7° still showed the tops of the radar echo from the cloud shifted slightly to the east (Figure 7). Analysis of the vertical cross-section of the radar echo indicated that the incus was at an altitude of about 10 km while its horizontal dimensions remained unchanged; however, the maximum value of radiolocation reflectivity decreased to 20–26 dBZ (Figure 8).

Quantitative analysis of the convective clouds development process

Analysis of the convective cloud development was conducted using the Gdańsk-Rębiechowo radar data acquired from measurements made on July 7th, 2014 between 11.40 and 13.00 UTC at 10-minute intervals. Upper air sounding data acquired from the Łeba station on July 7th, 2014 at 12.00 UTC were also used.

The maximum radiolocation reflectivity changes for antenna scans at beam elevation angles between 0.5° and 7.7° are presented in Figure 9. The maximum radiolocation reflectivity observed for the scanning elevation angles between 0.5° and 5.3° increased in the period from 11.40 UTC (measurement #1) to 12.00 UTC (measurement #3). The radiolocation reflectivity reached its maximum values for all scanning angles in the period from 12.00 UTC to 12.30 UTC (measurement #6). In the same time interval, the maximum radar echo at the highest elevation angle (7.7°) was also recorded. In the phase of maximum cloud development, at the antenna beam elevation angle of 3.4°, the maximum radiolocation reflectivity of 54 dBZ was recorded at an altitude of about 4 km. Vertical development of the cloud was also observed until it reached the tropopause (12 km), along with increasing values of radiolocation reflectivity of the radar echo height from 24.5 to 42 dBZ. Between 12.30 UTC and 13.00 UTC (measurement

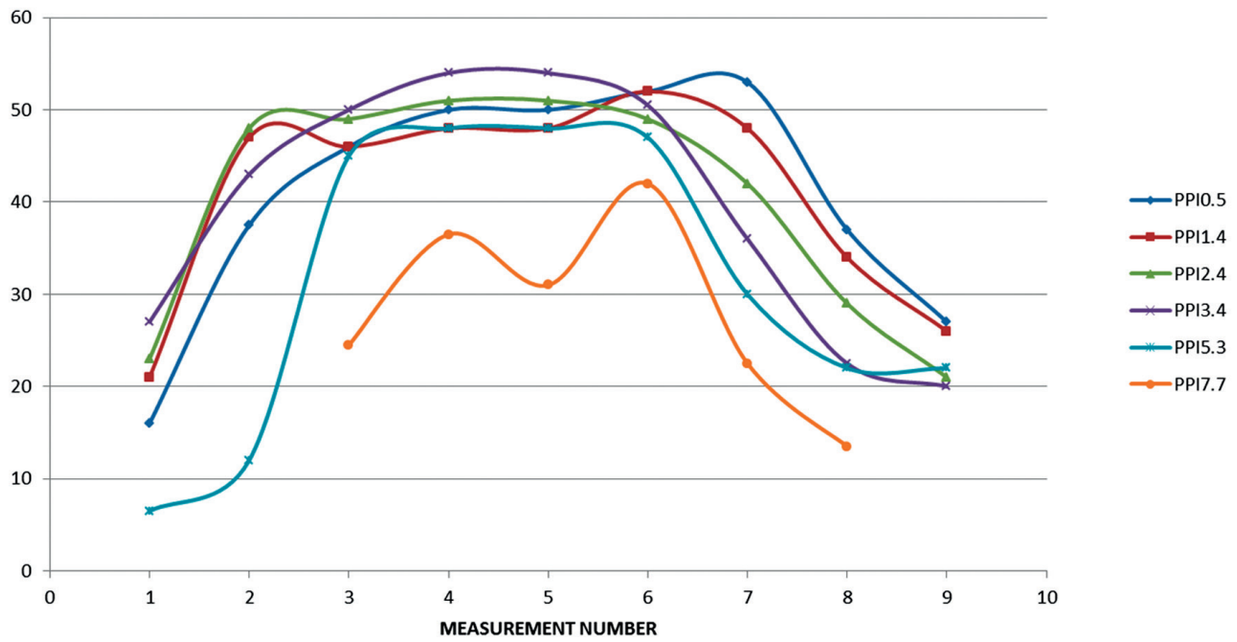

Figure 9. The maximum radiolocation reflectivity changes for antenna scans at beam elevation angles between 0.5° and 7.7° on July 7th, 2014 between 11.40-13.00 UTC

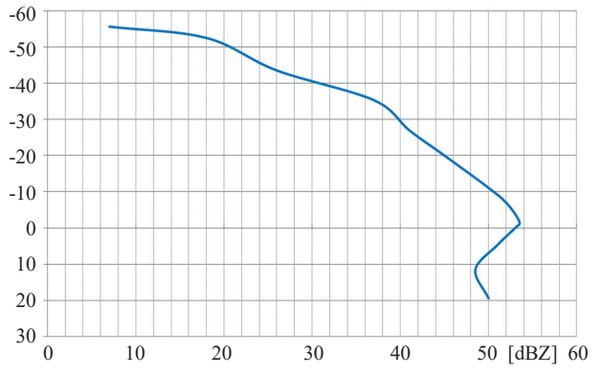

Figure 10. The maximum radiolocation reflectivity changes with temperature. Radar data of July 7th, 2014 at 12.30 UTC, upper air sounding data at 12.00 UTC

#9) the beginning of cloud dissipation was observed, along with rapidly decreasing values of radiolocation reflectivity to 27–22 dBZ and decreasing altitude of the cloud tops to 10 km.

Vertical profiles of maximum radiolocation reflectivity changes were determined to assess the structure of the cloud. The vertical profile of air temperature along the vertical axis was derived from upper air sounding data (Figure 10).

In the lower part of the cloud, composed of water droplets of various sizes, up to the 0°C isotherm level (3.6 km), the radiolocation reflectivity increased up to 54 dBZ. The large values of radiolocation reflectivity were due to the increasing size of water droplets, beyond the limit assumed for cloud droplets and up to the range of size of rain droplets. In radar meteorology, water droplets with radius larger than 100 μm are considered as rain droplets (Moszkowicz & Tuszyńska, 2006).

At higher altitudes, a gradual decrease of radiolocation reflectivity, up to 48 dBZ, was observed in the freezing layer with air temperature between 0°C and –12°C (5.8 km). This part of the cloud is a mixture of water droplets, super cooled water and ice crystals. The physical state of cloud particles significantly influences radiolocation reflectivity, which is related with the change of the effective scatter surface of the particles (1).

Above the –12°C isotherm the value of radiolocation reflectivity significantly decreases to 7 dBZ, which is related with varying concentration of ice crystals (1), (2).

The radar and upper air sounding data were used to the derive values of parameters and indicators (Table 1) that describe the thermodynamic state of the atmosphere. They are also used to formulate forecasts concerning weather phenomena that may pose threats to land, air and sea transport.

Analysis of the measurement results and meteorological observations at the Łeba station indicate that there was a storm in the vicinity of the station between 12.00 and 13.00 UTC.

Conclusions

Radar data are a reliable source of information about the state of the atmosphere and developing processes. Cloud system studies should use raw radar data acquired by scanning the atmosphere at selected antenna beam elevation angles. Radar products commonly available in weather data exchange networks, in most cases, do not enable to conduct quantitative analysis of the radar echoes.

It is important to take into account the impact of environmental and microclimatic conditions on the studied processes in order to obtain reliable results of radar data processing. Further research including

Table 1. Parameters describing convection conditions and weather phenomena occurrence probability for the region of the Łeba station in the afternoon of July 7th, 2014

Parameter	Value	Interpretation
	Radar data	
Y Algorithm	43.2	Radar echo from the thunderstorm cloud
ZHAIL Algorithm	$H_{max} > H_{45+5\,dBZ}$	Moderate hail
	Upper air sounding data	
Showalter Index – SSI	–1.14°C	Increased probability of thunderstorm
Convection Index – LI	–1.86°C	Thunderstorm possible (when strong forcing occurs)
Global Index – TT	50°C	Single intensive thunderstorms
Whaitinge Index – K	34.30	Probability of thunderstorm – 60 to 80%
Convective Available Potential Energy – CAPE	360.50 J/kg	Weak convection
Equilibrium Level – EL	241.83 hPa	Convective cloud height – ~10 900 m
Free Convection Level – LFC	770.13 hPa	Strong convection
Richardson Number – R_b	29.66	Conditions favorable to supercells formation

comparison and verification of radar data against direct measurements, upper air soundings and satellite data is necessary to increase the reliability of the computational results that qualitatively and quantitatively characterize the specific processes and weather phenomena.

The interpretation of radar measurements requires consideration of the influence of the atmosphere on electromagnetic wave propagation (atmospheric refraction). It is also necessary to take into account the impact of radar technical parameters on the results. The selected beam width and emitted impulse length cause an in increase, with increasing distance from the radar, in the measured geometric dimensions of the observed elements of the atmosphere (to which the radiolocation reflectivity is related).

Digital processing applied to radar echoes enables to determine additional characteristics of the state of the atmosphere, e.g. detecting turbulence, recognizing weather phenomena classes, intensity of precipitation and water sums over a selected region.

For operational hydrometeorological support, an important feature of radar measurements is the capability of covering an area of about 30,000 km^2 in real time with high temporal resolution (practically continuous measurement cycles).

Acknowledgments

The research was conducted and the paper was prepared by the personnel of the Department of Geographic Information Systems within Research project No. 23-933.

References

1. Büyükbas, E. et al. (2005) Training course on weather radar systems. Module A: Introduction to radar, WMO, Turkey.
2. Geçer, C. (2005) Training course on weather radar systems. Module D: Radar products and operational applications, WMO, Turkey.
3. Moszkowicz, S. & Tuszyńska, I. (2006) *Meteorologia radarowa. Podręcznik użytkownika informacji radarowej IMGW*. Warszawa: Instytut Meteorologii i Gospodarki Wodnej.
4. Szturc, J. (2004) *Teledetekcja satelitarna i radarowa w meteorologii i hydrologii*. Bielsko-Biała: Wydawnictwo Akademii Techniczno-Humanistycznej.
5. Tuszyńska, I. (2011) *Charakterystyka produktów radarowych*. Warszawa: Instytut Meteorologii i Gospodarki Wodnej – Państwowy Instytut Badawczy.
6. wetter3 (2014) [Online] Available from: www1.wetter3.de [Accessed: April 20, 2016]

Scientific Journals
of the Maritime University of Szczecin

Zeszyty Naukowe
Akademii Morskiej w Szczecinie

2016, 48 (120), 88–95
ISSN 1733-8670 (Printed)
ISSN 2392-0378 (Online)
DOI: 10.17402/181

Received: 29.04.2016
Accepted: 07.07.2016
Published: 15.12.2016

Analysis of ship domains in traffic separation schemes

Zbigniew Pietrzykowski✉, **Janusz Magaj**

Maritime University of Szczecin, Faculty of Navigation
1–2 Wały Chrobrego St., 70-500 Szczecin, Poland
e-mail: {z.pietrzykowski; j.magaj}@am.szczecin.pl
✉ corresponding author

Key words: navigation, safety, ship domain, Traffic Separations Schemes, natural limitations, criterion

Abstract
The ship domain is a criterion of safety assessment in ship encounter situations. This criterion allows us to identify dangerous situations in open sea and restricted areas, the latter characterized by natural limitations such as the shore line, or artificial ones e.g., boundaries of Traffic Separation Schemes (TSSs). This article analyzes ship domains in TSSs. These schemes, being established in areas where vessel traffic is intensive, as a rule have virtual *traffic lanes* that indicate the direction of vessel traffic flow. The influence of the ship size and type on domain shape and size in a TSS has been examined. The domains have been defined on the basis of AIS data and statistical methods. The analyzed ship domains have been approximated by ellipses. The authors have determined intervals of changes in domain parameters.

Introduction

Heavy vessel traffic in frequented shipping routes and port approaches, increasingly larger ships, and higher shipping velocities create real threats to the safety of navigation. Traffic Separation Schemes (TSSs) are introduced in such areas to assure navigation safety and aim at proper management of traffic flows. The areas where a TSS is in operation are regarded as restricted areas. However, the constraining boundaries of these areas are virtual boundaries, as opposed to the physical boundaries of a shipping waterway (breadth, depth, navigational obstructions and dangers).

As the virtual restrictions of the area must be observed, and taking into account the volume of vessel traffic, it is often difficult or just impossible to use the situation assessment criteria commonly used in the high seas i.e. the closest point of approach (CPA) and the time to the closest point of approach. The Ship Domain, an alternative to CPA, is defined as the area around the ship which should be kept clear of other objects (Fuji & Tanaka, 1971; Zhao, Wu & Wang, 1993; Pietrzykowski, 2008). Unlike the CPA, using the Ship Domain, the navigator can change its shape and size. This criterion allows the navigator to identify dangerous situations in both open waters and restricted areas, where maneuvering is limited by natural and man-made restrictions. A number of factors, including the human element, make the formal description difficult and limit its applicability (Fuji & Tanaka, 1971; Zhao, Wu & Wang, 1993; Rutkowski, 1998; Śmierzchalski & Weintrit 1999; Zhu, Xu & Lin, 2001; Pietrzykowski, 2008; Pietrzykowski & Uriasz, 2009; Wang et al., 2009; Wielgosz & Pietrzykowski, 2012; Hansen et al., 2013; Wang, 2013; Marcjan & Gucma, 2014; Pietrzykowski & Magaj, 2016). The research in this field aims at developing methods for Ship Domain determination and verification, mainly in restricted areas, where the maneuvering areas are limited by the physical dimensions of the area. One may expect that the shapes and sizes of Ship Domains proceeding in a TSS may differ from corresponding domains in the above mentioned areas.

The use of identified domains of ships moving in a TSS will enable automatic identification of dangerous situations and provide for appropriate countermeasures such as anti-collision maneuvers.

The research area

TSS Bornholmsgat

TSS is a traffic management route system governed by IMO regulations. Specific traffic lanes are designated to point out the general direction of traffic flow within the scheme. The responsibility of the International Maritime Organization for ships' routing is formulated in the SOLAS Convention, Chapter V, Regulation 10, according to which the Organization is the only international body for establishing such systems (SOLAS, 1974). Ships' routing systems contribute to safety of life at sea, safety and efficiency of navigation, and/or protection of the marine environment. Rule 10 of the COLREGs (IMO, 1972) prescribes the conduct of vessels when navigating through traffic separation schemes adopted by the IMO. However, this in no way relieves ships from compliance with other COLREG rules. It should be noted that some TSSs exist that are not governed by the IMO.

The traffic lanes in these routing systems are marked by virtual boundaries, i.e. if a ship violates a lane boundary, it does not necessarily imply direct risk of grounding or collision with a land structure. In many cases the vessel intersects the TSS. In such situations, the ships shall cross on a heading orthogonal to the general direction of traffic flow.

Dense regions of vessel traffic, organized using separate lanes and virtual boundaries, allow us to expect that the safety criteria (safe distances to other objects) will be different from those determined in similar encounters in open waters or areas restricted, for example, by shore line.

The Baltic Sea has a number of traffic separation schemes: TSS Adlergrund, TSS Bornholmsgat, TSS North of Rügen and TSS Słupska Bank (Pietrzykowski, Wołejsza & Magaj, 2015). Figure 1 presents the TSS Bornholmsgat with six traffic lanes.

Intensive traffic in that area includes vessels of various type and size, proceeding both to and from the Danish Straits and the Kiel Canal towards the Eastern Baltic Sea.

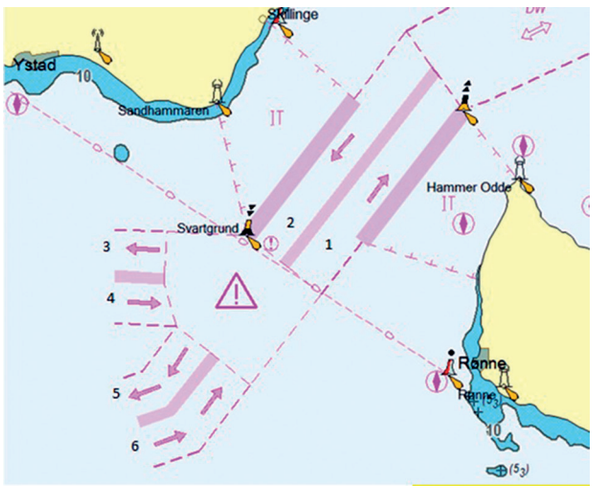

Figure 1. TSS Bornholmsgat; six areas of traffic lanes (Pietrzykowski, Wołejsza & Magaj, 2015)

Vessel traffic

This analysis, based on vessel traffic data from the AIS over four days in June 2011, examines traffic in lanes No. 1 and 2 TSS Bornholmsgat and takes into account various ship types and sizes.

332 ships were recorded on the traffic lane 1 and 347 ships on the traffic lane 2. The prevailing types were bulk carriers, tankers and passenger ships (Tables 1 and 2). One can see similar numbers of

Table 1. Vessel traffic flows in analyzed TSS. Traffic lane No. 1

Ship type	Length [m]					Total
	<50	<100	<150	<200	≥200	
passenger	2	–	5	10	10	27
bulker	3	75	80	48	9	215
tanker	1	5	20	16	14	56
Total	6	80	105	74	33	298

Table 2. Vessel traffic flows in the analyzed TSS. Traffic lane No. 2

Ship type	Length [m]					Total
	<50	<100	<150	<200	≥200	
passenger	2	–	3	4	13	22
bulker	1	74	82	62	16	235
tanker	3	4	25	18	6	56
Total	6	78	110	84	35	313

Table 3. Vessel traffic flows in the analyzed TSS

Ship type	2011 – 4 days traffic lanes 1 and 2		Year 2011*	
	Number	%	Number	%
passenger	49	7	2 823	5
bulker	450	67	35 576	61
tanker	112	17	10 700	18
other**	64	9	9 577	16
Total	675	100	58 676	100

* source (HELCOM, 2011), ** without unidentified crafts.

ships within the examined traffic lanes for each corresponding ship type and size.

The comparison of these data to statistical data on vessel traffic in the examined area in the years 2006–2012, published in (HELCOM, 2011) shows a similar percentage share of each type of vessel.

The process of domain determination

The domain identification process is complex due to a large number of variable factors affecting domain shape and size. For example, these factors may include the type and parameters of the area, or whether or not a traffic separation scheme is present in the case under consideration. Various methods of domain determination using analytical techniques, statistical methods, or artificial intelligence may be found in the literature (Fuji & Tanaka, 1971; Rutkowski, 1998; Śmierzchalski & Weintrit 1999; Zhu, Xu & Lin, 2001; Pietrzykowski, 2008; Pietrzykowski & Uriasz, 2009; Wang et al., 2009; Hansen et al., 2013; Marcjan & Gucma, 2014; Pietrzykowski & Magaj, 2016). Approaches based on statistical methods or artificial intelligence make use of simulation studies based on operator controlled ship handling simulators and real data records on vessel movements, primarily AIS data.

In this study, ship domain determination in TSS areas makes use of ship tracks recorded in the AIS system. The distances between ships are analyzed. The procedure of ship domain determination consisted of the following steps (Pietrzykowski & Magaj, 2016):

1. Transformation of the data of ships moving within the TSS from real motion display to relative motion display, where the origin of the coordinate system is fixed to the AIS antenna position on the ship.
2. Determination of ship track density.
3. Selection of the domain determination method.
4. Ship domain determination – identification of domain parameters for the examined shipping areas, taking into consideration the types and dimensions of the recorded ships.

Figure 2 presents ship tracks recorded in the real motion display and, after transformation, relative motion display.

Densities of ship tracks were determined by dividing the area around the vessel into 37 m long squares (0.02 Nm) and counting the recorded tracks in each square. Then the track density values were standardized to the interval [0, 1] (Figure 3).

The ship domain was defined on the basis of ship track densities. To this end, the area around the ship

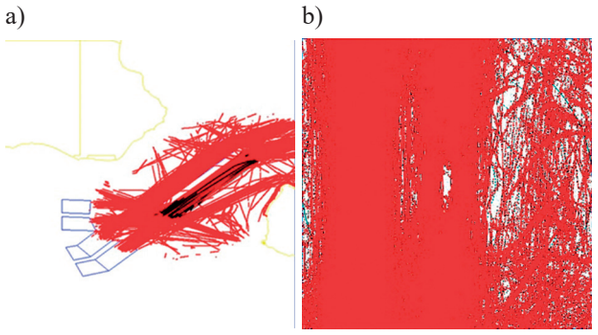

Figure 2. Tracks of ships in TSS Bornholmsgat, traffic lane 1: a) true motion, b) relative motion

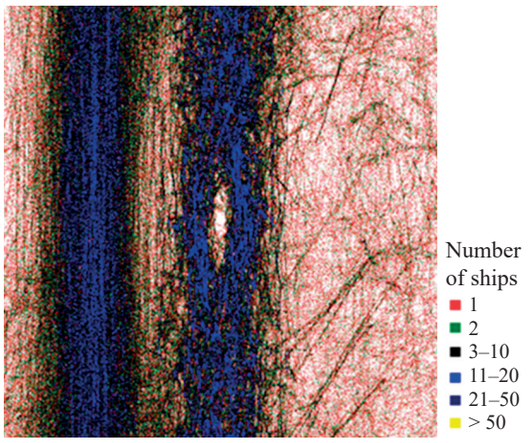

Figure 3. Ship track density in TSS Bornholmsgat, traffic lane 1 (Pietrzykowski & Magaj, 2016)

was divided into 72 five-degree sectors. Each sector was assigned a point defining the ship domain boundary/limit. The following criteria were used in this step: cut-off mechanism (7.5%) and the first maximum (Figure 4).

Due to irregularities of the shape, the determined domains were approximated to ellipses. The ellipses were described using the following parameters: x, y – shift of the ellipse center relative to the ship's antenna position, a, b – lengths of the ellipse minor and major semi-axes, α – angle of ellipse rotation (Figure 5).

The research

Domains of selected type ships

The presented method of domain determination was used to identify ship domains in the selected traffic lane 1 of the TSS Bornholmsgat. Table 4 shows the domain parameters for three types of ships: passenger, bulk carrier and tanker. TSS Bornholmsgat. The previously mentioned method of domain determination has been used.

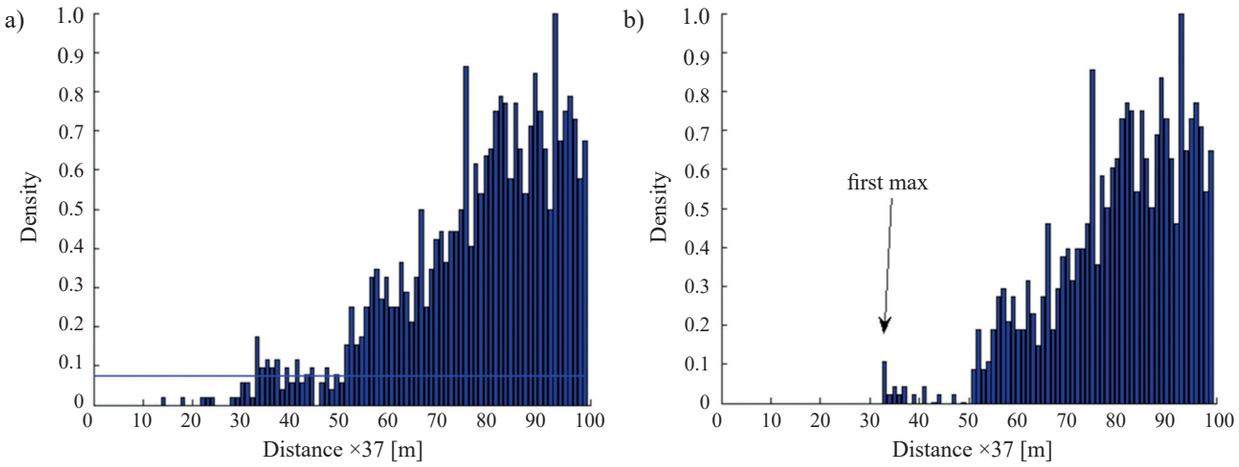

Figure 4. The method of determining the domain boundary for a selected sector 0–5°: a) cut-off mechanism; b) determination of the first maximum (Pietrzykowski & Magaj, 2016)

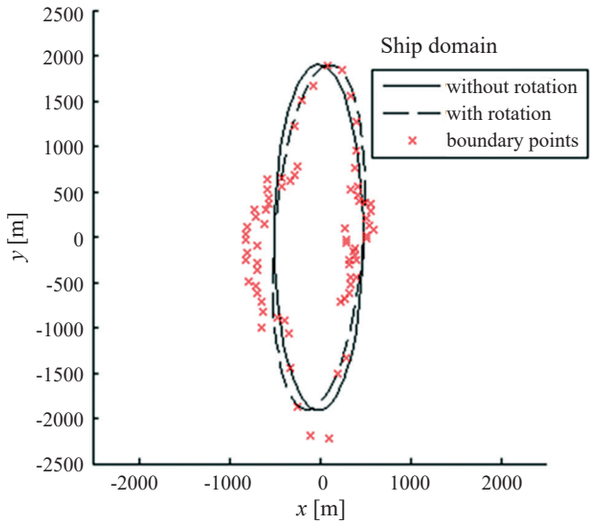

Figure 5. Ship domain boundary points and ship domains for the traffic lane No. 1 TSS Bornholmsgat (1) ellipse rotation angle α is not taken into account; (2) with ellipse rotation angle α

Figure 6 depicts the determined ship domains.

Figure 7 presents values of the determined ellipse parameters for each ship group. Tankers, with average length of 161 m, were observed to have larger domains compared to other cargo vessels (average length 90 m), which may be explained by the differences in ship size and the number of ships sailing in the area.

Because the incoming and outgoing TSS traffic is disturbed, we performed more detailed research. To this end, the traffic at the 3 Nm sections where ships enter and leave the TSS was neglected, only the central section of the traffic lane 1 was analyzed. Tables 5 and 6 show the domain parameters with and without domain rotation.

Figure 8 presents the values of determined ellipse parameters for the selected cases. A slight increase of domain size was observed for the central section

Table 4. Elliptical domain parameters of a ship for the traffic lane 1 TSS Bornholmsgat, without and with taking into account the ellipse rotation angle α; a – semi-major axis; b – semi-minor axis; c – shift of the ellipse center in x-direction; d – shift of the ellipse center in y-direction

Type	Parameter				
	α [deg]	a [m]	b [m]	c [m]	d [m]
passenger, bulker and tanker	0	503	2054	–10	–8
	5.1	499	1924	–9	–1
bulker	0	444	2128	–15	–6
	3.7	431	1962	–7	0
tanker	0	600	2356	–8	–6
	6.1	599	2123	–7	–3

Table 5. Domain parameters of a ship (ellipse) for selected sections of the traffic lane 1 TSS Bornholmsgat (without rotation); a – semi-major axis; b – semi-minor axis; c – shift of the ellipse center in x-direction; d – shift of the ellipse center in y-direction

Ships' type	Parameter				
	Traffic lane	a [m]	b [m]	c [m]	d [m]
passenger, bulker and tanker	whole	503	2054	–10	–8
	the central section	545	2165	–21	–8
bulker	whole	444	2128	–15	–7
	the central section	489	2188	–15	–10
tanker	whole	600	2356	–8	–6
	the central section	605	2356	–15	–7

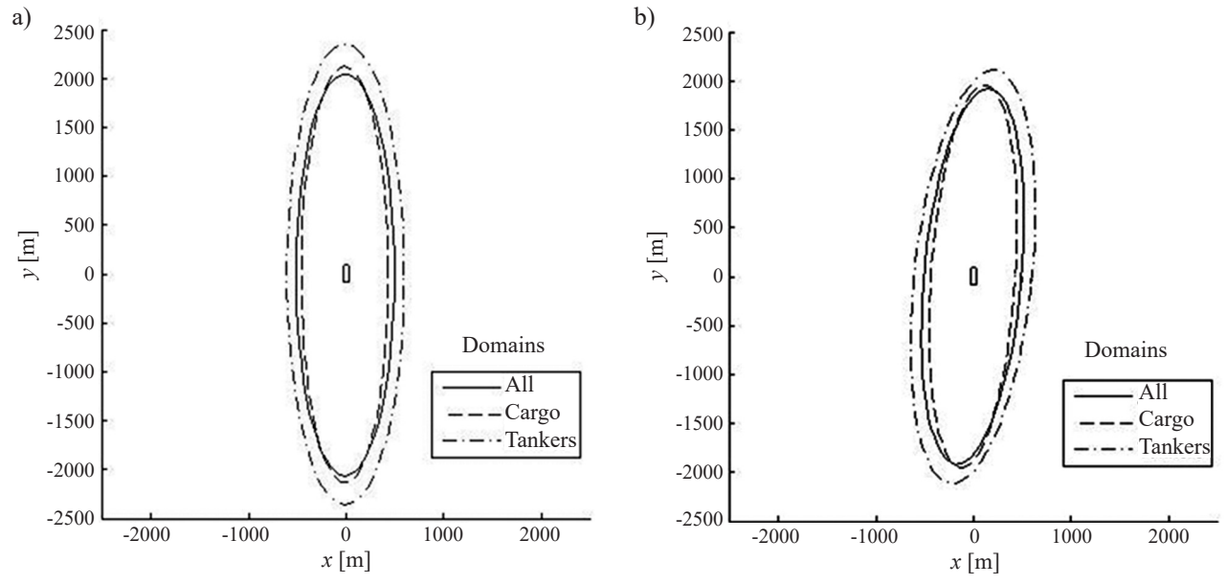

Figure 6. Ship domain for traffic lane 1 TSS Bornholmsgat: a) without the ellipse rotation angle *α*; b) with the ellipse rotation angle *α*

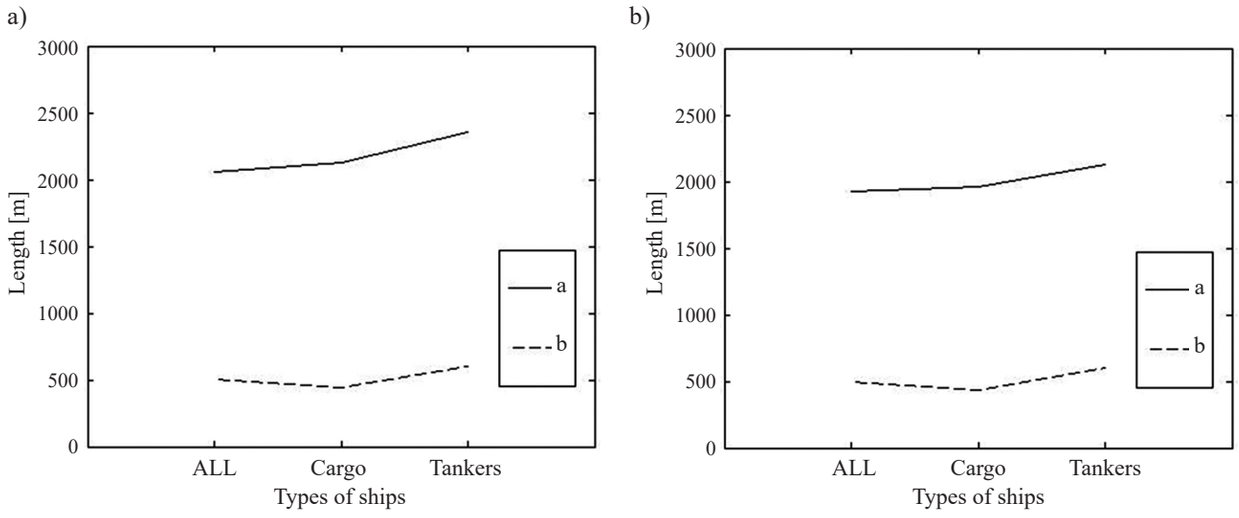

Figure 7. Ship domain parameters a and b for the traffic lane 1 TSS Bornholmsgat: a) without the ellipse rotation angle *α*; b) with the ellipse rotation angle *α*

Table 6. Domain parameters of a ship (ellipse) for selected sections of the traffic lane 1 TSS Bornholmsgat (with rotation); *a* – semi-major axis; *b* – semi-minor axis; *c* – shift of the ellipse center in *x*-direction; *d* – shift of the ellipse center in *y*-direction

Ships' type	Parameter					
	Traffic lane	*α* [deg]	*a* [m]	*b* [m]	*c* [m]	*d* [m]
passenger, bulker and tanker	whole	5.1	499	1924	–9	–1
	the central section	3.9	542	2237	–8	–1
bulker	whole	3.7	431	1962	–7	0
	the central section	3.3	495	2125	–4	–4
tanker	whole	6.1	599	2123	–7	–3
	the central section	4.6	599	2456	–4	–1

of the traffic lane 1. Besides, a significant increase of the major axis b was found in the rotated ellipse. Supposedly, this increase is an effect of less ordered traffic at both ends of the traffic lane.

Domains of various size ships

Various size ships were analyzed, where ship length was the size criterion. All ships were divided into four size groups by length: 1) 50–100 m; 2) 100–150 m; 3) 150–200 m; 4) over 200 m. Like in the case of various ship types, we examined the traffic lane 1 TSS Bornholmsgat. Table 7 shows the domain parameters for the mentioned ships sizes. The same method of domain determination has been used.

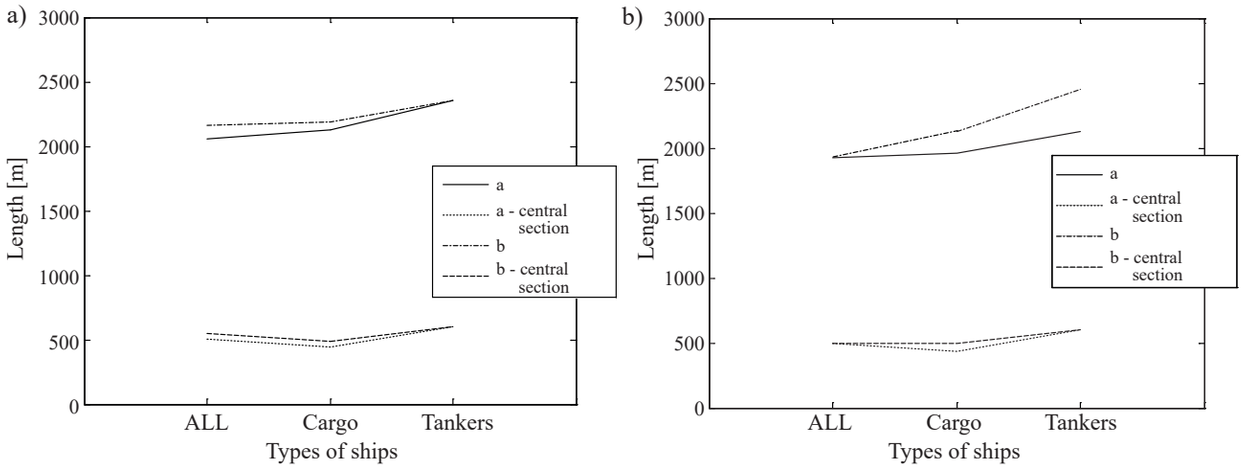

Figure 8. Ship domain parameters a and b for selected sections of the traffic lane 1 TSS Bornholmsgat: a) without the ellipse rotation angle *α*; b) with the ellipse rotation angle *α*

Table 7. Domain parameters of a ship (ellipse) for the traffic lane 1 TSS Bornholmsgat, without and with taking into account the ellipse rotation angle α; *a* – semi-major axis; *b* – semi-minor axis; *c* – shift of the ellipse center in *x*-direction; *d* – shift of the ellipse center in *y*-direction

Ship's length [m]	Parameter				
	α [deg]	*a* [m]	*b* [m]	*c* [m]	*d* [m]
50–100	0	390	2222	–20	–8
	3.6	401	2193	–8	1
100–150	0	437	2049	–18	–11
	1.6	430	2058	–6	–8
150–200	0	656	2448	–17	14
	0.7	648	2620	–5	3
> 200	0	529	2915	20	7
	1.6	526	2905	6	1

Figure 9 depicts the determined ship domains. The observed domain size increase was in line with ship length. No significant size difference was found between domains with or without rotation. A slight angle of rotation decreases with ship size, except for ships > 200 m, which may be due to a small size of the sample (The sample size of ships >200 m was half that for ships 150–200 m in length).

Figure 10 presents the values of determined ellipse parameters for the selected cases.

In this case, too, more detailed research was done due to less ordered traffic of vessels at the entrance and exit of the TSS lane. In this connection, the traffic at the 3 Nm sections where ships enter and leave the TSS lane was neglected, and only the central section of the traffic lane 1 was analyzed.

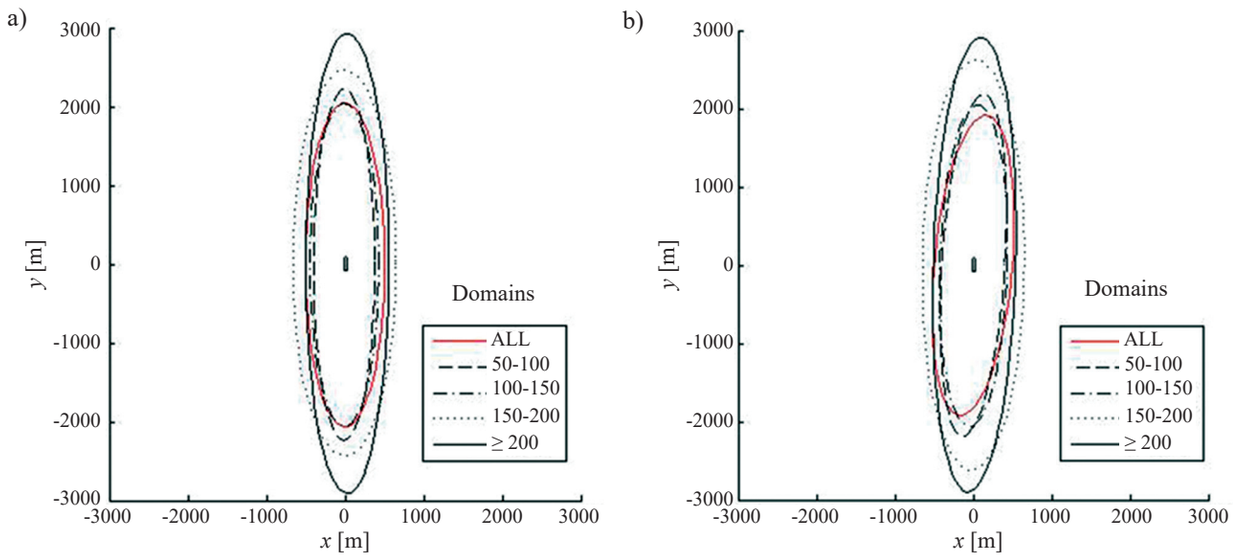

Figure 9. Ship domain for traffic lane 1 TSS Bornholmsgat: a) without the ellipse rotation angle *α*; b) with the ellipse rotation angle *α*

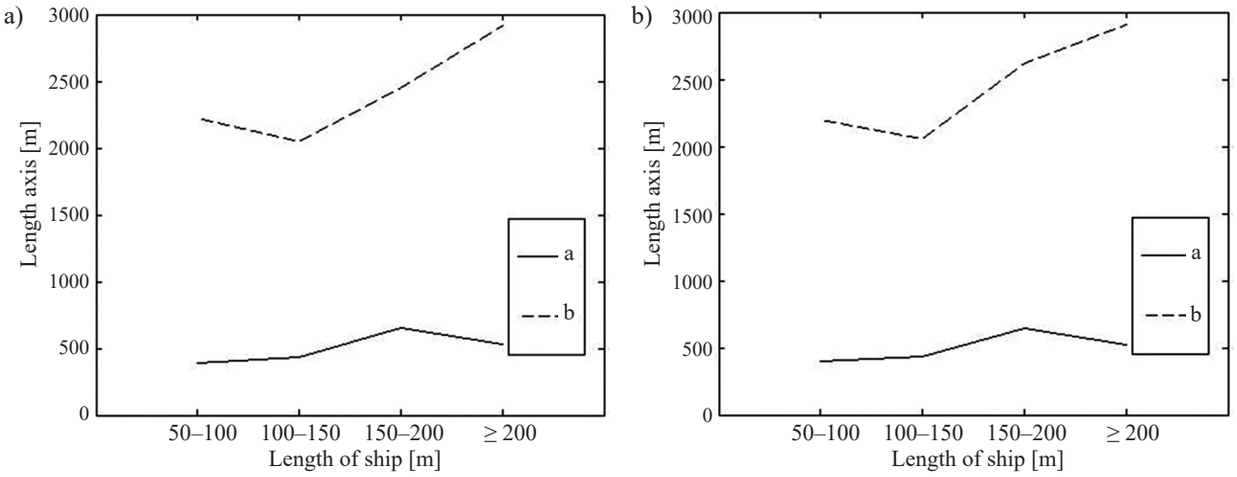

Figure 10. Ship domain parameters a and b for traffic lane 1 TSS Bornholmsgat: a) without the ellipse rotation angle *α*; b) with the ellipse rotation angle *α*

Table 8. Domain parameters of a ship (ellipse) for selected sections of the traffic lane 1 TSS Bornholmsgat (without rotation); *a* – semi-major axis; *b* – semi-minor axis; *c* – shift of the ellipse center in *x*-direction; *d* – shift of the ellipse center in *y*-direction

Ship's length [m]	Parameter				
	Traffic lane	*a* [m]	*b* [m]	*c* [m]	*d* [m]
50–100	whole	390	2222	–20	–8
	the central section	445	2329	–21	–21
100–150	whole	437	2049	–18	–11
	the central section	538	2002	–16	10
150–200	whole	656	2448	–17	14
	the central section	720	2307	–19	7
> 200	whole	529	2915	20	7
	the central section	585	3146	20	–6

Table 9. Domain parameters of a ship (ellipse) for selected sections of the traffic lane 1 TSS Bornholmsgat (with rotation); *a* – semi–major axis; *b* – semi–minor axis; *c* – shift of the ellipse center in *x*-direction; *d* – shift of the ellipse center in *y*-direction

Ship's length [m]	Parameter					
	Traffic lane	*α* [deg]	*a* [m]	*b* [m]	*c* [m]	*d* [m]
50–100	whole	3.6	401	2193	–8	1
	the central section	0.5	436	2499	–10	3
100–150	whole	1.6	430	2058	–6	–8
	the central section	3.9	522	2156	–4	2
150–200	whole	0.7	648	2620	–5	3
	the central section	0.1	704	2369	–5	7
> 200	whole	1.6	526	2905	6	1
	the central section	0.2	574	3144	8	0

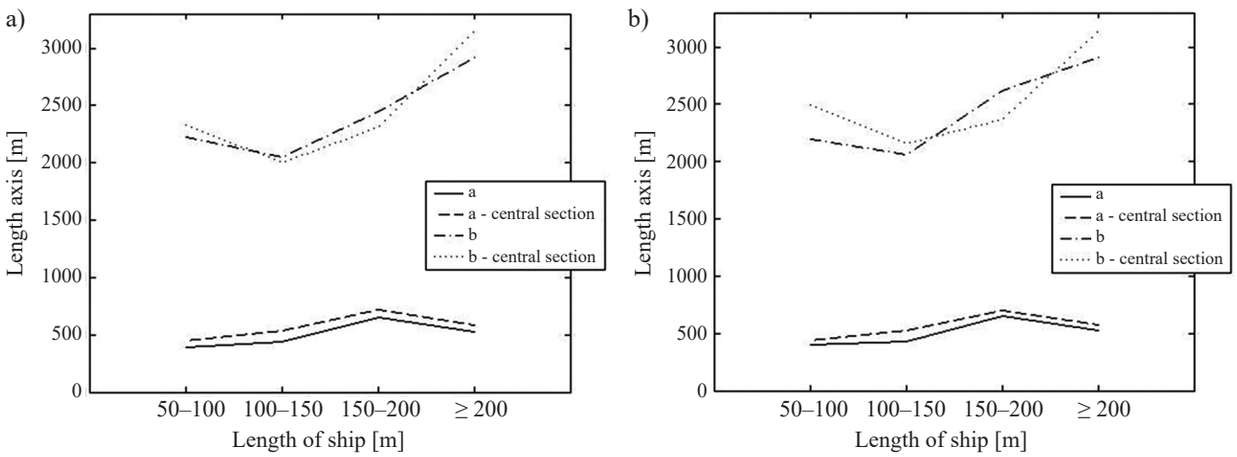

Figure 11. Ship domain parameters a and b for selected sections of the traffic lane 1 TSS Bornholmsgat: a) without the ellipse rotation angle *α*; b) with the ellipse rotation angle *α*

Tables 8 and 9 show domain parameters with and without domain rotation.

Figure 11 depicts values of the determined ellipse parameters for the selected cases. The domain length significantly increases (major axis b) as the ship length increases, while the domain breadth (minor axis a) changes slightly.

Conclusions

The authors have made a preliminary analysis of ship domains for various types and sizes of ships. The ship size visibly affects the ship domain, although its breadth grows slightly. Tankers were observed to have larger domains compared to bulk carriers. It should be noted, however, that the average length of tankers was greater than the average length of bulk carriers. Hence we may conclude that the ship type does not have much impact on ship domain size.

We plan to continue the research to cover the other traffic lanes in the TSS Bornholmsgat and other TSSs to verify the conclusions derived in this article.

Acknowledgments

This research outcome has been achieved under the research project No. 1/S/ITM/2016 financed from a subsidy of the Ministry of Science and Higher Education for statutory activities of Maritime University of Szczecin.

References

1. Fuji, Y. & Tanaka, K. (1971) Traffic Capacity. *Journal of Navigation* 24. pp. 543–552.
2. Hansen, M., Jensen, T., Lehn-Schiøler, T., Melchild, K., Rassmussen, F. & Ennemark, F. (2013) Empirical ship domain based on AIS data. *Journal of Navigation* 66.
3. HELCOM (2011) Helsinki Commission, Baltic Marine Environment Protection Commission, Report on shipping accidents in the Baltic Sea area during 2011. [Online] Available from: http://www.helcom.fi/Lists/Publications/Annual%20report%20on%20shipping%20accidents%20in%20the%20Baltic%20Sea%20area%20during%202011.pdf [Accessed: April 28, 2016]
4. IMO (1972) COLREGs, Międzynarodowe przepisy o zapobieganiu zderzeniom na morzu (MPZZM).
5. Marcjan, K. & Gucma, L. (2014) Wykorzystanie analizy incydentów nawigacyjnych w celu oceny bezpieczeństwa nawigacyjnego na obszarach Morza Bałtyckiego o dużym zagęszczeniu ruchu statków. *Prace Naukowe Politechniki Warszawskiej. Transport* 102. 77–86.
6. Pietrzykowski, Z. & Magaj, J. (2016) Ship Domains in Traffic Separation Schemes. *Scientific Journals of the Maritime University of Szczecin* 45 (117). pp. 143–149.
7. Pietrzykowski, Z. & Uriasz, J. (2009) The ship domain – a criterion of navigational safety assessment in an open sea area. *Journal of Navigation* 62.
8. Pietrzykowski, Z. (2008) Ship's fuzzy domain – a criterion of navigational safety in Narrow Fairways. *Journal of Navigation* 61.
9. Pietrzykowski, Z., Wołejsza, P. & Magaj, J. (2015) Navigators' Behavior in Traffic Separation Schemes. *Journal on Marine Navigation and Safety of Sea Transportation* (TRANSNAV) 9, 1. pp. 123–128.
10. Rutkowski, G. (1998) Domena statku a bezpieczeństwo nawigacji na akwenach trudnych pod względem nawigacyjnym. *Prace Wydziału Nawigacyjnego Akademii Morskiej w Gdyni* 6.
11. SOLAS (1974) Międzynarodowa konwencja o bezpieczeństwie życia na morzu. IMO.
12. Śmierzchalski, R. & Weintrit, A. (1999) *Domeny obiektów nawigacyjnych jako pomoc w planowaniu trajektorii statku w sytuacji kolizyjnej na morzu*. III Sympozjum Nawigacyjne, Gdynia.
13. Wang, N. (2013) A novel analytical framework for dynamic quaternion ship domains. *Journal of Navigation* 66.
14. Wang, N., Meng, X., Xu, Q. & Wang, Z. (2009) A unified analytical framework for ship domains. *Journal of Navigation* 62.
15. Wielgosz, M. & Pietrzykowski, Z. (2012) Ship domain in the restricted area – analysis of the influence of ship speed on the shape and size of the domain. *Scientific Journals Maritime University of Szczecin* 30 (102). pp. 138–142.
16. Zhao, J., Wu, Z. & Wang, F. (1993) Comments of ship domains. *Journal of Navigation* 46.
17. Zhu, X., Xu, H. & Lin, J. (2001) Domain and its model based on neural networks. *Journal of Navigation* 54.

Scientific Journals
of the Maritime University of Szczecin

Zeszyty Naukowe
Akademii Morskiej w Szczecinie

2016, 48 (120), 96–104
ISSN 1733-8670 (Printed)
ISSN 2392-0378 (Online)
DOI: 10.17402/182

Received: 29.04.2016
Accepted: 02.11.2016
Published: 15.12.2016

Navigational and legislative constraints for optimization of ocean routes in the Northern Pacific Ocean

Maciej Szymański✉, **Bernard Wiśniewski**

Maritime University of Szczecin, Faculty of Navigation, Institute of Marine Navigation
1–2 Wały Chrobrego St., 70-500 Szczecin, Poland
✉ corresponding author, e-mail: mszymanski@interia.pl, b.wisniewski@am.szczecin.pl

Key words: route programming, SPOS system, Bon Voyage system, navigational constraints, legislative constraints, Northern Pacific

Abstract
A ship sailing between the coasts of China, Japan, Korea and the Western coast of North America must cross navigational and geographical barriers of the Kuril Islands Archipelago and Aleutian Chain. Passes between the islands are particularly difficult and hazardous in winter. Most of them are covered by drifting ice for 5 months of the year. A number of allowed passes and offshore routes had been established by the maritime authorities of Alaska on the Bering Sea and in Aleutian Chain. However, use of other passes and routes is limited to exceptional cases only. Similar regulations exist in the Okhotsk Sea and other waters under Russian jurisdiction. The ship must then give grounds for a deviation from recommended or allowed passes and tracks and report other required information. Since January 1, 2015, it is mandatory to use the low sulphur fuel oil (sulphur content no higher than 0.01%) in the main propulsion system and auxiliary machinery when navigating inside the Emission Control Area (ECA) zone. Ships face a constant dilemma whether to remain in the ECA zone for the shortest or longer period of time, if the fuel and cost gain in relation to the entire route justify that. Available decision making support systems, like SPOS and Bon Voyage, do not solve that issue satisfactorily.

Introduction

A navigator solving the task of a voyage planning in the Northern Pacific Ocean is restricted in his/her choice of routes by a number of legislative and navigational constraints existing in the area. The article aims to highlight these practical problems that mariners currently face when solving the issues of route programming and optimization in the Northern Pacific Ocean.

Weather conditions in the northern Pacific Ocean

In general, the choice of route in the Northern Pacific is determined by the shape of the coast: they generally follow the Great Circle. The Great Circle route from Luzon Strait to the coast of British Columbia in Canada leads through the Japan Sea and Bering Sea and the Great Circle linking the Luzon Strait with the coast of California leads close to the port of Yokohama and South of Aleutian Chain. This is the shortest track, however, in most cases it leads through areas of inclement weather and unfavorable currents (UK Hydrographic Office NP136, 2014).

Weather in the Northern Pacific is shaped by the high pressure systems over the ocean and low pressure systems travelling eastwards along the Aleutian Chain. In summer, north of latitude 40N, favorable and warm weather prevails over the eastern part of the Northern Pacific, which favors sailing along the Great Circle. Also possible are low-pressure areas, or depression, which bring poor weather conditions over the eastern part of the region and intense fogs over the western part. In winter the Aleutian Low deepens and moves west of Bristol Bay (57° 30' N, 160° 30' W) over the western Aleutian Chain. Violent storms move from the coasts of China and

Japan towards the center of the Aleutian Low and the storms from the central Pacific travel north-west over the Gulf of Alaska. These storms bring rain, snow, and strong violent storms more often than on the Northern Great Circle routes (UK Hydrographic Office NP136, 2014).

Climatic routes in the Northern Pacific Ocean

Routes in the Northern Pacific Ocean do not show seasonal changes. The same routes can be used both in winter and in summer. Much more important is the direction, eastward or westward, in which the ship travels through the ocean. The Eastward route (from Japan to Canada), depends mainly on the actual surface pressure situation and navigational considerations of the voyage. Routes through the Bering Sea should be chosen when the high pressures systems are located there (UK Hydrographic Office NP136, 2014).

Ships proceeding westward should choose either the northern routes, north of Aleutian Chain, or the routes south of 35°N when the northern routes are excluded due to unfavorable weather conditions. Routes north of Aleutian Chain are located north of average storm routes. The Aleutian Chain is a natural breakwater, limiting the height of seas and swell arriving from the Northern Pacific Ocean (UK Hydrographic Office NP136, 2014).

Navigational constraints in route planning and programming in the Northern Pacific Ocean

Ocean routes based on the Great Circle in the Northern Pacific leading both west and east encounter certain geographical barriers which can significantly constrain navigation and affect the choice of route and its programming. A ship sailing between the cost of China and the western coast of North America must cross the following geographical and navigational constraints:

- Passes from the Sea of Japan to the Northern Pacific through the Tsugaru Strait and Soya/La Perouse Strait;

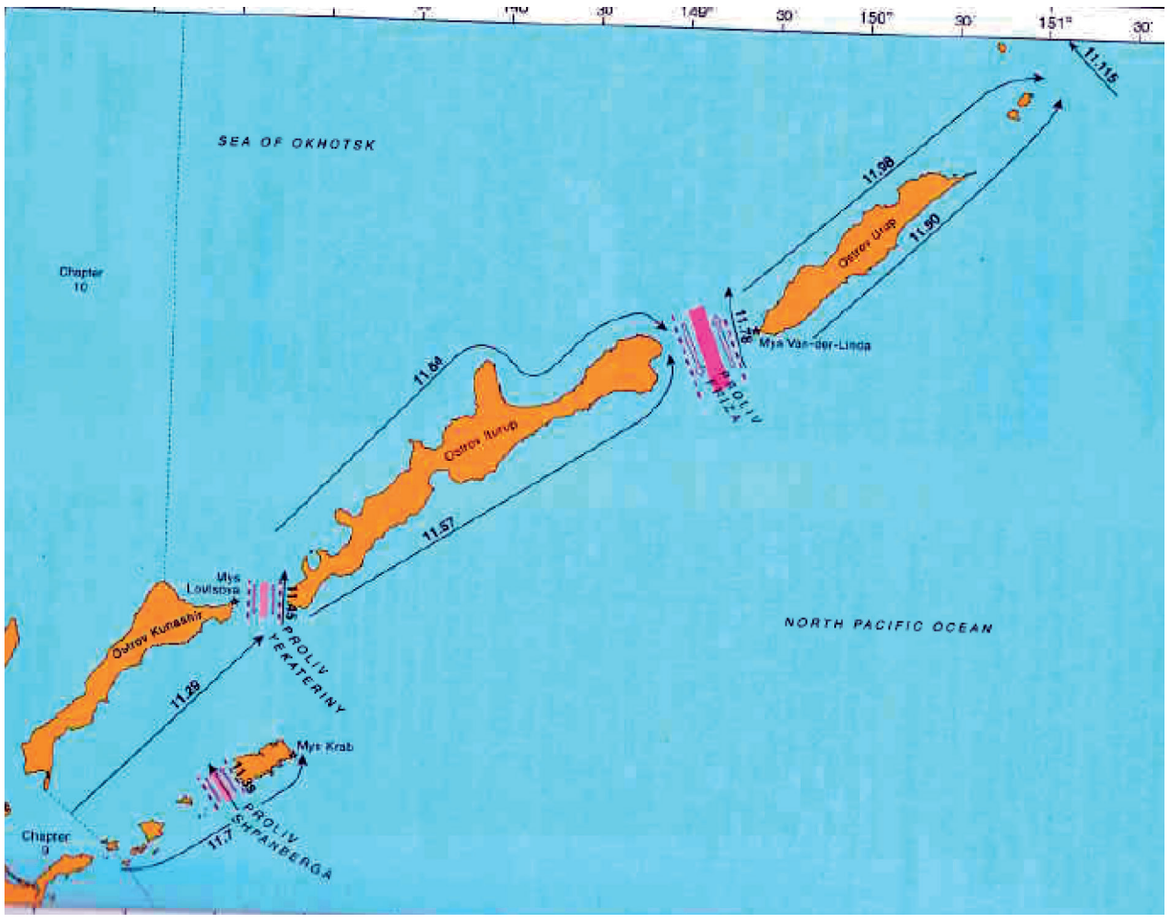

Figure 1. Kuril Islands – southern part (UK Hydrographic Office NP41, 2014)

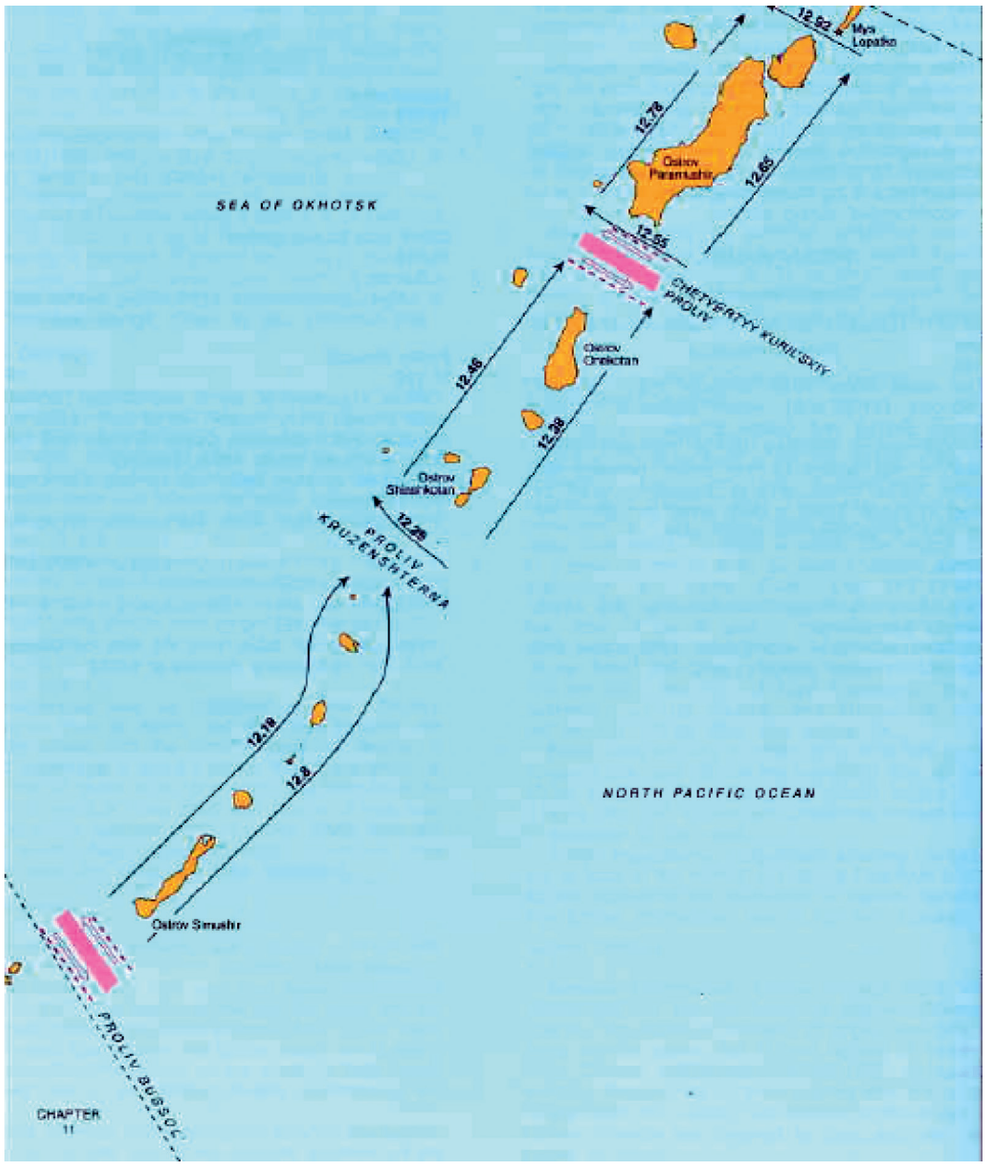

Figure 2. Kuril Islands – northern part (UK Hydrographic Office NP41, 2014)

- Sea of Okhotsk;
- Passes from the Okhotsk Sea to the Northern Pacific Ocean between the islands in Kuril Archipelago;
- Aleutian Chain and passes from the Northern Pacific Ocean to the Bering Sea and Unimak Pass.

Tsugaru Strait is the most convenient pass linking the Sea of Japan and the Pacific Ocean, between the Japanese islands of Honsiu and Hokkaido. It is broad, deep, and ice free all year round. Soya (La Perouse) Strait between the Japanese island of Hokkaido and Russian island of Sakhalin is navigationally less favorable. It is constrained or even blocked by ice for a large part of the year. Fast ice is usually present along the northern shores of Hokkaido and in the southern part of the Soya (La Perouse) Strait from mid-December until the end of March, and sometimes even longer. Drift ice forms along the eastern coast of Sakhalin and travels southward with current and wind reaching the northern shores of Hokkaido in mid-January. The greatest concentration of drift ice in Soya (La Perouse) Strait and along the northern Hokkaido occurs in February and March. Surrounding waters are then one big ice field consisting of dense ice floats 1–2 m thick in which it is impossible for ships to navigate. Ice gets also into the Sea of Japan. Drift ice remains in the Soya (La Perouse) Strait until the end of April and sometimes even until mid-May. As a result, navigation in the Strait for these 5 months of the year is possible only with icebreaker assistance. Moreover, between

February and April even the icebreakers have great difficulty keeping the waterway open for sea traffic.

There are a number of passes to the Pacific Ocean in the Kuril Archipelago (Figures 1 and 2). They are: Nemuro Strait, Proliv Yekateriny, Proliv Friza, Proliv Bussol, Proliv Kruzenshterna, Chetvertyj Kurilskyj Proliv, Pervyj Kurilskyj Proliv. Only three of them: Proliv Bussol, Proliv Kruzenshterna and Chetvertyj Kurilskyj Proliv are ice free all year round. Navigation in the remaining ones between February and mid-May is only possible with great deal of difficulty or not possible at all.

The Southern part of Okhotsk Sea is in principle ice free, however drift ice can be encountered occasionally.

The Southern part of the Bering Sea and all passes from the Bering Sea into the Pacific Ocean in Aleutian Chain are ice free all year round. The following passes are navigationally accessible for large, ocean faring ships: Unimak Pass, Akutan Pass, Umnak Pass, Samalga Pass and Amukta Pass Fox Islands, Seguam Pass, Atka Pass, Adak Strait, Tanaga Pass, Oglala Pass and Amchitka Pass in Andreanof Islands, the pass between the islands Amchitka and Semisopochnoi, the pass between the islands of Buldir and Kiska in Rat Islands, and passes east and west of Near Islands – respectively Buldir/Agattu Pass and north and west of Attu.

The Aleutian Chain and some of the passes in the archipelago are shown on Figures 3 and 4.

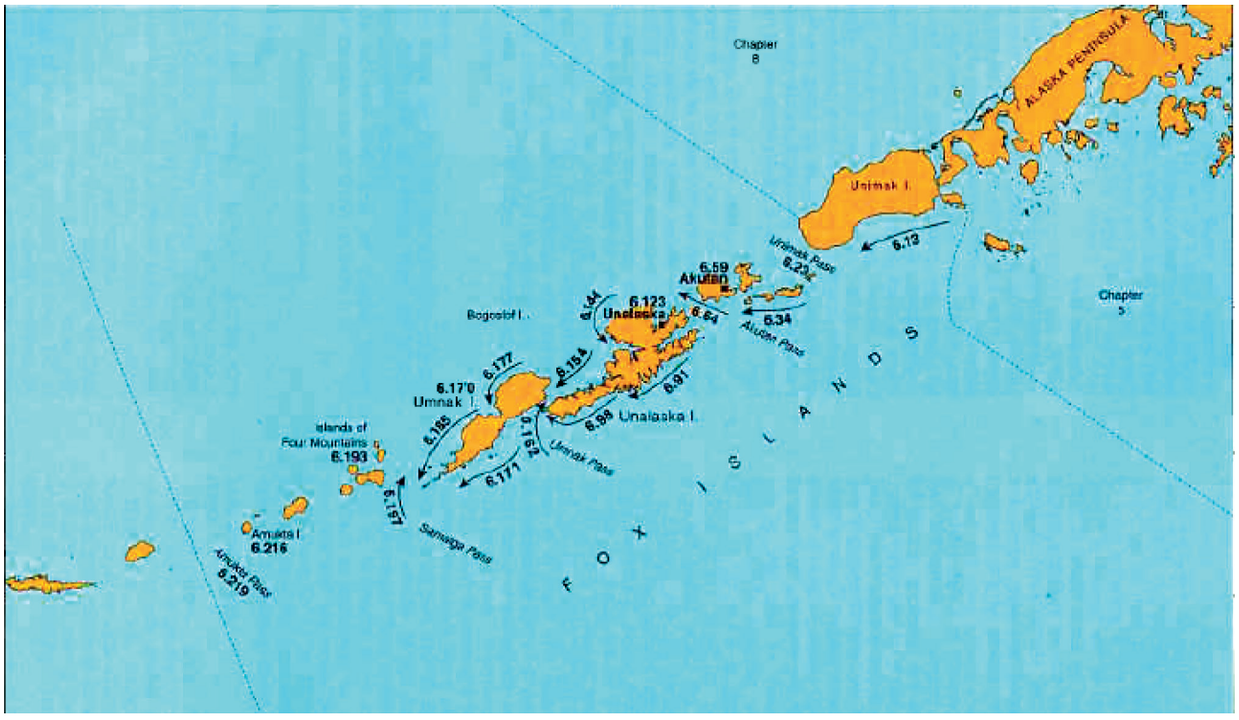

Figure 3. Aleutian Chain – eastern part (UK Hydrographic Office NP23, 2013)

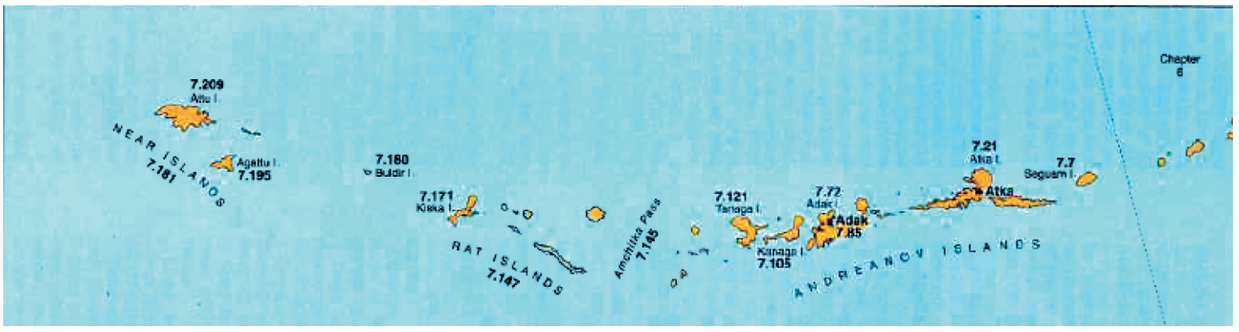

Figure 4. Aleutian Chain – western part (UK Hydrographic Office NP23, 2013)

Legislative constraints in route planning and programming in the Northern Pacific

Aleutian Chain and Bering Sea

The maritime Authorities for the State of Alaska (Alaska Maritime Prevention and Response Network) have established a number of procedures and measures reducing the risk of marine casualties (collision, grounding, oil spill) in order to protect the environment. One of them is the "offshore routing" – a procedure establishing specific routes which should be used by foreign ships transiting the Alaska waters. Foreign flagged ships should keep to those routes, despite the Innocent Passage Status, on the basis of which the voyage takes place. Offshore routing is one means of reducing the risk of marine casualties. The offshore distance provides more time for repairs to be effected by the vessel's crew if a hazardous condition develops, and provides time to respond to navigational errors and time for an assist vessel to arrive on scene before a vessel grounds (Alaska Maritime Prevention & Response Network, 2014).

Ships should keep at least 50 nautical miles offshore unless they proceed to or from the port located on the coast of Alaska, or unless they transit the Aleutian Chain through one of the allowed passes. These passes are: Unimak Pass, Amutka Pass, Amchitka Pass Buldir/Agattu Pass (Figure 5). The minimum distance from shore during transit should be at least 12 nautical miles (Alaska Maritime Prevention & Response Network, 2014).

Use of other passes is acceptable when the ship's Captain determines that, due to weather or other factors, it is safer to make use of an alternative route. In these instances, and before the deviation is made, a Notice of Deviation from Approved Route shall be made addressed to either the *Alaska Maritime Prevention and Response Network* or to the *Captain of the Port Western Alaska* as appropriate, together with the explanation of the reason for the deviation from the risk mitigation measures. The deviation is permissible only when granted by one of the above authorities. A notification to the above authorities is also required when the deviation is no longer necessary (Alaska Maritime Prevention & Response Network, 2014). Ships using the transit routes north or south of the Aleutian Chain should keep the distance of at least 50 nautical miles offshore. Transit routes are shown on Figure 6.

Recommended tracks in the Okhotsk Sea

The Russian Maritime Authorities have introduced the system of recommended routes between

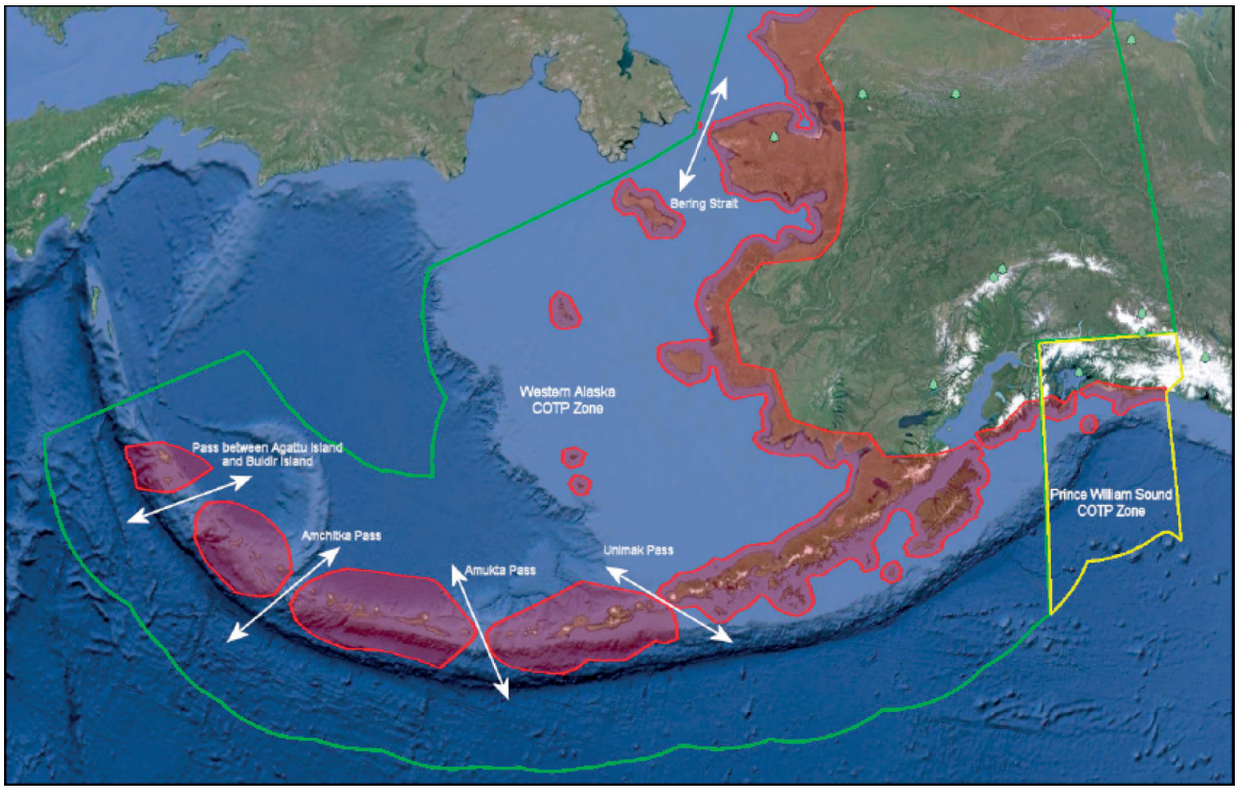

Figure 5. Allowed passes in the Aleutian Chain (Alaska Maritime Prevention & Response Network, 2014)

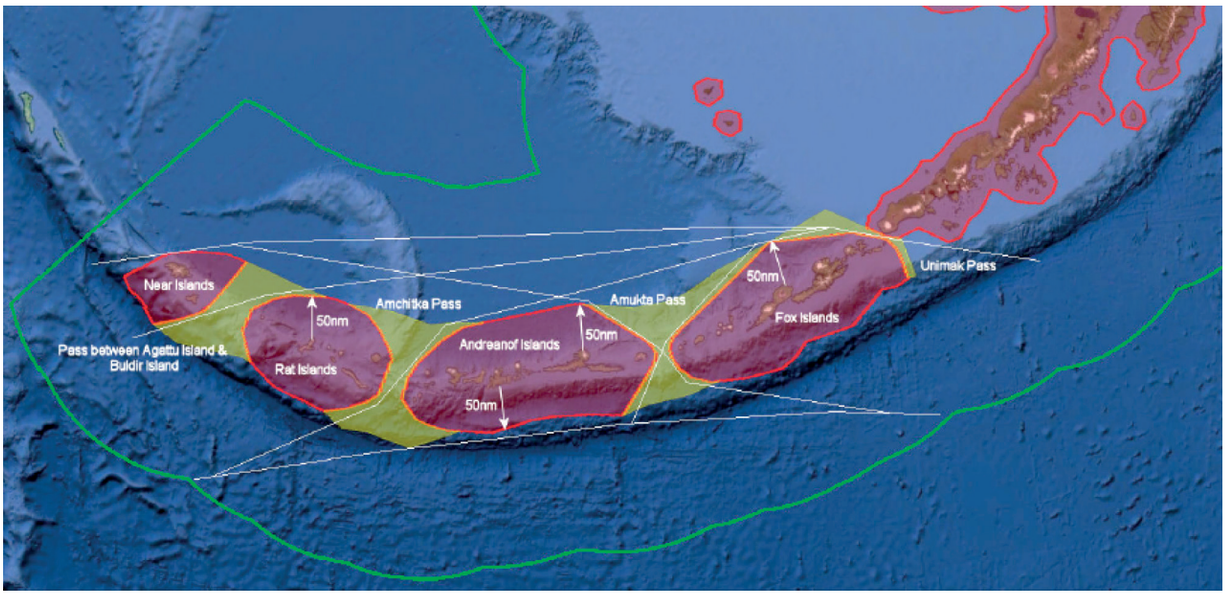

Figure 6. Offshore routes north and south of the Aleutian Chain and allowed passes in the Aleutian Chain (Alaska Maritime Prevention & Response Network, 2014)

passes in the Kuril Islands and ports on the coasts of the Federation in the Okhots Sea and on the parts of the Sea of Japan subjected to Russian maritime jurisdiction. The following routes are of the greatest significance for route optimization and weather navigation:

- Recommended route No. 1: from Nakhodka to La Perouse Strait and recommended route No. 2: from La Perouse Strait to Nakhodka.
- Recommended route No. 3: from La Perouse Strait to Chetvertyj Kurilskyj Proliv and recommended route No. 4: from Chetvertyj Kurilskyj Proliv to La Perouse Strait.

All those recommended routes are shown on Figure 7.

The recommended routes are not obligatory, however it is important to note that the local authorities may try to force the foreign flagged ships (also

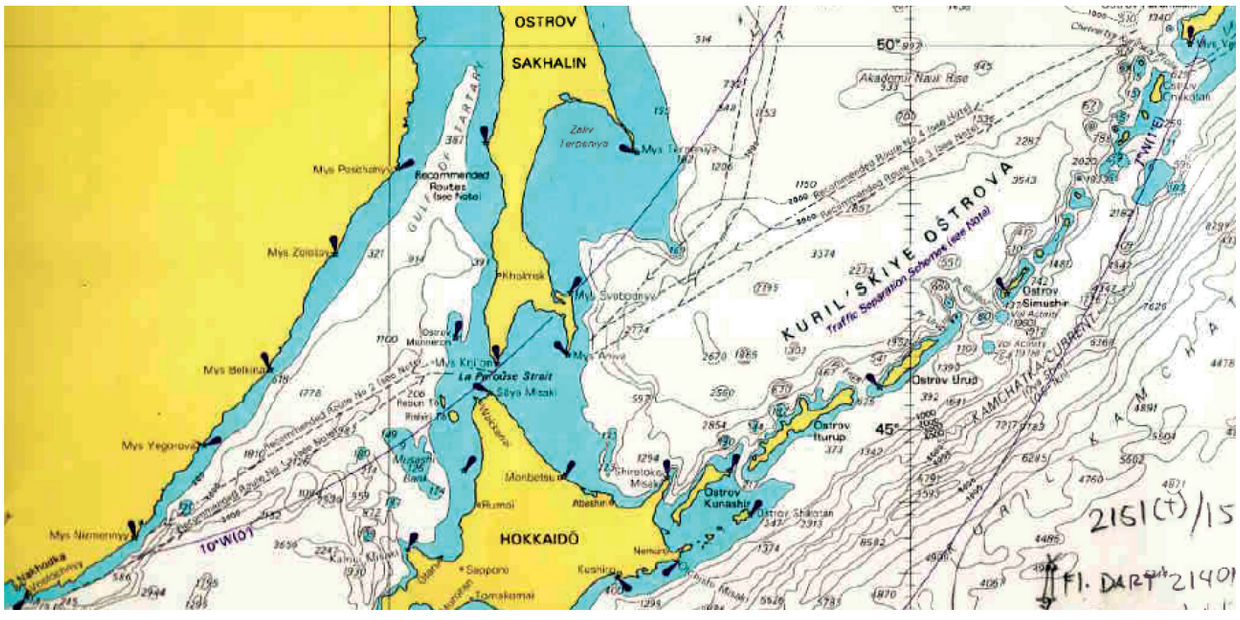

Figure 7. Recommended tracks in the Okhotsk Sea (UK Hydrographic Office BA Chart 4503)

those being in transit under the Innocent Passage rule) to use them.

North American ECA Zone

The North American ECA zone (Emission Control Area) is shown on Figure 8. The ships are obliged to use the fuel oil of sulphur content of less than 0.1% (ULFSO – Ultra Low Sulphur Fuel Oil) inside this zone starting from January 1, 2015. The necessity to switch over from HFO (High Sulphur Fuel Oil) to ULFSO may create, apart from a large scale of technical problems, also significant considerations at planning, programming and optimizing the route of the voyage.

There are technical problems related to the switchover procedure. When a ship is not equipped with two independent fuel systems (a rare and expensive solution) mixing of the fuel must be commenced soon enough in order to have pure ULFSO fuel at the moment of entry into the ECA zone. Sometimes, depending on the type of the engine, fuel mixing can last a couple of days. Such a complicated procedure requires careful planning and strict time management. The latter requirement is particularly difficult to comply with. Each amendment made to previously calculated and planned RPM (revolution per minute) settings of the main propulsion system affects the speed of fuel consumption and thus the time needed to have pure ULFSO in the system. In practice, if a correction in ship's speed is needed, it is increased rather than decreased for fuel purity. The switchover operation itself is also sometimes also long and complicated, with the need to reduce the RPM, usually to maneuvering RPM. After the changeover, RPM build up procedure is usually a complicated process as well.

All these problems result in voyage route optimization difficulties. The time necessary for fuel change over should be included in the overall route planning process. Another ever present issue is the question of how long to remain in the ECA zone: minimize the time to minimize the distance the vessel is running on a more expensive fuel, or to travel

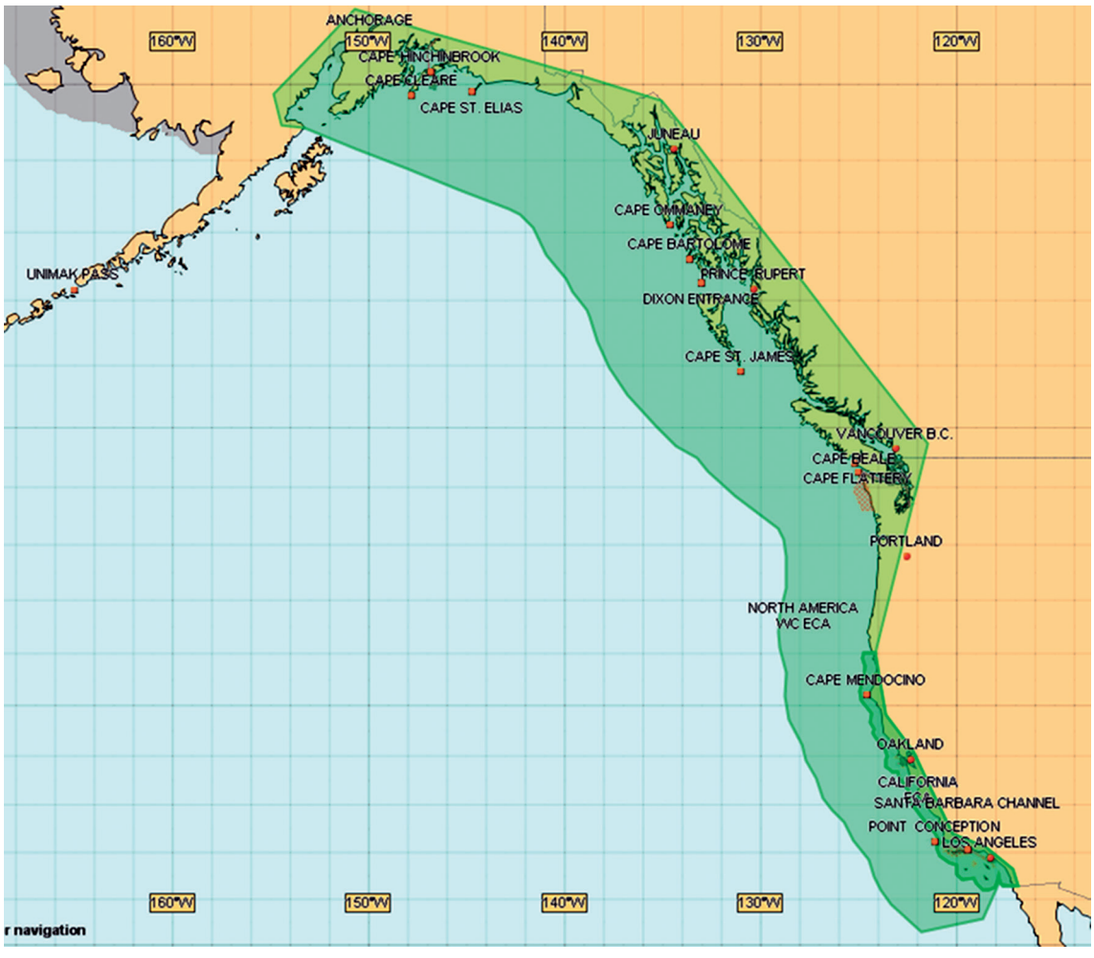

Figure 8. North American ECA Zone – western coast (Applied Weather Technologies, 2014)

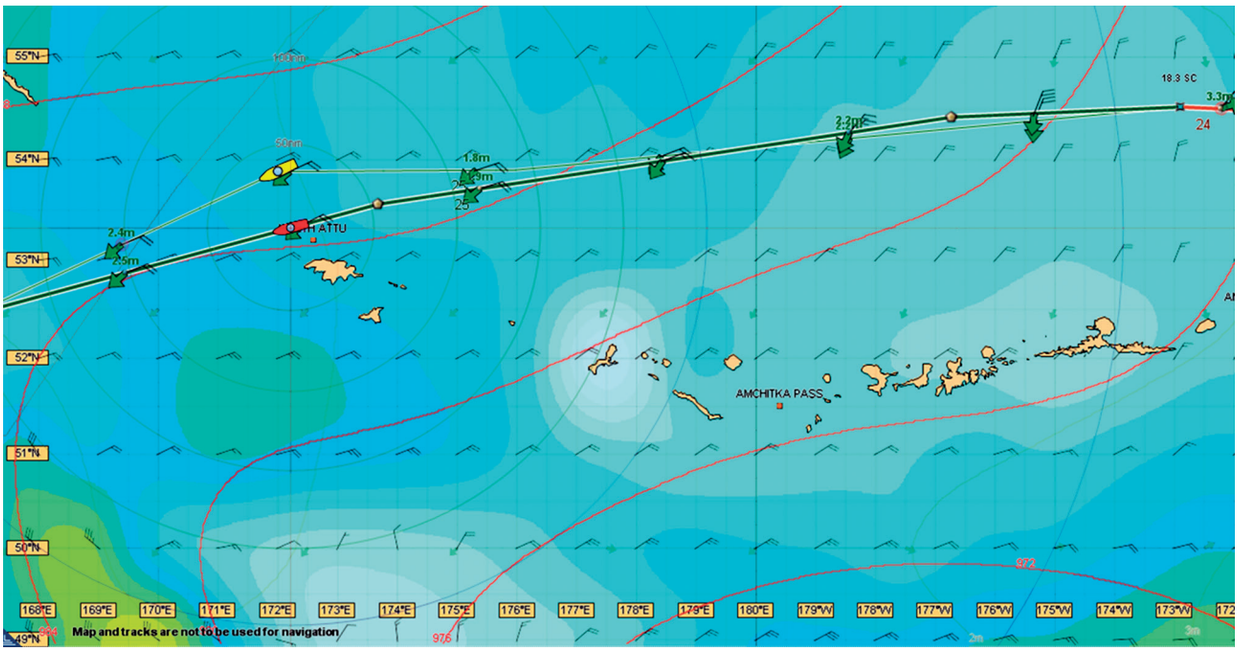

Figure 9. Route optimized in the Bon Voyage system and route programmed manually. The BV route does not meet the requirements of offshore routing (Applied Weather Technologies, 2014)

for longer period time on ULFSO to minimize fuel consumption and exposure to inclement weather conditions en route.

In most of the available route optimization systems (SPOS, Bon Voyage) this task is not solved satisfactorily and optimal solutions must be arrived at manually.

Problems in optimizing and programming of routes in the Northern Pacific Ocean – examples

Figure 9 presents the route, optimized in the *Bon Voyage* system which runs too close to the shore – less than 50 nautical miles off the Attu island (bold route, red vessel symbol). It was necessary to correct it manually (yellow vessel symbol) in order to comply with *offshore routing* requirements.

Figures 10–12 present an example of incorrect optimization of the route leading through the ECA zone with the use of *Bon Voyage* system. The route has been optimized according to the least fuel with fixed ETA (Estimated Time of Arrival) method. The route was optimized in such a way as to have the least possible distance in the ECA zone. However in this instance, the required deviation from the main route was so big that the cost of the burnt fuel had exceeded greatly the gain achieved on minimization of time and distance in the ECA zone.

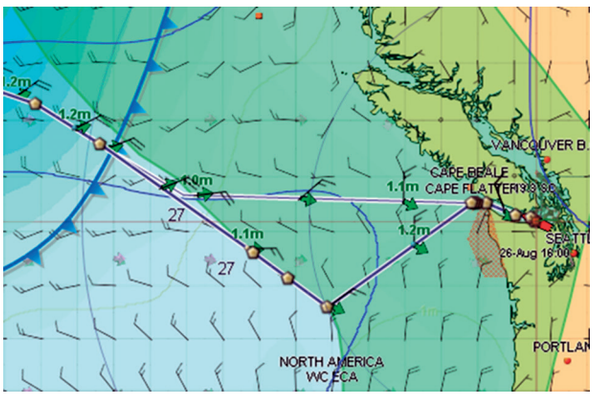

Figure 10. Route leading through the ECA Zone, optimized in the BV system (bold) and route programmed manually (Applied Weather Technologies, 2014)

Conclusions

A relatively simple and uncomplicated task of planning and programming a route of a ship in the Northern Pacific Ocean becomes a difficult and challenging one due to recently introduced (ECA, Alaska Maritime Prevention & Response Network) and already existing (recommended routes) legal frameworks and circumstances. Achieving an economical passage in terms of a total voyage cost is not always possible. Decision support and optimization tools, currently available and in use onboard the ships, like SPOS and Bon Voyage systems, do not always solve this issue properly and satisfactorily.

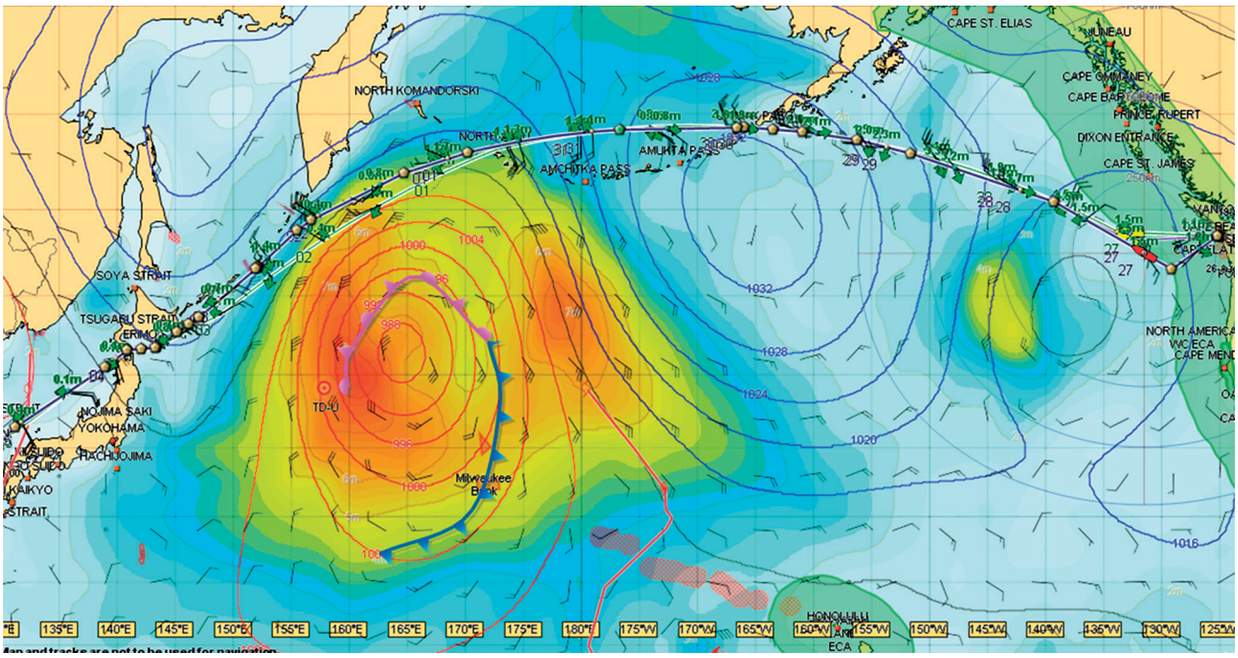

Figure 11. Route from Seattle (USA) to Pusan (South Korea)

Voyage Details Graph

Actions | Clone | Save | Close | Delete

	ETD	Departure	ETA	Arrival	Troll	nm	Hrs	T_FO	HSFO	LSFO	MDO	LSMDO	SC	WxF	CuF	SOG	Fuel(USD)
	2015/08/26 16:00	*SEATTLE*	*2015/09/05 21:00*	*BUSAN*	*19.4*	*4576*	*245.0*	*1313.3*	*1204.4*	*108.8*	*0.0*	*0.0*	*19.0*	*-0.25*	*-0.04*	*18.7*	*348795*
	2015/08/26 16:00	SEATTLE	2015/09/05 20:59	BUSAN	19.4	4661	245.0	1369.0	1289.7	79.3	0.0	0.0	19.3	-0.24	-0.02	19.0	352217

Figure 12. Calculation of costs: route optimized in BV (bold) and route programmed manually

References

1. Alaska Maritime Prevention & Response Network (2014) Western Alaska Alternative Planning Criteria for Nontank Vessels Cargo and Passanger Vessels. AK-APC-NTV Operating Porcedures for Cargo and Passengers Non Tank Vessels Transiting and Operating in Alaska Waters, August 13.
2. Applied Weather Technologies (AWT) (2014) Bon Voyage System (BVS) voyage optimization software, v. 7.0. 140 Kifer Court, Sunnyvale CA 94086.
3. UK Hydrographic Office BA Chart 4503. North Pacific Ocean. North Western Part.
4. UK Hydrographic Office NP136 (2014) Ocean Passages for the World, 6th Edition.
5. UK Hydrographic Office NP41 (2014) Admiralty Sailing Directions, Japan Pilot Volume I, 11th Edition.
6. UK Hydrpgraphic Office NP23 (2013) Admiralty Sailing Directions, Bering Sea and Strait Pilot, 8th Edition.

Scientific Journals
of the Maritime University of Szczecin

Zeszyty Naukowe
Akademii Morskiej w Szczecinie

2016, 48 (120), 105–113
ISSN 1733-8670 (Printed)
ISSN 2392-0378 (Online)
DOI: 10.17402/183

Received: 29.04.2016
Accepted: 23.11.2016
Published: 15.12.2016

Remarks on the further development of an integrated navigation system

Ryszard Wawruch

Gdynia Maritime University
3 Jana Pawła II Ave., 81-234 Gdynia, Poland, e-mail: wawruch@am.gdynia.pl

Key words: integrated navigation system, integrated bridge system, e-navigation, development, safety, restrictions

Abstract

According to the recommendation of the IMO Resolution MSC.252(83), "Adoption of the revised performance standards for integrated navigation system (INS)", the INS is introduced in order to enhance navigational safety by providing integrated and augmented functions to avoid geographic, traffic and environmental hazards. Its main task is to provide 'added value' for the officer of the watch (OOW), ship's captain and pilot, to plan, monitor or control the navigational safety and progress of the ship. The system should support navigational safety by combining, processing and evaluating inputs from different connected sensors and sources to provide information, giving timely warnings of dangerous situations, system failures and degradation of the integrity of delivered and presented information. An INS is defined as such if workstations provide multifunctional displays integrating at least the following navigational tasks (functions): route monitoring, collision avoidance and alert management. The output data contains a description of the subsystems and devices included in the INS, and the principles of their cooperation and presentation of data, but it does not present recommendations for interfacing the INS with the ship's radio communications equipment or standardised rules of operation by the user and presentation of information. These restrictions limit the possibilities of using this system in e-navigation. This paper identifies the importance of these limitations with respect to the need for further development of INSs, and presents proposals to solve this problem.

Introduction – legal aspects related to the integrated navigation system (INS)

The International Convention for the Safety of Life at Sea (SOLAS) of 1974, as amended, does not require maritime merchant vessels to be fitted with integrated navigational and/or bridge systems. According to the SOLAS Regulations V/18 and V/19.6, they may be installed on ships under the following conditions (IMO, 2014):

- They shall be subject to approval by the ship's flag state administration in accordance with the SOLAS Regulation V/18 and shall, as far as practicable, comply with performance standards not inferior to those defined in the IMO Resolution MSC.64(67) adopted on 4 December 1996, Annex 1, "Performance standard for integrated bridge systems (IBS)", and MSC.86(70) adopted on 8 December 1998, Annex 3, "Performance standard for integrated navigational systems (INS)", or MSC.252(83) adopted on 8 October 2007, "Adoption of the revised performance standards for integrated navigation systems (INS)";
- Integrated bridge systems (IBS) shall be so arranged so that failure of one sub-system is brought to the immediate attention of the officer in charge of the navigational watch (OOW) by audible and visual alarms, and does not cause failure to any other subsystem;
- In case of failure in one part of an integrated navigation system (INS), it shall be possible to operate each other individual item of equipment or part of the system separately;

- Each part of the INS performing functions assigned in the SOLAS Regulation V/19 to a specific piece of equipment or system must meet all IMO performance standards assigned to this piece of equipment or system in the resolutions mentioned in the SOLAS Regulation V/18.

As recommended by the Resolution MSC.252(83), an INS installed on ship on or after (IMO, 2007a):

- 1 January 2011, shall conform to performance standards not inferior to those specified in the Annex to this resolution;
- 1 January 2000 but before 1 January 2011, shall conform to performance standards not inferior to those specified in the Annex 3 to Resolution MSC.86(70).

Recommendation of the IMO Resolution MSC.86(70)

According to the Resolution MSC.86(70), an INS is any combination of navigational aids that provides functions beyond that of the general intent defined in the respective performance standards adopted by the IMO for individual equipment. It shall evaluate inputs from several independent and different sensors and sources, and combine them to provide information giving timely warnings of potential dangers and degradation of integrity of this information. This means that it should provide 'added value' to the functions and information needed by the officer in charge of the navigational watch (OOW) to plan, monitor and/or control the progress of the ship (IMO, 1998).

Integrity means the ability of the system to provide the user with information within a specified accuracy in a timely, complete and unambiguous manner, and alerts the user *via* alarms and indications within a specified time when the system should be used with caution or not at all. Functional integration shall meet the following requirements (IMO, 1998):

- The integrity of information should be checked by comparison of data derived independently from two or more sources if available, and verified before essential information is displayed or used;
- Information with doubtful integrity should be clearly marked and should not to be used for automatic control systems;
- Data latency should be consistent with the data requirements of the individual parts of the system;
- The validity of each part of data shall be checked before its integration;
- A failure of data exchange inside the INS should not affect any independent functionality of the integrated equipment and systems;
- A multifunction display unit shall present information and control redundantly;
- The INS shall request confirmation of the manual inputs that may cause unintended results before their acceptance, thus providing a plausibility check.

The INS shall acquire, process, store and distribute different types of information and data while applying an agreed consistent common reference system. An alarm management system complying, as a minimum, with the recommendation of the IMO Resolution A.830(19) adopted on 23 November 1995, "Code on alarms and indicators", should be provided by the INS.

Resolution MSC.86(70) defines three categories of INS (IMO, 1998):

- Category A for a system providing as a minimum, the information of position, speed, heading and time, each clearly marked with an indication of integrity;
- Category B for a system able, in addition to the functions realised by INS category A, to automatically, continually and graphically indicate the ship's position, speed and heading and, where available, depth, in relation to the planned route as well as to known and detected hazards, and correspondingly able to provide information needed for decision support in avoiding hazards;
- Category C for a system providing means to automatically control heading, track or speed and monitor the performance and status of these controls, in addition to the functions realised by INS category B.

Amendments introduced by the Resolution MSC.252(83)

The purpose of the performance standards defined in this resolution is to support the proper and safe integration of navigational functions and information, to allow the installation and use of an INS on-board ships, instead of stand-alone navigational equipment, and to promote safe procedures for the integration process both for comprehensive integration and partial integration of navigational functions, data and equipment. The INS supplements the functional requirements of the individual performance standards for particular navigational equipment and systems adopted by the IMO. Depending on the position of the ship's flag state

administration, Resolution MSC.252(83) may permit an INS being allowed to substitute for some carriage requirements of navigational equipment, as equivalent to other means under SOLAS Regulation V/19. In this case, the INS should comply with the performance standards mentioned in this resolution, and for the relevant tasks of these performance standards, with the applicable modules of the performance standards for the following navigational equipment: automatic identification system (AIS), electronic chart display and information system (ECDIS), echo sounding system (ESS), electronic position fixing system (EPFS), heading control system (HCS), radar system, speed and distance measuring device (SDMD) and track control system (TCS) (IMO, 2007a).

The described resolution does not change the general definition of an INS. According to its recommendation, the purpose of an INS is to enhance the safety of navigation by providing integrated and augmented functions to avoid geographic, traffic and environmental hazards. It supports safety of navigation by evaluating inputs from several sources, combining and integrating them to provide 'added value' for the operator to plan, monitor and/or control safety of navigation and progress of the ship, and to give them timely alerts of dangerous situations, system failures and degradation of integrity of the presented information. The system shall present timely, correct and unambiguous information to the users, and provide subsystems and subsequent functions within the INS and other connected equipment with this information, also supporting mode and situation awareness (IMO, 2007a).

Resolution MSC.252(83) removes the division of the INS into three categories (A, B and C), distinguishing them instead by the functions (tasks) performed by the system. An INS is defined as such if workstations provide multifunctional displays integrating at least the three following tasks (IMO, 2007a):

- Route monitoring;
- Collision avoidance;
- Alert management.

Additionally, the INS may provide manual and/or automatic navigation control functions, and comprise navigational tasks such as: 'Route planning', 'Navigation control data' and 'Navigation status and data display', including the respective sources, data and displays which are integrated into one navigation system.

As previously (according to the Resolution MSC.86(70)), an INS shall verify the availability, integrity, plausibility and validity of the acquired, combined, processed, evaluated, distributed and presented data. The integrity of information should be checked by comparison of the data derived independently from at least two sensors and/or sources, if available, but an approved back-up should be available for the following INS sensors and sources only (IMO, 2007a):

- EPFS;
- Heading measurement;
- Speed measurement;
- Radar;
- Chart database.

Data which does not pass the plausibility and validity checks with a positive result should not be used by the INS and should not affect functions that are not dependent on these data, unless the relevant performance standards specifically allow use of invalid data.

Available updated electronic navigational charts (ECS) and other navigational databases (tide tables, list of radio signals, *etc.*) should be used as common data sources for an INS. Implementing ship's route planning tasks, the system should allow voyage planning as recommended by the IMO Resolution A.893(21) on Guidelines for voyage planning, and shall provide means for (IMO, 2007a):

- Storage, loading and dissemination of the route plan;
- Checking of the defined (introduced) route plan against hazards based on the planned minimum under keel clearance (UKC) as specified by the mariner and manoeuvring limitations of the ship (allowed turning radius, the maximum value of the rate of turn (ROT), etc.), if available in the INS;
- Drafting and refining the route plan against meteorological information if available in the INS.

In the 'Route monitoring' task, an urgency manoeuvring procedure should be available at the display, taking set and drift into consideration. The display of additional different route-related information on the chart display is permitted, *inter alia* (IMO, 2007a):

- Tracked radar targets and AIS objects;
- Received safety related messages – so-called maritime safety information (MSI), such as AIS safety-related and binary messages and warnings received by NAVTEX;
- Initiation and monitoring of man-over-board and SAR manoeuvres (search and rescue and man-over-board modes);
- Tidal, current, weather and ice data.

Limitations in the INS development

One of the major constraints in the further development of integrated navigation systems is the lack of recommendations in the Resolution MSC.252(83):

- For interfaces connecting the INS to the radio communications equipment installed on ships according to the requirements of the of the SOLAS Chapter IV "Radio communications", Part C "Ships requirements";
- Regarding operational questions associated with the usage of the system and methods of presentation of information on a multifunction display.

In accordance with the requirements of the SOLAS Convention, one of the mandatory INS functions, route monitoring, can be realised only on an updated electronic navigation chart (ENC) presented on a multifunction display unit fulfilling all IMO performance standards for ECDIS. Regulation V/27 of the SOLAS Convention, "Nautical charts and nautical publications", states that nautical charts and nautical publications, such as sailing directions, lists of lights, notices to mariners, tide tables and all other nautical publications necessary for the intended voyage, shall be adequate and up to date (IMO, 2014).

In addition, as already noted in the previous chapter, the INS shall provide a means for drafting and refining the route plan against meteorological information, and may present additional different route-related information such as received maritime safety information (MSI), information from updated navigational publications, navigational and weather warnings, and tidal, current, weather and ice data if available in the INS. ENC and digital navigational publication may be corrected manually by the officer of the watch (OOW), but the process of their updating will be more efficient and less time-consuming if it is carried out automatically by the system after receiving corrections through the ship's radio communications (GMDSS) equipment. Technically, this is already possible and implemented on some ships, but it requires connection of an INS or an ECDIS as its subsystem to the ship's GMDSS equipment. The issue is that Resolution MSC.252(83) does not require that connection, and the IMO did not specify performance standards for interfaces necessary for this purpose. The aforementioned resolution contains only two general recommendations (IMO, 2007a):

- In cases where sources perform functions of the INS, these functions and interfaces should conform with the relevant parts of the performance standards defined in this resolution;
- Standardised and approved communication protocols for interfaces fulfilling the requirements of the IEC Standard 61162 for digital interfaces for navigational equipment within a ship should be used where possible.

The second limitation is the operational problems associated with the usage of the system and methods of presentation of information on a multifunction display. According to the recommendations of the points 1.3 and 2.1.1 of the analysed resolution, an INS aims to ensure that, by taking human factors into consideration, the workload is kept within the capacity of the operator in order to enhance safe and expeditious navigation and to complement the mariner's capabilities, while at the same time to compensate for their limitations. Currently manufactured systems do not fully meet these recommendations. There are not uniform rules for handling and presenting information and manufacturers offer systems which vary greatly in this respect. For this reason, there is a need to learn the principles of use of each system separately, as in the case of ECDIS where the IMO introduced two obligatory courses: the basic generic ECDIS course, and training in order to acquire skills in the use of a particular system. The biggest problems are for sea pilots, e.g. Baltic pilots, who may encounter ships operated on systems from different manufacturers, integrating and presenting different types of data and information in different manners. For this reason, they refer to the indications on multifunction displays very conservatively and mistrust them. There is IMO Circular SN/Circ.243 dated 15 December 2004, "Guidelines for the presentation of navigation-related symbols, terms and abbreviations", and issued on its basis Standard of the International Electrotechnical Commission IEC 62288, "Maritime navigation and radio communication equipment and systems – Presentation of navigation-related information on shipborne navigational displays – General requirements, methods of testing and required test results". They apply to all shipborne navigational systems and equipment but their implementation shall ensure that abbreviations and symbols used for the display of navigation-related information in all shipborne navigational systems and equipment are presented in a consistent and uniform manner only; therefore they do not solve the identified problem.

It seems that these two operational limits mean that INSs do not always fully meet the requirement of SOLAS Regulation V/15, "Principles relating to bridge design, design and arrangement of navigational systems and equipment and bridge procedures".

According to this regulation, all decisions which affect bridge design, the design and arrangement of navigational systems and equipment on the bridge, and bridge procedures, shall be taken with the aim of, *inter alia* (IMO, 2014):

- Facilitating the tasks to be performed by the bridge team and the pilot in making a full appraisal of the situation and in navigating the ship safely under all operational conditions;
- Promoting effective and safe bridge resource management;
- Enabling the bridge team and the pilot to have convenient and continuous access to essential information which is presented in a clear and unambiguous manner, using standardised symbols and coding systems for controls and displays;
- Allowing for expeditious, continuous and effective information processing and decision-making by the bridge team and the pilot;
- Preventing or minimising excessive or unnecessary work and any conditions or distractions on the bridge which may cause fatigue or interfere with the vigilance of the bridge team and the pilot;
- Minimising the risk of human error and detecting such error, if it occurs, through monitoring and alarm systems, in time for the bridge team and the pilot to take appropriate action.

INS operational limitations and recommendations of the IMO Circular MSC/Circ.982

As mentioned earlier, an INS is defined as such if workstations provide multifunction displays integrating at least 'Route monitoring', 'Collision avoidance' and 'Alert management' tasks. Particular workstations are defined in the IMO Circular MSC/Circ.982 dated 20 December 2000, "Guideline on ergonomic criteria for bridge equipment and layout", and two standards published by the International Organization for Standardization: ISO 8468, "Ships and marine technology – Ship's bridge layout and associated equipment – Requirements and guidelines", and ISO 14612, "Ships and marine technology – Ship's bridge layout and associated equipment – Additional requirements and guidelines for centralised and integrated bridge functions".

Circular MSC/Circ.982 lists two workstations corresponding to the INS tasks (IMO, 2000):

- Workstation for navigating and manoeuvring;
- Workstation for monitoring.

The first is a main workstation for ship's handling conceived for working in a seated or standing position with optimum visibility and integrated presentation of information and operating equipment to control and consider ship's movement. It should be possible from this place to operate the ship safely, in particular when a fast sequence of actions is required. The second is a workstation from which operating equipment and surrounding environment can be permanently observed in a seated or standing position. When several crew members are working on the bridge, it serves for relieving the navigator at the workstation for navigating and manoeuvring and/or for carrying out control and advisory functions by master and/or pilot (IMO, 2000).

In the ISO standards the two above mentioned stations are named (ISO, 2004; 2007):

- Primary navigation, traffic surveillance and manoeuvring workstation;
- Secondary navigation workstation.

The first is defined as a workstation with a commanding view used by navigators when carrying out navigation, traffic surveillance and manoeuvring functions. The second is a back-up workstation for navigation, which may also be used by an assisting navigator when required (ISO, 2004; 2007).

Controls and displays at the workstations for navigation, traffic surveillance and manoeuvring should enable the user (ship master, OOW and pilot) to:

- Continuously monitor the automatically displayed position of the ship in relation to the route, the surrounding waters and other ships, and manoeuvre the ship, including performing of anti-collision manoeuvres;
- Monitor the accuracy of the electronic chart system by cross checking the chart and radar alignment when applicable;
- Monitor all alarm conditions on the bridge and acknowledge warnings and alarms when applicable;
- Contact by radiotelephone with other ships, vessel traffic service (VTS) operators, harbour master officers and submit reports required by a ship reporting system.

From the foregoing description, it arises that the INS should be installed on both mentioned workstations and that it allows the OOW to perform parts of his tasks only. Similarly, as shown below, the INS integrates part of the equipment, control units and indicators of those workstations only.

The MSC circular describes in detail the recommended minimum equipment of each bridge workstation. According to its recommendations, the workstation for navigating and manoeuvring (primary

navigation, traffic surveillance and manoeuvring) should be fitted *inter alia* with (IMO, 2000):

- Navigational equipment: AIS, automatic visual position indicator and information of position fixing systems, ECDIS, heading and/or track control system (adjustment), radar with radar plotting aids;
- Indications for: gyro and magnetic compass headings, pre-set heading, water depth including depth warning adjustment, time, wind direction and velocity, air and water temperature, speed (possibly longitudinal and lateral), rudder angle, rate-of-turn, propeller revolutions (actual and desired), main engine revolution in the case of reduction geared engine, propeller pitch in the case of controllable pitch propeller, torque, starting air, lateral thrust, group alarms (with aids for decision-making);
- Signal transmitter for: whistle, automatic device for fog signals, general alarm, Morse signalling light;
- Automatic device for emergency alarm;
- Controls for: main engine(s) including crash manoeuvres and emergency stop, thrusters and main rudder (including override facility);
- Controls for console lighting and remote control for search light;
- Two-way VHF radiotelephone (walkie-talkie) with charging connection and/or paging system;
- Internal communication equipment and public address system (if applicable);
- VHF point with channel selector;
- Steering mode and position selector switches and rudder pump selector switch;
- Sound reception system (if applicable);
- Acknowledgement of the bridge navigation watch alarm system BNWAS.

The workstation for monitoring (secondary navigation workstation) shall be fitted with (IMO, 2000):

- Radar and radar plotting aids;
- Signal transmitter for whistle;
- Acknowledgement of BNWAS;
- Indications for: propeller revolutions, pitch of controllable pitch propeller, speed, rudder angle, gyro compass heading, time, rate-of-turn, water depth and alarms;
- Internal communication equipment;
- VHF point with channel selector.

INS as a subsystem of the integrated bridge system (IBS)

Now 20 years of age but still valid and cited in the SOLAS Regulation V/19, IMO Resolution MSC.64(67) adopted on 4 December 1996, "Adoption of new and amended performance standards", recommends the ship's flag and port state administrations to ensure that integrated bridge systems (IBSs) installed on ships on or after 1 January 1999 conform to performance standards not inferior to those set out in the Annex 1 to this resolution, "Recommendation on performance standards for integrated bridge systems (IBS)". According to the recommendation of this annex, an IBS is defined as a combination of systems which are interconnected in order to allow centralised access to sensor information or command (control) from workstations, with the aim of increasing safe and efficient ship management by suitably qualified personnel. It should support systems performing two or more of the following operations (IMO, 1996):

- Passage execution;
- Communications;
- Machinery control;
- Loading, discharging and cargo control;
- Safety and security.

Interfacing to an IBS should comply with the IEC 1162 Publication as relevant to international marine interface standards.

An INS forming part of an IBS should allow the task of 'Passage execution' to be conducted. An IBS performing two operations – 'Passage execution' and 'Communication' – shall solve the problems indicated in chapter 3 associated with a lack of connection between the INS and ship radio communications (GMDSS) equipment. In order to achieve this, the IMO should amend Annex 1 to the Resolution MSC.64(67).

INS as a tool of e-navigation

The idea of e-navigation, the possibility of its development and implementation, as well as the Polish approach to this subject identified at an early stage of the work of the Correspondence Working Group on e-navigation created at the IMO are presented in the works published *inter alia* by A. Weintrit (Weintrit & Wawruch, 2006; Weintrit et al., 2007a; 2007b; Weintrit, 2007; 2011; 2013), D. Filipkowski (Filipkowski and Wawruch, 2010; Filipkowski, 2013) and D. Petraiko (Petraiko, Wake & Weintrit, 2009). The key structural components of e-navigation later defined the base of user needs, which as approved by the IMO Maritime Safety Committee (MSC) are *inter alia* (IMO, 2014a; Wawruch, 2014):

1. Accurate, comprehensive and up-to-date electronic navigational charts (ENC) covering the entire geographical area of a vessel's operation.
2. Accurate and reliable electronic positioning signals, with 'fail-safe' performance, probably provided through multiple redundancy, e.g. on-board receivers of different satellite and terrestrial radio navigation systems or inertial navigation devices.
3. Provision of information on vessel route, course, manoeuvring parameters and other status items (hydrographic data, ship identification data, passenger details, cargo type, security status, etc.), in electronic format.
4. Transmission of positional and navigational information in relations: shore-to-ship (e.g. by vessel traffic services (VTS), coastguard centres, hydrographic offices), ship-to-shore and ship-to-ship.
5. Accurate, clear, integrated, user friendly display of the above mentioned information on-board and ashore (e.g. using integrated bridge system (IBS) or integrated navigation system (INS)).
6. Information prioritisation and alert capability in risk situations (collision, grounding, etc.), both on-board and ashore.

The component listed in point 5 explicitly requires installation of the functions of 'Passage execution' and 'Communications' on the workstations for navigating and manoeuvring and for monitoring IBS performance, or connection of the INS to the ship's GMDSS equipment.

As potential e-navigation solutions defined on the basis of identified user needs and gap analysis were listed following tasks (Wawruch, 2014; IMO, 2014b):

- S1 Improved, harmonised and user-friendly bridge design;
- S2 Means for standardised and automated reporting;
- S3 Improved reliability, resilience and integrity of bridge equipment and navigation information;
- S4 Integration and presentation of available information in graphical displays received *via* communication equipment;
- S5 Information management;
- S6 Improved access to relevant information for search and rescue;
- S7 Improved reliability, resilience and integrity of bridge equipment and navigation information for shore-based users;
- S8 Improved and harmonised shore-based systems and services;
- S9 Improved communication of VTS service portfolio.

Five prioritised solutions numbered as S1, S2, S3, S4 and S9 were selected from the abovementioned list and recognised as those with the most priority on the basis of a formal safety assessment (FSA) conducted using two criteria (IMO, 2013a):

- Seamless transfer of data between various equipment on-board;
- Seamless transfer of electronic information and data between ship and shore and *vice versa*, and in relation to ship-to-ship and shore-to-shore.

An additional function of an integrated system, not currently constituent in the tasks mentioned as e-navigation solutions, that may be considered is a decision support system as proposed by Z. Pietrzykowski (Pierzykowski, Borkowski & Wołejsza, 2012) and presented by Poland at the IMO in 2013 (IMO, 2013b).

As part of the FSA, the following Risk Control Options (RCOs) were identified as providing effective risk reduction in a cost-effective manner (Wawruch, 2014; IMO, 2014b):

- RCO 1 Integration of navigation information and equipment including improved software quality assurance;
- RCO 2 Bridge alert management;
- RCO 3 Standardised mode(s) for navigation equipment;
- RCO 4 Automated and standardised ship-shore reporting;
- RCO 5 Improved reliability and resilience of on-board PNT systems;
- RCO 6 Improved shore-based services;
- RCO 7 Bridge and workstation layout standardisation.

In order to harmonise and standardise shore-based services rendered for ships under different situations and/or locations, they were grouped and are described as Maritime Service Portfolios (MSPs). The IMO Sub-Committee on Safety of Navigation (NAV) noted a preliminary list of 16 MSPs comprising the following services: maritime assistance (MAS), maritime safety information (MSI), telemedical maritime assistance (TMAS), nautical charts and publications, ice navigation, meteorological information, real-time hydrographic and environmental information, VTS, local port, pilot, tugs and vessel shore reporting, and search and rescue (SAR) (Wawruch, 2014).

An INS fulfilling the recommendations of the Resolution MSC.252 (83) provides key structural components of e-navigation mentioned in points: 1 and 2 fully, 3, 5 and 6 in part (in relation to navigation) and 4 (after connecting it to the ship's radio

communications equipment). Without an INS or IBS, it will be impossible to implement all of the nine aforementioned tasks of e-navigation. The discussed system allows the provision of effective risk reduction in a cost-effective manner, fulfilling risk control options (RCO) numbers 1, 3 and 5, and partially 2 (bridge alert management). This means that having been connected to the ship's GMDSS equipment, an INS will be a very useful tool for e-navigation.

Following the recommendations of the IMO Circular MSC/Circ.982, it should be possible for communication to be carried out with shore-based services in the scope of different MSPs by the master, OOW and pilot, sitting or standing at the workstations for navigating and manoeuvring or monitoring. Information and data received from shore-based services shall be automatically presented on monitors installed on those workstations too. The simplest technical solution for achieving this goal is to connect the INS to the ship's GMDSS equipment.

Conclusions

The bridge team and pilot are required to use 'any means available' to safely navigate the ship, including by visual position fixing and lookout as well as communications with external sources of information such as other traffic and VTS stations, and the design of integrated systems should therefore support the use of all means and their correlation (IMO, 2013c). An INS should enhance navigational safety by providing integrated and augmented functions to avoid geographic, traffic and environmental hazards. It shall be installed on the workstations for navigating and manoeuvring and for monitoring, enabling the ship's captain, OOW and pilot to execute the safe passage of the ship along a planned route. This means that it should facilitate the exchange and presentation of all data and information necessary to achieve these objectives. Planning of the ship's route and conducting sea passage in a safe and efficient manner requires access to current weather forecasts, navigational and meteorological warnings and other information transmitted by shore-based services described as Maritime Service Portfolios (MSPs).

As it was described in the previous chapters, the major constraints limiting the further development of INSs is the lack of recommendations in the Resolution MSC.252(83):

- For interfaces connecting the INS to the radio communications equipment installed on ships according to the requirements of the of the SOLAS Chapter IV, "Radio communications", Part C "Ships requirements";
- Regarding operational questions associated with the usage of the system and methods of presentation of information on a multifunction display.

The first limitation can be removed in two ways:

- By introducing, instead of an INS, an integrated bridge system (IBS) implementing two functions: 'Passage planning and execution' and 'Communications';
- By extending the functions performed by an INS.

The first solution requires a thorough amendment of the Annex 1, "Recommendation on performance standards for integrated bridge systems (IBS)", to the Resolution MSC.64(67) made in accordance with the recommendations of the IMO Circular SN.1/Circ.274, "Guidelines for application of the modular concept to performance standards" (IMO, 2008), and therefore can be time consuming. The second solution requires the development of new modules to the revised performance standards for integrated navigation systems (INS) described in the Resolution MSC.252(83), as it is suggested in the proposal presented by China and Norway during the third session of the IMO Sub-Committee on Navigation, Communications and Search and Rescue (NCSR) in March 2016 (IMO, 2015a; 2015b). This solution appears to be more effective and easier to implement. The revised performance standards for INSs are modular and can be revised in an easy manner by adding new modules to deal with the new demands and standards as the industry develops new systems and technology.

As recommended in the Circular SN.1/Circ.265, "Guidelines on the application of SOLAS Regulation V/15 to INS, IBS and bridge design", the bridge team and the pilot shall focus on handling the ship rather than on operating the INS (IMO, 2007b). Correspondingly, seafarers shall be provided with a standardised, simple and effective interface for the control and monitoring of navigational systems. This can be achieved by introducing guidance on the standardised mode (S-Mode) of operation of navigational equipment and systems. Equipment and systems, after switching on S-Mode with a single button action, shall default to a standard display and present a standard user interface for pre-defined tasks. Currently there is no definition of this mode of operation. It should be prepared and accepted by the IMO, but the introduction of an INS with an S-Mode should solve operational questions associated with the usage of an integrated system, and different

methods of presentation of information on a multifunction display.

References

1. Filipkowski, D. & Wawruch, R. (2010) *Concept of "One window" data exchange system fulfilling the recommendation for e-navigation system*. In Mikulski J. (ed.) Transport Systems Telematics, 10th International Conference on Transport Systems Telematics, TST 2010. Selected Papers. Springer International Publishing.
2. Filipkowski, D. (2013) *Data transmission system architecture for e-navigation*. In Mikulski J. (ed.) 13th International Conference on Transport Systems Telematics, TST 2013. Selected Papers. Springer International Publishing.
3. IMO (1996) *Resolution MSC.64(67) adopted on 4 December 1996. Adoption of new and amended performance standards, Annex 1. Recommendation on performance standards for integrated bridge systems (IBS).* London: IMO.
4. IMO (1998) *Resolution MSC.86(70) adopted on 8 December 1998, Annex 3. Performance standard for integrated navigational systems*. London: IMO.
5. IMO (2000) *Circular MSC/Circ.982 dated 20 December 2000. Guidelines on ergonomic criteria for bridge equipment and layout*. London: IMO.
6. IMO (2007a) *Resolution MSC.252(83) adopted on 8 October 2007. Adoption of the revised performance standards for integrated navigation systems (INS)*. London: IMO.
7. IMO (2007b) *Circular SN.1/CIRC.265 dated 19 October 2007 Guidelines on the application of SOLAS regulation/15 to INS, IBS and bridge design*. London: IMO.
8. IMO (2008) *Circular SN.1/Circ.274 dated 10 December 2008. Guidelines for application of the modular concept to performance standards*. London: IMO.
9. IMO (2013a) *Report to the Maritime Safety Committee. NAV 59/20*. London: IMO.
10. IMO (2013b) *Development of an e-navigation strategy implementation plan. Report on research project in the field of e-navigation submitted by Poland. NAV 59/INF.2*. London: IMO.
11. IMO (2013c) *Development of an e-navigation strategy implementation plan. Report of the Correspondence Group on e-navigation to NAV 59 submitted by Norway. NAV 59/6*. London: IMO.
12. IMO (2014) *The International Convention for the Safety of Life at Sea (SOLAS), 1974, as amended. Consolidated Edition*. London: IMO.
13. IMO (2014a) *Development of an e-navigation strategy implementation plan. Report from the Correspondence Group on e-navigation. NCSR 1/9*. London: IMO.
14. IMO (2014b) *Development of an e-navigation strategy implementation plan. Background information related to the development of e-navigation submitted by Norway. NCSR 1/9/INF.5*. London: IMO.
15. IMO (2015a) *Proposals on drafting new modules to Performance standards for integrated navigation system (INS) (Resolution MSC.252(83)) submitted by China. NCSR 3/6/1*. London: IMO.
16. IMO (2015b) *Proposals to draft additional modules to the Revised Performance standards for Integrated Navigations Systems (INS) (Resolution MSC.252(83)) submitted by Norway. NCSR 3/6/2*. London: IMO.
17. ISO (2004) *Standard ISO 14612:2004. Ships and marine technology. Ship's bridge layout and associated equipment. Additional requirements and guidelines for centralized and integrated bridge functions*. Geneva: ISO.
18. ISO (2007) *Standard ISO 8468:2007 Ed.3. Ships and marine technology. Ship's bridge layout and associated equipment. Requirements and guidelines*. Geneva: ISO.
19. Patraiko, D., Wake, P. & Weintrit, A. (2009) E-navigation and the human element. In Weintrit A. (ed.) *Marine Navigation and Safety of Sea Transportation*. CRC Press, Taylor & Francis Group.
20. Pierzykowski, Z., Borkowski, P. & Wołejsza, P. (2012) *Marine integrated navigational decision support system*. In Mikulski J. (ed.) Telematics in the Transport Environment, 12th International Conference on Transport Systems Telematics, TST 2012. Selected Papers. Springer International Publishing.
21. Wawruch, R. (2014) Status of the work on e-navigation conception and plan of its implementation at the beginning of 2014. *Archives of Transport System Telematics* 7, 4. Katowice.
22. Weintrit, A. & Wawruch, R. (2006) *Future of maritime navigation, e-navigation concept*. In 10th International Conference Computer Systems Aided Science, Industry and Transport, TRANSCOMP 2006. Proceedings, Vol. 2. Radom: Kazimierz Pułaski Technical University of Radom, Faculty of Transport.
23. Weintrit, A. (2007) Development of e-navigation strategy. In Mikulski J. (ed.) *Advances in Transport Systems Telematics*. Katowice: Silesian University of Technology.
24. Weintrit, A. (2011) *Development of the IMO e-navigation concept – common maritime data structure*. In Mikulski J. (ed.) Modern Transport Telematics, 11th International Conference on Transport Systems Telematics, TST 2011. Selected Papers. Springer International Publishing.
25. Weintrit, A. (2013) *Technical infrastructure to support seamless information exchange in e-navigation*. In Mikulski J. (ed.) Activities of Transport Telematics, 13th International Conference on Transport Systems Telematics, TST 2013. Selected Papers. Springer International Publishing.
26. Weintrit, A., Wawruch, R., Specht, C., Gucma, L. & Pietrzykowski, Z. (2007a) An approach to e-navigation. *Coordinates*, Vol. III, Issue 6.
27. Weintrit, A., Wawruch, R., Specht, C., Gucma, L. & Pietrzykowski, Z. (2007b) Polish approach to e-navigation concept. In Weintrit A. (ed.) *Advances in marine navigation and safety of sea transportation*. Gdynia: Gdynia Maritime University.

Transportation Engineering

Scientific Journals
of the Maritime University of Szczecin

Zeszyty Naukowe
Akademii Morskiej w Szczecinie

2016, 48 (120), 117–124
ISSN 1733-8670 (Printed)
ISSN 2392-0378 (Online)
DOI: 10.17402/184

Received: 29.04.2016
Accepted: 30.11.2016
Published: 15.12.2016

Theoretical foundations of the implementation of controlled pyrotechnical reactions as an energy source for transportation from the sea bed

Wiktor Filipek, Krzysztof Broda✉

AGH University of Science and Technology, Faculty of Mining and Geoengineering
30 Mickiewicz Ave., 30-059 Krakow, Poland, e-mail: {Wiktor.Filipek; broda}@agh.edu.pl
✉ corresponding author

Key words: deep sea mining, transport from the sea floor, blasting materials, pyrotechnics, implementation, exploitation

Abstract
The depletion of inland deposits of natural resources and the increasing demand for some raw materials have resulted in the growing interest in deep sea exploitation of natural deposits. This gives an impulse to the mounting research and development of methods of exploitation of natural deposits from the sea and ocean floors, which are not limited to petrol and gas. The main area of difficulty in opencast mining methods conducted at considerable depths is the transportation process from the sea floor to the surface. The methods employed so far, such as continuous line bucket (CLB), hydraulic pumping (HP) and air-lift pumping (ALP), have both advantages and disadvantages. The most salient problem is their considerable energy consumption resulting in great costs, hence the need for the development of less expensive methods. The authors have suggested a new method, involving the use of pyrotechnical materials as a source of energy in the transportation from the sea floor and have presented its theoretical grounding. Special emphasis has been placed on determining the depth to which the method can be applied and the energy needed in transportation in relation to the density of the transported substance (output).

Introduction

Transport from the sea floor to the surface poses major difficulties when employing opencast marine mining at extreme depths. The solutions used to date (Karlic, 1984; Depowski et al., 1998), such as: CLB (continuous line bucket), HP (hydraulic pumping) or ALP (air-lift pumping) have proved to have their advantages and disadvantages. The biggest disadvantage is their energy consumption and, thus, high cost.

In this paper the authors want to present the use of pyrotechnical materials for the transport in water environment. The method is designed for the cyclical transport from big depths, over 200 meters. The transport module is based on the average alteration of density, which is inherently connected to the buoyant force affecting an immersed body. When the average density of the module is bigger than that of the surrounding medium, the buoyant force is lower than the weight of the body and the body falls down (sinks), whereas in the opposite case the buoyant force is higher than the body weight and the body emerges (floats). The situation in which the average density of the module equals the density of the surrounding medium is a particular case in which the buoyant force equals the body weight. In this condition, the body remains inert and floats in the liquid.

There are two ways in which we the average density of an immersed object can be changed. The first is used in submarines and is based on the use of ballast tanks, which, according to the need, are filled with water or emptied by using compressed air. The method is used when the depth does not exceed

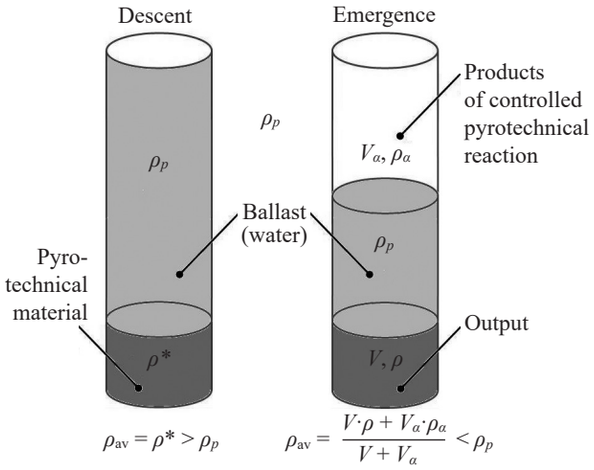

Figure 1. The concept of the implementation of controlled pyrotechnical reaction for transportation from sea bed

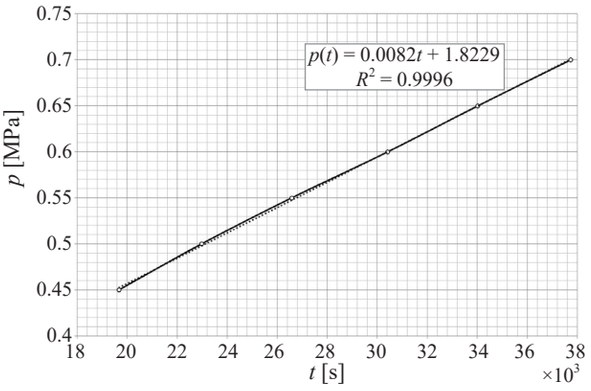

Figure 2. The graph shows the relation between the growth of pressure (*p*) over time obtained during explosive deflagration time (*t*)

several hundred meters. For technical reasons, this resurfacing method cannot be employed beyond depths of a few hundred meters and is it necessary drop the ballast, losing it irreversibly.

In order to present our concept of the use of pyrotechnic materials for transportation from the seabed (Figure 1) we show that, in the proposed solution, the weight of the structure of the transport unit does not change during either the descent to the bottom or the ascent to the surface. Therefore, in the following discussion we assume that we can balance the weight of the structure of the transport unit, affecting its buoyant force (Archimedean force). We focused on the processes taking place in the internal volume of the module, consisting of pyrotechnic material, having density ρ^*, and water, which acts as the ballast and whose density is indicated with ρ_p. In order for the module to descend, the density of the pyrotechnic material must be greater than the density of water. During the ascent, the volume occupied by the water will be then occupied by the gaseous products of the pyrotechnic reaction, having volume V_α and density ρ_a, which are pyrotechnic reaction products. The remaining volume V, of density ρ_a, is occupied by solid reaction products and the pyrotechnical output. The condition of emergence of the module is that the average density of the module, ρ_{av}, must be lower than ρ_p.

The pyrotechnical materials thus act as the energy source for the transport process, providing the energy input necessary to empty the ballast task. This concept is the subject of patented applications of the authors (Filipek & Broda, 2015a; 2015b). Through the research conducted to date, the authors have managed to devise a method for prolonging the deflagration method time of explosive materials belonging to the category of propellant explosives (powder).

Experimental research shows that in order to decrease the abrupt pressure gradient, which is harmful to the application, it is necessary to prolong the time of the reaction that triggers the pressure increase. The shorter the combustion time is, the more abrupt the energy surge. As shown in Figure 2, it was possible to prolong the explosive deflagration time (the paper submitted for print by the authors).

Transport from the sea floor based on the use of pyrotechnical material is a complex system. In order to make the system fully operational it is vital to solve the problems concerning particular stages of utilization. As mentioned earlier, the research carried out to date has allowed to solve the problem of pressure increase in the pyrotechnical reaction. This was as indispensable step for the continuation of work. In the controlled pyrotechnical process, we achieved the possibility of carrying out a phase change from solid body (or fluid) to gas, obtaining the required parameters of pressure growth velocity, facilitating safe ballast tank emptying.

This paper focuses on the next stage of system operation – defining the maximum depth at which the transport system is fully operational. The way in which we sought to achieve the objective is shown in Figure 3. In the first step, we set the relationship enabling to determine the dependence of the energy needed to ascend from the depth h (6).

In the second step, based on knowledge of potential energy, we determined the maximum ρ_a value and the added γ factor (10). We then analyzed the course of the controlled pyrotechnic reaction for the desired size (Step 3). Selected results are presented in Figures 5 and 6. In the last step, we focused on determining the maximum depth of

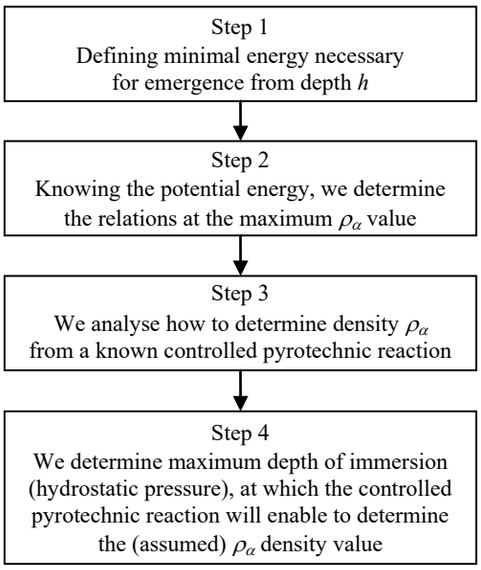

Figure 3. Algorithm for determining the maximum depth of immersion

immersion (hydrostatic pressure) in correspondence of which it is possible to achieve emergence of the module without surpassing the maximum allowable density.

Determination of conditions for preliminary considerations

In order to make the proposed method competitive against currently adopted solutions, it should be characterized by a higher energy efficiency. The minimum energy required to move a mass between two points in the gravitational field is determined by potential energy. It is this energy that we took as a reference point in our research. In order to accept the concept of free emergence of the body under the influence of buoyant forces, the work load of the gas must be determined. The pyrotechnical reaction product should be such that the value of the buoyant force can be bigger than the weight of the equipment.

The typical relation used for determining pressure at a given depth h (1) (Halliday, Resnick & Walker, 2005; Orzechowski, Prywer & Zarzycki, 2009) is:

$$p = p_o + p_h = p_o + g\,\rho\,h \tag{1}$$

Due to the fact that both the gravitational acceleration, g, and liquid density, ρ_p, are not constant values, the influence of these values on pressure should be taken into consideration and can be presented through the equation (2):

$$p = p_o + \int_0^H g(\varphi,h)\rho(s,T,h)\,\mathrm{d}\,h \tag{2}$$

in which it was assumed that fluid density (Brahtz, 1974; Perry & Walker, 1982) is a function of three parameters: salinity (s), temperature (T) and depth (h). Gravitational acceleration, in turn, was determined by two parameters: latitude and distance from the center of the Earth. The relation between g and latitude (φ) can be determined by (3) (Hinze, Frese & Saad, 2013):

$$g \approx \left(9.7803267714\frac{1+0.00193185138639\sin^2\varphi}{\sqrt{1-0.00669437999013\sin^2\varphi}}\right) \tag{3}$$

where the spherical shape of the Earth was taken into consideration. However, because of the irregular structure of the lithosphere, the relations employed offer only approximate values of the gravitational acceleration. In order to determine pressure at a given depth, local anomalies have to be taken into consideration as shown in relation (4).

$$p = p_o + \int_0^H g(r,\varphi,\lambda)\rho(s,T,h)\,\mathrm{d}\,h \tag{4}$$

In this equation, gravitational acceleration depends on three parameters: distance from the center of the Earth, r, and two parameters determining geographical position, namely φ and λ.

It turns out that determining pressure distribution as a function of depth is practically impossible without data on the changes with altitude of the local fluid and of the local change of gravitational acceleration with depth. Thus, with a significant degree of approximation, we assumed as reference that a pressure of 1 bar corresponds to that of a 10 m column of water and thus the pressure of 100 bar corresponds to the pressure at the depth of 1 km.

$$1\ [\mathrm{bar}] \approx 10\ \mathrm{mH_2O} \approx 10^5\ [\mathrm{Pa}]$$
$$100\ [\mathrm{bar}] \approx 1\ \mathrm{kmH_2O} \approx 10^7\ [\mathrm{Pa}] \approx 10\ [\mathrm{MPa}]$$

Determining energy and buoyancy depending on density

Let us consider the work performed during the movement of weight of density ρ from a certain depth, h, to the surface of liquid. Let us assume that weight lifting takes place in a non-viscous liquid of density ρ_p in order not to consider the influence of flow resistance at emergence of the object in question. The amount of work performed to move the object in question can be expressed through the following relation (5):

$$\Delta E_p = W = mgh = ghV(\rho - \rho_p) \tag{5}$$

where V stands for the volume occupied by the object in question. Of course, equation (5) is only reasonable when the density of the lifted weight (ρ) is bigger than the density of the surrounding liquid (ρ_p). In the opposite case, the calculation of the work would be meaningless because the object would emerge on its own.

Now let us consider the work of the isobaric transformation which we would have to perform at the depth h in order to change the density of the object in question by changing its volume. The initial volume and density of the object are, respectively, V and ρ. The volume of liquid that has to be pumped into the object in order to increase its volume is V_α and its density is ρ_α . The relation describing isobaric transformation takes the form of equation (6). Pressure p at depth h is going to be determined from relation (1) by subtracting ambient pressure p_o. Omitting ambient pressure in equation (6) results from the fact that we do not calculate absolute work but the work up to the moment of emergence of the object. Besides, the pumped-in liquid carries an energy equal to $p_o V_\alpha$, which, when subtracted from the absolute work, will give us the result described in equation (6).

$$W = pdV = p((V_\alpha + V) - V) = pV_\alpha = \rho_p g h V_\alpha \quad (6)$$

By comparing equations (5) and (6), we obtain the following:

$$V(\rho - \rho_p) = \rho_p V_\alpha \Rightarrow V_\alpha = V\left(\frac{\rho}{\rho_p} - 1\right) \quad (7)$$

Equation (7) carries the information on the maximum volume V_α when the theoretical work performed at depth h equals the potential energy and thus coincides with the hypothetical work which would have to be performed for the surfacing of the object from depth h if the work is performed in non-viscous fluid. Equation (7) does not provide, however, any information on whether the object will sink, float or emerge. In order know this, we have to evaluate the coefficient, marked as n, which is the multiplication factor in $V_\beta = nV$. This coefficient must be chosen so that the average density of the whole object is equal to the density ρ_p of the surrounding liquid and is going to be determined from the inequality (8):

$$\left.\begin{aligned} \frac{\rho_\alpha V_\beta + \rho V}{V_\beta + V} \le \frac{\rho_p\left(V_\beta + V\right)}{V_\beta + V} = \rho_p \end{aligned}\right\} \Rightarrow n \ge \frac{\rho - \rho_p}{\rho_p - \rho_\alpha} \quad (8)$$

By putting into equation (7) the solution of the inequality (8) we will obtain relation (9):

$$\left.\begin{aligned} \frac{V_\beta}{V_\alpha} &= n\frac{\rho_p}{\rho - \rho_p} \\ n &= \frac{\rho - \rho_p}{\rho_p - \rho_\alpha} \end{aligned}\right\} \Rightarrow \frac{V_\beta}{V_\alpha} = \frac{\rho_p}{\rho_p - \rho_\alpha} \quad (9)$$

When analysing equation (9) it is easy to notice that the relationship V_β/V_α is actually the relationship between the theoretical work required to create a volume, V_β, filled with liquid of density ρ_α at depth h, and the hypothetical work which we would be required to take out the object in question from depth h to the surface. By introducing the additional coefficient, γ, which is the relationship between ρ_α/ρ_p, we will obtain the following expression (10):

$$\delta = \frac{V_\beta}{V_\alpha} = \frac{E}{E_p} = \frac{1}{1-\gamma} \quad (10)$$

Equation (10) explains, inter alia, that the work performed in creating the volume V_β at depth h will be always bigger than the hypothetical work which we would have to be performed to extract the object from the depth h.

Figure 4, which is a graphic representation of equation (10), shows that a mutual correlation exists between the coefficients γ and δ defined in the equation (10). In order to create an equation in which the work required to create a fluid-filled volume V_β (fluid of ρ_α, depth h), equals the potential energy E_p, assumed as a reference point, the value of ρ_α at the depth h would have to amount to zero (vacuum). The more ρ_α approaches ρ_p, the more work has to be performed. This is justifiable because a higher value of ρ_α implies that a bigger volume V_β must be generated so that the density of the whole object is at least equal to the one of the surrounding liquid.

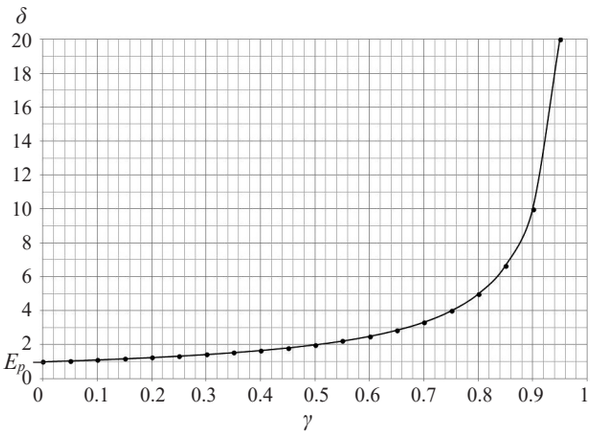

Figure 4. Graphic interpretation of the dependence of δ on γ

Analysis of selected pyrotechnical reactions

By conducting research on pyrotechnic reactions (Błasiak, 1956; Urbański, 1985; McLean, 1992; Brown, 2000; Dyja, Maranda & Trębiński, 2001; Papliński, Surma & Dębski, 2009), we have learned to control their progress. The control of pyrotechnical reaction that its spontaneous (uncontrolled) course is not allowed. This enables us to eliminate, or significantly reduce, most products of combustion, typical of uncontrolled pyrotechnical reaction, e.g. CO, CH_4, H_2.

The solutions were based on three types of reactions taking place during the combustion of explosives:

$$4KNO_3 + 5C \rightarrow 2K_2CO_3 + 2N_2 + 3CO_2 \quad (11)$$

$$4KNO_3 + 5C \rightarrow 2K_2O + 2N_2 + 5CO_2 \quad (12)$$

$$C_8(NO_2)_8 \rightarrow 4N_2 + 8CO_2 \quad (13)$$

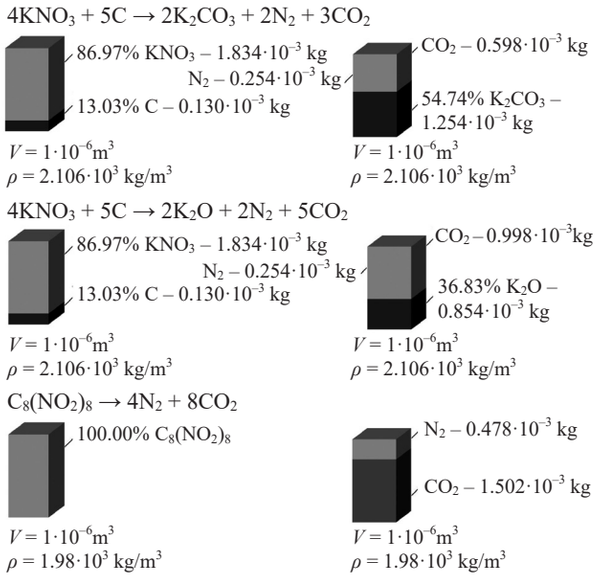

Figure 5. Graphic illustration of mass balance of products and substrates for the three paths of pyrotechnic reactions in the case of immersion and emergence of the transportation module

Reaction (11) is a typical deflagration reaction of the black powder without sulphur and with insignificant traces of chemical compounds resulting from combustion of charcoal. Pyrotechnical reaction (12) takes place in ordinary black powder deflagration; however, because of the considerable chemical affinity between potassium oxide and carbon dioxide, these compounds react with each other, resulting in reaction (11). When controlling the process, it is possible to favor reaction (12) while suppressing the secondary reaction between potassium oxide and carbon dioxide.

Reaction (13) is detonation of one of more modern explosives – octanitrocubane – and it is treated by the authors as a comparative reaction. It is unlikely to be used for our purpose because of the short detonation time (short duration ca. 10 km/s). However, the authors considered this reaction to be worth analyzing because there are two products of combustion: nitrogen and carbon dioxide.

Process analysis requires gathering all the physical and chemical data available in literature (Mizerski, 2013; Tablice fizyczno-astronomiczne, 2013; PubChem, 2016).

Figure 5 presents a graphical representation of pyrotechnical reactions for three courses of reaction (11), (12), (13). On the left-hand side of Figure 5, the input composition of the pyrotechnical material for each reaction, with the respective density, was presented. On the right-hand side, the products of reaction with percentage share of volume of the solid phase and weight share of the products are shown. These mass fraction, were the input point for further calculations after having been converted to moles.

In the analysis of the model, three states of aggregation were assumed. It was also assumed that potassium carbonate (K_2CO_3) from reaction (11) and potassium oxide (K_2O) from reaction (12) are present in the solid state. We also assumed, due to the lack of data in literature, that solid state is non-compressible (is not subject to compression) in comparison to other discussed phases and that CO_2 is always present in the liquid state. This assumption made us keep within the critical temperature limit

Table 1. Physical and chemical data of substances used for analysis

Molecular formula	Potassium nitrate	Carbon	Octanitrocubane	Potassium oxide	Potassium carbonate	Nitrogen	Carbon dioxide
	KNO_3	C	$C_8(NO_2)_8$	K_2O	K_2CO_3	N_2	CO_2
Molar mass	0.1011032 kg/mol	0.0120107 kg/mol	0.4641296 kg/mol	0.094196 kg/mol	0.138205 kg/mol	0.0280134 kg/mol	0.0440095 kg/mol
Density	2.109 10^3 kg/m³ (20°C)	2.09–2.23 10^3 kg/m³	1.98 10^3 kg/m³	2.32 10^3 kg/m^3 (20°C)	2.29 10^3 kg/m³		

for CO_2, amounting to 30.98°C (304.15 K). The relationship between density change of the liquid phase and pressure function was determined on the basis of the equation as proposed by Span and Wagner (1996). An algorithm (EMS Energy Institute, 2015) (tool software) is available online to determine the density of the liquid phase as a function of pressure and temperature. We assumed, for the purpose of our research, that nitrogen is always in the gas phase. The change of the density as a function of pressure was determined from the Van der Waals equation (14) (Szargut, 2005):

$$\left(p + \frac{an^2}{V^2}\right)(V - nb) = nRT \tag{14}$$

where:

n – amount of gas (in moles);
V – volume (in m^3).

In our research, the following values were assumed (Mizerski, 2013; Tablice fizyczno-astronomiczne, 2013):

R = 8.314462 J/(mol K) – universal gas constant;
a = 0.141 $(J \cdot m^3)/mol^2$ – experimental constant – parameter of particle attraction;
b = $3.91 \cdot 10^5$ m^3/mol – experimental constant – volume excluded from the movement of particles.

Determination of maximum pressure

An iterative method was applied to determine the immersed object density. The research excluded the construction mass because it can be balanced (buoyancy will be balanced at zero), for example by employing floats (tanks filled with oil). The calculations initially included the assumed density of the products resulting from reactions (11), (12), and (13). The following step involved the assumption of the temperature at which these densities should be determined. In most cases, this value was set at 5°C (278.16 K). We then determined pressure at the interface between liquid CO_2 and gaseous N_2, assuming insolubility of one phase in the other. This pressure was determined with an accuracy of three decimal points, using iterative methods to solve the system of two equations consisting of the Van der Waals equation (14) for the gas phase and the EoS equation for the liquid phase.

Figure 6 presents the result of pressure determination, obtained when the density of the product of the three reactions amounted to 1 g/cm^3. The percentage share for each product was also shown for the reactions considered. We can conclude from Figure 6 that the maximum depth guaranteeing emergence depends heavily on the amount of solid phase in the reaction products. Therefore, the least beneficial result (21.9 MPa) equivalent to the depth of ca. 2.19 km can be obtained for the reaction (11). Far more beneficial is the case of reaction (12), characterized by a smaller share of the solid phase with a depth of ca. 3 km. The third course reaches the depth of ca. 21 km.

Figures 7 and 8 present the maximum obtainable pressure as a function of reaction product density (for three courses of reaction (11), (12), (13)).

All the curves were determined for the ambient temperature of 5°C (278 K). Moreover, the graphs with average product density of 1000 kg/m^3 show how the pressure will increase with temperature (empty circles on the graph correspond to temperature values 278 K, 283 K, 293 K, 303 K). Additionally, the curve depicting the relationship between maximum pressure and density is presented, relative to the condition in which the transport system works with clean carbon dioxide in the liquid phase and solid and liquid products are removed from the operational area of the device. The relationship between reaction product densities for a transport system working with clean nitrogen was not shown because of the excessively big values in the scale of figures. For instance, with an average density amounting to 0.6 g/cm^3, we obtain a maximum pressure value

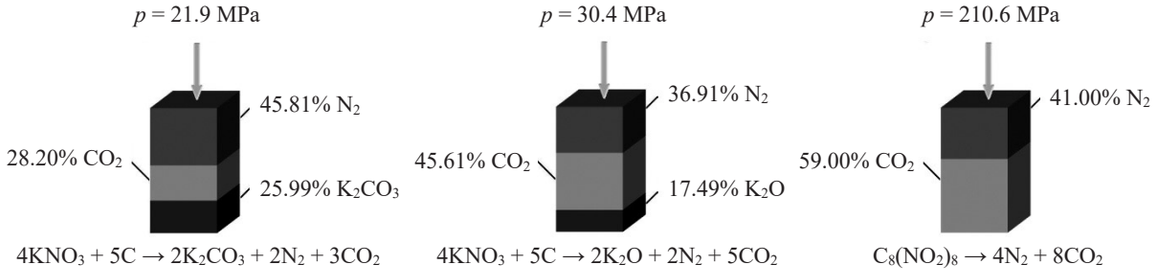

Figure 6. Comparison of maximum pressures for three pyrotechnical reactions with the assumed average density of the reaction products equal to 1000 kg/m^3

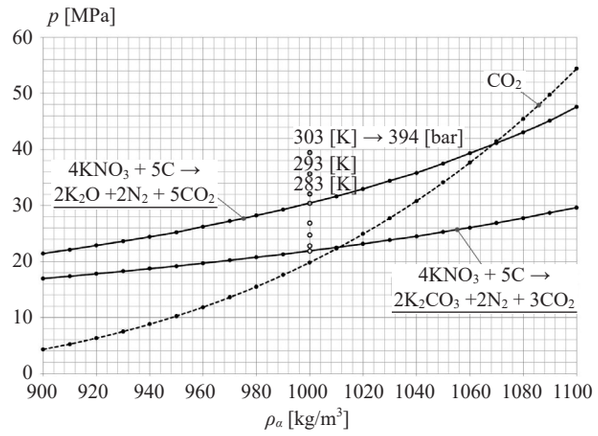

Figure 7. Relationship between the maximum pressure p and the product density ρ_α at $T = 278$ K for the first ($4KNO_3 + 5C \rightarrow 2K_2CO_3 + 2N_2 + 3CO_2$) and second ($4KNO_3 + 5C \rightarrow 2K_2O + 2N_2 + 5CO_2$) reactions and clean carbon dioxide

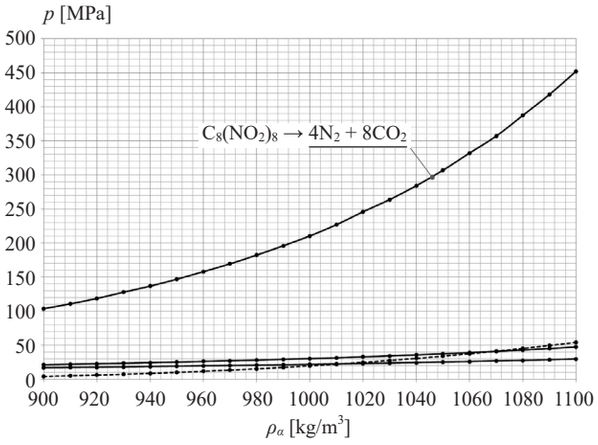

Figure 8. Relationship between maximum pressure p and density ρ_α for three reactions and clean carbon dioxide

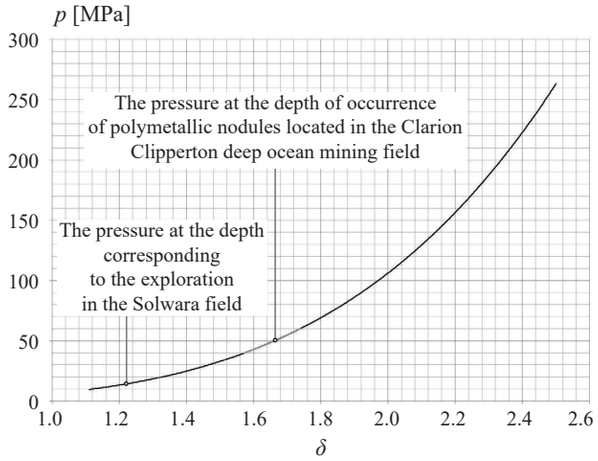

Figure 9. Graph of relation of coefficient δ (energy consumption rate) and pressure p for clean nitrogen N_2 determined for temperature $T = 278$ K

of 261.5 MPa at the temperature 5°C (278 K), while the density scale assumed for our graphs starts with 900 kg/m^3.

By analyzing Figure 9, we can see that in the case in which the system works on clean nitrogen, the theoretical value of δ would not exceed two.

In any case, the authors of this publication claim that, except for the value of δ the most important point affecting the feasibility of this transport system is the cycle of storage and recovery with respect to the energy obtained from explosive deflagration. The efficiency of the process determines the future application of this method.

Conclusions

From the analysis of the obtained pyrotechnical reaction products (Figures 6, 7, 8) we can conclude that the solid phase significantly limits the maximum pressure and thus the depth from which the system can get back to the surface. If, after emergence, solid reaction products were removed from the device, greater depths could be achieved thanks to the greater "supply" of potential energy.

On the basis of the discussions it can be concluded that the transport system should work with CO_2 and N_2 as working agents due to the fact that carbon dioxide is easily liquefied with increasing pressure and the system becomes more flexible in comparison to the system working on clean nitrogen.

In order to obtain maximum energy efficiency, the system should work at the lowest coefficient δ, equal to 1; however, this case is theoretically impossible because vacuum conditions would have to be created. On the other hand, the density ρ_α should not be close to ρ_p because, in this situation, δ approaches infinity.

The authors are aware of the possible impact of the proposed concept on the environment. At the current stage of research, the authors have reduced this impact by eliminating sulphur from the pyrotechnic material. Further investigations are being carried out and will be successively published.

Acknowledgments

This article was written within Statutes Research AGH, No. 11.11.100.005.

References

1. Błasiak, E. (1956) *Technologia związków azotowych. T. 2. Kwas azotowy, azotany i azotyny, sole amonowe, związki cyjanowe i inne*. Warszawa: Państwowe Wydawnictwa Techniczne.

2. Brahtz, J.F. (1974) *Oceanotechnika*. Gdańsk: Wydawnictwo Morskie.
3. Brown, G.J. (2000) *The Big Bang. A History of Explosives*. Sutton Publishing.
4. Depowski, S., Kotliński, R., Rühle, E. & Szamałek, K. (1998) *Surowce mineralne mórz i oceanów*. Warszawa: Wydawnictwo Naukowe Scholar.
5. Dyja, H., Maranda, A. & Trębiński, R. (2001) *Zastosowania technologii wybuchowych w inżynierii materiałowej*. Częstochowa: Wydawnictwo WMiIM PC.
6. EMS Energy Institute (2015) *CO_2 Calculator*. [Online] Available from: http://www.energy.psu.edu/tools/CO2-EOS [Accessed: March 12, 2016]
7. Filipek, W. & Broda, K. (2015a) Sposób transportu i urządzenie transportujące ładunek w wodzie, zwłaszcza z dużych głębokości. Zgłoszenie do Urzędu Patentowego RP nr P-414 387.
8. Filipek, W. & Broda, K. (2015b) Sposób transportu i urządzenie transportujące ładunek w środowisku płynnym, zwłaszcza z dużych głębokości. Zgłoszenie do Urzędu Patentowego RP nr P-414 388.
9. Halliday, D., Resnick, R. & Walker, J. (2005) *Podstawy fizyki. T. 3*. Warszawa: PWN.
10. Hinze, W.J., Frese, R.R.B. & Saad, A.H. (2013). *Gravity and Magnetic Exploration: Principles, Practices, and Applications*. Cambridge University Press. p. 130.
11. Karlic, S. (1984) *Zarys górnictwa morskiego*. Katowice: Wydawnictwo „Śląsk".
12. Mclean, D. (1992) *The Do-It-Yourself Gunpowder Cookbook*. Paladin Press.
13. Mizerski, W. (2013) *Tablice chemiczne*. Warszawa: Adamantan.
14. Orzechowski, Z., Prywer, J. & Zarzycki R. (2009) *Mechanika płynów w inżynierii i ochronie środowiska*. Warszawa: WNT.
15. Papliński, A., Surma, Z. & Dębski, A. (2009) *Teoretyczna i eksperymentalna analiza parametrów balistycznych prochu czarnego*. Materiały Wysokoenergetyczne, Warszawa.
16. Perry, A.H. & Walker, J.M. (1982) *System ocean – atmosfera*. Gdańsk: Wydawnictwo Morskie.
17. PubChem (2016) [Online] Available from: https://pubchem.ncbi.nlm.nih.gov [Accessed: March 12, 2016]
18. Szargut, J. (2005) *Termodynamika*. Warszawa: PWN.
19. Tablice fizyczno-astronomiczne (2013) *Tablice fizyczno-astronomiczne*. Warszawa: Adamantan.
20. Urbański, T. (1985) *Chemistry and Technology of Explosives*. Oxford: Pergamon Press.

Scientific Journals
of the Maritime University of Szczecin

Zeszyty Naukowe
Akademii Morskiej w Szczecinie

2016, 48 (120), 125–133
ISSN 1733-8670 (Printed)
ISSN 2392-0378 (Online)
DOI: 10.17402/185

Received: 24.05.2016
Accepted: 18.08.2016
Published: 15.12.2016

Optimization of Świnoujście port areas and approach channel parameters for safe operation of 300-meter bulk carriers

Stanisław Gucma

Maritime University of Szczecin, Faculty of Navigation, Marine Traffic Engineering Centre
1–2 Wały Chrobrego St., 70-500 Szczecin, Poland, e-mail: s.gucma@am.szczecin.pl

Key words: marine traffic engineering, waterways, computer simulation of ship movement, safety of navigation, seaport, approach

Abstract

This article presents the optimized parameters of the Świnoujście seaport entrance and three-kilometer fairway linking Świnoujście and Szczecin, extended to allow the safe entry of 300-meter bulk carriers drawing up to 13.5 meters. The parameters were determined by a simulation-based optimization method, where the objective function and its constraint were, respectively, the reconstruction costs of that waterway section and the vessels' navigation safety. The study made use of real-time simulation in coordination with the vessel's human operator.

Introduction

The Commercial Port of Świnoujście can accommodate ships with an overall length of 270 m and draft of 13.2 m. The approach channel to the outer port has been modernized to accept Q-Flex type LNG tankers up to 315 m in length. The approach channel stretching from buoy N-2, 35.6 km away from the entrance heads of the outer port, has a depth of 14.5 m, while its width at the bottom ranges from 200 to 220 m.

The approach waterway leading to the Świnoujście outer port provides safe passage of bulk carriers with overall length L_{oa} = 300 m and maximum draft T = 13.5 m. The Port Authorities intend to upgrade the Chemików, Hutników, Górników and Portowców quays to handle unloading of similarly sized ships. There is only one four-kilometer section of the waterway that is still not suitable for such ships, stretching from the outer port entrance heads to the Commercial Port quays. Possible solutions to these limitations through waterway modernization are discussed, by formulating the following research problems:

1. Determination of parameters for the Świnoujście entrance and a three-kilometer section of the Świnoujście-Szczecin fairway, which will provide for safe approach and berthing at the Commercial Port of bulk carriers with L_{oa} = 300 m and T = 13.5 m, based on the criterion of project cost minimization.
2. Determination of safe operational conditions for bulk carriers with L_{oa} = 300 m entering the Commercial Port of Świnoujście.

The assumed preliminary operational conditions for 300 m bulk carriers entering the port of Świnoujście have been defined as follows:

- arrival and departure of a bulker loaded to a draft of 13.5 m;
- turning of a ballasted bulker in the Northern Turning Basin at maximum forward and aft drafts of, respectively, T_F = 6.0 m and T_A = 9.0 m;
- visibility above 2 Nm, day or night without restrictions;
- wind speed up to 10 m/s, from any direction;
- mean incoming or outgoing current at 0.8 knots.

For these conditions, the following factors were taken into consideration:

- restrictions concerning the project scope, which does not include the reconstruction of the quays on the eastern bank of the River Odra (*Kanał Zbiorczy*);
- bathymetric and hydrometeorological conditions in the port of Świnoujście;
- maneuvering restrictions of loaded ships turning at the Northern Turning Basin;
- previous operational practices relating to large bulk carriers in the Commercial Port of Świnoujście.

The optimal parameters of the Świnoujście port entrance, the approach channels to the Chemików, Hutników, Górników and Portowców quays (the first section to 3.1 km of the Świnoujście-Szczecin fairway) and the Northern Turning Basin were determined through a simulation procedure for sea waterway system optimization.

Waterway system optimization procedure

The optimization of sea waterways was carried after determining the parameters characterizing the basic elements of a reconstructed system (waterway and navigation subsystems). These parameters are a function of designed (assumed) conditions for the safe operation of the ship (state vector of ship's safe operation).

The objective function in optimization problems related to marine waterway systems is the cost of upgrading the waterway system components and the cost of subsystem operation. With the above assumptions, we can write the objective function of waterway parameter optimization in the form (Gucma & Ślączka, 2015; Gucma et al., 2015):

$$Z = (A1 + A2 + N1 + N1 + S) \rightarrow \min \tag{1}$$

where
$A1 = f_1(\mathbf{D_i}, h_{xy})$, given that $(x, y) \in \mathbf{X1} \times \mathbf{Y1}$;
$A2 = f_2(\mathbf{D_i}, h_{xy})$;
$N1 = f_3(\mathbf{D_i}, h_{xy})$;
$N2 = f_4(\mathbf{D_i})$;
$S = f_5(\mathbf{D_i})$,
that is

$$Z = F(\mathbf{D_i}, h_{xy}) \rightarrow \min \tag{2}$$

with the constraint

$$\left.\begin{array}{r}\mathbf{d_i}(1-\alpha) \subset \mathbf{D_i} \\ \underset{p(x,y)\in \mathbf{D_i}}{\wedge} h_{xy}(t) \geq T_{xy}(t) + \Delta_{xy}(t)\end{array}\right\} \tag{3}$$

where
$\mathbf{D_i}$ – navigable area meeting the condition of safe depth at the *i*-th waterway section;
$\mathbf{d_i}(1–\alpha)$ – safe maneuvering area in the *i*-th section of the waterway of the *j*-th ship under preset navigational conditions, determined at confidence level $1–\alpha$;
Z – cost of construction and operation of waterways;
$A1$ – cost of construction (reconstruction) of the waterway;
$A2$ – cost of operation of the reconstructed waterway;
$N1$ – cost of the construction of a subsystem for determining ship position (navigation systems);
$N2$ – cost of navigation systems operation;
S – ship operating costs associated with waterway passage (pilotage, tug assistance, etc.);
h_{xy} – water depth at point (x, y);
T_{xy} – ship's draft at point (x, y);
Δ_{xy} – under keel clearance at point (x, y).

For sea waterways of constant depth (h_{xy} = constant), the objective function can be written in the form:

$$z = F(\mathbf{D_i}) \tag{4}$$

with the constraint:

$$\mathbf{d_i}(1 - \alpha) \subset \mathbf{D_i}(t) \tag{5}$$

This type of function was applied for the determination of safe parameters of a turning basin. On the other hand, the critical parameter for navigational safety in fairways (entrance to the port of Świnoujście and Świnoujście-Szczecin fairway) is the width at bottom. Therefore, the objective function was written as:

$$Z = F(D_j) \rightarrow \min \tag{6}$$

with the constraint:

$$D_j \geq d_j(1 - \alpha) \tag{7}$$

where
D_j − available fairway width at bottom, at the *j*-th point of the fairway center line;
$d_j(1–\alpha)$ − safe width at fairway bottom for a ship maneuvering in preset navigational conditions at the *j*-th point of the fairway center line determined at confidence level $1–\alpha$.

The safe maneuvering area during a turning maneuver, $\mathbf{d_i}(1–\alpha)$, and safe fairway width, $d_j(1–\alpha)$, were determined through real-time simulation using non-autonomous models (Gucma, Gucma & Zalewski, 2008). In non-autonomous simulation models the ship is steered by the human navigator.

Simulation tests were carried out on a Polaris full mission bridge simulator from Kongsberg, located at the Marine Traffic Engineering Center, Maritime University of Szczecin. The simulation tests

followed a procedure typically used in designing marine waterways:

- formulation of a research problem, including the identification of design objective, simulation methods used and the type of simulators;
- design of models for ship movement on the chosen simulator and their verification;
- design of the experimental system and performance of the experiment;
- statistical processing and analysis of test results.

The mathematical models developed and verified in the course of the present work represented the movement of a bulk carrier with L_{oa} = 300 m, lightered to a draft of T = 13.5 m and in ballast. Technical and operating parameters of the tested bulk carrier were based on an online database Sea-web (LR), covering a population of more than 10,000 bulk carriers (Analysis, 2014). The parameters of that bulk carrier are shown in Table 1. The models were verified by testing the speed, stopping, turning circle and a zigzag tests.

Table 1. Technical and operating parameters of a 300-m bulk carrier

No.	Notation	Bulk carrier
1.	L_{oa} [m]	300
2.	L_{bp} [m]	288.5
3.	B [m]	48.1
4.	T_{max} / $T_{lightered}$ [m]	17.8 / 13.5
5.	T_{aft} [m] in ballast	9.0
6.	t [m] trim in ballast	3.2
7.	P_n [kW] ME power	14 500
8.	D [t] for $T_{13.5}$ – displacement	157 500

Experimental system

The simulation tests consisted of running a reliable number of maneuver trials (entering / leaving / turning ship) for the tested variants defining the problem under consideration. The comparison of the results of each variant was carried out using the criteria of navigational safety. The test variants were specified by taking into account:

- port operational conditions;
- previous test results for the same port;
- objectives of the study;
- examined water area;
- examined ships;
- prevailing navigational conditions;
- maneuvering tactics based on established practices.

General assumptions of the simulation tests are as follows:

- due to the characteristics of the ships, local bathymetry and the established practice, it was assumed that incoming ships (loaded) would be berthing portside, alongside the Hutnikow quay;
- incoming maneuver is more difficult than departure;
- turning is performed only by a ship in ballast condition;
- least favorable wind direction for incoming ships is N combined with the incoming current;
- least favorable wind direction in the turning basin is N when combined with incoming current, and S when combined with outgoing current;
- adopted maximum wind speed, V_w = 10 m/s;
- adopted maximum current speed, V_p = 0.8 knot (incoming) and V_p = 0.6 kn (outgoing);
- four tugs assisted all entering, leaving, and turning maneuvers of the vessel:
  - 3 tugs with cycloidal propulsion, 45 ton bollard pull;
  - 1 conventional tug with 30 ton bollard pull.

Specific assumptions of the simulation tests were as follows:

- the tests included port entry maneuvers, berthing, unberthing, turning and departure;
- the maneuvers were performed using 4 tugs;
- entry maneuvers started abeam the entrance to the outer port at a speed of 4 knots with two tugs connected, one fore and one aft;
- when the ship was departing, turning was always performed around the sideboard side;
- trial maneuvers were conducted by pilots of the Szczecin-Świnoujście Pilot Station and experienced;
- each series, performed by each pilot and captain, consisted of two passages in a series.

The simulated trials consisted of five series of 16 passages each. The test conditions adopted in each series are presented in Table 2. A diagram of the electronic chart area is shown in Figure 1 (Analysis, 2014).

Table 2. Simulations test plan

Series No.	Ship	Maneuver type	Wind	Current
1.	300 loaded	entry, no turning	0	0
2.	300 loaded	entry, no turning	N 10 m/s	0.8 kn incoming
3.	300 in ballast	departure, turning	0	0
4.	300 in ballast	departure, turning	N 10 m/s	0.8 kn incoming
5.	300 in ballast	departure, turning	S 10 m/s	0.6 kn outgoing

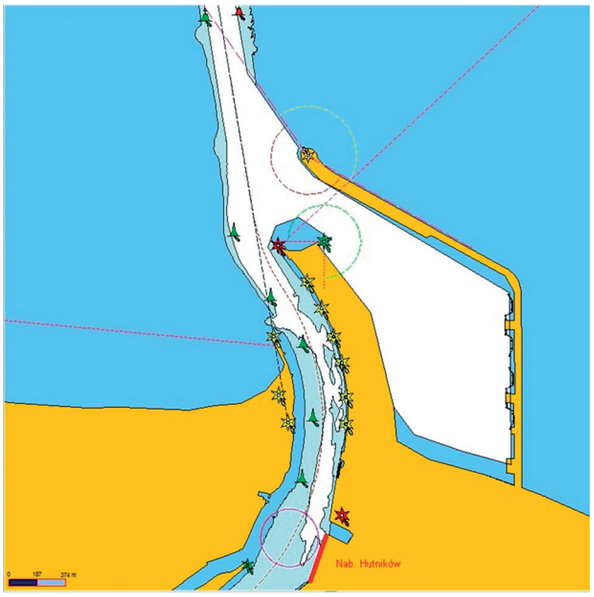

Figure 1. A fragment of electronic chart of the trials area

Optimal port area and Świnoujście entrance parameters based on the results of simulation tests

The tests made use of the basic criterion of navigational safety (performed maneuver). The safe maneuvering area was determined on the basis of the widths of the ship's swept paths (Gucma, 2001). The swept path width was determined by a random variable representing the maximum distance of extreme points of the ship on the left and right-hand sides of a hypothetical axis of the examined area. The swept path width for a specific series of tests is calculated at three levels:

- medium;
- maximum, as the maximum envelope in a specific series;
- 95% confidence level.

An analysis of the results of simulation tests was based on a quantitative assessment of the safety of navigation, estimated using the risk theory. In global terms, the method used to estimate the risk of navigation is a most modern one (Gucma, 2007). The condition of safe maneuver (port approach, turning etc.) fulfills the following relation:

$$R_{ijkxy} \le R_{akc} \tag{8}$$

given that

$$R_{ijkxy} = I_{ijkxy} \cdot P_{ijkxy} \cdot S_{ijkxy} \tag{9}$$

where

R_{ijkxy} – risk of performing the j-th maneuver by the i-th type ship in the k-th variant of navigational conditions at point (x, y) of the area;

R_{akc} – acceptable navigational risk of passing a given fairway section;

I_{ijkxy} – mean annual intensity of performing the j-th maneuver in an area defined by coordinates (x, y) by the i-th type ship in the k-th navigational conditions;

P_{ijkxy} – probability of navigational accident when performing the j-th maneuver by the i-th type ship in the k-th navigational conditions at point x, y of the area;

S_{ijkxy} – consequences of an accident of the i-th ship performing the j-th maneuver in the k-th navigational conditions at point (x, y) of the area.

We can define the probability of a navigational accident as:

$$P_{ijkxy} = 1 - P_{nijkxy} \cdot P_{tijk} \tag{10}$$

where

P_{nijkxy} – navigational probability of performing the j-th maneuver by the i-th ship in the k-th navigational conditions at point (x,y);

P_{tijk} – probability of reliable operation of technical systems and equipment when performing the j-th maneuver by the i-th ship in the k-th navigational conditions.

After substitution and transformation we get the condition of safe performance of the examined maneuver:

$$P_{nijkxy} \ge \frac{I_{ijkxy} \cdot S_{ijkxy} - R_{akc}}{I_{ijkxy} \cdot S_{ijkxy} \cdot P_{tijk}} \tag{11}$$

The navigational probability of making a smooth, accident-free, maneuver can be expressed in terms of the normal distribution by writing the following inequality (Gucma, 2007):

$$P\left(\frac{X_{ijkn} - \overline{X}_{ijkn}}{\sigma_{ijkn}} \le \frac{\frac{B_{ijkn}}{2} - \overline{X}_{ijkn}}{\sigma_{ijkn}}\right) \ge \frac{I_{ijkn} \cdot S_{ijkn} - R_{dop}}{I_{ijkn} \cdot S_{ijkn} \cdot P_{tijk}} \tag{12}$$

where

X_{ijkn} – maximum distance of the extreme points of the i-th type ship to the left and right from the n-th point of real fairway center line for the j-th type maneuver and k-th navigational conditions;

$\overline{X}_{ijkn}$; σ_{ijkn} – parameters of normal distribution at the n-th point of the fairway center line to left and right from swept path axis of the i-th ship, j-th type maneuver and k-th navigational conditions.

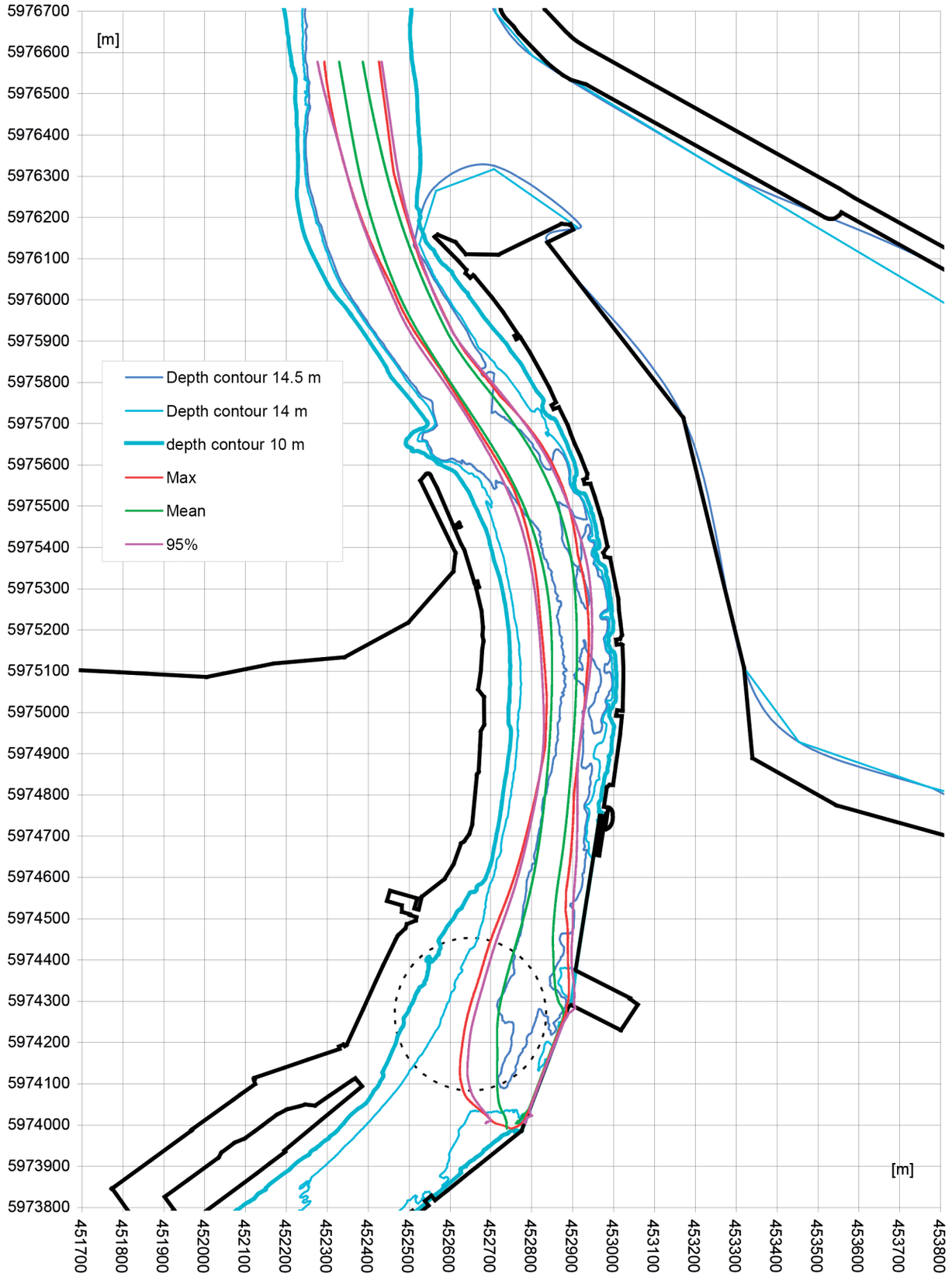

Figure 2. Swept paths of a loaded bulk carrier L_{oa} = 300 m during its entry and berthing to Hutników Quay in Świnoujście, wind N 10 m/s, incoming current 0.8 kn (Analisis, 2014)

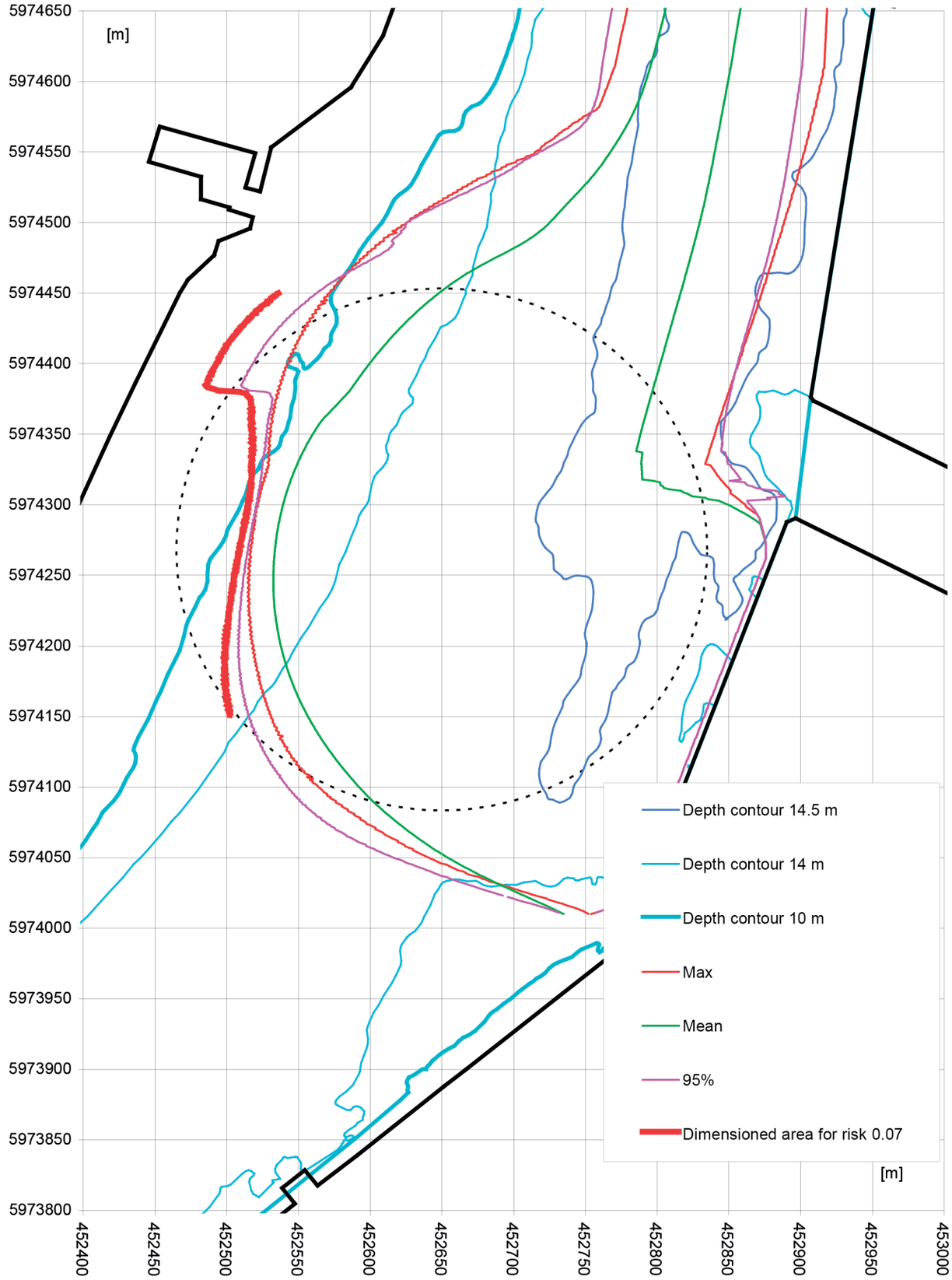

Figure 3. Safe maneuvering area for risk 0.07. Turning maneuver. Bulk carrier L_{oa} = 300 m; wind S 10 m/s; outgoing current 0.6 knot (Analisis, 2014)

After the simulation tests and the determination of the distribution parameters to the right and left of each *n*-th point of the fairway center line ($\overline{X}_{pijkn}$; σ_{pijkn}; $\overline{X}_{lijkn}$; σ_{lijkn}) the limit values of the inequality for both sides of the fairway were determined.

Using the standardized functions of normal distribution we calculate the minimum values of safe widths of right and left sides of the fairway: $B_{lijkn}/2$ and $B_{pijkn}/2$, where the safe bottom width at the *n*-th fairway point is defined as a sum of the two parts:

$$B_{ijkn} = \frac{B_{pijkn}}{2} + \frac{B_{lijkn}}{2} \tag{13}$$

with

$B_{lijkn}/2$; $B_{pijkn}/2$ – width of the right-hand (p) and left-hand (l) part of the fairway for the *i*-th ship, *j*-th maneuver and *k*-th navigational conditions at the *n*-th point of the fairway center line;

B_{ijkn} – minimum safe width of the fairway at bottom for the *n*-th point of the fairway center line, with *i*-th type ship, *j*-th maneuver, *k*-th navigational conditions.

The area defined by the safe minimum bottom width at the *n*-th point is called the safe maneuvering area and contains all margins related to measurement uncertainties, navigational errors, the process of maneuvering and accident consequences. The parameters that must be met by the safe maneuvering area were previously determined by optimization.

It is assumed that acceptable navigational risk of performing a specific maneuver in non-tidal areas equals 0.07 of the total number of accidents per year (major and minor accidents) (Gucma, 2001), while the average annual intensity of entry/exit maneuvers of a "maximum" vessel was assumed to equal 10. The physical method, utilizing the results of simulation tests, was used to calculate accident consequences, based on the comparison of kinetic energy (Gucma, 2001).

Figure 2 shows statistical results of simulation tests presented in the form of swept paths at different confidence levels. These data represent vessel entry to Świnoujście and berthing portside alongside a loaded bulk carrier, having T = 13.5 m and L_{oa} = 300 m, with wind N 10 m/s and incoming current of 0.8 knots.

Figure 3 presents the safe maneuvering area evaluated at a risk R = 0.07 for a 300 m bulk carried engaging in a turning maneuver in ballast, with S 10 m/s wind and an outgoing current of 0.6 knots.

The navigable area of the port entrance (depth contour 14.5 m) including the Świnoujście approach channel (0.0 km ÷ 1.0 km) and Świnoujście-Szczecin fairway (0.0 km ÷ 3.1 km) was determined on the basis of simulation test results referring to bulk carriers with an overall length of 300 m. The parameters

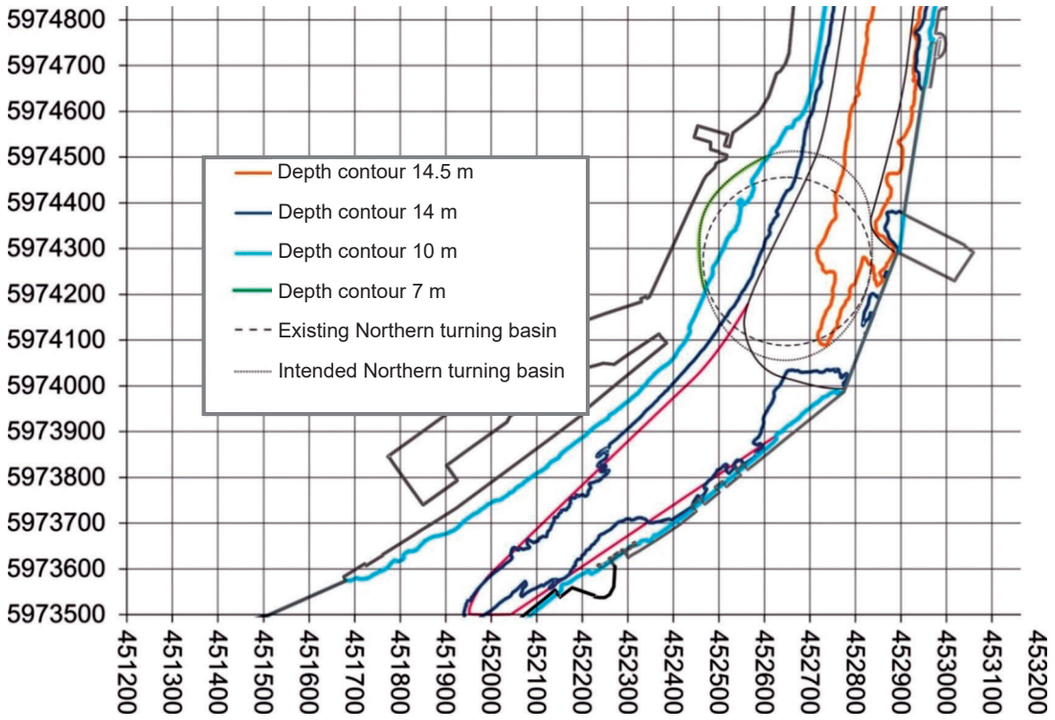

Figure 4. Navigable area (safe depth contour 7.0 m) of the Northern Turning Basin and the approach channel (safe depth contour 14.5 m) (Analisis, 2014)

of this area meet the optimization criterion, i.e. minimization of waterway system reconstruction and operation. From the results of simulated turning maneuvers of a 300 m bulker, the navigable area of the Northern Turning Basin with a contour depth of 7.0 m was also determined, as illustrated in Figure 4.

Conditions for safe operation of 300-metre bulk carriers entering the port of Świnoujście

The system of sea waterways is defined by parameters of its subsystems. The optimal system of sea waterways discussed in the present work consists of two elements:

- entrance to the port of Świnoujście and three-kilometer long section of the Świnoujście-Szczecin fairway with optimized parameters;
- existing fixed aids to navigation of that area plus slightly modified floating seamarks.

These two components of the sea waterway system are a function of conditions for the safe operation of the ship. Such conditions are described by a vector of conditions of the safe operation of a "maximum ship" in the *i*-th section of the examined waterway, written in the form (Gucma et al., 2015):

$$\mathbf{W_i} = [t_{yp}, L_{oa}, B, T, H_{st}, V, C, \mathbf{H_i}] \qquad (14)$$

where

t_{yp} – type of "maximum ship";
L_{oa} – length overall of "maximum ship";
B – breadth of "maximum ship";
T – draft of "maximum ship";
H_{st} – airdraft of "maximum ship";
V_i – allowable speed of "maximum ship" in the *i*-th waterway section;
C_i – tug assistance in the *i*-th waterway section (required number and bollard pull of the tugs);
$\mathbf{H_i}$ – vector of hydrometeorological conditions allowable for "maximum ship" in the *i*-th waterway section.

$$\mathbf{H_i} = [d/n, \Delta h_i, V_{wi}, KR_{wi}, V_{pi}, h_{fi}, KR_{fi}] \qquad (15)$$

where

d/n – allowable day/night time (daylight or no restrictions);
Δh_i – allowable drop of water surface level;
V_{wi} – allowable wind speed in the *i*-th section;
KR_{wi} – wind direction restrictions (if present, in the *i*-th section);
V_{pi} – allowable current speed in the *i*-th section;
h_{fi} – allowable wave height in the *i*-th section;
KR_{fi} – restrictions to wave direction (if any).

The conditions of safe operation of a "maximum" bulk carrier for the port of Świnoujście can be defined as follows:

1. The term "maximum" bulk carrier includes bulkers with overall length in the range:
   $$270 \text{ m} < L_{oa} \leq 300 \text{ m}$$
   and with draft:
   - loaded: $13.0 \text{ m} < T \leq 13.5$ m;
   - in ballast: $T_{forw} \leq 6$ m.
2. Entering or leaving the Commercial Port of Świnoujście, berthing of a loaded bulk carrier and its turning in ballast condition:
   - time of day: no restrictions;
   - visibility: good ≥ 2 Mm;
   - ship's speed during entry and departure maneuvers: $V \leq 4$ knots;
   - wind speed: $V_w \leq 10$ m/s;
   - wind direction: No restrictions;
   - current speed: $V_p \leq 0.8$ knots;
   - current direction: no restrictions;
   - positioning systems: PNS, PNDS, terrestrial;
   - tug assistance: 3 tugs with bollard pull of minimum 45 tons (cycloidal or azimuth) and 1 tug with a bollard pull of 30 tons.

The notations:

- PNS – Pilot Navigation System,
- PNDS – Pilot Navigation Docking System.

Conclusions

This article discusses the determination of new parameters of port entrance area in Świnoujście, and in the three kilometer stretch of the Świnoujście-Szczecin fairway and the Northern Turning Basin (Figures 2 and 4). Such reconstruction of the waterway will allow safe entry into the Commercial Port of Świnoujście of bulk carriers with an overall length of 300 m and a maximum draft of 13.5 m.

These parameters are calculated using a simulation-based optimization method developed by the author. The relevant objective function is the minimization of reconstruction and operation costs of the examined waterway section, while navigational safety is the constraint. The method used was real time simulation based on non-autonomous models with a human operator (navigator). The study was conducted on the full mission bridge simulator Polaris from Kongsberg, run by the Marine Traffic Engineering Centre, Maritime University of Szczecin.

Using the test results, the author has determined conditions for the safe operation of bulk carriers with L_{oa} = 300 m, capable of entering the Commercial Port of Świnoujście after the reconstruction of this

section of the waterway. The primary conditions for safe operation of the bulk carrier is the entry/departure of a loaded ship with $T \leq 13.5$ m and turning the ship in ballast with a forward draft lower than or equal to 6 m. These maneuvers can be used for maximum wind and current speeds of 10 m/s and 0.8 knots, respectively, and minimum visibility of two nautical miles.

The new parameters of the Świnoujście port entrance, Świnoujście-Szczecin fairway section (3.1 km) and Northern Turning Basin allowed the technical design of fairway reconstruction and planning of the relevant project.

Acknowledgments

This research outcome has been achieved under the research project No. 1/S/CIRM/2016 financed from a subsidy of the Ministry of Science and Higher Education for statutory activities of Maritime University of Szczecin.

References

1. Analysis (2014) Analiza nawigacyjna przebudowy toru podejściowego północnego do Świnoujścia od 0,0 km do 1,0 km oraz toru wodnego Świnoujście-Szczecin od 0,0 km do 3,1 km. Praca naukowo-badawcza pod kierunkiem S. Gucmy; zlecona przez Biuro Projektowo-Inżynierskie REDAN Sp. z o.o. w Szczecinie. Szczecin: Akademia Morska w Szczecinie.
2. Gucma, S. (2001) *Inżynieria ruchu morskiego*. Gdańsk: Okrętownictwo i Żegluga.
3. Gucma, S. (2007) Optimization method of port parameters and its application for design of the newly build outer harbour in Świnoujście. *Archives of Transport* 4, 19. pp. 43–55.
4. Gucma, S., Gucma, L. & Zalewski, P. (2008) *Symulacyjne metody badań w inżynierii ruchu morskiego*. Monografia pod redakcją Stanisława Gucmy. Szczecin: Wydawnictwo Naukowe Akademii Morskiej w Szczecinie.
5. Gucma, S. et al. (2015) *Morskie drogi wodne. Projektowanie i eksploatacja w ujęciu inżynierii ruchu*. Pod redakcją Stanisława Gucmy. Gdańsk: Fundacja Promocji Przemysłu Okrętowego i Gospodarki Morskiej.
6. Gucma, S. & Ślączka, W (2015) Methods for optimization of sea waterway systems and their application. *Polish Maritime Research* 3(87), 22. pp. 14–19.

Scientific Journals
of the Maritime University of Szczecin

Zeszyty Naukowe
Akademii Morskiej w Szczecinie

2016, 48 (120), 134–137
ISSN 1733-8670 (Printed)
ISSN 2392-0378 (Online)
DOI: 10.17402/186

Received: 29.04.2016
Accepted: 14.07.2016
Published: 15.12.2016

The role of stray currents in the evolution of damage in transport systems

Elwira Kałkowska

Maritime University of Szczecin
1–2 Wały Chrobrego St., 70-500 Szczecin, Poland, e-mail: elwira.kalkowska@wp.pl

Key words: stray currents, electric currents, catenary, circuit, corrosion, erosion, resistance

Abstract
The aim of the present work is the influence of stray currents on transport systems, especially rail and city systems. Therefore, a study was conducted that simulated flow of stray currents on elements of the transportation system. Steel DOMEX, which has enhanced resistance to corrosion, was used as research material. It is rarely understood that transport systems can have reciprocal negative effects on each other. For example, the urban and long-distance rail transport systems influence the transmission systems (gas pipelines, information systems). A side effect of the functioning of railways is the formation of stray currents, which cause electrochemical corrosion in all undergrounded metal components. It has been demonstrated that the impact of stray currents on the metal parts is of corrosive nature, and their effects can be presented graphically and numerically. It has also been proven that the anodic potential causes a greater loss than the cathodic potential. Furthermore, the exposure to the elements, both in the process of corrosion and erosion, accelerates the destruction of the material.

Introduction

The concept of stray currents is inevitably associated with the development of the catenary. With the launch of the first experimental electrically powered trams in Berlin, in 1881, and the subsequent electrification of all tram lines in the world, the phenomenon of stray currents was observed. In the first power networks, the propulsion of electric traction was supplied by DC (in Poland today traction network is powered by a DC voltage of 3000 V). The presence of electric currents was noticed to partially interfere with working circuits in the ground, causing significant corrosion of items such as metal pipe and cable sheathing. The local corrosion rate reached 5 mm per year (sometimes even more) leading to studies on the phenomenon of excessive corrosion, which resulted in significant losses and damages. As research work started the electrochemical nature of the problem had not been immediately identified.

Definition of stray currents

According to the encyclopedia, the phenomenon of stray currents is defined as "electricity flow via buildings, ground or equipment due to electrical supply system imbalances or wiring flaws. It refers to an existence of electrical potential that can be found between objects that should not be subjected to voltage". More specifically the above phenomenon in the catenary, reverse current flowing in the circuit should theoretically flow to the traction substation by rail; however, due to the lack of perfect isolation of the transition section of the rail – ground resistance of the longitudinal rails – part of the current branches out, in accordance with the second law of Kirchhoff. Some of the currents returning to the substation through the ground, where the resistance is small, stray – hence the name of stray currents. These branches of the main current flow use all underground metal parts. During the flow of the current at the boundary between ground and metal

components, there is a corrosion phenomenon of metal parts (Sokólski, 2007).

Due to the common power catenary circuit and the current used to generate traction in the rail system, the leakage phenomenon used to eddy currents is usually the only one considered, overlooking the influence of alternating currents. The source of these currents can be network traction powered by alternating current (used in some European countries), or the phenomenon of self-induction (the process may occur in long pipelines located near the high-voltage alternating current power line through the interaction of power cables, telecommunications, high-voltage lines and sometimes rail). Although the phenomenon of corrosion resulting from alternating currents is fairly well known, methods to protect metal components from this type of corrosion are still unknown. The reason for this is the lack of use of cathodic protection. Furthermore, the corrosion speed of the process, compared to the effect of DC on the metal parts, is fairly small (Stochaj, 2013).

Currently in Poland there are four standards for protection against stray currents, summarized in Table 1.

Table 1. List of standards in force in Poland (Sokólski, 2007)

PN-EN 50122-2:2002	Railway applications – stationary devices – Means of protection against the effects of stray currents caused by electric traction current.
PN-EN 50162:2006	Protection against corrosion due to stray current from direct current systems.
PN-W--89510:1997	Protection of metal objects against corrosion by stray current in shipyards and ports. General requirements and tests.
PKN–CEN/TS 15280	Assessment of the likelihood of corrosion of buried pipelines caused by alternating current. Application to cathodically protected pipelines.

The influence of stray currents on metal structures

As already mentioned, the main damage caused by stray currents is the electrochemical corrosion of metal parts, which occurs at the intersection between metal structures and electric traction lines. To prevent significant decrease in metal volume, the so-called cathodic method is usually adopted as a means of protection. Its basic functioning principle is the compensation of the effect of stray currents by applying an appropriate negative polarity metal structure, thus reducing or even completely eliminating, the discharge current. When the protection current from an external source is insufficient (e.g. poor insulation coating), the process of draining the stray current back to the electric traction network may be used in addition to cathodic protection (Balitskii & Chmiel, 2015).

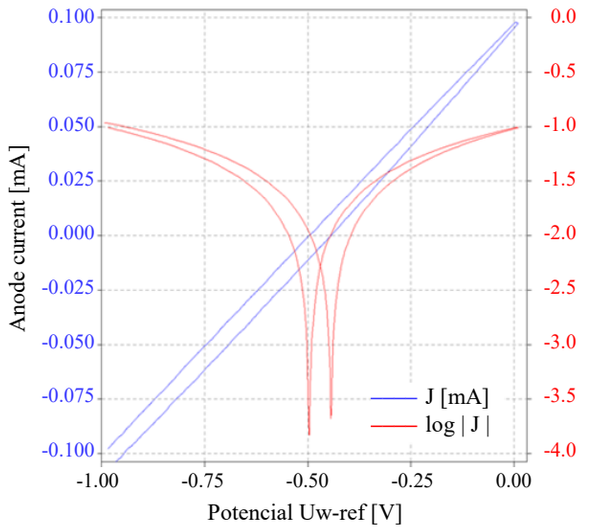

Figure 1. Voltammetric curves Domex steel in the soil solution

In Figure 1, the blue curves show the current value, while red curves represent the logarithm of the absolute value of the current for increasing and decreasing potential.

On the basis of tests, it was determined that potential changes ranging from –0.5 V to –0.2 V are particularly important. Additional tests indicated a change in polarity of the potential from –0.3 V (for the HNO_3 solution) to –0.35 V (for NaCl). A significant shift of the peak potential during the return cycle in the NaCl solution, due to the formation of a layer of iron chlorides, was observed. A negative value of the anodic current in the circuit is a sign that conditions of cathodic polarization were created at the working electrode, with the consequent evolution of hydrogen (Norma PN, 2004).

It is noted that the current density in a 0.1 M soil solution and in a 0.1 N nitric acid solution reaches 50 mA. Therefore, it can be assumed that the scaling factor is approximately 500. It follows that 15 minutes of exposure of Domex steel in a 0.1 N nitric acid solution corresponds to about a week's exposure in a natural soil environment.

Corrosion and erosion research

The test was conducted based on the dynamic cyclical process potentiometer, which allows to determine the oxidation potentials (Figure 2).

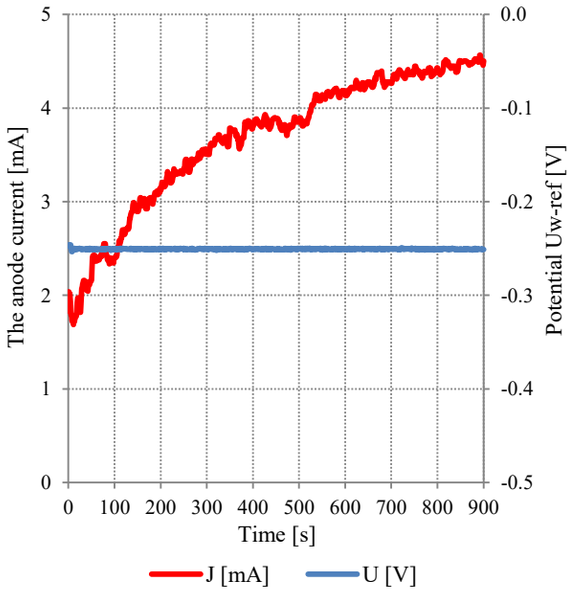

Figure 2. Changes in the conditions of corrosion current anode

The material used consists of Domex steel in the form of discs of 13 mm diameter and 4 mm thickness (cut elec).

The samples were prepared for the test according to the following procedure:

- Grinding flat surfaces on paper abrasive grit 500;
- Grinding test surface to grit 1000;
- Polishing test surface with a 3 micrometer diamond (Struers DP);
- Washing sample in methyl alcohol and drying in warm air;
- Weighing samples;
- Exposing samples to corrosion;
- Washing sample in methyl alcohol and drying in warm air;
- Weighing samples;
- Exposing erosion;
- Washing sample in methyl alcohol and drying in warm air;
- Weighing samples;
- Purifying the contact surface (grinding grit 1000).

Erosion Research was performed in the blasting shock chamber in accordance with ASTM G134 conditions:

- Pressure stream, PS – 12.5 MP;
- Counter-pressure in the chamber, PK – 0.25 MPa;
- Nozzle diameter, DD – 0.4 mm;
- Distance nozzle – sample, L – 10 mm;
- Temperature, TO – 22÷25°C (Norma ASTM, 2010).

The aim of the study was to evaluate the erosion resistance of the material degraded in the process of corrosion by stray currents.

Determination of the evolution of erosion through gravimetric analysis

The aim of the study was to evaluate the erosion resistance of the material degraded by corrosion caused by stray currents. The simulation results are shown in Table 2. All results indicate material losses of DOMEX steel and are expressed in mg. A separate overview shows the cathodic and anodic conditions.

Table 2. Intensity of the erosion for individual processes

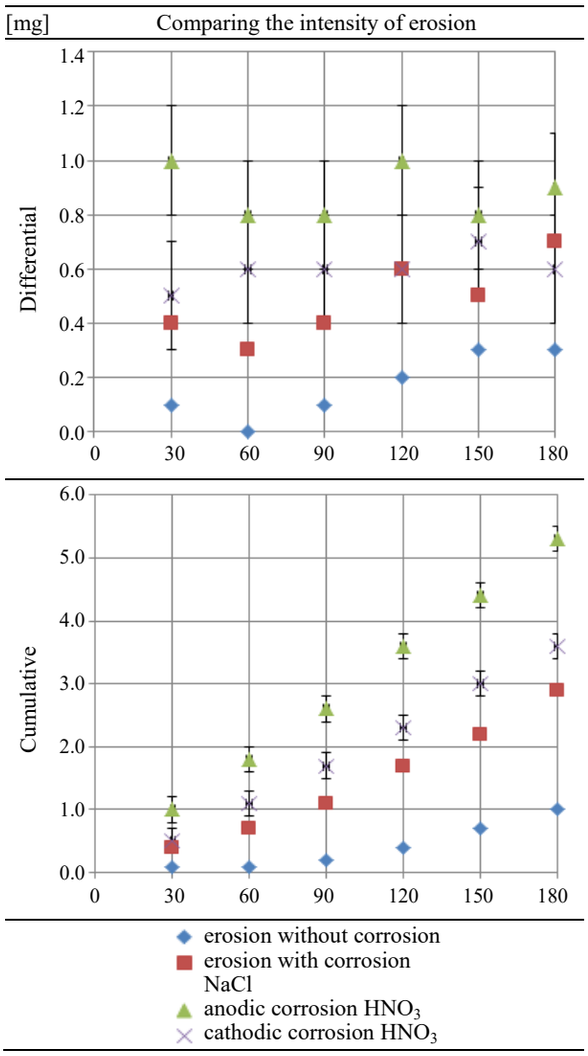

Conclusions

The flow of currents in traction networks produces the undesirable phenomenon of stray currents. These currents have a negative impact on all metal parts in the soil as they cause electrochemical corrosion. The components most vulnerable to this phenomenon are those found in the passage of these currents to the substation, where the surface of the anode takes on a high potential.

A small change in capacity with respect to the passive state is sufficient to cause corrosion of significant intensity. For example, 10 mV of difference is able to cause a corrosion current density up to 10 mA/cm^2. The anode current density is the cause of the relatively large corrosion destruction.

Cathodic polarization is not sufficient to maintain the service life of the object due to the risk of hydrogen degradation of the metal. Beloglazov has shown that currents having a density greater than 3 mA/cm^2 promote intense absorption and diffusion of hydrogen into the metal material.

The simultaneous exposure of object to the phenomena of corrosion and erosion is particularly dangerous. The synergistic effects can be divided into the following classes:

- Erosion accelerates corrosion as a result of the removal of the passive layer. Under the conditions of the experiment, the accelerating agent can be quantified as 50;
- Reduction of the erosion resistance of the material as a result of electrochemical corrosion and hydrogen degradation by a factor of 3 to 5, compared to conditions in which corrosion does not occur;
- Creation of areas sensitive to corrosion as a result of the accumulation of stress and strain in the surface layer during the erosion process.

The presence of stray currents can disrupt conventional systems of anticorrosive protection and cause premature destruction of the object as a result of the simultaneous action of corrosion and mechanical degradation processes.

Steel with a micro supplement of boron showed relatively good resistance to degradation in hydrogen under the simulated cathodic polarization currents (Beloglazov, 2011).

Under the conditions of the corrosion experiment, the erosion process does not display the annular distribution of damage characteristic of pure erosion. On the contrary, the damage extends almost evenly over the entire surface, as is common with electrochemical phenomena. The process of erosion consists mainly in the removal of a layer degraded by corrosive phenomena. The effect of erosion is several times higher than in the case of corrosion-free conditions after only 90 minutes following the appearance of erosion in the central part of the sample. This can be explained as a consequence of hydrogen, which gradually deteriorates the material as a result of the electrochemical process and of cavitation (Chmiel & Łunarska, 2012). The presence of boron as micro-alloying additive can slow down the process.

References

1. Balitskii, A. & Chmiel, J. (2015) Resistance of Plate Shipbuilding Steels to Cavitation-Erosion and Fatigue Fracture. *Materials Science* 50 (5). pp. 736–739.
2. Beloglazov, S.M. (2011) *Electrochemical Hydrogen and Metals*: *Absorption, Diffusion and Embrittlement Prevention in Corrosion and Electroplating*. Nova Science Pub Inc.
3. Chmiel, J. & Łunarska, E. (2012) Effect of cavitation on absorption and transport of hydrogen in iron. *Solid State Phenomena* 183. pp. 25–30.
4. Norma ASTM (2010) Norma ASTM G134-95(2010)e1. Standard Test Method for Erosion of Solid Materials by a Cavitating Liquid Jet.
5. Norma PN (2004) Norma PN-E-05030-10:2004. Ochrona przed korozją. Elektrochemiczna ochrona katodowa i anodowa. Terminologia.
6. Sokólski, W. (2007) Prądy błądzące – prądy niechciane. *Magazyn Ex* 3. p. 61.
7. Stochaj, P. (2013) Prądy błądzące jako źródło zagrożenia korozyjnego gazociągów stalowych. *Nafta-Gaz* 9. pp. 683–689.

Scientific Journals
of the Maritime University of Szczecin

Zeszyty Naukowe
Akademii Morskiej w Szczecinie

2016, 48 (120), 138–145
ISSN 1733-8670 (Printed)
ISSN 2392-0378 (Online)
DOI: 10.17402/187

Received: 05.05.2016
Accepted: 23.09.2016
Published: 15.12.2016

User charges for road infrastructure in certain European Union member states

Piotr Lewandowski

Maritime University in Szczecin, Faculty of Economics and Transport Engineering
Institute of Transport Management
11 H. Pobożnego St., 70-507 Szczecin, Poland
e-mail: p.lewandowski@am.szczecin.pl

Key words: infrastructure, transport, charges, EU Member States, regulations, roads

Abstract

New regulations enforced by the European Commission have greatly extended the possibilities to levy charges. The regulations include not only the TEN-T network, but also all motorways in Europe. The directive has given Member States the opportunity to charge heavy goods vehicles in a way to balance not only the costs of infrastructure but also those connected to noise and pollution caused by road traffic. The new provisions have enabled Member States to increase the charge during peak periods and to lower it in the off-peak hours in order to reduce traffic more effectively. The binding norms provide that the revenue from the charges should be destined to enhancing the stability of the transport section. The new rules provide a strong incentive to set aside new revenues from charging to finance certain types of transport projects. Poland has adapted very well to this new situation. The ever-increasing network of toll roads gives new opportunities for the development of transport. The increasing number of national and foreign hauliers guarantees constant investment in the development of road infrastructure and therefore a good use of the country's geographical location.

Introduction

The liberalisation of provisions concerning international transport in EU Member States has been subject to criticism by certain groups of road hauliers, in reference to equal opportunities in the use of road infrastructure.

The transport of cargo within the Community is subject to tolls. The 1999 Eurovignette Directive on the charging of heavy goods vehicles weighing over 3.5 tonnes for the use of certain infrastructures made it possible to recover the costs sustained in the maintenance of road infrastructure. The directive authorises Member States to levy time-based 'user charges' (e.g. per day, per week, per year) or distance-based tolls (e.g. per kilometre). Said provisions prohibit the recovery of the so-called external costs, such as those related to air and acoustic pollution, currently borne by society at large and tax payers in particular.

On June 1st, 2011 the European Parliament passed new regulations allowing Member States to levy additional charges on heavy goods vehicles, connected not only with the maintenance of infrastructure but also with noise and pollution. Since 2012, this new regulation has allowed Member States to address the issue of heavy traffic, allowing them to regulate the amount of the charge (with the possibility to increase it up to 175%), according to the time of day (European Commission, 2008; 2011). Additionally, a new mechanism allows assigning the revenue from the new charges to new investment projects for the modernisation of transport infrastructure.

The EU provisions therefore send price signals to operators, thanks to which heavy goods vehicles bear the entire cost connected with the noise and pollution they create. The tolls also constitute a tool to regulate traffic depending on the time of day, discouraging the entrance on the roads of heavy goods vehicles during peak hours (etransport.pl).

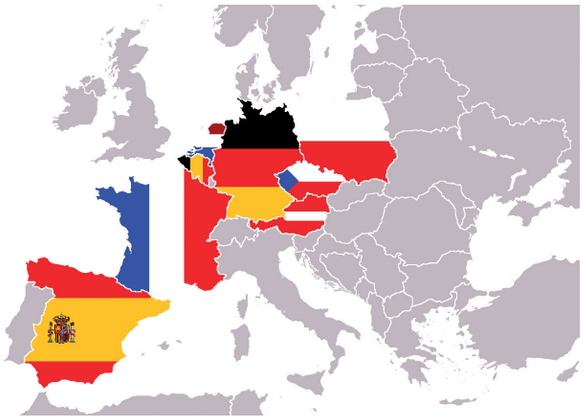

Figure 1. States whose user charges are subject to analysis

In practice, the charges for external costs amount to 3–4 cents per kilometre, depending on the Euro class of the vehicle, the location of the road and the traffic. According to the European Commission's decision, the charges are to be collected via electronic systems and the drivers are to be issued a proof of payment, directly stating the amount of external costs so that these can be transferred to the finale clients.

Member States determine individually the roads for which they wish to charge user fees and they also individually settle the amounts. The charging systems also vary from country to country.

The analysis of the rates of charges for the use of road infrastructure and the systems used for their calculation in chosen EU states will allow to evaluate some of the problems faced by professional road hauliers (DKV Euro Service, 2016).

The following states have been subject to analysis: Poland, Austria, Belgium, the Netherlands, the Czech Republic, Spain, France and Germany (Figure 1).

Poland – electronic toll collection system viaTOLL

Poland has an electronic toll collection system for the passage on national roads. The charge is collected on the chosen sections of the road and goes to the National Road Fund.

The amounts of electronic charges that apply in the viaTOLL system have been advised by the Ministry of Transport, Construction and Marine Economy (formerly the Ministry of Infrastructure).

The categories of vehicles subject to charges are (Eurovignette, 2016):

- a vehicle or a combination of vehicles of MPW (maximum permissible weight) over 3.5 tonnes but below 12 tonnes;
- a vehicle or a combination of vehicles of MPW over 12 tonnes;
- buses, regardless of their maximum permissible weight.

Road categories:

- Class A and S national roads, with class A referring to motorways and S referring to express ways (Table 1);
- Class GP and G national roads, with GP referring to major trunk roads and G referring to major roads (Table 2).

The viaTOLL system is based on the short-range wireless communication technology. The system consists of the following elements: above the toll roads there are gantries fitted with antennas. The antennas allow the communication between

Table 1. Electronic toll rates for Class A and S roads

Vehicle category	Toll rate per 1 km of national road (in PLN)			
	EURO class, according to exhaust emissions (1)			
	max. EURO 2	EURO 3	EURO 4	min. EURO 5
Vehicles with MPW (2) over 3.5 tonnes but below 12 tonnes	0.40	0.35	0.28	0.20
Vehicles with MPW (2) over 12 tonnes	0.53	0.46	0.37	0.27
Buses regardless of MPW	0.40	0.35	0.28	0.20

Table 2. Electronic toll rates for Class GP and G roads

Vehicle category	Toll rate per 1 km of national road (in PLN)			
	EURO class, according to exhaust emissions (1)			
	max. EURO 2	EURO 3	EURO 4	min. EURO 5
Vehicles with MPW (2) over 3.5 tonnes but below 12 tonnes	0.32	0.28	0.22	0.16
Vehicles with MPW (2) over 12 tonnes	0.42	0.37	0.29	0.21
Buses regardless of MPW	0.32	0.28	0.22	0.16

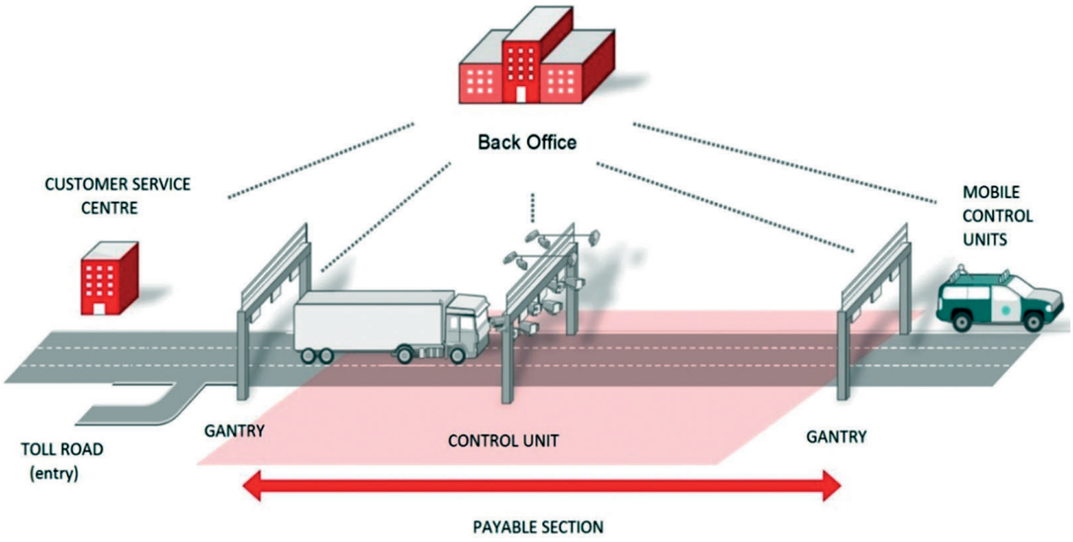

Figure 2. The viaTOLL operation principle

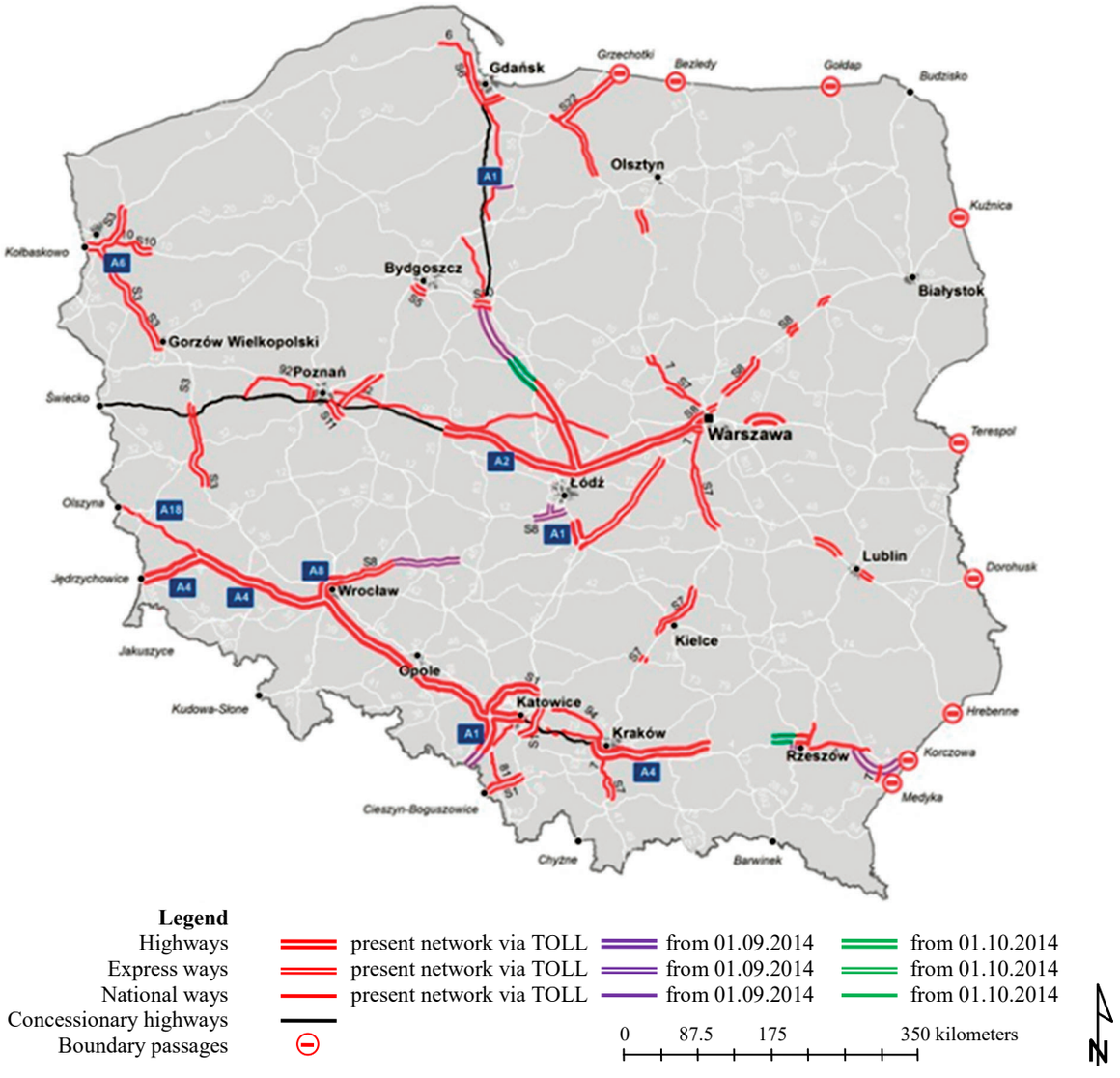

Figure 3. Poland – a map of toll roads (author's own compilation based on GDDKiA data)

transmitters and viaBOXes installed in cars. Every time a car (equipped with a viaBOX) passes under a gantry, a toll is calculated for the passage on a toll-charging section (Figure 2).

The viaTOLL system was introduced in March 2011. Initially it covered express ways and motorways, for a total length of 1565 km. Poland (using primarily EU funds) is still introducing new transit sections, with 325 km being added in 2012, 300 km in March 2013, 465 km in October 2013 and 265 km in September 2014.

The 22 February 2015 Regulation of the Council of Ministers has introduced an additional extension. Since June 30th, 2015, 251 km of national roads (35 km of motorways and 216 km of express ways) are being added to the system. Within four years, the total length of toll roads has doubled and currently amounts to 3171 km. However, the map presented in Figure 3 shows how much there is still to be done and how the topography and location of Poland facilitates the use of EU laws to collect charges, which substitute EU funds expected in the future. This is best seen by considering the increase of profits from e-toll. In 2014, the viaTOLL system collected PLN 1.42 billion, i.e. a third more than in the previous year. The number of users and first-time registrations has also increased (843 000 in 2014 in comparison with 766 000 in 2013).

The comparison between the total size of infrastructure and the amount of toll roads in the chosen EU states proves truly interesting.

Austria

In the territory of Austria there is an electronic toll system for lorries and buses over 3.5 tonnes using highways and freeways. Vehicles under 3.5 tonnes are subject to a different type of toll, as they are obliged to buy motorway vignettes (Table 3). The automatic system, called GO, has replaced both the vignettes and the road tax. The toll collection system has been designed by the Kapsch TrafficCom Company. The amount of toll differs according to the EURO emission class, the number of axles of a vehicle and the length of the section.

Increased rates are applied to particular sections of highways and freeways. The following are the special toll routes:

- A9 – Bosrucktunnel (km 57–67), Gleinalmtunnel (km 133–157);
- A10 – Kataschbergtunnel / Tauerntunnel (km 104–113);
- A11 – Karawankentunnel (km 11–21);
- A13 – Hangbrücken Schönberg-Matrei (km 10–19);
- S16 – Arlbergtunnel (km 22–39).

Belgium and the Netherlands

The Eurovignette system applies in Belgium and it is required from any vehicle over 12 tonnes using motorways in Belgium, the Netherlands, Luxemburg, Denmark and Sweden. The Eurovignette is bought for a specified period of time: day, week, month, or year. The charges are calculated according to the period of use, emission class and the number of axles. From 2016 the Viapass, a satellite toll system for vehicles over 3.5 tonnes MPW, will be applicable in the territory of Belgium (European Commission, 2016).

For all categories, a day vignette costs EUR 8.00. The other charges are described in Tables 4 and 5.

Table 4. Charges for passage – weekly tariff

Charges for passage on motorways and expressways, according to the EURO emission class for vehicles over 12 tonnes MPW – weekly tariff		
Emission class	1–3 axles	4 or more axles
EURO 0	26.00	41.00
EURO 1	23.00	37.00
EURO 2 and over	20.00	33.00

Table 3. Toll rates per one kilometre of highway

Tolling according to EURO emission classes Rates for vehicles with a max. permissible gross weight of more than 3.5 tonnes from 01-01-2015			
Rate group	Category 2 2 axle	**Category** 3 3 axle	**Category** 4+ 4 a. more axle
A EURO – emission class EURO VI	**0.156**	**0.2184**	**0.3276**
B EURO – emission class EURO EEV	**0.170**	**0.2380**	**0.3570**
C EURO – emission class EURO IV a. V	**0.188**	**0.2632**	**0.3948**
D EURO – emission class EURO 0 to III	**0.211**	**0.2954**	**0.4431**

Table 5. Charges for passage – monthly tariff

Charges for passage on motorways and expressways according to the EURO emission class for vehicles over 12 tonnes MPW – monthly tariff		
Emission class	1–3 axles	4 or more axles
EURO 0	96.00	155.00
EURO 1	85.00	140.00
EURO 2 and over	75.00	125.00

The Czech Republic – the electronic toll system MYTO CZ

The Czech toll system MYTO CZ (Figure 4) is applied to all motor vehicles over 3.5 tonnes MPW. In this system the charge is based on the actual number of kilometres covered by the vehicle, EURO emission class and the number of axles, and it is calculated electronically by an on-board equipment Premid-Box (Table 6). The government of the Czech Republic decided to increase the toll as of January 1st, 2015 and to introduce a new Euro 6 tariff category. The Euro 6 Tariff is designated for vehicles belonging to the EURO VI category or EEV emission class and maintains a favourable rate.

Spain – the electronic toll system DKV

All vehicles are charged for using Spanish motorways ("Autopistas") (Figure 5). The charges for the passage on motorways and via tunnels may be settled by the use of DKV CARD or an on board toll equipment DKV BOX (Table 7). The DKV CARD enables also non-cash settlements when using secured car parks.

France – the electronic toll system TIS PL

The abbreviation TIS PL ("Télépéage Inter-Sociétés Poids Lourds") refers to the French toll system for trucks of categories 3 and 4. Approximately 9,000 km of French motorways, several bridges and tunnels are subject to toll for all vehicles weighing 3.5 tonnes or more (Figure 6).

Road tolls in France can be settled via DKV BOX or DKV CARD. In case of using the DKV BOX, the

Figure 4. The Czech Republic – a map of toll roads

Table 6. The Czech Republic – charges for passage

Rates for the passage on highways and motorways, according to the emission class and the number of axles for vehicles over 3.5 tonnes MPW in Czech korunas												
Emission class	EURO 0–2			EURO 3–4			EURO 5			EURO 6, EEV		
Number of axles	2	3	≥ 4	2	3	≥ 4	2	3	≥ 4	2	3	≥ 4
Highways and motorways	3.34	5.70	8.24	2.82	4.81	6.97	1.83	3.13	4.52	1.67	2.85	4.12
1st class roads	1.58	2.74	3.92	1.33	2.31	3.31	0.87	1.5	2.15	0.79	1.37	1.96

Acceptance DKV BOX/CARD	Acceptance DKV BOX
AP1	AP2
AP8	AP4
AP9	AP6
AP12	AP7
AP15	AP51
AP17	AP61
AP18	AP68
AP19	AP71
AP36	C31
AP37	C32
AP41	(former AP16)
AP46	C33
AP53	
AP55	
AP57	
AP66	
M12	
R2	
R3	
R4	
R5	

Tunnel:

① Túnel del Cadi (North of Barcelona); ② Túneles de Artxabda (Bilbao): But only for coaches, two axle-mini van and cars
③ Túneles de Vallvidrera (Barcelona)

Figure 5. Spain – the system of toll roads

Table 7. Spain – charges for passage

Section	Class 1 (vehicles with 2 or 3 axles) [EUR]	Class 2 (vehicles with 4 or more axles) [EUR]	
Alicante (Crevillente) → Cartagena (Beatos)	4.30	5.20	A37
Ávila → Adanero	10.20	11.70	A51/A6
Ávila → Villacastín (A 6)	3.00	3.75	A51
Barcelona (Mataró) → Malgrat / Palafolls	5.44	6.77	C32 (A19)
Barcelona (Martorell) → Tarragona	13.55	17.05	A7
Barcelona (Molins de Rei) → El Vendrell	11.00	13.80	A7
Bilbao → Zaragoza	58.30	67.60	A68
Burgos (Castanares) → A68 (Bilbao)	12.45	12.45	A1
Burgos (Castanares) → Arminón	13.00	13.00	A1
Castelldefels Sud (Barcelona) → El Vendrell	10.28	18.14	C32 (A16)
El Campello (Alicante) → Monforte del Cid / A–31	5.15	6.15	A7
Girona – Norte → Granollers	12.95	16.45	A7
Irun (Behobia) → San Sebastian (Donostia)	3.95	4.72	A8
La Coruna → Ferrol	8.20	10.70	A9

Table 8. France – charges

Motorway No. / payable section	Category	
	3 (2-axle vehicle)	4 (3-axled or more vehicle)
Paris – Arras (A26)	23.6	30.9
Paris – Metz (A4)	49.3	65.2
Paris – Strasburg (A4)	74.1	98.6
Bordeaux – Toulouse (A62)	38.3	50.6
Lyon – Les Abrets (A43)	13.2	16.8
Reims – Troyes (A5)	23.2	30.9

toll system operators generally offer an additional 13% discount (Table 8).

Germany – the electronic toll system TOLL COLLECT

In Germany, all trucks with a total weight of 7.5 tonnes or over must pay distance-based tolls for the use of motorways. German toll amounts depend on (Table 9):

Figure 6. France – the network of motorways

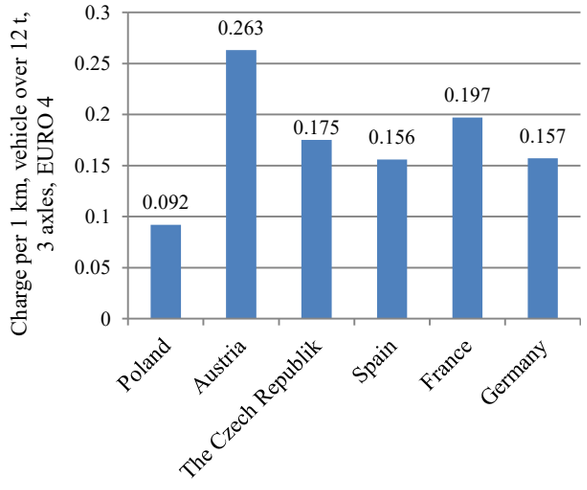

Figure 7. The cost of 1 km by a 3-axle, Euro IV-class vehicle over 12 tonnes

- emission class,
- number of axles,
- length of the toll stretch.

In addition, circa 1,000 km of four-lane main roads are subject to toll charges.

Charges for the use of infrastructure are calculated on the basis of environmental protection. Member States base their fees on the EURO class. The higher the engine class, the lower the price. As a consequence, road hauliers are forced to invest continuously in eco-friendly equipment (Go-Maut, 2016). Figure 7 shows the cost per kilometre for a EURO IV Class vehicle, which is one of the most common engine classes. Charges in Poland, which is still in the early stages of toll introduction, are very low.

Table 9. Germany – charges

Category	Proportion of toll rate (in cents) Costs for air pollution	Number of axles	Proportion of toll rate (in cents) Costs for infrastructure	Toll rate (in cents)
A (EURO 6)	0	less than 3	12.5	12.5
		more than 4	13.1	13.1
B (EURO 5)	2.1	less than 3	12.5	14.6
		more than 4	13.1	15.2
C (EURO 4)	3.2	less than 3	12.5	15.7
		more than 4	13.1	16.3
D (EURO 3)	6.3	less than 3	12.5	18.8
		more than 4	13.1	19.4
E (EURO 2)	7.3	less than 3	12.5	19.8
		more than 4	13.1	20.4

Conclusions

The new regulations enforced by the European Commission have greatly extended the possibilities to levy charges. The regulations include not only the TEN-T network, but also all motorways in Europe. The directive has given Member States the opportunity to charge heavy goods vehicles with charges which not only balance the costs of infrastructure but also the costs of noise and pollution caused by road traffic.

The new provisions have enabled Member States to increase the charge during peak periods and to lower it in the off-peak periods in order to reduce traffic more effectively. The toll may be increased by as much as 175% over the average amount, with the highest charges to be collected for maximum five peak hours daily (for the rest of the time lower charges must apply).

The binding norms provide that the revenue from the charges should be reserved to enhancing the stability of the transport section. The new rules provide a strong incentive to set aside new revenues from charging to finance certain types of transport projects. Member States can also decide to earmark 15% of the total revenue collected for projects on the trans-European network. There is also an obligation for transparent reporting, as Member States will have to report regularly on how the total revenues of tolls are used.

Special provisions are made for mountain areas which will be allowed to simultaneously apply the existing mark-up and the new external cost charges, which will have to be spent on financing TEN-T priority projects situated on the same TEN-corridor.

The "rendez-vous" clause keeps the issue of "polluter pays" and internalisation of external costs under constant review. It allows the Commission to produce reports on further internalisation of external costs, including the extension to other transport modes, for other vehicles and to ensure a more harmonised approach.

Poland has adapted very well into this new situation. The ever-increasing network of toll roads gives new opportunities for the development of transport. The increasing number of national and foreign hauliers guarantees constant investment in the development of road infrastructure and therefore a good use of the country's geographical location.

References

1. DKV Euro Service (2016) [Online] Available from: www.dkv-euroservice.com [Accessed: May 04, 2016]
2. etransport.pl (2016) [Online] Available from: www.etransport.pl [Accessed: May 04, 2016]
3. European Commission (2008) Documents MEMO/08/492. *Greening Transport Package – Frequently asked questions*. [Online] Available from: http://europa.eu/rapid/press-release_MEMO-08-492_en.htm [Accessed: May 04, 2016]
4. European Commision (2011) Documents MEMO/11/378. *Road charging: Heavy lorries to pay for costs of air and noise pollution*. [Online] Available from: http://europa.eu/rapid/press-release_MEMO-11-378_en.htm [Accessed: May 04, 2016]
5. European Commission (2016) National Reform Programme 2016 [Online] April 2016. Available from: http://ec.europa.eu/europe2020/pdf/csr2016/nrp2016_belgium_en.pdf [Accessed: May 04, 2016]
6. Eurovignette (2016) [Online] Available from: www.eurovignettes.eu [Accessed: May 04, 2016]
7. Go-Maut (2016) [Online] Available from: www.go-maut.at [Accessed: May 04, 2016]

Scientific Journals
of the Maritime University of Szczecin

Zeszyty Naukowe
Akademii Morskiej w Szczecinie

2016, 48 (120), 146–152
ISSN 1733-8670 (Printed)
ISSN 2392-0378 (Online)
DOI: 10.17402/188

Received: 29.04.2016
Accepted: 15.11.2016
Published: 15.12.2016

Legal aspects of using inland surface waters to satisfy residential needs in Poland

Dorota Łozowicka[1], Magdalena Kaup[2]✉, Zbigniew Machowski[3]

[1] Maritime University of Szczecin, Faculty of Navigation
1–2 Wały Chrobrego St., 70-500 Szczecin, Poland, e-mail: d.lozowicka@am.szczecin.pl
[2] West Pomeranian University of Technology, Faculty of Maritime Technology and Transport
41 Piastów Ave., 71-065 Szczecin, Poland, e-mail: mkaup@zut.edu.pl
[3] Solicitor, PhD student at the Faculty of Law and Administration of the University of Szczecin,
sekretariat@kancelaria-machowski.pl
✉ corresponding author

Key words: inland waters, floating rules, residential purposes, houseboats, perspectives, legal aspects

Abstract
This article attempts to determine the rules for lawful use of floating objects for residential purposes. It presents the currently existing legal solutions applied in Europe for such floating structures. Further, the article describes a classification of residential floating objects from the legal perspective. The existing regulations are analyzed with regard to the provisions of the Water Law Act and the Inland Navigation Act. Moreover, the paper describes three different types of water usage, i.e. common, ordinary and special, and discusses in which of these forms the residential use of public waters falls. The analysis allows for the determination of the directions of further research, so that an accurate procedure ensuring a lawful use of houseboats can be adopted.

Introduction

It is a cliché to say that satisfying a person's residential needs is one of the most fundamental objectives in their life, but this may entail the necessity to implement novel solutions. One common and established way to secure one's residence is to use real estate designed for that purpose. However, the range of options available is actually substantially wider than this. It is becoming more and more common to come up with concepts for locating residential structures in aquatic settings. This way of meeting residential needs has been present on a wider scale in the Netherlands, Sweden and France. "Houseboats" have started to be encountered in Poland, as well, particularly on public inland surface waters, i.e. rivers and lakes.

Different companies are offering to build and sell floating objects that are technically fully adapted to live in, as they are equipped with complete bathroom and toilet facilities, as well as the wiring and heating systems. They also carry all the required documents allowing such structures to be used on water.

The formal and legal aspects of building and using an object of this sort in Poland are beyond the purpose of this article. Rather, it focuses on determining the rules to follow in order to secure a lawful residential use of floating structures. To this end, the paper endeavors to appropriately classify these structures by type, and then analyze the legal opportunities for using surface waters under the Polish Water Law Act and the Polish Law of Inland Navigation Act, for the purpose of determining the available options for the residential use of public waters.

Existing legal solutions allowing for various forms of residential use of water

In Europe and the USA, the use of houseboats gained momentum in the early 1980s. It came as a response to growing affluence of societies with a simultaneous increase in land prices. In such

countries as the Netherlands, Germany, England and Sweden, riverside towns and cities have seen a growing popularity of the use of floating barges to live on. Poland can already boast a few similar solutions, as well (Kaźmierczak & Zaremba, 2013).

Some of the most important reasons for riverside town inhabitants migrating towards rivers are the development of urban agglomerations, growing prices of building land, limited resources of building land, growing affluence of societies, environmentally-friendly lifestyles or esthetic qualities.

The Netherlands can serve as an example of how architecture can be adapted to the environmental conditions, where approx. 60% of the country's area is below the sea level (Figure 1). Currently, there are 16 thousand floating homes that are legally sanctioned residential buildings. The floor area of a single one of these homes may reach 200 square meters. Until recently, the rules governing the erection of floating buildings were complex, but in 2009 the government passed new resolutions regulating the classification of buildings on water. It is now possible to permanently and legally dwell on them while taking advantage of all the privileges enjoyed by buildings on land, including rights to obtain insurance and credit. The applicable legal regulations have standardized the construction and ownership issues thus adapting them to the needs of the residential use of water (DNW, 2006).

Figure 1. An example of floating residential structure in Amsterdam

In Germany, particularly in Hamburg, the recent years have witnessed extensive investments in developing and managing riverside areas and harbor wharfs, as they have been discovered to contain a huge economic potential. Nevertheless, there are no separate regulations governing the issues of technical conditions for erecting floating buildings and, depending on the location, different rules are applied. For a house located in the river channel at the entrance to the harbor, the water law and the German inland navigation law are applied, while floating buildings located on urban canal waters are subject to different regulations (DNW, 2006; Sibilak, 2014).

Similarly, the Polish law does not provide for any established set of regulations concerning the residential use of water. Also, there is no standardized approach to interpreting the already existing regulations, which could help in carrying out this sort of investment. The procedures and regulations that apply in any given case are strictly dependent on the structure's parameters, the mooring technique to be used, and the potential mooring places.

Legal classification of floating objects intended for residential use in Poland

A floating object intended for residential use is expected to play an identical role to that of a residential building, i.e. immovable property erected on land in accordance with the requirements of the Building Law Act of 7 July 1994 (Official Journal of 1994) (Ustawa, 1994). However, a mere look at the fact that it is meant to be used and located on water alone, meaning that it has no permanent ties to the land, makes it absolutely clear that it is not immovable property. On the other hand, if it is to be used on water areas as a floating device it should be deemed to be a ship.

According to art. 5.1.1.h of the Inland Navigation Act of 21 December 2000 (O.J. 2013.1458 of 2013.12.06) (hereinafter referred to as the Navigation Act) (Ustawa, 2000), a ship is a floating device with or without a motor drive, including a ferry, a hydrofoil or a hovercraft, meant for use or used on inland waterways, also for residential purposes. The wording of this provision leaves no doubt that ships can be used to satisfy residential needs. This, however, raises the question of what conditions should be met in order to be able to take advantage of this possibility, and what is the actual scope of this option.

The rules for developing lands not covered by waters by erecting buildings and flats on them and using such structures, along with the formal and legal requirements to be fulfilled in this respect, have been made precise and clear by the Polish regulators. The same cannot be said of the legal regulations that could be applied to assessing the lawfulness of using water surface for residential purposes.

An analysis of the regulations applicable in this respect should first of all invoke the provisions of the Water Law Act and the Inland Navigation Act. Such

an analysis leads to the conclusion that permanent residential use of floating objects is not banned by these two statutes, therefore it is allowed and does not violate the law. It can certainly be found that there is no straightforward ban on residing on water. A ban of this sort, for instance, does apply to plots within the premises of Family Garden Plots, and is directly provided for in art. 12 of the Family Garden Plots Act of 13 December 2013 (O.J.2014.40 of 2014.01.09) (Ustawa, 2013).

General rules for use of surface waters, and surface water management options in Poland

The rules for using waters and managing them, as well as administering water resources, are to a considerable extent regulated in the Water Law Act (Ustawa, 2001b). This statute provides that water management should take into account the common interest rule and be implemented through cooperation between public administration authorities, water users and local community representatives so that maximum social benefits can be achieved.

Art. 31 of the aforementioned Act contains general rules determining the manner in which water can be used. According to this provision, water usage is allowed to satisfy the needs of people and economy. Three types of water usage are enumerated: common usage, ordinary usage and special usage (Figure 2). It should be added that none of these forms of water usage may cause deterioration of water condition and of the ecosystems dependent on such water, or lead to water wastage, water energy wastage, or damage.

The regulators have expressly ruled out the following from the usage right to surface waters:

1) extraction of stone, gravel, sand and other material from inland marine waters together with the inland marine waters of Gdańsk Bay and territorial seawaters;
2) removal of vegetation from waters or banks;
3) extraction of stone and gravel from mountain streams;
4) use of water in water bodies intended for breeding and raising of fish and other aquatic organisms, situated on lotic waters;
5) inflow of wastewater.

The following have been ruled out from the ordinary usage of water:

1) irrigation of soil or crops with groundwater using sprinkler irrigation systems;
2) extraction of surface water or groundwater in an amount exceeding 5 cubic meters per 24 hours;
3) use of water for the purposes of business activity;
4) agricultural use of wastewater or entering of treated wastewater to water or soil if the combined amount of such wastewater exceeds 5 cubic meters per 24 hours.

There is no obligation to obtain the owner's permission, or any special permits, for the common usage of waters, which applies to public waters that are owned by the State Treasury or local government units. However, the special usage of such waters requires that a relevant permit under the Water Law

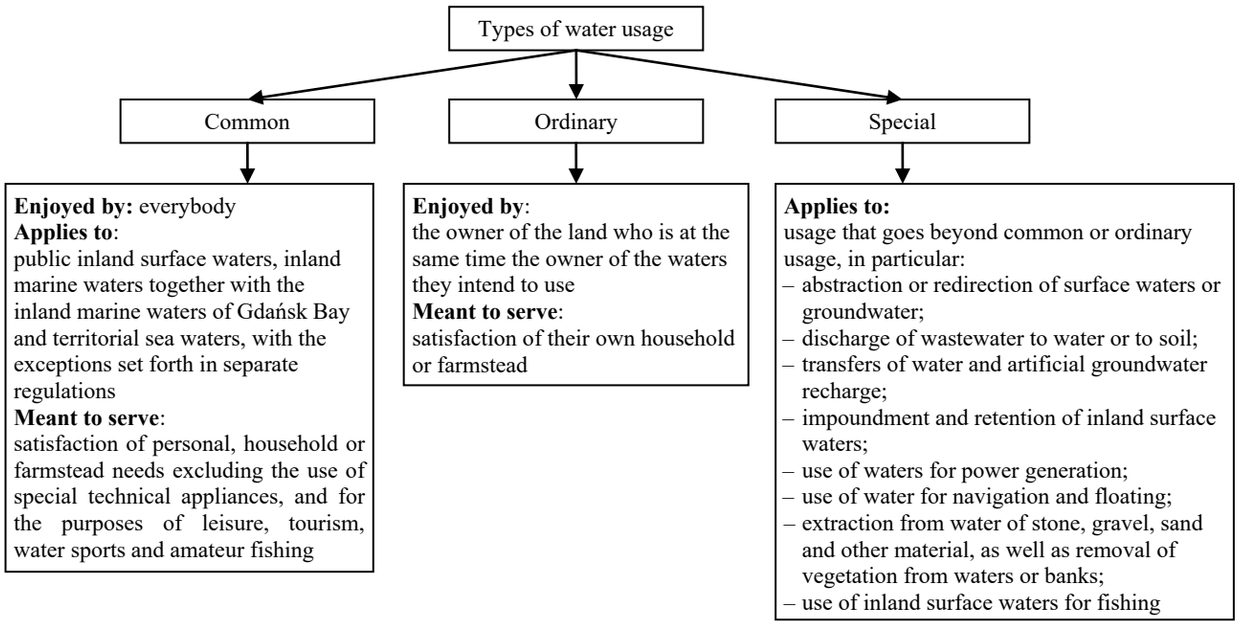

Figure 2. Types of water usage in Poland

Act be obtained. The scope of this paper is limited to public waters.

Residential use of public waters in Poland

This situation calls for an analysis of which of the usage forms discussed in chapter 2 of this article covers the residential use of public waters. Since the purpose of common usage is to satisfy the personal needs of water users, it should raise no doubt that this concept includes satisfying their residential needs, as well. Bearing this in mind, it can be concluded that the holders of a habitable vessel can use it for this purpose on all public waters of their choice.

Nevertheless, this right does not include the possibility of fixing the vessel permanently to some place, i.e. immobilizing it. It is obvious that in order to prevent uncontrolled relocation of the vessel it must be fixed to a designated water facility. According to art. 9.1.19 of the Water Law Act, a water facility shall be any facility used for shaping water resources and using them. Among such facilities, the Act lists wharfs, piers and marinas. Clearly, the practical purpose of the facilities concerned is to allow watercrafts to stop and be properly immobilized. Before these facilities can be built, one is required to obtain the title to the land on which they are to be located and a relevant permit under the Water Law Act. Whether the title to the land covered by public waters can be obtained, and the scope of such a title, will depend on the type of land.

According to art. 14.1 of the Water Law Act, the lands covered by surface waters are property of the owner of such waters. As mentioned before, public inland waters are owned by the State Treasury, or a relevant local government unit. Therefore, it is these entities that hold the freehold title to the lands covered by these waters and the right to dispose of such lands, which are construed so to be the beds and banks of natural flows, lakes and other natural water bodies, within the boundaries of the shorelines. Figure 3 depicts a division of inland surface waters.

This division is of essential importance in terms of the possibility of and rules for trading in land covered by lentic waters or land covered by lotic waters.

Article 14.2 of the Water Law Act provides that lands covered by lotic surface waters may not be used for trading under the civil law, except cases that are expressly named in the Act. Such exceptions are related to r use by fishing districts and other undertakings that are explicitly listed in art. 20.1 of the Water Law Act (Ustawa, 2001b).

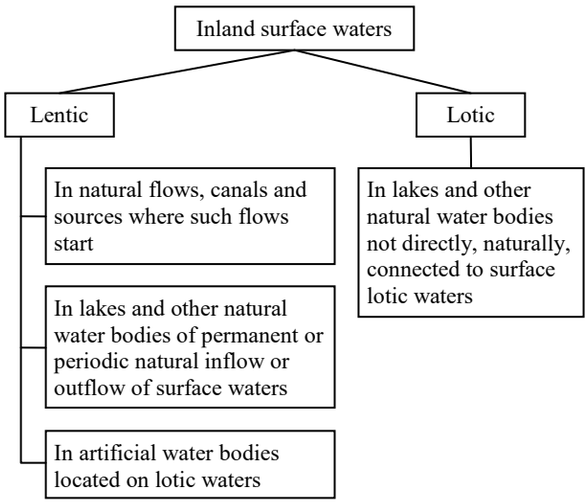

Figure 3. Types of inland surface waters

The provision discussed herein provides that lands covered by waters owned by the State Treasury shall only be released for use only if they are indispensable for the purpose of carrying out undertakings related to:

1) water power generation;
2) transport by water;
3) extraction of stone, gravel, sand and other material or removal of vegetation from water;
4) building transport infrastructure;
5) building industrial, municipal or agricultural infrastructure;
6) activity intended for recreation, tourism, water sports and amateur fishing;
7) services designed for other purposes than those specified in point 6 above;
8) building telecommunication infrastructure.

Certainly, the building of a facility designed for the parking of a watercraft used for satisfying a specific person's residential needs does not fall within any of the categories listed above. However, pursuant to art. 20.6a of the Water Law Act, lands covered by water that are owned by the State Treasury and are indispensable for the purposes of running undertakings other than those specified in item 1 shall be granted for use under the rules provided for in the Civil Code Act of 23 April 1964 (Ustawa, 1964).

The limitations referred to above do not apply to lands under inland lentic surface waters owned by the State Treasury. Such lands may be sold by the minister having jurisdiction over State Treasury matters upon receipt of permission from the minister with jurisdiction over water management matters and according to the rules provided for in the Real Estate Management Act of 21 August 1997 (O.J.2015.1774

of 2015.11.03) (Ustawa, 1997). In turn, the President of the National Water Management Authority represented by directors of local regional water management authorities is the one with jurisdiction to administer and dispose of the remaining lands covered by water.

As it comes to the necessity of obtaining the Water Law Act permit to build a facility required for mooring a houseboat, art. 122 of the Water Law Act must be invoked. According to item 1.3 of that article, the erection of water facilities requires that the Water Law Act permit be first obtained. The following documents must be attached to the application for the Water Law Act permit:

1. a Water Quality Impact Assessment and Water Management Survey Statement (Polish: operat wodnoprawny);
2. a decision on the site location of a public-purpose project or a zoning decision if it is required – in the case of an application for the Water Law Act permit to build a water facility;
3. a description of the intended activity drawn up in non-technical language.

The Water Quality Impact Assessment and Water Management Survey Statement are the basic documents on the grounds of which the permit under the Water Law Act is issued. These documents must be presented in both descriptive and graphical forms. The Statement indicates, among other things, the purpose and the scope of the intended water usage, a specification of the waters covered by the Water Law Act permit, and the water facilities plan, presented in the form of a sketch or on a map.

Not all facilities will require a permit issued under the Water Law Act. Art. 123a of the Water Law Act specifies the building undertakings and the activities that only require to be reported to the competent authority. Hence, depending on the facility chosen to be built, the requirements that secure it is lawfully erected will differ. For instance, the erection of a pier of a total length of up to 25 meter will only need to be reported. The same will be true for floating objects or ships meant for residential or service-related purposes on lotic waters.

As a rule, such reports should be made to the district administrator (head of the country) with jurisdiction over the locality. Only if the planned undertaking is to be carried out in closed areas, as defined by the Environmental Protection Act of 27 April 2001 (O.J.2013.1232 of 2013.10.23) (Ustawa, 2001a), will the report be made to the director of the regional water management authority with jurisdiction over the locality.

The report should be made before the planned commencement date for the works or activities. Pursuant to art. 123a.3 of the Water Law Act, the report should contain the following information:

1. name of the reporting entity, its seat and address;
2. definition:
   a) purpose of the planned activities, works or water facilities;
   b) the impact of such activities, works or water facilities on surface waters and groundwater, particularly on the condition of such waters and on the implementation of the environmental objectives defined for such waters;
3. description of the planned works, their location, basic parameters, and conditions of performance;
4. the commencement date for the works or activities.

Moreover, pursuant to item 4 of the aforementioned article, the following documents should be attached to the report:

1) a copy of the up-to-date cadastral map bearing the diagram of the actions planned and the extent of their impact;
2) relevant sketches or drawings;
3) statements of compliance of the planned undertaking with the water usage conditions for the water district and with the requirements provided for in separate regulations;
4) the permission from the owner of the water or the artificial water body.

Case studies of the floating residential structures legalization in Poland

An analysis of the legalization of two floating residential constructions will be described below. The first case concerns a house on the water built by Kamil Zaremba in Wroclaw (Kaźmierczak & Zaremba, 2013). The second investment concerns a floating house planned in Szczecin following the initiative of Patrick Paluszek (wspieram.to, 2015).

The example of the investment in Wroclaw indicates that in Poland there is currently no standardized procedure related to planning such an investment. A lot of time is required to gather information from many different offices (including Municipality, the Regional Water Management Board (RZGW)). The moorage depends on permission from the RZGW. The location of the floating structure in the city center requires an additional verification of the Local Development Plan (whether a site provides residential buildings) and the issue of a building permit. In addition, part of the center of Wroclaw is under the protection of the Municipal Conservator,

which requires other permits. In the Office of Inland Navigation there was a problem regarding the classification of the object in order to allocate the appropriate laws regulating its construction and usage.

An investor considered buying and renovating old barges; however, the cost of repairing the hull, classifying the structure in the PRS (Polish Register of Shipping) and providing residential functions, could be considerable (about PLN 1 million) (Kaźmierczak & Zaremba, 2013).

Comfortable living in the houses on the water requires sufficient infrastructure and connection with running water, sewage disposal, and electricity and gas connections. In the absence of these amenities, a Feasibility Study should be prepared introducing the necessary amendments to the existing Local Development Plan. Naturally, this procedure takes time.

The floating house to be realized in Szczecin will be built with prefabricated elements manufactured near Wroclaw. These elements will be transported by road vehicles and placed in a designated place of storage. The expected construction period of the floating house is 3 months. The house is intended to be located on Grodzka island, in Szczecin, behind the bridge of the marina city. It is a place near the city center and also with a nice view. An important aspect is the fact that this section of the Oder experiences minimal freezing during the winter. The house will be a fully autonomous unit, but moorage will allow connection to the media infrastructures. The construction does not possess it own propulsion system for displacement and pushers will be used. The house has been designed by a person who lives in a similar construction in Wroclaw (wspieram.to, 2015).

For this investment, the biggest problem was the determination of its legal status and obtaining the necessary permits. By law, house construction was treated as homemade, which allowed to avoid its classification (in this case PRS) and registration in the Polish Yachting Association. The planned mooring place determines which authority should issue appropriate permission. In the case of marine waters, it is the Maritime Office, while in the case of inland waters, it is the Office of Inland Navigation. The same design parameters determine whether it will be considered as a water platform or ship. According to Polish law, the residential address cannot be assigned, which generates residency problems. In addition, there is not possibility of obtaining a mortgage for this type of investment. On the contrary, such a possibility does exist in Western Europe, so it would benefit to learn from the experience of other countries (wspieram.to, 2015).

The analysis of these cases allows to determine the presence of 3 main stages for this type of investment:

Stage I. Conceptual design of floating residential structures and selection of a mooring place:
- legal classification of the object and definition of its parameters,
- definition of the nature of mooring,
- choice of mooring place.

Stage II. Obtaining the necessary documents and permits:
- water permit or notification,
- the right to use the land,
- necessity of obtaining a building permit,
- registration,
- rules related to flood protection,
- rules related to the protection of the environment,
- the possibility of obtaining credit and insurance.

Stage III. Realization of investments:
- agreements with subcontractors,
- assembly of individual sections,
- furnishing,
- technical acceptance.

The analysis of the law in Poland showed that in case of mooring the house on the water, there is no requirement to obtain a building permit as defined in the Building Law Act of 7 July 1994. In addition, the house on the water, which is not permanently connected with the ground, does not fall within the definition of a building, structure or temporary building, and therefore does not fall under the provisions of the Building Law Act.

Conclusions

As it can be concluded from an analysis of the regulations concerning water construction, the formalities that need to be taken care of in order for the investor to be lawfully allowed to erect a water facility indispensable for immobilizing a houseboat and using such a facility are abundant. However, the lack of precision of the existing regulations does not allow to identify with certainty the specific procedure to be adopted.

In order to choose the appropriate procedure, one should first of all determine the parameters of the watercraft (its size), and define the mooring technique and location, which will then help determine the legal regulations that apply. Before choosing the mooring location, one should check the urban land development plan and verify whether the town/city

already has plans for investments in the given area (for example, the erection of residential estates with access to water, marinas, or others). The choice of location is of crucial importance. If one wants the object to be located on a river or a lake with a naturally flowing tributary, they will be subject to the Water Law Act, in which the ownership of lands covered by water is regulated in different ways, depending on whether the waters are lentic or lotic.

Acknowledgments

This research outcome has been achieved under the research project No. 2/S/INM/2016 financed from a subsidy of the Ministry of Science and Higher Education for statutory activities of Maritime University of Szczecin.

References

1. Kaźmierczak, I. & Zaremba, K. (2013) Paradoks budynków pływających. *Warunki Techniczne* 2. pp. 57–61. [Online] Available from: https://miedzyrzeczami.files.wordpress.com/2013/11/paradoks-budynkc3b3w-pc582ywajc-485cych_ik_wt02_2013.pdf [Accessed: February 25, 2016]
2. wspieram.to (2015) *Mieszkamy na Odrze – pływający dom w Szczecinie*. [Online] Available from: https://wspieram.to/mieszkamynaodrze [Accessed: February 20, 2016]
3. DNW (2006) *Pierwszy w Polsce Dom na Wodzie*. [Online] Available from: http://www.domynawodzie.pl [Accessed: February 20, 2016]
4. Sibilak, M. (2014) Mieszkanie na barce. [Online] May 2014. Available from: http://biznes.onet.pl/mieszkanie-na-barce/x6w8v [Accessed: February 25, 2016]
5. Ustawa (1964) Ustawa z dnia 23 kwietnia 1964 r. Kodeks cywilny. Dz.U. 1964 Nr 16 poz. 93.
6. Ustawa (1994) Ustawa z dnia 7 lipca 1994 r. Prawo budowlane. Dz.U. 1994 nr 89 poz. 414.
7. Ustawa (1997) Ustawa z dnia 21 sierpnia 1997 r. o gospodarce nieruchomościami, Dz.U. 2015.1774.
8. Ustawa (2000) Ustawa z dnia 21 grudnia 2000 r. o żegludze śródlądowej, Dz.U. 2013.1458.
9. Ustawa (2001a) Ustawa z dnia 27 kwietnia 2001 r. Prawo ochrony środowiska, Dz.U. 2013.1232.
10. Ustawa (2001b) Ustawa z dnia 18 lipca 2001 r. Prawo wodne. Dz.U. 2001 nr 115 poz. 1229.
11. Ustawa (2013) Ustawa z dnia 13 grudnia 2013 r. o rodzinnych ogrodach działkowych, Dz.U. 2014.40.

Scientific Journals
of the Maritime University of Szczecin

Zeszyty Naukowe
Akademii Morskiej w Szczecinie

2016, 48 (120), 153–158
ISSN 1733-8670 (Printed)
ISSN 2392-0378 (Online)
DOI: 10.17402/189

Received: 29.04.2016
Accepted: 18.09.2016
Published: 15.12.2016

The ship safety zones in vessel traffic monitoring and management systems

Mirosław Wielgosz

Maritime University of Szczecin, Faculty of Navigation, Institute of Navigation
1–2 Wały Chrobrego St., 70-500 Szczecin, Poland, e-mail: m.wielgosz@am.szczecin.pl

Key words: navigational danger, safety, safety frame, safety zone, ship domain, traffic monitoring

Abstract

This paper presents the problem of the "know-how" needed by the operators of vessel traffic supervision, monitoring, advisory and safety zone management systems required and maintained by marine navigators on their ships. The problem of the proper and correct interpretation of these systems is raised. Different types of ship safety zones, concerning both anti-collision and navigational purposes are presented, introducing the concept of hydrographic ship domain. Anti-collision and hydrographic domains were compared in order to establish mutual dependence. The factors influencing the two types of ship domains were analysed. The author proposed their merging and replacement with one universal domain, discussing its advantages and disadvantages. The analysis of the factors influencing the shape and size of such ship safety zones in conducted. The results in the different phases of research were presented and conclusions were drawn.

Introduction

Monitoring and management of vessel traffic in narrow channels and in proximity of ports is usually performed by shore based centres known as VTS (Vessel Traffic Service) or VTMS (Vessel Traffic Management Service). They are engaged in control, advisory, information services and direction of movement of vessels in the subordinate waters (IALA, 2016, Wawruch, 2001).

At its simplest, the main objectives of a VTS are to (IALA, 2016):

- aid the mariner in the safe and efficient use of navigable waterways;
- allow unhindered access to pursue commercial and leisure activities while respecting any restrictions that may exist;
- contribute to keeping the seas and adjacent environment free from pollution.

Their tasks, depending on the specific service provided, may also include, but are not limited to:

- monitoring the traffic of vessels;
- monitoring of compliance to rules and regulations;
- advice on passing the supervised area;
- guiding ships by:
  - passing information about position relative to the fairway centre;
  - advising about course and speed changes;
  - information about other traffic in the area.

For the operator of such a system to issue advice, instructions or recommendation to change course or sail along specified routes, knowledge is required regarding at least the approximate size of the zones that the navigator wants to keep free from other objects – domains or ship safety zones. This involves responsibility for the decisions taken. Although not all the transmitted commands and recommendations are mandatory, navigators generally trust the information and willingly submit to and expect the recommendations of the operator, who has experience and knowledge of the area and the specifics of local traffic.

When sending information, recommendation or advice, the VTS operator should take into account the movement of other vessels, the presence of navigational hazards (such as wrecks and fishing nets),

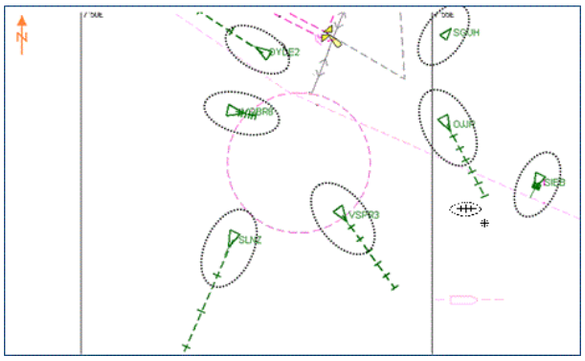

Figure 1. Pre analysed anti-collision domains on ECS screen

and areas that are restricted or well-known for their special conditions. At the same time, they should understand the degree of risk they represent for individual ships, depending on the size, type, speed, and other specific characteristics of the vessel in question.

Safety zone – domain from VTS operator point of view

The expression "ship domain" was introduced for the first time in the 1970s (alternatively, one can use the term "safety zone") and refers to the safety zones in terms of collision avoidance. By definition, this is an area in which the navigator wants to keep, or keeps, free from other objects (Goodwin, 1975; Śmierzchalski & Weintrit, 1999; Pietrzykowski & Uriasz, 2009).

Nowadays, with the new electronic equipment implemented and installed on board ships, it seems to be reasonable to distinguish between the "anti-collision domain", which refers to floating objects such as other ships, and the "hydrographic domain", defined in the following subchapter.

By observing the image of navigational situation in the supervised waters, the operator keeps track of vessels in accordance with the distance and range of automatic identification system (AIS) and ARPA/radar equipment. In general, the navigational situation is reported in accordance with the requirements (if applicable), so that the operator has enough information about the object. If not reported, detailed data is read and obtained from the AIS.

When information about the size and current speed of ship is available, it is possible to generate on-screen a chart system of the ship's domain. Generally, VTS systems are established in restricted areas, where physical and legal restrictions exist (proximity to the land and navigational hazards as well as special areas). It is thus possible to introduce (Figure 1) and input the ship domain described in the author's previous research works and publications (Rutkowski, 2010; Wielgosz & Pietrzykowski, 2012; Wielgosz, 2016).

The VTS operator must not only take into account the navigator's anti-collision domains, but also consider their safety zones in hydrographic terms.

Anti-collision domain

The term "anti-collision domain" refers to a ship domain taking into consideration floating objects only and excludes underwater objects and fixed navigational hazards.

Research works conducted by the author and other researchers allow assigning to a ship of known size and speed an individual elliptic domain of predefined size (Pietrzykowski, Wielgosz & Siemianowicz, 2012; Hansen et al., 2013).

The mathematical model of a ship's domain in the restricted area, taking into account its size and the speed, is shown below (1, 2, 3, 4, 5, 6) (Wielgosz, 2015a; 2015b).

The parametric equation of the ellipse for the mean effective domain of such a ship, taking into accounts its size and speed, takes the form:

$$x(t) = x_0 + a \cdot \cos(t) \tag{1}$$

$$y(t) = y_0 + b \cdot \sin(t) \tag{2}$$

where:

$$a = \left(a_{1L} \cdot L^{b_{1L}} + c_{1L}\right) + a_{1v}\left(v^{b_{1v}} - 2^{b_{1v}}\right) \tag{3}$$

$$b = \left(a_{2L} \cdot L^{b_{2L}} + c_{2L}\right) + a_{2v}\left(v^{b_{2v}} - 2^{b_{2v}}\right) \tag{4}$$

$$x_0 = p_x \cdot L + q_x \cdot v + r_x \tag{5}$$

$$y_0 = p_y \cdot L + q_y \cdot v + r_y \tag{6}$$

where:

L – ship's length [m];
v – ship's speed;
$a_{1L}, b_{1L}, c_{1L}, a_{2L}, b_{2L}, c_{2L}$ – length influence coefficients;
$a_{1v}, b_{1v}, c_{1v}, a_{2v}, b_{2v}$ – speed influence coefficients;
t – relative bearing;
p_x, q_x, r_x – X-axis centre displacement coefficient;
p_y, q_y, r_y – Y-axis centre displacement coefficient.

Function coefficients for different domains are available as groups of coefficients relating to the length of semi-axes and displacement of ellipse centre (Wielgosz, 2015a).

The process of generating and visually presenting such a domain on the VTS operator's electronic chart system screen should be very simple – comparable to the automatic acquisition zones used in the ECDIS and ARPA systems.

This will, according to the author, improve decision-making and increase the safety level of both life and the environment.

The VTS operator, when making a decision and advising the navigator, should take into account the problem (known from the practice and literature) of partially overlapped ship domains. Figure 2 illustrates a situation (in this case overtaking), where the domain of a smaller ship (ship A), with a smaller domain, remains intact, while the bigger ship domain (ship B) has been breached. Later in time, ship B may require action by ship A or undertake its own action.

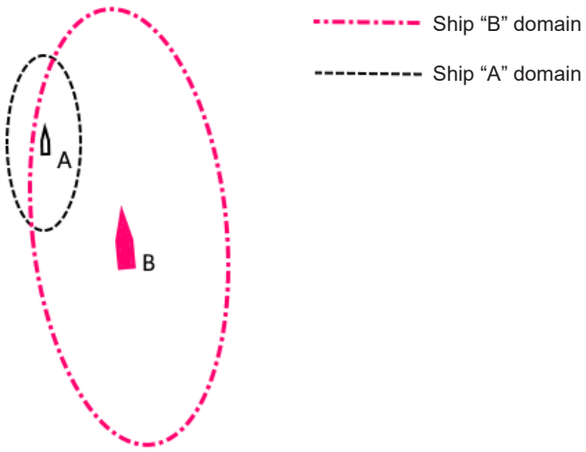

Figure 2. Partially overlapped domains

A useful solution would be the introduction in VTS systems of applications that are already known as navigational decision support systems, e.g. NAVDEC. These systems have the possibility to input the domain as a criterion for assessing the safety of navigation. Such a system will allow planning the manoeuvres of two or more ships in the area considering their domains (Pietrzykowski et al., 2011).

Hydrographic domain

The concept and term "hydrographic domain" is still not known in literature. It can be defined, based on the other anti-collision domains, as the area around the ship that navigators want to keep or keep free from all kinds of navigational hazards that may be identified on an electronic navigational chart encoded in vector format. The possibility to use such domain appeared with the implementation of systems, such as ECDIS and ECS (Electronic Chart System), working with vector format charts. Such systems are able to read and interpret navigational chart content. The extra task remaining to the navigator is the selection and activation of corresponding alarms and, setting safety parameters appropriate to the situation.

In the situation shown in Figure 3, the VTS operator is going to order ship with call sign ABCD to leave the fairway and give way to ship with call sign IJKL, yet he will not be able to quickly and precisely determine the limits – the safety zone in hydrographic terms.

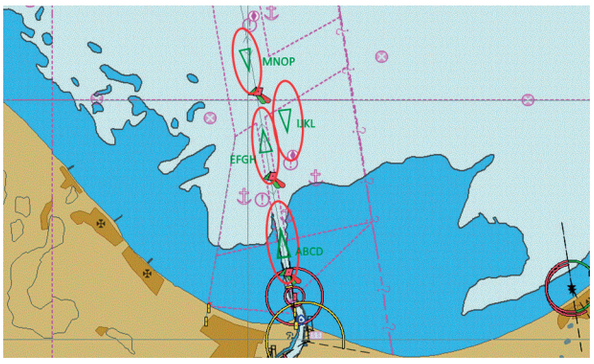

Figure 3. Proposed ship domain on VTS operator screen

Research work

The scope of research was setting the safety parameters in standard tools used in ECDIS systems. The research has been conducted in two forms: questionnaire research and recording of a/m parameters set by ECDIS course participants.

One of such tools is the "Safety Frame", introduced in their systems by several ECDIS manufacturers (Figure 4). This frame is a rectangle, set by a navigator, containing the ship's position and giving the ability to detect, with the necessary advance:

- user defined safety contour and safe depth;
- underwater navigational hazards (wrecks, rocks);
- special areas selected for the detection by navigator (military area, restricted area, etc.);
- user inserted objects on the chart, which have been given the attribute "danger".

They can vary in technical details in systems of different manufacturers, but the task is always the same: to detect in advance the above mentioned navigational dangers and obstructions.

Figure 5 presents the frame, as designed by the company Transas, that gives the possibility to set

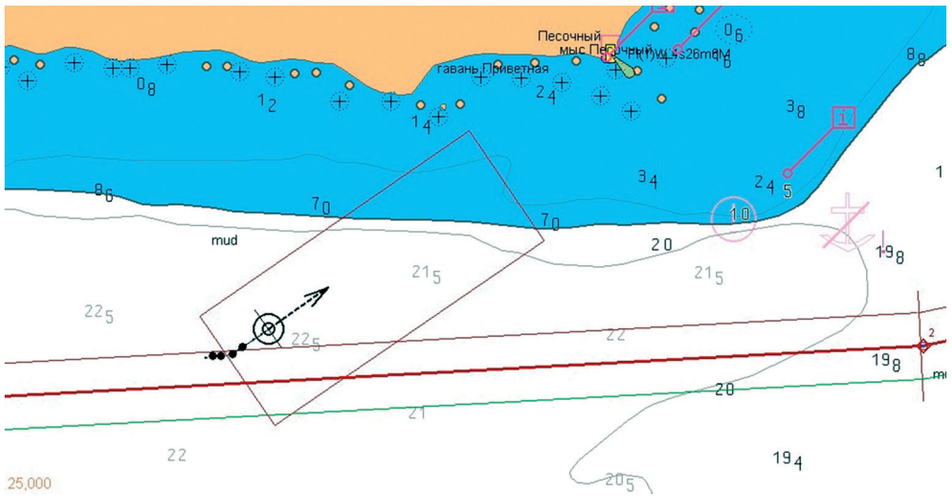

Figure 4. Safety frame in ECDIS system (Transas ECDIS NS 4000)

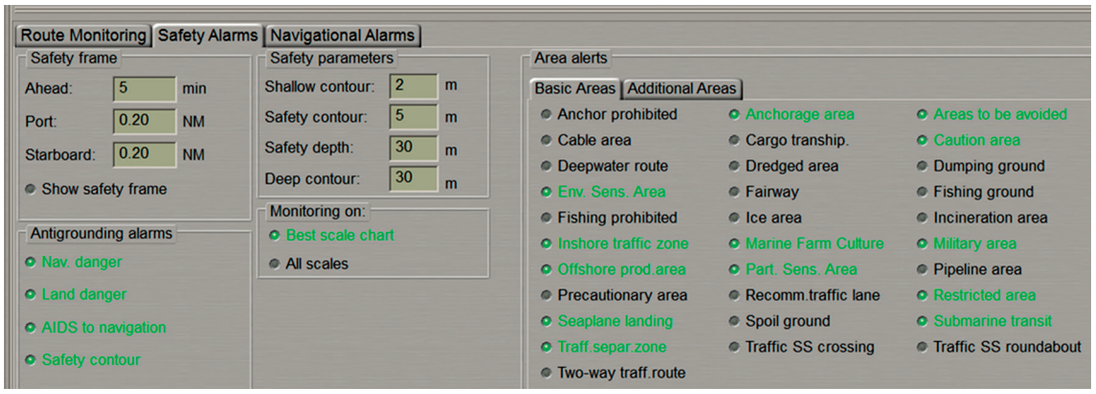

Figure 5. Route monitoring window (Transas ECDIS NS 4000)

detection time to 0–15 min (representing the ship's motion at current COG and SOG). The width of the frame, both of the port and starboard side of the ship, is set in nautical miles. The stern distance is associated with a lower value set on the side of the ship (Transas ECDIS NS4000), as it is not very important when the ship is moving forward. Figure 5 shows the "Safety Alarms"/"Route monitoring" window, with the possibility of editing the parameters of the frame and selecting items to detect.

Such a tool is not present in the electronic chart system used by VTS operators. VTS operators giving instructions or sending information or recommendation and analysing the collision domain only, may suggest to the navigator an incorrect execution of course alternation or deviation from the course.

It was therefore decided to introduce the concept of hydrographic domain, in all aspects known to both parties, and conduct research works concerning its size. Suggested hydrographic domains are

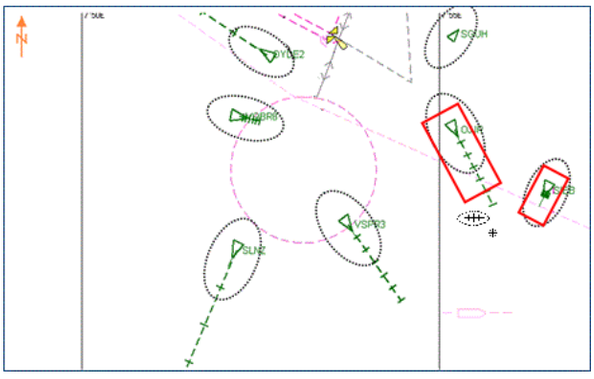

Figure 6. Electronic chart system screen with anti-collision and proposed hydrographic domains

shown as red rectangles in Figure 6, together with the anti-collision domains shown as black dotted ellipses.

The values set by navigators were researched through questionnaires and practical settings of safety frame parameters in the ECDIS system.

Three different types of ships, considered as representative ships, were analysed: large, medium, and small (Table 1).

Table 1. Particulars of the researched ships

Parameter	Ship's size		
	Large	Medium	Small
Length (LOA) [m]	261.3	173.5	95.0
Breadth (B) [m]	48.0	23.0	13.0
Draft (T) [m]	9.0	8.1	3.7
Displacement (D) [t]	63 430	19 512	3 510
Speed (v) [knots]	16.3	18.9	11.1

A total of 35 course participants have been questioned, each of them setting parameters for three above mentioned ships. Example results for "Ahead" parameter settings are shown in Figure 7 in histogram mode.

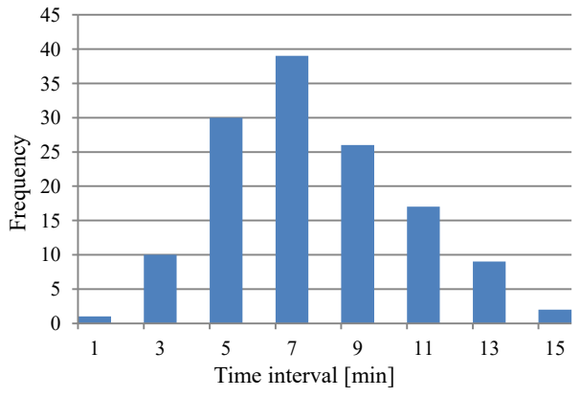

Figure 7. "Ahead" settings of safety frame in histogram mode

All detailed results for safety frame parameters settings are presented in Tables 2, 3 and 4 below. Column 5 – "Ahead [NM]" contains "Ahead' value recalculated in nautical miles for corresponding ship speed.

Table 2. Large-sized ship

	Ahead [min]	Starboard [NM]	Port [NM]	Aft [NM]	Ahead [NM]
Min	3	0.5	0.25	0.25	0.82
Mean	8.47	1.24	0.88	0.88	2.30
Max	15	2	2	2	4.08

Table 3. Medium-sized ship

	Ahead [min]	Starboard [NM]	Port [NM]	Aft [NM]	Ahead [min]
Min	2	0.25	0.15	0.15	0.63
Mean	8.22	1,11	0.74	0.74	2.59
Max	15	1,5	2	2	4.73

Table 4. Small-sized ship

	Ahead [min]	Starboard [NM]	Port [NM]	Aft [NM]	Ahead [min]
Min	1	0.25	0.10	0.10	0.19
Mean	8,05	0.76	0.48	0.48	1.49
Max	15	1	1	1	2.78

Concept of universal, total domain

Operating with two independent types of domains may lead to serious misunderstandings, mistakes and even cause serious dangerous situations in navigation. The question arises is then whether it is possible to substitute two different, independent domains with one universal, total domain containing both of their features.

The answer, until now, has been very ambiguous. The two proposed domains are shown together in Figure 8. It is easily understood that it is very difficult to substitute them with one geometric figure and further research is necessary. The hydrographic domain is significantly shorter behind the ship because the fixed object has already been passed and is no longer considered dangerous, contrarily to the target ship manoeuvring behind the ship's own stern.

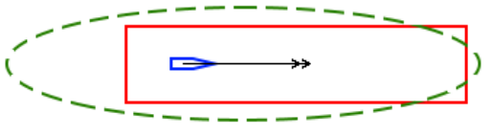

Figure 8. Proposed anti-collision and hydrographic domains

The overlapping and comparison of the two domains raises the question of whether it is more convenient to substitute the rectangle with the ellipse. Theoretically, for some reasons it may be the case, but further research is required for navigators to accept it. It should be, for example, more practical to automatic plan and check the route.

The main problem is visible when the two discussed domains are shown for the same vessel (Figure 9). The hydrographic domain presents an

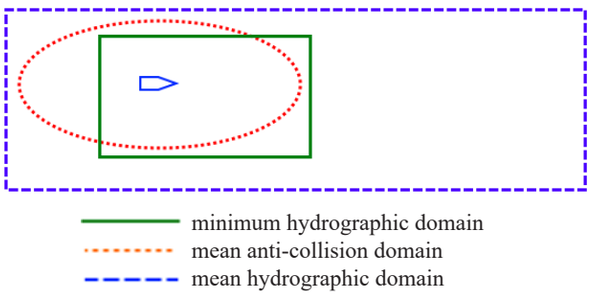

Figure 9. Anti-collision and hydrographic domains

unexpectedly large size. This observation only leads to the conclusion that researched domains are declarative only, and similarly to anti-collision domains, smaller effective hydrographic domains exist and need to be identified by simulation and research (Wielgosz, 2015a).

Conclusions

The problem of determining the shape and size of the ship safety zones is complex for navigators. The problem increases for someone who is not on board the ship and is using the standard electronic chart system, which is not pre-set for individual ship dangers (e.g. specific safety contour).

Research carried out by the author allows to draw the following conclusions:

- implementation of the proposed hydrographic domain will increase safety in VTS monitored areas;
- the domains described are to be considered as declarative only;
- further, detailed research on effective hydrographic domain is necessary.

Analysing the two domains together it is possible to determine whether the major risk for the navigator is a fixed wreck or the manoeuvring target ship.

The wreck is fixed and won't move, but the target ship, although it is also monitoring the situation, could perform the wrong manoeuvre.

A single, universal domain should find a compromise solution to this problem.

Acknowledgments

This research outcome has been achieved under the research project No. 1/S/ITM/2016 financed from a subsidy of the Ministry of Science and Higher Education for statutory activities of Maritime University of Szczecin.

References

1. Goodwin, E.M. (1975) A Statistical Study of Ship Domain. *Journal of Navigation* 28. Cambridge
2. Hansen, M., Jensen, T., Lehn-Schiøler, T., Melchild, K., Rassmussen, F. & Ennemark, F. (2013) Empirical Ship Domain Based on AIS Data. *Journal of Navigation* 66. Cambridge.
3. IALA (2016) *Vessel Traffic Services Manual*. Digital Publication, Edition 6.
4. Pietrzykowski, Z. at al. (2011) *The Navigational Decision Support System on a Sea – going Vessel*. Szczecin: Maritime University.
5. Pietrzykowski, Z. & Uriasz, J. (2009) The Ship Domain – a Criterion of Navigational Safety Assessment in an Open Sea Area. *Journal of Navigation* 62. Cambridge.
6. Pietrzykowski, Z., Wielgosz, M. & Siemianowicz, M. (2012) Ship domain in the restricted area-simulation research. *Scientific Journals Maritime University of Szczecin* 32 (104) z. 2. pp. 152–156.
7. Rutkowski, G. (2010) Wykorzystanie przestrzennego modelu domeny do oceny bezpieczeństwa nawigacyjnego kontenerowca typu post-panamax podczas manewrów podchodzenia do terminalu DCT Gdańsk Port Północny. *Prace Wydziału Nawigacyjnego Akademii Morskiej w Gdyni* 24. Gdynia.
8. Śmierzchalski, R. & Weintrit, A. (1999) *Domains of navigational objects as an aid to route planning in collision situation at sea*. Proceedings of 3rd Navigational Symposium, Gdynia.
9. Wawruch, R. (2001) *Assumptions decision-making automated control system of maritime traffic*. Proceedings of the International Scientific Conference "Transport XXI century", Warsaw University of Technology, 2001.
10. Wielgosz, M. (2015a) *Domena statku w ocenie bezpieczeństwa żeglugi*. Unpublished Phd theses [in Polish]. Szczecin: Maritime University.
11. Wielgosz, M. (2015b) Efektywna domena statku na akwenie ograniczonym i jej zastosowanie w systemach statkowych [in Polish]. *Technika Transportu Szynowego* 12. Radom.
12. Wielgosz, M. (2016) Declarative ship domain in restricted area. *Scientific Journals of the Maritime University of Szczecin* 46 (118). pp. 217–222.
13. Wielgosz, M. & Pietrzykowski, Z. (2012) Ship Domain in the Restricted Area – Analysis of the Influence of Ship Speed on the Shape and Size of the Domain. *Scientific Journals Maritime of the University of Szczecin* 30 (102). pp. 138–142.

Miscellaneous

Scientific Journals
of the Maritime University of Szczecin

Zeszyty Naukowe
Akademii Morskiej w Szczecinie

2016, 48 (120), 161–170
ISSN 1733-8670 (Printed)
ISSN 2392-0378 (Online)
DOI: 10.17402/190

Received: 29.04.2016
Accepted: 07.11.2016
Published: 15.12.2016

Development and research of additional parameters of steganographic systems

Olesya Afanasyeva

Technical Institute in Kraków
e-mail: olesya@afanasyev.kiev.ua

Key words: steganosystem, digital environment, hiding messages, parameter of data concealing, steganogram

Abstract

This paper contains research on and methods of determining values for basic parameters of steganographic systems. In particular, a parameter of concealing the presence of information in a digital environment is researched. Using this particular parameter increases the degree of protection of a message introduced into a digital environment. This parameter is one of the fundamental ones in case of implementation of a steganalysis system. Besides that, this paper contains a review of parameters of redundancy of a digital environment and the parameter of steganogram resistance to technological transformations in digital environments.

Introduction

Steganography methods, such as those to hide messages from unauthorized use, are effective and can be widely used in naval information systems for various purposes. For example, in naval applications, it is used to protect information being communicated between ships or between ships and ports and can be implemented via satellite-communication channels. Another example is protection of limited-access information, like electronic logs and other tasks, related to use of naval-information systems. For successful use of steganography systems in graphical, digital environments it is necessary to conduct analysis of parameters, characterizing the steganography systems, with the aim to select optimal parameters of the information-hiding task.

In this work, new parameters are introduced that characterize steganography systems and methods of evaluating their values and the aim of use of each parameter are reviewed.

One of the new parameters introduced in this work is the parameter of secrecy, which characterizes the level of hiding of the existence of the hidden message in the digital environment. With that parameter, it becomes possible to increase the level of protection of the hidden messages from steganography-analysis (steganalysis) systems, used for detection of such messages in any environments, including digital ones.

Basic tasks

When creating steganographic systems, several requirements for this kind of system have to be taken into account. These requirements are defined, firstly, by providing given values of fundamental parameters that characterize a steganographic system. Thus, several tasks are necessary that are related to defining basic parameters which characterize a steganosystem: tasks of determining values of the corresponding parameters, tasks of extending parameters representing certain possibilities of such system, and some other tasks related to the problems of creating a steganographic system.

Interpretation of parameters of a steganosystem

Steganographic methods of concealing information in a digital environment can be divided into the

following ways of implementing the corresponding concealment: a technical way of placing information in the environment that leads to its distortion within acceptable limits; a method of using semantic analysis of information with the purpose of determining changes that would save the information with semantics intact; a method of placing a hidden image by hidden components, implemented so that it would not distort the main image; a method of using the plot analysis in order to modify the image without changing the plot of the main image; and a method of generating new images oriented towards placing hidden information within them.

To create more-effective steganography systems, it is necessary to:

- add additional parameters that better reflect the requirements of providing the invisibility of messages, injected into the digital media; or
- develop the determination methods of the values of the input parameters.

Since the algorithm of hiding messages in steganography systems is aimed at providing the invisibility of the messages, adding the new parameters and development of methods of their values' calculation are actual tasks for steganography.

One of the key parameters characterizing the concealment of stenographic information is the degree of invisibility, which is subjective because this parameter is correlated with subjective characteristics of a human. A development in informatics leads to creating a great variety of different information converters, among which may be found some that make invisible-data fragments reveal themselves. From the point of view of conceptions of objective invisibility, the latter has to be defined while considering those kinds of converters that are not oriented towards revealing hidden information. We can introduce the following definitions of information invisibility in a digital environment.

Definition 1. Subjective invisibility of information is a property of a digital environment (DE) that contains the information, which is not visible under an ordinary examination of the corresponding environment by a user. Such invisibility is personalized. Obviously, steganographic methods of information concealment have to ensure objective invisibility.

Definition 2. Objective invisibility of information is a property of a DE that ensures information concealment when using various standard tools for analysis of a DE that are not designed for detecting steganographically-hidden information.

Another important characteristic of a steganosystem is absence of information regarding hidden information being present in the DE. We will call this parameter the parameter of information concealment. A parameter of concealment of hidden information in the DE defines the capability of DE elements that carry hidden information to be interpreted as DE elements that do not carry hidden information. To ensure constructiveness and unambiguity of interpretation of this parameter, let us review the following definition.

Definition 3. The parameter of concealment of hidden information characterizes a degree of deviation of parameter values of DE fragments that contain the hidden information from the parameter values that characterize components that do not contain hidden information and are surrounded by them.

This definition is constructive because with it we can discuss the signs of presence of hidden information. Based on the invisibility definition, criteria of invisibility of hidden information can be discussed (Afanasyeva, 2006; 2009). The invisibility parameter is written as η, and the concealment parameter is written as $\Im$. Definitions of the parameter of objective invisibility η and the parameter of concealment $\Im$ allow creation of algorithms of their definition.

Any environment that displays some information must have a certain interpretation. For example, if we have some symbols $x_1,\ldots,x_n$, that can be used to display certain information, then each symbol and its chosen combinations must have an interpretation that is independent of a specific steganogram. Suppose that symbol interpretation is written as $J(x_i)$, and interpretation of symbol combinations is written as $J(x_{i1},\ldots,x_{ij})$. Information will be such a set of symbols and their combinations, each one of which has an interpretation. Formally, this can be represented as the following relation:

$$U(x_{i1},\ldots,x_{ijn}) = [J_1(x_{i1}),\ldots,J_m(x_{ij}*x_{ik}*\ldots*x_{ir})],\ldots,J_n(x_{im})] \quad (1)$$

where "*" is a symbol that describes correlation between x_{ij} and x_{ik} within the scope of their semantic interpretation. Interpretation of $J(x_1,\ldots,x_n)$ will be called an interpretational extension of the corresponding data set or symbols $(x_1,\ldots,x_n)$. Because each interpretational extension is different from another one, if it relates to different symbols or their combinations (thanks to determining a single element $J(x_i)$) it becomes possible to introduce a way to describe interpretational extensions by numeric values. Given definitions of η and $\Im$ parameters in this case, they can be defined not only qualitatively but quantitatively as well. The latter allows for an introduction of numeric criteria to define the

invisibility measure or the concealment measure of information in the DE. In information systems, converters and analyzers of DE are widely used that are not oriented towards the tasks related to steganography. Examples of these known converters of DE are compression systems widely used in data transfer systems and such (Katzenbeisser & Petitcolas, 2000; Provos & Honeyman, 2003). These tools and other tools of examination of DE will be considered technological tools of DE conversion and analysis. Thus, from the point of view of steganographic systems, we should review one more parameter that characterizes a steganogram, which is a capability of the latter to withstand technological tools of conversion and modification of elements that contain the hidden information.

Definition 4. The resistance of a steganosystem (SS) to technological transformations $\varkappa$ ensures impossibility to destroy elements of hidden information in the DE or to detect their interpretational extensions with the help of technological tools and DE transformations.

It is incorrect to claim that certain converters or analyzers of DE cannot detect components that carry hidden information in the DE. Thus, we have to assume that methods that are not related to steganalysis tasks exist that can reveal elements which carry hidden information and which will be called steganoelements (SE). A set of SE will be called a steganogram (SG). Because steganography is not so much about concealing the information carriers as about concealing the that there are hidden data in the DE, a certain steganosystem has to solve, at least, the following tasks: a task of concealing the carriers of hidden information, or carriers of steganoelements; and the task of concealing interpretational extensions of the corresponding SE carriers. A degree of information concealment, defined by the invisibility and concealment parameters, is implemented by concealing SE carriers and concealing SE interpretation. In most graphic DEs that are representations of versatile and rich information there are semantic redundancies. This means that in some DEs that represent information with a certain richness, regardless of whether a SE set is introduced into this environment, there always are components interpretation of which can be, with various degree of coherence, related to the interpretation of the whole DE. This is caused by the following factors: information generated without special limitations of its way of representation always has redundancies that do not essentially affect the content of key information stored in this DE; when generating information in the DE, components can be introduced in this DE resulting from technological tools of generating the corresponding information; and there is a whole set of random factors that cause generation in the DE of non-basic elements represented in the DE. All of these factors influence the parameters that characterize an informational image and information concealed in it, generated in the DE.

In cases with η and $\Im$ parameters, it is valuable to review possible approaches to determining the value of the $\varkappa$ parameter. Resistance of SGs against technological conversions is closely related to DE properties. Technological processes acting on the DE can lead to the following consequences: destroying certain SE and, respectively, the modification of the hidden information; revealing the hidden information; and distorting the main information in the DE, which can be its radical change or its destruction. We will not consider the last case because it is not so much related to SG as to the image stored in the DE. Let us assume that influences of technological tools on the SG are not related to steganalysis tasks. The main danger that can arise when using technological tools is the destruction of SE components as a result of conversions of the corresponding DE by these tools.

Revealing hidden information by technological tools is only possible when information is concealed not only by placing symbols defining certain information elements but by placing the interpretation itself of these elements, as well. An example of this situation can be a case when alphabet-letter codes, describing the corresponding interpretation, are used to display information stored in the DE. In this case, texts that describe the corresponding interpretation on the users' native language are the corresponding description as interpretational extensions. This situation is typical for those technological tools that use interpreters of symbols in some alphabets. Among these technological tools are various editors that could be used for converting elements detected in the description environment of a certain image. It should be noted that such an informational image could be a text image stored in the DE.

Generally, steganography never uses direct placement of concealed information as a description of its interpretation. A way to separate carriers of concealed information, or separate symbols embedded in the DE from their interpretational extensions, is performed by the following methods: on the basis of using transformations of interpretation description; on the basis of space distribution of symbols used to describe the information introduced in the DE and to

describe interpretational extension of these symbols; and on the basis of using the rules of forming interpretational extensions for a certain set of symbols, using a known interpretation of certain used symbols to describe concealed information in the digital environment.

The first way lies in using various cryptographic algorithms to encrypt the texts that describe the corresponding interpretations or the concealed information itself in the user language (Doubechies, 1990; Babash & Shangin, 2002).

A space distribution of symbols used to describe information and the description of their interpretational extensions that describe the corresponding symbol in the user language is based on using vocabularies for symbols used when coding the information embedded in the DE. This method is rather cumbersome, but when considering the specifics of the subject of steganographic information concealment, using personal vocabularies by two subscribers that use steganography to exchange information is quite well founded. Essentially, using vocabularies is quite popular in the branch of message encryption.

A third way is a modification of a method based on using vocabularies. The point is that personal vocabularies can grow in time, requiring a large amount of memory, and in time these vocabularies can be accessed by third parties, which can lead to compromising the corresponding steganosystems. Thus, in the third approach, it is proposed to shorten this vocabulary to a degree necessary for defining a certain symbol. On the basis of interpretations that are single-text descriptions in the user language, rules are formed to generate phrases and sentences that could describe information that has to be embedded in the DE for the transfer to a subscriber. These rules are the secret part of a steganosystem, or a part that is personalized for users of the corresponding steganosystem. These rules can be represented in a compact way and do not require big amounts of memory and vocabularies for a certain symbol set that can be available to all.

Reasoning from the above, the main threat from technological processes is unforeseen destruction of information embedded in the DE. Let us determine possible approaches to calculate the values of the corresponding parameter, which lie in the following: based on the detected fact of destruction of information, to determine the number of SE elements that were distorted or removed from the DE by the corresponding tools; to determine the DE parameters that could be used to predict the amount of distortion of hidden information, which could allow an estimate of the possible resistance of the steganosystem as a value opposite to the amount of distortions; and based on an analysis of basic characteristics of technological tools of DE transformation, parameters are defined that allow an estimate of distortions in the DE that could be caused by using technological tools.

Parameter-evaluation methods of steganography system based on a usage example of graphical, digital media

Parameters that characterize a steganosystem (SS) have to be described qualitatively in order to obtain estimates for characterizing SS and SG (Yhang & Ping, 2003; Noda, Niimi & Kawaguchi, 2006). Let us review the possible methods of measurement of parameters, among which are: a degree of invisibility (η) of information introduced in the DE and its varieties: a subjective degree of invisibility η_s, an objective degree of invisibility η_b, and a technological degree of invisibility η_t; a degree of redundancy of DE (μ), which has the following varieties: semantic redundancy μ_s, technical redundancy μ_t, technological redundancy μ_p, and natural redundancy μ_n; and a degree of carrying capacity of a steganographic channel π. Let us examine the possible ways of measuring the parameters that are their basic sort.

The invisibility degree has to be measured within the limits of psychophysiological invisibility. A value of these limits is determined on the basis of psychovisual research that lie in generating experimental dependencies, displayed as curves or data tables where a value of change of brightness ΔJ_i is measured in one of selected colors on the distance between the two dots where two values of brightness are measured, which is formally written as the following expression:

$$\eta^{+} = \frac{\left(\alpha\left(\Delta J\right)\right)^{J}}{\left|l_1\left(J_1\right) - l_2\left(J_2\right)\right|} \tag{2}$$

Let us assume that the upper limit of invisibility η is set on the basis of experimental data corresponding to the relation (2). Let us review the definition of the lower limit of invisibility for changes in the image caused by introducing information in the digital environment. A graphical image can be represented in the following forms: as brightness of pixels creating the image field; as codes of value of single pixels depending on the color model; or as an image semantic description. Choosing these three forms of image representation is based on the fundamental difference in the methods of these

representations and different possibilities to interpret the conceptions of information concealing. On the level of a semantic-image representation, certain heterogeneities within its placement, if they do not distort codes and symbols that are semantic-image elements, are not factors that are taken into consideration when reviewing the corresponding image. The upper limit of the invisibility value, described by the expression (2), is placed below the level of semantic invisibility that is defined by the degree of semantic distortion of the image where the concealed information is introduced. Within this degree, visual heterogeneities, that could be visible, are acceptable. Semantic invisibility is mostly used in text environments. The upper limit of invisibility values η^+ is defined on the basis of analysis of psychophysiological features of visual perception of graphical images. The lower invisibility limit η^- has to be defined on the level of codes representing the brightness values and color values of the corresponding dots. Although different models of generating colors exist, as well as vector methods of generating an image, a method of representing the lower limit of visibility η^- will be added up to representations that use conceptions of pixel codes. We will define the lower limit of η^- value as a degree of change of code values describing the corresponding pixels.

The role of the lower limit of the invisibility value of the introduced element of a hidden-information code could be taken by a single change of the least-significant bit. But in practice, depending on the purpose of using the steganographic method of information concealing, the digital environment is affected by factors of a various nature that could lead to unforeseen changes in the corresponding environment. These changes are normally called noise. The main characteristic that represents the degree of noise in the signal is the signal-to-noise ratio. Because of this, there is no sense in talking about η^- values that are less than the noise. Thus, the lower limit of the invisibility value of the concealed information in the digital environment will be defined on the basis of the following relation:

$$\eta^+ \geq \alpha_p \beta \sum_{i=1}^{n} \frac{\Delta d_{si} - \Delta d_{szi}}{\Delta d_s} \tag{3}$$

where Δd_s is the value of the signal change caused by introducing the hidden information, Δd_{sz} is a noise value within the signal, α_p is a factor of a usage mode of a steganogram, and β is a factor that represents description features of certain image dots or fragments. In this case, the source of noise can be technological transformations, compression, decompression, and so on. In order to get η^+ and η^- to a common-measurement unit, let us transform the relation (2) to the form that has the same unit as the relation (3). Transforming the unit $\eta^+ \rightarrow \eta^-$ (not vice-versa $\eta^- \rightarrow \eta^+$, although it is possible) is caused by the fact that the process of embedding the element of concealed information lies in modifying codes by introducing bits or codes of information elements. When introducing information codes causes modification of the components that describe the image not in the coordinate space (such as the (x, y) system, but in the time-frequency system, for instance, (ω, t)), the degree of invisibility of information embedded in the image is defined after the reverse transformation of the image representing space from (ω, t) space to (x, y) space.

Let us review transforming $\eta^+ \rightarrow \eta^-$ to a common measurement unit. Brightness values J_1 and J_2, as well as ΔJ, are brightness values of certain pixels. A value of the code d_i, which defines the brightness value, is related to the brightness degree at least in the visibility range of the user, which can be written as:

$$J_i = f(d_i) \tag{4}$$

where J_i is the brightness of the pixel i and d_i is a value of the code written in the register corresponding to the pixel i. If we assume that brightness in the visible range can be directly proportional to the value of the code written in the corresponding register, the relation (3) can be written as:

$$\eta^+ = \frac{\alpha\left(a\Delta d + b\right)}{\left|l_1\left(a_1 d_1 + b_1\right) - l_2\left(a_2 d_2 + b_2\right)\right|}$$

where $J_1 = a_1 d_1 + b_1$, a is a factor of proportionality that adjusts the value of code change with the value of brightness change of a certain pixel, and b is a constant in the linear dependence $\Delta J = a\Delta d + b$.

Let us review methods of measurement of redundancy parameter value SG, or redundancy of a container where hidden information is stored. In this case, the analysis is conducted on the level of technical implementation of a method when introducing a message in the DE, so we will review the technical redundancy μ_t, which will be written as μ. Practical redundancy μ_P is a parameter that ensures the possibility to implement a required invisibility degree of other types, such as η_S. If redundancy $\mu = 0$, it means that every register that stores the brightness code $d_i\,(J_i)$ can be used to store an element of information being concealed. However, because the function f_i in the expression (4) is not linear, it means that on

the level of displaying an image fragment, due to optical laws, various effects can take place, especially in the fragments that carry semantic load where brightness or colors change. This is illustrated in cases that create an effect of tridimensionality of an image (Katzenbeisser & Petitcolas, 2000; Provos & Honeyman, 2002). This leads to the necessity to use not only η parameters of various types, but μ parameter as well. It can be asserted that redundancy of a parameter that characterizes DE is closely related to SS. Moreover, a parameter μ can be interpreted as the one that is necessary in order to make it possible to implement processes of concealing information by a SS system. For steganography, only DEs with redundancy are used. Because DE redundancy is closely related to the invisibility level, methods of measuring redundancy μ have to be compatible with methods of measuring the invisibility parameter. Within a single DE redundancy can be several levels: redundant number of places that can be selected for storing the introduced information; redundant coding of single-image pixels; redundant number of image elements from the point of view of their semantic significance; etc. These redundancies are closely related to redundancies μ_s, μ_p, μ_t, and μ_n. Because redundancies μ and the invisibility degree η are related to each other, to define μ we will use the η parameter that is already transformed to the unit defined by a numeric value. The value of μ can be determined from the following relation:

$$\mu^1 = \alpha \frac{\eta^+ - \eta^-}{\Delta d_{\mathrm{SG}}} - 1$$

where Δd_{SG} is a value of modification of a single environment element that is necessary for, at least, introducing the minimal element of concealed information, α is a proportionality factor and μ^1 is redundancy of DE within a single element that can be modified. Redundancy of a DE in general is composed of the following components: a redundancy component μ^1, a redundancy component μ^2 that determines this value regarding all environment elements where, based on technical requirements, and an information element that can be introduced. Redundancy μ^2 depends on the size of the information code that has to be introduced, and will be written as R. If we define N(SG) as the number of elements in a DE suitable for storing information elements, and N(R) as the number of information-elements embedded in the DE, we can write the following relation:

$$\mu^2 = N(\mathrm{SG}) - N(\mathrm{R}).$$

In this case, redundancy due to unused environment elements for storing information codes within them will be defined by the relation:

$$\mu^3 = \mu^2 \alpha \frac{\eta^+ - \eta^-}{\Delta d_{\mathrm{SG}}}$$

Full redundancy of the DE environment with introduced information of the size N(R) equals to: $\mu = \mu^3 + \mu^1 \cdot \mu^2$. This relation can be written in the form reduced to the common measurement units:

$$\mu = (N(\mathrm{CS}) - N(\mathrm{R}))\left(2\alpha \frac{\eta^+ - \eta^-}{\Delta d_{\mathrm{SG}}} - 1\right).$$

Let us examine the parameter of carrying capacity of a steganochannel π.

Definition 5. A steganochannel (SCh) is a name of a system that consists of a DE, where the DE and steganosystems SS are planned to be placed, and that performs this placement, formally written as:

$$\mathrm{SCh} = F(\mathrm{DE}, \mathrm{SS}) \tag{5}$$

In most cases, the idea of an SK is limited by its comparison to the possibilities of a digital environment where some information can be stored secretly (Katok & Hasselblat, 1999). These possibilities mostly depend on the steganosystem type. In the known approaches, determining the carrier capacity SK depends on the possibility to transfer data without errors during the counter-actions from an opponent. In this case, only such properties of SS are indirectly accounted for as the ability of the latter to generate an SG that is resistant to the attacks, although it is reasonable to be estimated using a separate parameter.

Within the scope of this approach, function F from the expression (5) describes the fusion of an SS with a DE so that, on the basis of this fusion-solving task of optimizing the process of using SCh, it would be possible. In this case, the carrying capability is examined independently from the parameter that defines resistance of an SG related to the attacks. Thus, the π parameter for SCh has to be defined not only on the basis of DE, but also on the basis of analysis of functional abilities of SS. Let us assume that the function F from the expression (5) is linear. This means that the two components DE and SS can be reviewed independently, if we accept the conditions for SS that will represent limitations regarding the functioning way of SS. The redundancy parameter μ of the DE environment is a key one to determine the carrying capability SCh. So, the carrying capability of a channel π has to be directly proportional to the redundancy degree of DE, which can be written

as follows: $\pi_m = \beta f(\mu)$, where β is a proportionality factor.

Definition 6. A momentary carrying capability of a steganochannel π_m characterizes the maximal amount of information hidden in the DE that could be stored in the SG while saving the given level of invisibility of hidden data, or $\pi_{CS} = \beta\mu$.

Analysis of a concealment parameter

Known parameters that characterize not only steganographic systems (SSs), but the principle of steganographic concealment, is a parameter of invisibility degree of information embedded in the digital environment η and a parameter of concealing degree of presence of information $\Im$ hidden in the DE. Parameter $\Im$, as well as parameter η, have subjective nature regarding the user who is not authorized (NAU to detect the steganographically-hidden information. In general, in this case we can assume that parameter $\Im$ mostly represents subjective properties of certain NAU, because one NAU_i can think that there is a steganographically-hidden element of an information image (IO_i) in some environment, while another NAU_j can think that there is none. In order to evade such subjectivity when determining the value of $\Im$ parameter, let us assume the following. We will examine a certain DE where single fragments of DE_i can be distinguished where information intended to be concealed will be stored. These fragments DE_i from DE will be called steganographic containers (SC). In this case, we will review the parameter $\Im$ within the following conditions.

Condition 1. The NAU knows that there is no SC in the DE where concealed information could be stored, or there is no SG in the DE.

Then, subjective factors that could distinguish NAU_i from NAU_j from the point of view of parameter $\Im$, and will be eliminated by the next condition that needs to be accepted because of the introduction of parameter $\Im$.

Condition 2. The DE, in general, does not have to be divided into fragments DE_i that, from the point of view of NAU, can be used for concealing information.

Qualitatively, the given conditions lie in the following. A subjective decision of a single NAU_i regarding possibility of existence of concealed information in the given DE_i is considered a random event regarding all fragments of information images present in the DE. This event depends on a random event of appearance of an NAU_i among all possible NAU. Besides, in a certain DE there is always some set DE_i that is suitable for placing a DE in it, which can also add to the randomness factor that could be used to compensate the subjectivity factor from the side of NAU_i. Obviously, the *Condition 2* does not mean that absolutely all fragments DE_i from the DE can be suitable for embedding IO_i. There must be algorithms within the SS that, corresponding to certain criteria, select some DE_i for their usage as containers. Let us assume that the selection of DE_i from DE is performed according to this relation: $DE_i = SKl(DE)$, where SKl is a steganographic key for the container selection. Thus, the properties of SKl can affect the value of the parameter $\Im$. Because the value of the parameter $\Im$ is determined by different factors that characterize the degree of suitability of certain SC elements for invisible concealing of information image elements (EIO) in the selected container or a certain DE_i that is directly related to the concealment degree, it is reasonable within the scope of the algorithm of SC selection and, respectively, within SKl to foresee the features and criteria which would not lead to a decrease of invisibility degree and, respectively, concealment when placing the corresponding IO in the selected SC. There are the following possible ways to solve this problem: using integral parameters, similar to the parameters used in the SS when placing IO in SG that are generated on the basis of analysis of parameters used on the level of SG analysis by the SS system; defining the parameters that characterize DE, in general, and can be related to technical aspects connected to embedding information in the DE; and defining the parameters that characterize DE from the point of view of external features related to the corresponding environment.

The first approach looks the most natural, because defining the concealment parameter can be considered a development of invisibility parameter that is researched quite intensively and has a commonly-accepted interpretation. Let us review the second approach in more detail. One of the basic conditions of using DE for selecting a container within it is a condition corresponding to the size of the DE, which has to be bigger than the foreseen container: $\{[CS = k(SKO) \,\&\, (k \geq 1)\}$. For the parameter $\Im$, within the scope of this relation, it is natural to assume that $\Im$ increases together with k. If $\Im = 0$ and $k = 1$, then DE = SC and a place for storing IO is unambiguously determined by the size of SC. In order to be able to use the given starting condition, $\Im$ has to be related to k by a logarithmic dependency, which will be written as:

$$\Im = A \ln k \tag{6}$$

where A is a certain expression that describes the dependency of $\Im$ from other parameters of DE that could characterize $\Im$. The next parameter closely related to the parameters that characterize SS is a noise pollution in the DE. Let us assume that any DE environment, especially if it is transferred in the space of an electronic network, suffers from noise pollution. Introducing information in the selected fragments of DE or in the SG can also be considered as some sort of noise pollution. In this case, there can be heterogeneous noise pollution throughout all DE environments. Let us assume that noise pollution of the DE throughout the entire environment is uniform from the point of view of noise-spectral power because it can be assumed that during the transfer of DE through the same channel along all the length of this channel DE is affected by the same reasons of noise pollution. So, one of DE parameters that could be considered as independent, from the point of view of methods of introducing information in DE, from the parameter $\Im$, if the latter ensures the given concealment degree, is a spectral thickness of a noise pollution signal. In this case, the spectral thickness of noise in the DE is examined at the input and the output of DE channel. Channel input and output will be identified with the source where the SG is generated and the users among which there is a recipient whom SG is addressed to. The spectral thickness of noise is calculated at the channel input and is defined as D_{xx} and is determined by the embedded message, while spectral thickness of noise at the channel output, which is also determined by the channel noise pollution, is defined as D_{yy}. For noise analysis in DE, the mutual-spectral thickness D_{xy} is examined. Then, a coherence function can be used for analysis (Kharin, Bernik & Matveev, 1999; Popov, 2000) that is described by the following relation:

$$\gamma_{xy}^2(f) = \frac{\left|D_{xy}(f)\right|^2}{[D_{xx}(f), D_{yy}(t)]}.$$

Substantial essence of $\gamma^2_{xy}(f)$ allows the following interpretation within the range of $\Im$. If, in the DE environment, a value of $\gamma^2_{xy}(f)$ for the noise existing in the DE is changed heterogeneously, it could mean that there is a SG in the DE with an embedded IO that leads to a change in uniformity of value of $\gamma^2_{xy}(f)$ in the corresponding DE fragment. Because the embedded IO is implemented at the channel input of SS, in order to determine the value of $\gamma^2_{xy}(f)$ we will differentiate it by the x variable, and then the following relation can be written:

$$\delta_x[\gamma_{xy}^2(f_{sz})] = d[\gamma_{xy}^2(f_{sz})]/d[x(t_{sz})]$$

where f_{sz} is a frequency of a noise component of the information signal described in DE. Regarding the size of the DE that is defined by the value of k, the frequency component can be considered, with respect to k, an additive variable. So, the relation (6) can be written as follows:

$$\Im = A_1\{\delta_x[\gamma_{x,y}^2(f_{sz})] + \ln k\} \tag{7}$$

where A_1 is a possible extension of the dependency (7).

External characteristics that characterize DE are firstly related to semantic features. Among these features, the following can be mentioned: different DE types; informational uniformity of DE, parameters of DE that characterize semantic properties of information in IO; and functional orientation of information placed in the corresponding environment.

Informational uniformity is determined by the degree of integrity of information stored in the DE environment. Informational uniformity has different degrees depending on the DE type. This is caused by the possibility of recreating one or another plot in different environments.

Semantic parameters of information in IO are important parameters because any user, including one not authorized to receive concealed information, first uses semantic content of the corresponding IO. Different IO types have different measures of semantic representation as interpretational descriptions. Text types of DE are the ones most covered by interpretational descriptions of IO. The next one, based on its interpretational abilities, is the graphical type of DE. The ones with the least interpretational abilities are musical images. In this case, their musical essence is emphasized, because sound images can be represented in the symbolic form.

Within the scope of problems related to determining the $\Im$, an important task is to determine the value of $\Im$ for each single case of steganographic information concealment in the DE. At the same time, the $\Im$ value must not be affected by the modification of the IO implemented by technological tools. So, let us formulate a definition.

Definition 7. A technical modification of DE takes place when the latter does not lead to change of IO semantics.

The change of IO in DE will be understood not only as changes regarding the output IO, but also changes that could extend semantics of the modified IO. For example, if, as a result of modification of a DE fragment containing IO, elements of an image appear that do not directly affect the semantics of the

main IO and are dots, spots, etc., these elements can lead to a change in semantics of the IO.

Definition 8. A semantic modification of DE takes place in a case when, as a result of embedding information in DE, changes are introduced in the IO that lead to change of IO semantics.

An example of these modifications can be a color change of certain elements of an IO image and others. Let us assume that an arbitrary IO has a standard IO, or IO^E, if there is an interpretational description of the corresponding image. Obviously, in most cases the following relation takes place:

$$\forall(\mathrm{IO}_i)[\Delta\mathrm{IO}_i = [\mathrm{IO} - \mathrm{IO}^E]] \tag{8}$$

This means that IO^E is a standard only in case when there is a certain set of such IO that the following relation is true:

$$\{[\mathrm{IO}^k = \{\mathrm{IO}^k_1,\ldots,\mathrm{IO}^k_n\}] \,\&\, \forall(\mathrm{IO}^k_i)[\Delta I_i \neq 0]\} \rightarrow \forall(\mathrm{IO}^k_i)\,\exists\,(\mathrm{IO}^{Ek}) \tag{9}$$

The accuracy of image descriptions and their deviations from standards in the relations (8) and (9) is determined by the accuracy of interpretational descriptions of the corresponding images, which will be written as $j(\mathrm{IO}_i)$. Let us assume that an interpretational description of $j(\mathrm{IO}^k_i)$ is represented in the user's native language in the normalized form that is ordered corresponding to semantic accents of importance of certain IO elements (Sayood, 2002; Vatolin et al., 2002). Normalization of the description lies in using only determined words in the text descriptions and excluding redundancies, additional grammatical expressions and words. The ordering accent is understood as such placement of text of interpretation description when at the beginning of the $j(\mathrm{IO}_i)$ description those elements of $j_i(\mathrm{IO}_i)$ are placed that within this IO_i have the biggest semantic significance from the point of view of information transferred through IO_i. In the next element $j_{i+1}(\mathrm{IO}_i)$, a fragment of IO_i description is placed that has the next value of semantic significance that is determined from IO_i interpretation, etc. Let us assume that $j(\mathrm{IO}_i)$ is a single phrase of a text $\varphi_i(\mathrm{IO}_i)$. One of the basic functions of the standard IO^E of an image IO_i is determining the ordering accents of description $j_i(\mathrm{IO}_i)$ for images IO^K of a certain class K. Let us assume that IO^E for the image class K contains the full semantic representation of the corresponding $IO^K{}_i$. We will assume that $j_i(\mathrm{IO}_i)$ can be represented as a description of IO_i semantics that has a varying value of significance depending on the number of components $j_i(\mathrm{IO}_i)$ included in $j(\mathrm{IO}_i)$. With regards to the conception of accented ordering of $j(\mathrm{IO}_i)$ let us assume that the measure of semantic significance of $j_i(\mathrm{IO}_i)$ for description of IO_i semantics is determined by the value of the accent assigned to phrases $\varphi_i[j_i(\mathrm{IO}_i)]$ that compose a text description of $j(\mathrm{IO}_i)$ and a number of place of φ_i storage in $j(\mathrm{IO}_i)$. With respect to the normalization of $j(\mathrm{IO}_i)$ description, let us assume that φ_i with the highest accents are placed at the beginning of $j(\mathrm{IO}_i)$ description. We can represent $j(\mathrm{IO}_i)$ as series of phrases φ_i, or $j(\mathrm{IO}_i) = \varphi^i{}_1 * \varphi^i{}_2 * \ldots * \varphi^i{}_m$, where each $\varphi^i{}_j$ has a value of accent ξ_j, and also, $(g < k) \rightarrow (\xi_g > \xi_k)$. To step aside from the absolute values of ξ_j, let us assume that $(\Sigma^m{}_{j=1}\xi_j) = 100\%$ for IO_i. In graphical images a situation can take place when IO_i in DE corresponds to the standard image only at $\alpha\%$. This, in turn, means that such semantic modification of IO_i from DE can be performed, that:

$$[(\mathrm{IO}_i) + (\Delta(\mathrm{IO}_i))] \rightarrow [j(\mathrm{IO}_i + \Delta I_i) \leq j(\mathrm{IO}^E)].$$

In order to move to the qualitative estimation of value of semantic modification that will be a next component of parameter $\Im$, let us assume the next conditions and definitions.

Definition 9. An IO_i image will be represented in an incomplete semantic form, if the value of sum of its accents is less than sum of accents of its full standard, or:

$$\sum\nolimits_{i=1}^{k} \xi_i(\mathrm{IO}^k) < \sum\nolimits_{i=1}^{m} \xi_i[P(j(\mathrm{IO}^{kE}))],$$

where $P(j(\mathrm{IO}^{kE}))$ is a full-interpretation description of an IO^k image of K class that is a standard for IO^k.

When introducing a message V_i in DE, it is impossible to adjust, throughout the whole DE or all the elements IO^k, the modification of their semantics so that the corresponding modification would be the same for all IO^k components, so the following is true:

$$\lambda_i(\mathrm{IO}_i) = \left| \sum\nolimits_{i=1}^{k(i)} \xi_i(\mathrm{IO}_j) - \xi_p(\mathrm{IO}^E_P) \right|.$$

A component for $\Im$ that represents the semantic modification in IO_i with DE will be written as s_i. To define it, let us use the following relation:

$$\{[[\lambda_i(\mathrm{IO}_i) - \delta] \geq 0] \rightarrow (s_i = s_i + 1)\} \,\&$$
$$\{[[\lambda_i(\mathrm{IO}_i) - \delta] < 0] \rightarrow (s_i = s_i)\}$$

where δ is a threshold value of difference of sums ξ_i between images IO_i and $IO^E{}_P$. This relation can be extended like following:

$$\Im = s_i(\mathrm{CS}) + \delta_x\left[\gamma^2_{xy}(f_{sz})\right] + \ln k \tag{10}$$

Let us assume the following condition of using certain components of EIO_i from IO_i.

Condition 3. If in IO_i from DE a component EIO_i from IO_i is used that has its own semantic meaning that causes the presence of the corresponding standard IO^E_i, and EIO_i has incomplete semantic interpretation, then $j(EIO_i) = \varphi_1 * ... * \varphi_k$ has to have the highest value of acceptance from the complete interpretational description of $j(IO_i)$.

The given condition means that in cases when in graphic or any other symbolic images IO_i there are no components of interpretational description, the corresponding φ_i that describe single fragments of interpretational representation correspond to the elements of such representation in IO^E_i that have the highest values of ξ_i. At the qualitative level the given condition means that, when a graphical image is generated so that it represents a certain object or a certain entity with some semantic approximation, such elements of the corresponding image are used that are the most informative for this IO_i. This means that these components have greater values of ξ_i regarding the elements that are used during the implementation of IO_i.

Conclusions

In this paper, several basic parameters are developed and researched that characterize steganographic systems, regardless of the type of digital environment the steganographic system is oriented towards.

Along with the invisibility parameter of a message embedded in the DE, a parameter of concealment of a hidden message is researched. Thanks to using this parameter, it became possible to estimate the degree of detection of environment elements where the message elements can be stored. In many cases, this can be sufficient because, on the basis of estimation of this parameter, the detected DE can be eliminated from the whole environment in order to withstand the possibility to transfer a hidden message to a recipient. In this case, the invisibility parameter characterizes the degree of possibility to detect, based on the selected DE elements, when using the concealment parameter, the elements of the message itself.

Introducing the concealment parameter allows a division of the steganographic concealing of a message in the DE into two stages:

- a stage of selecting such DE fragments, to place a message within them, that would be hard to distinguish among the surrounding DE fragments;
- a stage of implementing such a way to introduce, in the selected DE fragments, the message elements that would make it hard to recognize certain elements of the concealed message.

The researched parameter of concealing the message placement in the DE is a description of a certain aspect of invisibility degree of a hidden message that increases the safety level of a message hidden in the DE.

The paper contains analysis of other parameters of a steganosystem and research of methods to calculate their values. Such parameters are the redundancy parameter of DE and the parameter of steganogram resistance regarding technological transformations of DE, foreseen by standard methods used in the digital information systems.

The results obtained in the paper allow the constructive approach to solving tasks that lie in creating new steganosystems.

References

1. Afanasyeva, O.Y. (2006) *Parameter of invisibility in steganosystems*. Science and techniDE conference of young scientists and engineers of modeling. Kyiv, Institute of modeling problems in energetiDE of NAS of Ukraine.
2. Afanasyeva, O.Y. (2009) *Analysis of parameters of steganosystems oriented towards using graphical digital environments.* Modeling and information technologies: collected articles (IMPE of NAS of Ukraine). Kyiv, Issue 50.
3. Babash, A.V. & Shankin, G.P. (2002) *The history of cryptography*. Moscow: SOLON-R.
4. Doubechies, I. (1990) The wavelet transform, time-frequency localization and signal analysis. *IEEE Transactions on Information Theory* 36, pp. 961–1005.
5. Katok, A. & Hasselblat, B. (1999) *Introduction to the modern theory of dynamical systems*. Moscow: Factorial.
6. Katzenbeisser, S. & Petitcolas, F.A.P. (Eds) (2000) *Information hiding techniques for steganography and digital watermarking*. Boston – London: Artech House.
7. Kharin, Y.S., Bernik, V.I. & Matveev, G.V. (1999) Mathematical basiDE of cryptology. Minsk: BSU.
8. Noda, H., Niimi, M. & Kawaguchi, E. (2006) High-performance JPEG steganography using quantization index modulation in DCT domain. *Pattern Recognition Letters* 27(5), pp. 455–461.
9. Popov, S.N. (2000) *PC video system*. St. Petersburg: BHV-Peterburg, Arlit.
10. Provos, N. & Honeyman, P. (2002) *Detecting Steganographic Content on the Internet*. Proc. 2002 Network and Distributed System Security Symp., Internet Soc.
11. Provos, N. & Honeyman, P. (2003) *Hide and Seek: An introduction to steganography*. University of Michigan. IEEE Security & Privacy.
12. Sayood, H. (2002) *Kompresja danych. Wprowadzenie*. Warszawa: RM.
13. Vatolin, D., Ratushnyak, A., Smirnov, M. & Yukin, V. (2002) *Methods of data compression. Structure of archivers, image and video compression*. Moscow: DIALOG-MIFI.
14. Yhang, T. & Ping, X. (2003) *A Fast and Effective Steganalytic Technique Against JSteg-like Algorithms*. Pric. 8th ACM Sym. Applied Computing, ACM.

Scientific Journals
of the Maritime University of Szczecin

Zeszyty Naukowe
Akademii Morskiej w Szczecinie

2016, 48 (120), 171–175
ISSN 1733-8670 (Printed)
ISSN 2392-0378 (Online)
DOI: 10.17402/191

Received: 29.04.2016
Accepted: 18.11.2016
Published: 15.12.2016

Projecting sale prices of new container ships built in 2005–2015 based on DWT and TEU capacities

Tomasz Cepowski

Maritime University of Szczecin, Faculty of Navigation
1–2 Wały Chrobrego St., 70-500 Szczecin, Poland, e-mail: t.cepowski@am.szczecin.pl

Key words: container ship, sale price, cost estimation, DWT capacity, number of containers, TEU capacity, design, artificial neural networks, linear regression, approximation

Abstract

This paper presents mathematical relationships that allow forecast of the estimated sale price of new container ships, based on data concerning vessels built in 2005–2015. The presented approximations allow estimation of the price based on deadweight capacity (DWT) or the number of containers the ship will carry (TEU). The approximations were developed using linear regression and the theory of artificial neural networks. The presented relations have practical relevance in the estimation of container ship sale price needed in transport studies or preliminary parametric design of the ship. It follows from the above that the use of artificial neural networks to predict the price of a container ship brings more accurate solutions than linear regressions.

Introduction

Maritime transport stakeholders often need to know the estimated price of different vessels. Depending on the available information, the pricing of new vessels can be either approximate or specific.

Price estimation of means of transport is most often carried out at the stage of general transport studies, aiming at the choice of the mode of transport (Rawson & Tupper, 2001; Watson, 2002). In regard to maritime transport means, factors taken into account include vessel's period of operation or possible sale of the vessel after that period. When a cargo ship is considered, this analysis also takes into account limitations of the port infrastructure and transport system adopted (Rawson & Tupper, 2001).

An estimated cost of a ship is also carried out at its design stage, to determine the construction costs and, possibly, the cost of ship operation. Since ship design is a multi-stage process, at each stage design parameters are optimized relatively to the criteria and design constraints, where economic analysis plays an essential role. The proper conduction of this analysis is the basis for the development of ship design of highest operational value (Buczkowski, 1974; Bertram 2000, Chądzyński, 2001).

Prediction of the estimated sale price of the ship is of particular importance when concurrent methods of ship design could be used. In this case, the estimated sale price should be known at the preliminary design stage.

The preliminary design stage consists of parametric and geometric design. Estimating the price of the ship in this phase is difficult. The problem arises from the fact that the price of the vessel depends, inter alia, on the unit costs of ship construction, which in turn include the costs of materials, equipment, labour and the additional costs of the yard (Schneekluth & Bertram, 1998; Michalski, 2004). In general, the total of these costs is not known at the stage of parametric design, because at this phase a detailed specification of materials and equipment is not known. During the parametric design, only general design parameters of the ship are known, such as main hull dimensions, general geometric indicators, and general assumptions regarding the cargo capacity or speed of the ship. For this reason, at this stage the economic analysis covers only basic

technical parameters of the vessel, such as weight/displacement, speed or cargo capacity.

In contrast, in the subsequent stages of design, when more information is available on the ship to be built, a detailed estimation is performed, considering the unit costs of materials, equipment, and labour and additional costs of the shipyard. Methods presented in (Schneekluth & Bertram, 1998; Abramowski, 2013; Michalski, 2004) apply to the detailed cost estimation of sea transport means, i.e. vessels.

Aim of the research

This article describes methods of cost estimation for the purpose of transport studies or preliminary parametric design of a container ship. The aim of the study was to develop mathematical relationships that allow performing cost estimation of container ships built in the years 2005–2015 on the basis of their basic operating parameters.

The practical aim of the research was to develop a mathematical function, f, for predicting the price of a container ship, P, using technical parameters, represented as $X_1X_2...X_n$.

$$P \approx f(X_1, X_2, \ldots, X_n) \tag{1}$$

where:
P – sale price;
$X_1X_2...X_n$ – technical parameters of the vessel;
n – number of parameters;
f – searched-for mathematical function.

The analysis took into account a set of 241 new container ships built in the years 2005–2015, whose parameters ranged as follows:

- DWT: 2,310–165,538 t;
- number of containers (TEUs): 58–13,344;
- service speed: 10–27 knots;
- sale price: 2.5–170 million USD.

In addition to the above parameters the study included:

- displacement and weight of ship;
- gross tonnage (GT);
- main hull dimensions: length between perpendiculars, breadth, moulded depth, moulded draft;
- power plant output, fuel consumption.

The study assumed that the function f in equation (1) can be determined using linear regression and the theory of artificial neural networks.

Use of linear regression for container ship price approximation

Statistical analysis showed that the price of a container ship is mainly dependent on container capacity (TEUs) and DWT capacity. Of all the investigated statistical relationships, the following proved to be the best:

$$P = 21{,}241{,}378 + 0.818338 \cdot \mathrm{TEU}^2 \tag{2}$$

$$P = 19{,}146{,}189 + 0.00602853 \cdot \mathrm{DWT}^2 \tag{3}$$

where:
P – price of a container ship in USD;
TEUs – number of containers;
DWT – deadweight capacity [t].

Equation (2) is characterized by:

- correlation coefficient $R^2 = 0.73$,
- standard error σ = \$ 16.8 million,

while equation (3) is characterized by:

- correlation coefficient $R^2 = 0.73$,

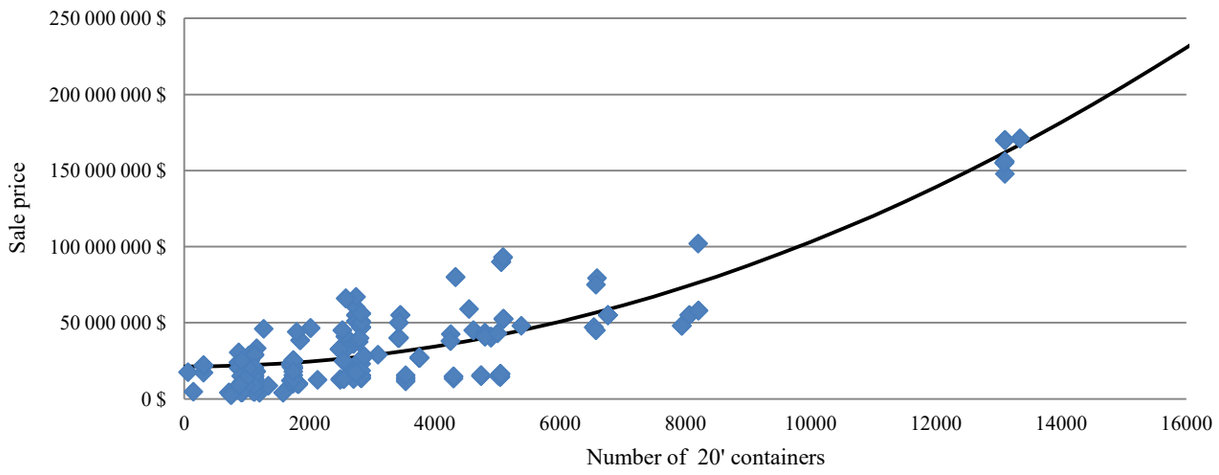

Figure 1. Approximations of container ship price depending on the number of containers. Relationship (2) in comparison with reference data

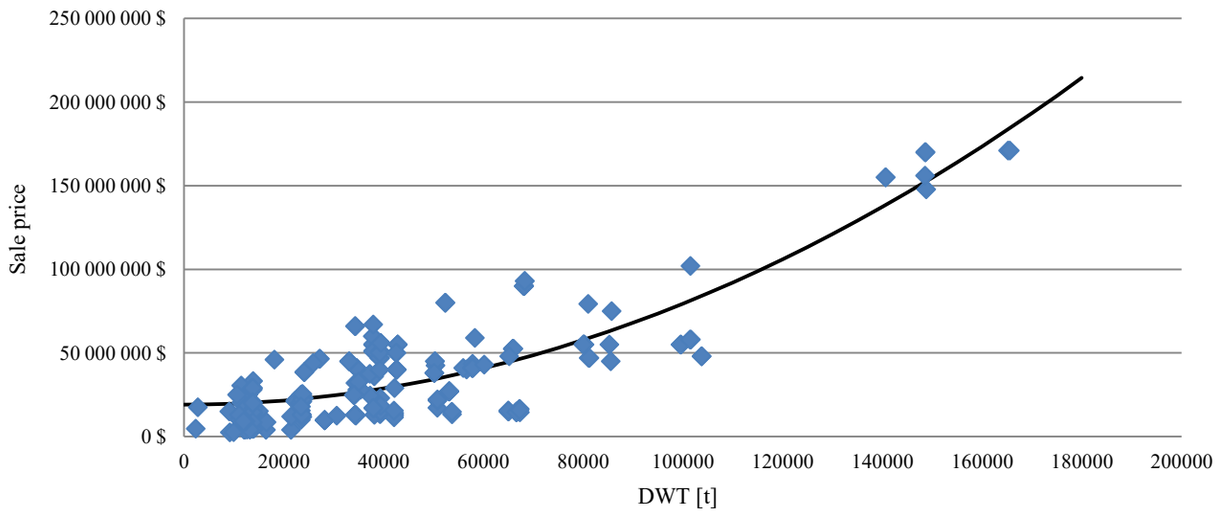

Figure 2. Approximations of container ship price depending on DWT capacity. Relationship (3) in comparison with reference data

- standard error σ = $ 17.2 million.

Figures 1 and 2 show the comparison between reference data and results obtained through the relations (2) and (3), respectively.

A model was then developed for predicting the sale price of a container ship based on the DWT capacity and TEU capacity:

$$P = -40{,}849{,}078 + \\ +639{,}829 \cdot \ln(\text{DWT})^2 \cdot 4.913 \cdot 10^{-5} \cdot \text{TEU}^2 \qquad (4)$$

where:
P – price of a container ship in USD;
TEU – number of containers;
DWT – deadweight capacity [t].

Equation (4) is characterized by:

- correlation coefficient $R^2 = 0.73$;
- standard error σ = $ 16.8 million.

Figure 3 shows the prediction of the price of a container ship based on the carrying capacity and the number of 20-foot containers according to formula (4).

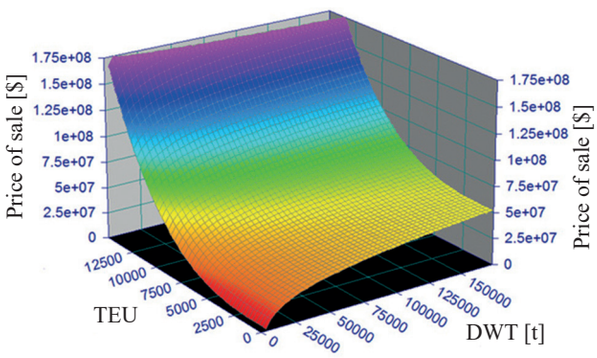

Figure 3. Projecting the price of a container ship depending on the DWT capacity and TEU capacity according to formula (4)

Use of artificial neural networks for container ship price approximation

In many scientific works on hydromechanics and ship design, the application of the theory of artificial neural networks to make approximations brought to good solutions. In the publications of Abramowski (2008; 2013) the author used the theory of artificial neural networks to build approximating functions, while Chądzyński (2001) shows the possibility of using an analysis of neural network sensitivity to a dependent variable for the selection of independent variables.

Equation (4) presented in the previous section has a slightly higher accuracy than equations (2) and (3). It means that this relationship is of little practical use, because it does not enable more accurate approximations than equations (2) and (3). On the other hand, the use of the theory of artificial neural networks for approximating the sale price depending on the TEU capacity produced more accurate solutions.

The artificial neural network was applied to determine a function approximating the sale of vessels. In this research, the following types of networks were tested:

- Multilayer Perceptron (MLP) of a sigmoidal activation function;
- Generalized Regression Neural Network (GRNN) – a regression network;
- Radial Basic Function Network (RBF).

The search for the most appropriate network was carried out through the following steps:

1. description of the best network structure by means of genetic algorithms;
2. learning a network (usually by using the back-propagation method);
3. testing a network;
4. assessment of approximation accuracy obtainable within a network on the basis of the testing data.

The MLP network of the structure: 2 (inputs) × 3 (hidden neurons) × 1 (output), appeared to be the most accurate (Figure 4). The network can be represented by this mathematical relationship:

$$P = \frac{\left(\frac{1}{1+e^{-(([\mathrm{DWT,TEU}]\times\mathbf{S}+\mathbf{P})\times\mathbf{A}-\mathbf{B})}}\times\mathbf{C}+0.211\right)+2.4\cdot10^{-2}}{5.99\cdot10^{-9}} \tag{5}$$

where:

P – price of a container ship in USD;
DWT – deadweight capacity [t];
TEU – number of containers;
A – matrix of weight values:

$$\begin{bmatrix} .6549 & .7148 & .6021 \\ 1.6543 & .4188 & -1.1279 \end{bmatrix};$$

S – matrix of coefficients:

$$\begin{bmatrix} 6.45\mathrm{E}-06 & 0 \\ 0 & 7.67\mathrm{E}-05 \end{bmatrix};$$

B – threshold vector
[3.1783 1.1353 –0.5476];
C – column vector of weights:
[2.4972 0.7511];
P – vector of offset values:
[–6.84E–02 2.35E–02].

Equation 5 allows the approximation of the price, *P,* based on deadweight capacity, DWT, and number of containers, TEU, using the matrix calculation method. The matrix and column vectors were described above.

The artificial neural network described by equation (5), compared to relations (2)–(4), is characterized by:

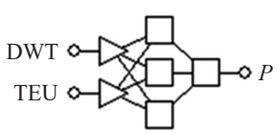

Figure 4. The structure of artificial neural network for the approximation of container ship price P according to equation (5), where: DWT – deadweight capacity, TEU – number of twenty-foot containers

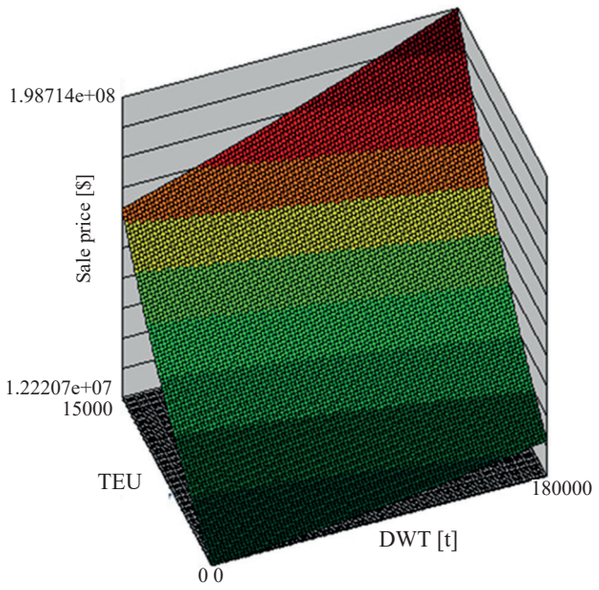

Figure 5. Projecting the price of a container ship depending on the DWT capacity and TEU capacity according to the formula (5)

- the highest value of the correlation coefficient, $R^2 = 0.86$;
- the lowest standard error, σ = $ 13.0 million.

Figure 5 presents container ship price prediction based on the DWT capacity and TEU capacity resulting from equation (5).

Conclusions

The study shows that the price estimate of a new container ship is influenced mainly by the TEU capacity and DWT capacity. The article presents a series of mathematical formulas that allow forecasting the price of a container based on these quantities. The relations have been developed from data on sale prices of 241 container ships built in 2005–2015.

Formulas (2) and (3) may be used interchangeably as the ship's carrying capacity depends mainly on the number of containers. Formula (4), which takes into account both DWT capacity and TEUs, is characterized by an accuracy that is only slightly higher than the one of formulas (2) and (3). Therefore, the practical value of this formula is low. Formula (5), on the other hand, includes the same independent variables, i.e. DWT capacity and TEU capacity, yet it is characterized by the highest accuracy and lowest error of the developed formulas.

It follows from the above that the use of artificial neural networks to predict the price of a container ship brings more accurate solutions than linear regressions.

References

1. Abramowski, T. (2008) Application of artificial neural networks to assessment of ship manoeuvrability qualities. *Polish Maritime Research* 2. pp. 15–21.
2. Abramowski, T. (2013) Application of Artificial Intelligence Methods to Preliminary Design of Ships and Ship Performance Optimization. *Naval Engineers Journal* 125 (3). pp. 101–112.
3. Bertram, V. (2000) *Practical Ship Hydrodynamics*. Butterworth-Heinemann.
4. Buczkowski, L. (1974) *Podstawy budownictwa okrętowego. T. I–III*. Skrypt Politechniki Gdańskiej, Gdańsk.
5. Chądzyński, W. (2001) *Elementy współczesnej metodyki projektowania obiektów pływających*. Prace Naukowe Politechniki Szczecińskiej, Szczecin.
6. Michalski, J.P. (2004) Parametric method of preliminary prediction of the building costs. *Polish Maritime Research*, Special Issue.
7. Rawson, K.J. & Tupper, E.C. (2001) *Basic Ship Theory* (5th Edition). Elsevier.
8. Schneekluth, H. & Bertram, V. (1998) *Ship Design for Efficiency and Economy*. Butterworth/Heinemann.
9. Watson, D.G.M. (2002) *Practical Ship Design*. Gulf Professional Publishing.

Scientific Journals
of the Maritime University of Szczecin

Zeszyty Naukowe
Akademii Morskiej w Szczecinie

2016, 48 (120), 176–181
ISSN 1733-8670 (Printed)
ISSN 2392-0378 (Online)
DOI: 10.17402/192

Received: 29.04.2016
Accepted: 02.12.2016
Published: 15.12.2016

Methodology for identification of potential threats and ship operations as a part of ship security assessment

Katarzyna Prill[1]✉, Marcin Szymczak[2]

Maritime University of Szczecin
[1] Education and Certification Department, [2] Ship Department
e-mail: {k.prill; m.szymczak}@am.szczecin.pl
✉ corresponding author

Key words: threats, security assessment, ISPS Code, terrorism, system, identification methods, safety of navigation

Abstract

This paper presents the development of a methodology for the identification of possible intentional threats and key ship operations that may be significant for a ship's security assessment, carried out by a Company Security Officer. The applicable international and domestic legal regulations regarding ship security systems are here analysed. Key factors and parameters that may provide support for the proper identification of realistic threats are also identified, giving practical relevance to this paper. The information reported here may be of support to those responsible for the development and revision of a ship's security assessment as it addresses an important part of the maintenance of navigational safety of ship operations under the provisions of the International Ship and Port Facility Security Code – ISPS Code.

Introduction

The adoption of the International Ship and Port Facility Security (ISPS) Code in 2002, which resulted from Conference Resolution 2 of the Contracting Governments to the International Convention for the Safety of Life at Sea (SOLAS), has led to an obligation for marine vessels to implement a system supporting security against intentional threats (IACS, 2008; UKMTO, 2011; IMB, 2016). An unlawful intentional act may be either a terrorist or a piracy act. An intentional threat is mostly defined as a use of force or violence against people or property in contravention of the law, aimed at intimidation and extortion on a group of people or country concessions to meet specific goals (Ślączka, Prill & Cieszyńska, 2010).

Legislative activities of the International Maritime Organisation (IMO) in regards to navigation safety improvement, including in particular an implementation of formal marine vessels' security systems, were a result of the events of September 11th 2001 (UKMTO, 2011). They led to the introduction of additional forces and measures improving navigation security, in particular in the areas specified as dangerous (e.g. the Somalia coast, the strait of Malakka) (Fernando et al., 2015; Knyazeva & Korobeev, 2015; IMB, 2016). The first part of this paper presents a legal analysis regarding maritime vessels' security systems, and also the legal requirements on ship security assessment, with respect to both domestic and international regulations (Stec, 2011). The second section of the paper refers to an identification process of key parameters, operations and factors that may affect a correct definition of threats. Therefore, this paper is of practical nature and may be of support for individuals responsible for the development and revision of ship security assessment as it addresses an important part of the maintenance of navigational safety of ship operations under the provisions of the International Ship and Port Facility Security Code – ISPS Code.

Ship security system with respect to domestic and international legal requirements

Under the Vienna Convention on the Law of Treaties (VCLT) of May 23rd 1969, each State adhering to the IMO is obliged to sign an international agreement, also known as a treaty, act or convention, respecting its provisions and implementing them into domestic law. The Republic of Poland, as a State belonging to the International Maritime Organisation and a Member State of the European Union, is obliged to comply with the requirements on ship security included in the following international acts:

1. International Convention for the Safety of Life at Sea concluded at London on November 1st 1974 (Journal of Laws of 1984, No. 61, Item 318 and 319 and of 2005, No. 120, Item 1016 as amended) along with the Protocol of 1978 relating to the International Convention for Safety of Life at Sea of November 1st 1974 concluded on February 17th 1978 (Journal of Laws of 1984, No. 61, item 320 and 321 and of 1986, No. 35, Item 177) hereinafter referred to as the "SOLAS Convention";
2. The International Ship and Port Facility Security Code (ISPS Code) adopted on December 12th 2002, Conference resolution 2 of the Contracting Governments to the International Convention for the Safety of Life at Sea, 1974 (Journal of Laws of 2005, item 1016) hereinafter referred to as the "ISPS Code";
3. Regulation No. 725/2004/EC of the European Parliament and of the Council of March 31st 2004 on enhancing ship and port facility security (O.J. WE L 129 209.04.2004, page 6; O.J. EU, Polish special edition, part 7, 7.8, page 74);
4. Directive No. 2005/65/EC of the European Parliament and of the Council of October 26th 2005 on enhancing port security (O.J. UE L/310/28 of November 25th 2005);
5. Commission Regulation (EC) No. 884/2005 of June 10th 2005 laying down procedures for conducting Commission inspections in the field of maritime security (O.J. UE L 148/25 of June 11th 2005).

The legal requirements included in the above mentioned international documents have been incorporated by the aforementioned Vienna Protocol to the domestic law. In the Polish legal system, provisions and requirements for the security system of ships may be found in the following documents:

1. The Ratification Act on the amendments to the International Convention for the Safety of Life at Sea 1974 SOLAS (Journal of Laws No. 2005.120.1016 of July 5th 2005);
2. The Maritime Security Act of September 4th 2008 (Journal of Laws No. 2016, item 49);
3. The Regulation of the Minister of Infrastructure of February 19th 2008 on the ship pre-arrival security information form (Journal of Laws No. 34, item 268);
4. The Regulation of the Minister of Infrastructure of February 25th 2009 on the form of declaration of security between a ship and a port facility (Journal of Laws No. 39, item 315);
5. The Regulation of the Minister of Infrastructure of February 25th 2009 on the forms regarding the Continuous Synopsis Record (CRS) for the ship and the list of last ports of call (Journal of Laws No. 39, item 314);
6. The Regulation of the Minister of Infrastructure of June 23rd 2009 on detailed activities and methods of actions for contact point designated to act upon receiving an alert and the requirements for the operation of alert systems (Journal of Laws No. 102, item 843);
7. The Regulation of the Minister of Infrastructure of November 5th 2010 on the transmission and information flow in the field of maritime security (Journal of Laws No. 217, item 1431);
8. The Regulation of the Minister of Infrastructure of November 17th 2010 on the list of prohibited items and substances and methods and means of securing the transport of weapons on ships (Journal of Laws No. 233, item 1529 as amended);
9. Regulation of the Council of Ministers of April 15th 2011 on the control methods and measures in the field of maritime security (Journal of Laws No. 93, item 539);
10. The Prime Minister Announcement of July 22nd 2015 on the publication of the consolidated text of the Regulation of the Council of Ministers on the procedure and method of co-operation of bodies in order to prevent threats to ships, port facilities and ports and related infrastructure, resulting from the use of ships or floating objects for terrorist attacks (Journal of Laws No. 2015, item 1139).

Ship Security System: goals and objectives

The goal of developing a ship security system is to identify and analyse potential threats that may occur with respect to a particular ship during its travel or

stay at a port, and to then implement activities that mitigate the threat. A key element of the entire security system is a company declaration stating that appropriate forces and measures shall be provided in order to perform basic ship security activities.

The basic tasks for the ship security system are (ISPS, 2004; Benny, 2015, pp. 41–42; Liwäng, Sörenson & Österman, 2015):

1. The prevention against unauthorised access on shipboard, in particular to special security areas.
2. The prevention against carrying weapons and other dangerous materials on board.
3. The prevention against smuggling drugs and other dangerous substances.
4. The prevention of sabotage, theft of goods or engineering solutions.
5. The protection of the ship and port facility against terrorist attacks, criminal assaults or threats caused by technical failures or natural disasters.
6. The establishment and implementation of procedures for responding to life or health-threatening situations of the shipboard personnel and any other individuals on board or at the port facility where the ship is berthed.

In order to complete the above mentioned tasks, the company, through the Company Security Officer – CSO, is obliged to verify periodically the actual state of the ship covered by the system, including (ISPS, 2004, A/8.4):

1. An identification of existing security measures, procedures and operations;
2. An identification and evaluation of key ship board operations that are important to protect;
3. An identification of possible threats to the key ship board operations and the likelihood of their occurrence, in order to establish and prioritize security measures;
4. An identification of weaknesses, including human factors, in the infrastructure, policies and procedures.

Correct identification of the actual status of the ship security allows to indicate the steps that should be taken in order to systematically increase the ship's degree of security (Urbański, Margaś & Sprecht, 2008). An obligation to possess, develop and review periodically the Ship Security Assessment (SSA) for each ship belonging to the company, in fulfilment of the requirements of the A/8 of the ISIP Code and Art. 4, point 12 of the Maritime Security Act, dated September 4th 2008. This constitutes the grounds for drawing up a Ship Security Plan – SSP. The correct identification of threats with a high probability of occurrence on an assessed ship

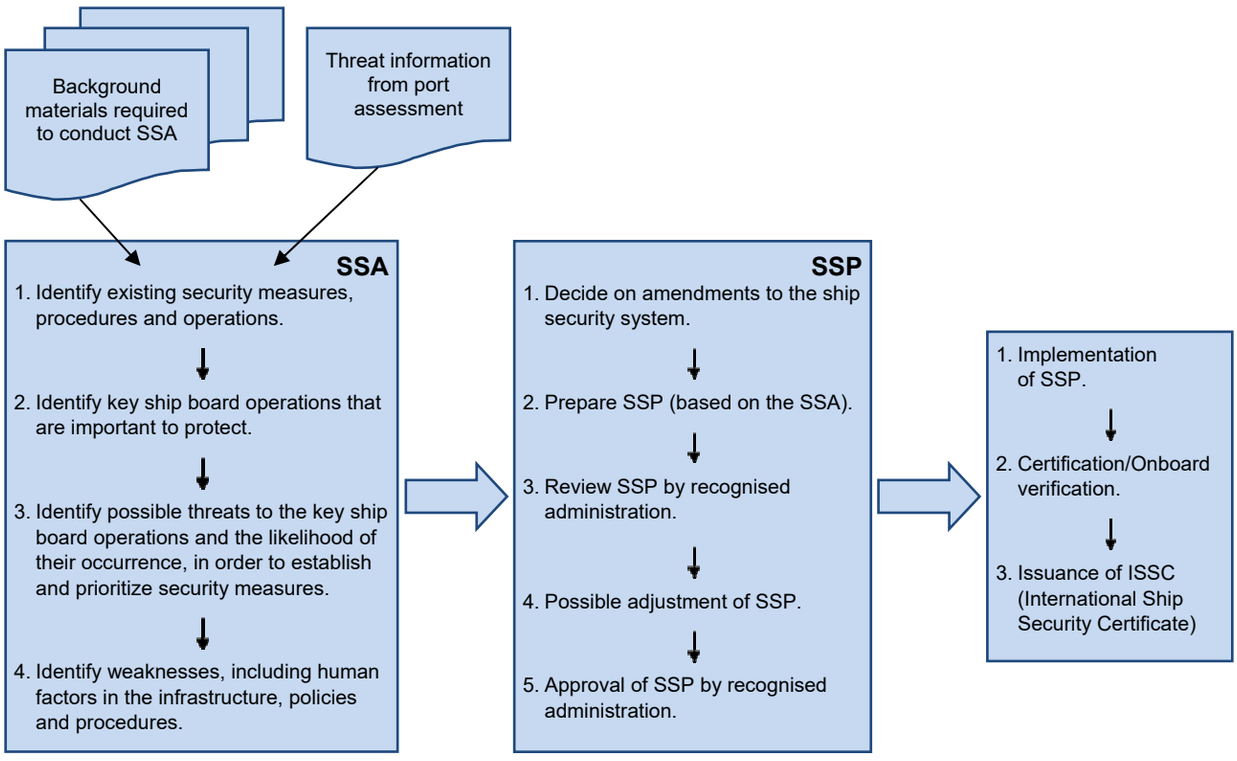

Figure 1. Mutual relations between SSA and SSP (based on NSA, 2012)

and the determination of key ship operations which may affect ship security should result when drawing up procedures and instructions that shall sufficiently protect a vessel against intentional threats.

The mutual relations between SSA and SSP are illustrated in Figure 1 (NSA, 2016).

Methods of assessment and review of SSA

The ship security assessment process is conducted periodically on the basis of the existing status, using methods such as FMEA, HAZID, and brainstorming (in contrast to the analysis of dynamic approach (Stróżyńska & Abramowicz, 2015)). It is divided into stages during which the Company Security Officer, on the grounds of the gathered information, identifies potential threats to the assessed ship and analyses the risk of their occurrence (Urbański, Margaś & Sprecht, 2008). The following steps of the ship security assessment process have been established (ClassNK, 2004; ABS, 2005).

Stage 1: Identification of the ship's characteristics and voyage areas.

Stage 2: Identification of possible threats and potential security risks for the ship and the crew (according to A/8.4.3, B/8.2 of the ISPS Code).

Stage 3: Identification and evaluation of key shipboard operations that are important to protect (according to A/8.4.1, A/8.4.2, B/8.3, B/8.6, B/8, 7, B/8.8 of the ISPS Code).

Stage 4: Identification of possible scenarios of threat to key shipboard operations and crew, and assessment of the likelihood of their occurrence (according to A/8.4.3, B/8.9, B/8.10 of the ISPS Code).

Stage 5: On-scene Security Survey (according to A/8.4.4, B/8.5, B/8.14 of the ISPS Code).

Stage 6: Re-identification of possible threat scenarios to key shipboard operations and crew and assessment of the likelihood of those occurrences (according to A/8.4.3, B/8.9, B/8.10 of the ISPS Code).

For the purpose of this paper, the first, second and third stages are subject to a detailed analysis.

Stage 1: Identification of the ship's characteristics and voyage areas

1. Prior to commencing the identification process of threats that may occur, with a specific probability, for the assessed ship, the vessel specification should be performed (Randić et al., 2015). The assessment should be conducted based on the criteria including, in particular: Design parameters of the assessed ship, voyage area and cargo description, legal requirements – When preparing for the identification process of intentional threats and key threats for the security of ship operations, one must pay attention to the parameters of the assessed ship. Apart from the ship design parameters, the knowledge of waters where the ship operates or will be operating in the near future is also very significant, as well as the specification of the type of cargo carried.
2. Characteristic factors for the ship requiring protection and possible weaknesses – It is necessary to report the devices and measures with which the ship is equipped by the company and the procedures applicable in the up-to-date operation. On the basis of this criterion, information should cover weaknesses in the field of the applicable procedures, infrastructure, crew qualifications and human factors.
3. External documentation providing information and affecting proper identification of threats and key operations of an assessed ship – During the threat identification process, the CSO should make use of, inter alia, the ship general arrangement plan, the list of restricted areas enumerated in the SSP and other spaces indicated in Chapter II-2 of the SOLAS Convention, including a description of every determined and potential access point to the ship as well as a list of key equipment for security purposes and safe ship operation, a list of exit routes and assembly points allowing for safe abandon of the ship. If available, all ship security procedures should be taken into consideration, including procedures regarding inspections, searches, people, supplies and property identification, monitoring, inspection of security equipment, alarms and access control.

Stage 2: Identification of possible threats and potential security risks for the ship and the crew

At this stage, the Company Security Officer should, based on the information gathered at the first stage, answer to the below questions to gradually determine the probability of occurrence of a threat (ClassNK, 2004):

1. Is there the existence of political (incl. religious, ideological, ethnical, nationalistic) threats that may affect the security of the ship, crew, or cargo? If so, what are the threats?
2. Does the ship operate in waters (enter ports) with unstable political situation? If so, which waters? What is the current political situation?

3. Can the ship, when staying in a port, be used to destroy/damage symbolic (historic) buildings/ structures?
4. Does the ship visit ports where mass events take place? If so, what kind of events?
5. Can the ship be used to damage ecologically important areas?
6. Does the ship itself possess a symbolic value?
7. Does the visibility or profile of the ship, company or brand represent a motive for unlawful acts?
8. Does the ship carry a special cargo? If so, what cargo?
9. Is it likely that terror related smuggling takes place from ports your ship is visiting?
10. Is it likely that your crew can take part in or embrace terror related smuggling? What are the ethnic characteristics of the crew? Are there any political – ethnic conflicts?
11. Does the ship operate in areas known for piracy?
12. Do the ship, cargo or passengers represent risk of hijacking? Can the ship damage infrastructure significant for industry and society?
13. Is the ship itself a critical infrastructure for society and industry?
14. Can the activities jeopardising ship security affect community safety and industry protection?
15. Can the ship be used as a means of threat and create fear in society?

Stage 3: Identification and evaluation of key shipboard operations that are important to protect

At the third stage, the subject of an analysis is the ship itself. The Company Security Officer should identify and specify the likelihood of an attack threat for every ship operation and its crew in the field of the procedures related with cargo loading, unloading or transportation and operations related with current ship operations (BV, 2003, Bichou, 2015). In order to identify correctly the operations affecting ship security, the CSO should take into consideration the following:

1. Control of access to the ship, ship spaces and rooms – the Company Security Officer should determine the security degree for the ship's structural elements such as: gangways, ladders, passages, corridors, platforms, doors, hatches, portholes, stairs, storage rooms for mooring lines and anchor chains, access to the ship from the sides, the bow, the aft, the storage room, loading equipment. The CSO should also identify every individual who is not a crew member and has an access to the ship rooms and spaces (company representatives, inspectors, technicians, guests, visitors etc.).
2. Limited access areas and restricted areas – the Company Security Officer should identify spaces that should be subject to a particular protection due to their function, and that would significantly affect the possibility of reacting to attacks if they were to be compromised. Such areas include, inter alia, the bridge, engine room, citadel, if present, emergency exit from the engine room, crew spaces, steering gear room, storage rooms, emergency power generator room, fire stations, battery rooms, air conditioning and fan rooms, storage rooms, anchor rooms, the Medical Room, hatches and access points to the air conditioning system and other specific for the assessed vessel.
3. Operations improving security – The Company Security Officer should identify equipment, systems, devices and procedures having an impact on the improvement of ship security. Such operations may include, inter alia, alarm procedures, drill schedule, monitoring systems, fire protection systems, signal systems, rescue systems, communication and alert systems, etc.
4. Deliveries and cargo management – Deliveries management should be understood as any operation related with loading and unloading cargo, ship storage and waste discharge from the ship. The CSO should determine the points where deliveries will be loaded and stored and waste discharged.

Conclusions

The ship security assessment process should be divided into stages at which the Company Security Officer, based on the gathered information, identifies potential threats for the assessed ship and analyses the risk of their occurrence. The identification of threats and key ship operations is a process that determines the development of the following elements of the ship security system against threats resulting in the deterioration of navigational safety. In order to complete successfully the security activities, specified by the international and domestic laws, the identification process should be comprehensive and cover the ship (its structure, equipment, systems, etc.), crew (trainings and engagement in the ship security process), transported cargo and the area where the ship operates. It must be noted that the above described identification process should be carried out individually for every assessed ship and should result in the development of appropriate procedures ensuring that ship security is maintained at a proper level.

References

1. ABS (2005) Guide for Ship Security (SEC) 3 ed. [Online] Available from: https://www.eagle.org/eagleExternalPortalWEB/ShowProperty/BEA%20Repository/Rules&Guides/Current/111_ShipSecurity(SEC)Notation/Pub111_ShipSecurity [Accessed: April 19, 2016]
2. Benny, D.J. (2015) *Maritime Security: Protection of Marinas, Ports, Small Watercrafts, Yachts and Ships*. CRC Press.
3. Bichou, K. (2015) The ISPS Code and the Cost of Port Compliance: An Initial Logistics and Supply Chain Framework for Port Security Assessment and Management. In: Haralambides H. *Port Management*. pp. 109–137.
4. BV (2003) *Ship security assessment – VentiSTAR, Maritime Division Ship in Service*. [Online] Available from: www1.veristar.com [Accessed: April 20, 2016]
5. ClassNK (2004) *Steps of Ships Security Assessment, ClassNK*. [Online] Available from: https://www.clasnk.org.jp [Accessed: April 19, 2016]
6. Fernando, D., Martinez, A., Sidoti, D., Mishra, M., Han, X. & Pattipati, K. (2015) *Context-based models to overcome operational challenges in maritime security, Technologies for Homeland Security (HST)*. IEEE International Symposium on Technologies for Homeland Security 14–15.04.2015. pp. 1–6.
7. IACS (2008) *Rec. No. 81. Guidance on the ISPS Code for Maritime Security Auditors*. [Online] Available for: www.iacs.org.uk/publications/publications.aspx?pageid=4&sectioned=5 [Accessed: April 04, 2016]
8. IMB (2016) *Violent attacks worsen in seas of West Africa despite global piracy downturn*. International Maritime Bureau report 27.04.2016. [Online] Available for: https://iccccs.org/icc/imb [Accessed: April 28, 2016]
9. ISPS (2004) Międzynarodowy Kodeks dla ochrony statków i obiektów portowych, przyjętym w dniu 12 grudnia 2002 r., Regulacja Nr 2 Konferencji Umawiających się Rządów – Stron Międzynarodowej Konwencji o bezpieczeństwie życia na morzu, 1974 r. (D.U. z 2005 r., poz. 1016), zwana „Kodeksem ISPS".
10. Journal of Laws (2008) Ustawa z dnia 4 września 2008 r. o ochronie żeglugi i portów morskich (D.U. nr 2016, poz. 49).
11. Knyazeva, N. & Korobeev, A. (2015) Maritime terrorism and Piracy: The Threat to Maritime Security. *Mediterranean Journal of Social Sciences* 6. pp. 226–232.
12. Liwäng, H., Sörenson, K. & Österman, C. (2015) Ship security challenges in high-risk area: manageable or insurmountable? *WMU Journal of Maritime Affairs* 14 (2). pp. 201–217.
13. NSA (2012) *Guideline for performing Ship Security Assessment*. p. 4. Norvegian Shipowners' Association. [Online] Available from: http://www.tradewindsnews.com/incoming/article262521.ece/binary/report%20report [Accessed: April 19, 16]
14. Randić, M., Matika, D. & Możnik, D. (2015) SWOT analysis of deficiencies on ship components identified by Port State Control Inspections with aim to improve the safety of maritime navigation. *Shipbuilding* 66 (3). pp. 61–72.
15. Ślączka, W., Prill, K. & Cieszyńska, K. (2010) Określenie potencjalnych zagrożeń dla terminali LNG na przykładzie terminala LNG w Świnoujściu. *Logistyka* 4. pp. CD–CD.
16. Stec, K. (2011) Wybrane prawne narzędzia ochrony infrastruktury krytycznej w Polsce. *Bezpieczeństwo Narodowe* 19, III. pp. 181–197.
17. Stróżyńska, M. & Abramowicz, W. (2015) A Dynamic Risk Assessment for Decision Support Systems in the Maritime Domain. *Studia Ekonomiczne* 165. pp. 295–307.
18. UKMTO (2011) *Best Management Practice for Protection against Somalia Based Piracy*. Livingston, Edinburgh: Witherby Publishing Group Ltd.
19. Urbański, J., Margaś, W. & Sprecht, C. (2008) Bezpieczeństwo morskie – ocena i kontrola ryzyka. *Zeszyty Naukowe Marynarki Wojennej* 2(173). pp.

Scientific Journals
of the Maritime University of Szczecin

Zeszyty Naukowe
Akademii Morskiej w Szczecinie

2016, 48 (120), 182–186
ISSN 1733-8670 (Printed)
ISSN 2392-0378 (Online)
DOI: 10.17402/193

Received: 29.04.2016
Accepted: 02.11.2016
Published: 15.12.2016

Application of Bon Voyage 7.0 (AWT) to programming of an ocean route of post-Panamax container vessel in transpacific voyage Seattle – Pusan 26.08.2015, 1600UTC – 05.09.2015, 2100UTC

Maciej Szymański✉, Bernard Wiśniewski

Maritime University of Szczecin, Faculty of Navigation, Institute of Marine Navigation
1–2 Wały Chrobrego St., 70-500 Szczecin, Poland
✉ corresponding author, e-mail: mszymanski@interia.pl, b.wisniewski@am.szczecin.pl

Key words: ocean voyage route optimization, ocean voyage route programming, voyage planning, Bon Voyage system, fuel criterion, ECA

Abstract
The results of testing the Bon Voyage system for an ocean voyage are presented in this paper. The main assumptions of testing were: ETD – 26.08.2016 and ETA – 05.09.2016, as established by the owner. All the data have been obtained from an actual voyage of a post-Panamax shipping container through the North Pacific. Testing was repeated again after completion of the voyage (post-voyage analysis). The data indicate that improved results with respect to fuel consumption could have been achieved using a different moment of second stage testing. Possible problems at planning, programming, and optimizing of the route leading through the ECA (Emission Control Area) zones with the use of onboard routing systems are also presented.

Introduction

Improper weather planning or incorrect execution of a ship's voyage can result in huge financial and operational losses for the ship-owner or charter company. Consequently, there are a number of decision support and optimization tools available on the market to assist the navigator in this task. We present here the practical application as well as the limitations of one of these tools, the Bon Voyage System, in planning and execution of a transpacific voyage.

Description of the ship, the voyage, its planning and optimization

The voyage of the post-Panamax container Vessel from Seattle, USA, to Pusan, South Korea, was been planned on the basis of the following weather data:

1. AWT BV 7.0 planning tool and weather products of AWT, applicable in this tool, in particular the 16 days weather prognosis (Applied Weather Technologies, 2014).
2. Surface analysis weather charts and 24- and 48-hrs surface prognosis charts, 3- and 5-days tropical cyclones track charts, 50 kts winds charts of the JMA (Japanese Maritime Agency).
3. Standard EGC warnings and information.

The vessel is a post-Panamax container vessel.
LOA: 335.7 m;
Breadth molded: 42 m;
GT: 97500;
TEU capacity: 8750;
Drafts: Fwd = 13.30 m, Aft = 13.30 m;
DWT: 84711 MT;
Cargo, fuel and ballast: 71 971 MT, 6736 TEU (77%), 3015 MT of fuel, 8340 MT of ballast.

In accordance with the owner's policy, once the ocean voyage had embarked, the vessel was

additionally assisted in weather routing by AWT. The AWT provided Routing and Monitoring service route recommendation before the commencement of the voyage, as well as constant monitoring throughout the whole duration of the voyage. Therefore, hydro-meteorological analysis and updated route recommendations were regularly provided to the ship. In fact, periodically throughout the voyage, the ship submitted position and weather reports to AWT which enabled the route monitoring and correct routing of the ship.

Symbols and abbreviations used in the paper

ETD – *Estimated Time of Departure*;
Departure – Point of departure;
ETA – *Estimated Time of Arrival*;
Arrival – Point of arrival;
Troll – vessel's own roll period (transverse) in sec;
nm – *nautical miles*, route distance;
Hrs – *hours*, required steaming time;
T_FO – *Total Fuel Oil*, Total fuel consumption en route;
HSFO – *High Sulphur Fuel Oil*, consumption en route;
LSFO – *Low Sulphur Fuel Oil*, consumption en route;
MDO – *Marine Diesel Oil*, consumption en route;
LSMDO – *Low Sulphur Marine Diesel Oil*, consumption en route;
SC – *Calm Sea Speed*, ship's speed on calm seas for the optimized route;
WxF – *Weather Factor*, influence of weather on ship's speed;
CuF – *Current Factor*, influence of ocean surface current on ship's speed;
SOG – *Speed Over Ground* for the optimized route;
Fuel(USD) – Total fuel cost in USD for the optimized route.

Testing before the commencement of the voyage

Preliminary testing of the voyage plan had been started several days ahead of the planned ETD, on August 22nd. It was assumed, according to the coastal schedule that the ETD would be on August 26, 2015 at 1600Z. Required ETA at Pusan pilot station was determined for September 5, 2015 at 2100Z. A preliminary simulation of the voyage was conducted on that day to demonstrate whether the northern route (based on the Great Circle) would be feasible with respect to the current weather conditions. The route and its calculated costs are presented in Figure 1. The method of testing was to consume the least fuel with a fixed ETA (Wiśniewski, 1991).

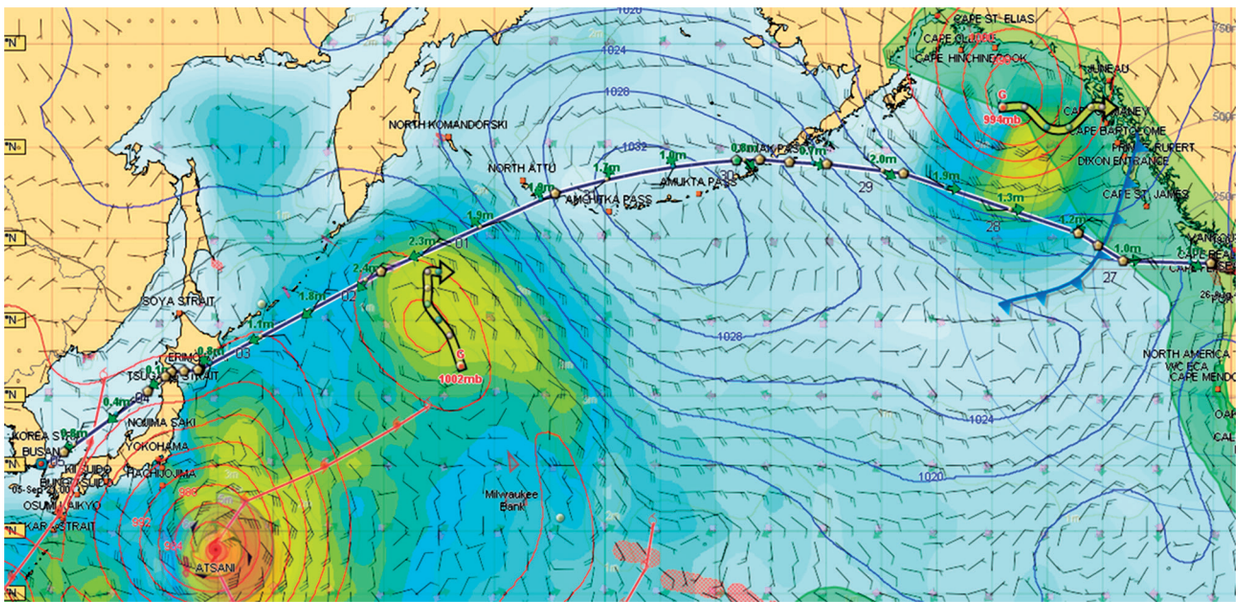

ETD	Departure	ETA	Arrival	Troll	nm	Hrs	T_FO	HSFO	LSFO	MDO	LSMDO	SC	WxF	CuF	SOG	Fuel(USD)
2015/08/26 16:00	SEATTLE	2015/09/05 20:59	BUSAN	19.4	4576	245.0	1342.5	1232.3	110.2	0.0	0.0	19.1	-0.38	-0.07	18.7	356221

Figure 1. The Preliminary simulation Aug. 22, 2015 – optimization least fuel consumption with fixed ETA and voyage costs

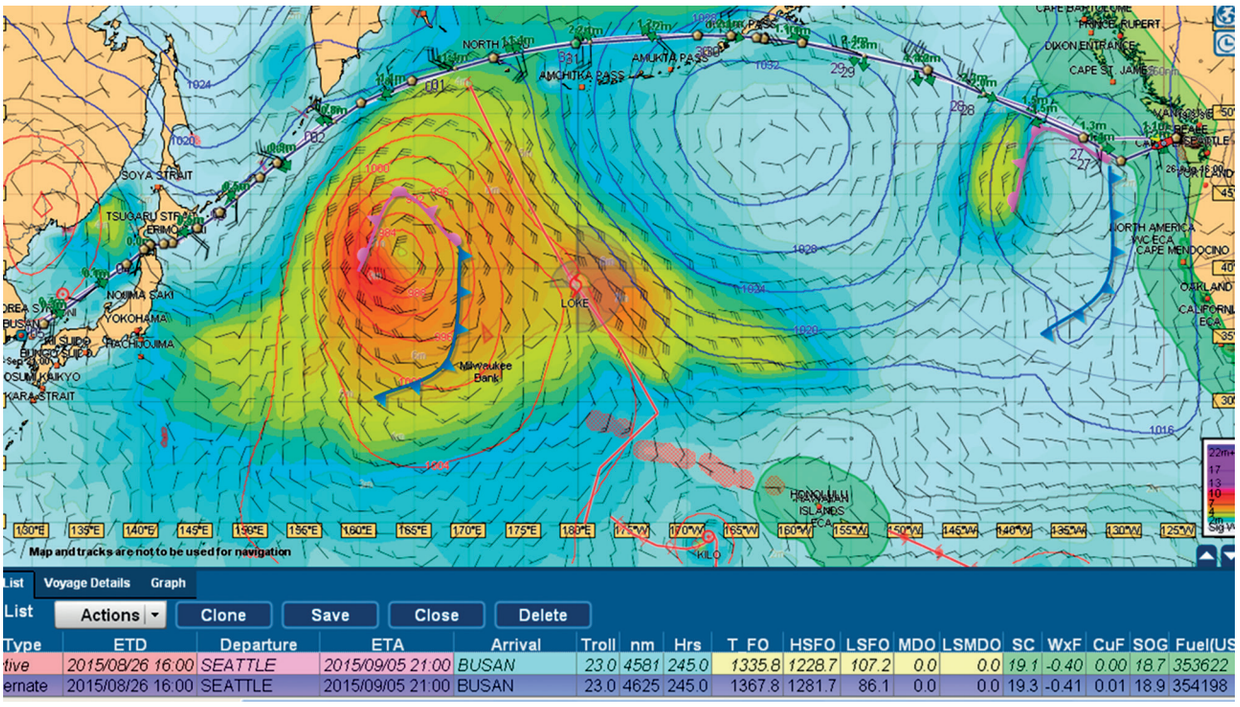

Figure 2. 2nd stage testing from August 26th. Optimization condition of least fuel consumption with fixed ETA. The route created by BVS (bold) and the route corrected manually together with voyage costs of both routes

Testing during the voyage

The 1st stage of route testing and optimizing was conducted on August 26th, 2015. The results of this test are presented on Figure 2. The 2nd stage testing was conducted (after dropping off the vessel's pilot) during the navigation through the waters of Puget Sound and Strait of Juan de Fuca, after the latest weather info had been received. These results are presented on Figure 2. The results for the route created by the BVS are presented as well as for the route created manually. The BVS route contains optimization errors regarding the navigation in ECA zone. They had been corrected in the route created manually. The BVS overall route is more expensive, despite the shorter distance in the ECA zone. Part of that route is presented on Figure 3. The above testing has proven that the choice of the northern route, based on the great circle was correct.

The ship must strictly comply with the voyage schedule. Earlier arrival is in general not viable. Regular liner operators and container operators in particular, operate according to port windows, prearranged with port terminal operators. The ship must enter the port, complete the cargo operations, and sail within those port windows' limits. Any changes and amendments to those time frames are generally not accepted. Noncompliance with the port window may result in the loss of port berth or a fine. Consequently, the ship tries to arrive exactly on ETA as determined in voyage schedule, with minimum possible fuel consumption, so as to not to lose her port window.

The true route chosen by the captain shows the gain of 44 Nm and 32 MT of fuel in comparison to the route created by BV, despite the 21 MT higher consumption of ULFSO in the ECA zone (107.1–86.2). This route, compared with the route from the preliminary testing simulations, is similar in terms of distance and leads partially through the

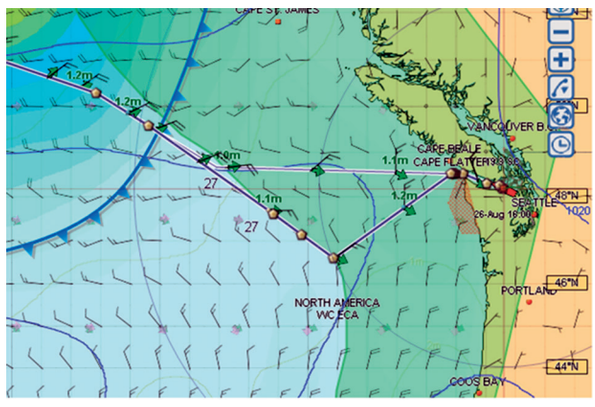

Figure 3. The Part of the route leading through ECA zone, optimized by BVS (bold) and true route

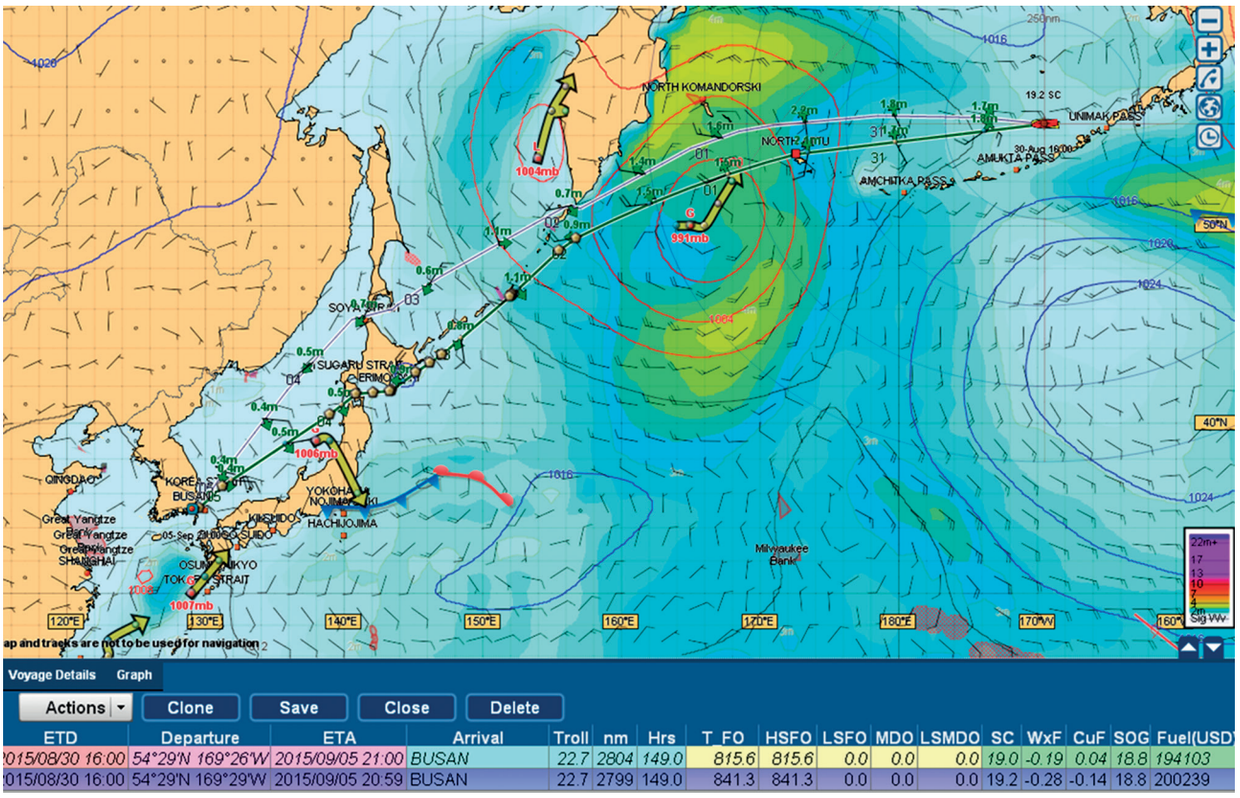

ETD	Departure	ETA	Arrival	Troll	nm	Hrs	T_FO	HSFO	LSFO	MDO	LSMDO	SC	WxF	CuF	SOG	Fuel(USD)
2015/08/30 16:00	54°29'N 169°26'W	2015/09/05 21:00	BUSAN	22.7	2804	149.0	815.6	815.6	0.0	0.0	0.0	19.0	-0.19	0.04	18.8	194103
2015/08/30 16:00	54°29'N 169°29'W	2015/09/05 20:59	BUSAN	22.7	2799	149.0	841.3	841.3	0.0	0.0	0.0	19.2	-0.28	-0.14	18.8	200239

Figure 4. The 3rd stage testing, optimization east fuel with fixed ETA – August 30th

Bering Sea. However, this testing shows that the weather conditions worsen, i.e. two low pressure systems at 40°N/160°E and 39°N/180° (Figure 2) intensify.

The 2nd stage testing had been conducted on August 30th, on the Bering Sea. The results of this testing are presented in Figure 4. The route created by BVS is slightly longer than the finally chosen route, however fuel-wise it is more favorable. This route would have led through Okhotsk Sea, Soya/La Perouse Strait and Sea of Japan to Pusan, through the Piervyj Kurilskyj Proliv pass (a waterway leading from the Pacific), to the Okhotsk Sea between Kamchatka Peninsula and the first island in the Kuril Archipelago. The more southern pass, through Chetvertyj Kurilskyj Proliv is safer (UK Hydrographic Office NP41, 2014; UK Hydrographic Office NP136, 2014) and it was considered as optional route. The route created by BVS in the 2nd stage of testing, leading through the Pervyj Kurilskyj Proliv was not accepted due to navigational considerations and, moreover, the fuel gain on route leading through the Chetvertyj Kurilskyj Proliv pass was negligible. Finally, the original route from the 1st stage of testing, leading through Tsugaru Strait between the Japanese Islands, was chosen.

Post-voyage analysis

Post-voyage analysis, using the true weather data had been conducted after the completion of the voyage. It was then compared with the true route. Both routes are presented on Figure 5. This analysis showed that the route leading south of Aleutian Chain would have been more favorable, both cost-wise and weather-wise. This leads to a conclusion that weather forecasts at that time could have been wrong and that the date of the 2nd stage testing had been chosen incorrectly. Weather conditions and the ship's position in the Gulf of Alaska along the true route and along the route programmed on the basis of true weather data on August 28th are presented on Figures 6 and 7. They show unequivocally that the route should have been amended to a more southern one in this particular moment. The 2nd stage testing was, however, greatly affected by the tropical system TS LOKE and its forecasted track (see Figure 2). It seems that a several stage testing was viable in this particular voyage. 1st stage testing should have taken place in Seattle, 2nd stage testing on departure from the ECA zone, 3rd stage testing in Unimak pass, 4th stage testing on the meridian 180 and 5th stage testing on the meridian 160 E. Errors in planning and programming the route were also greatly influence

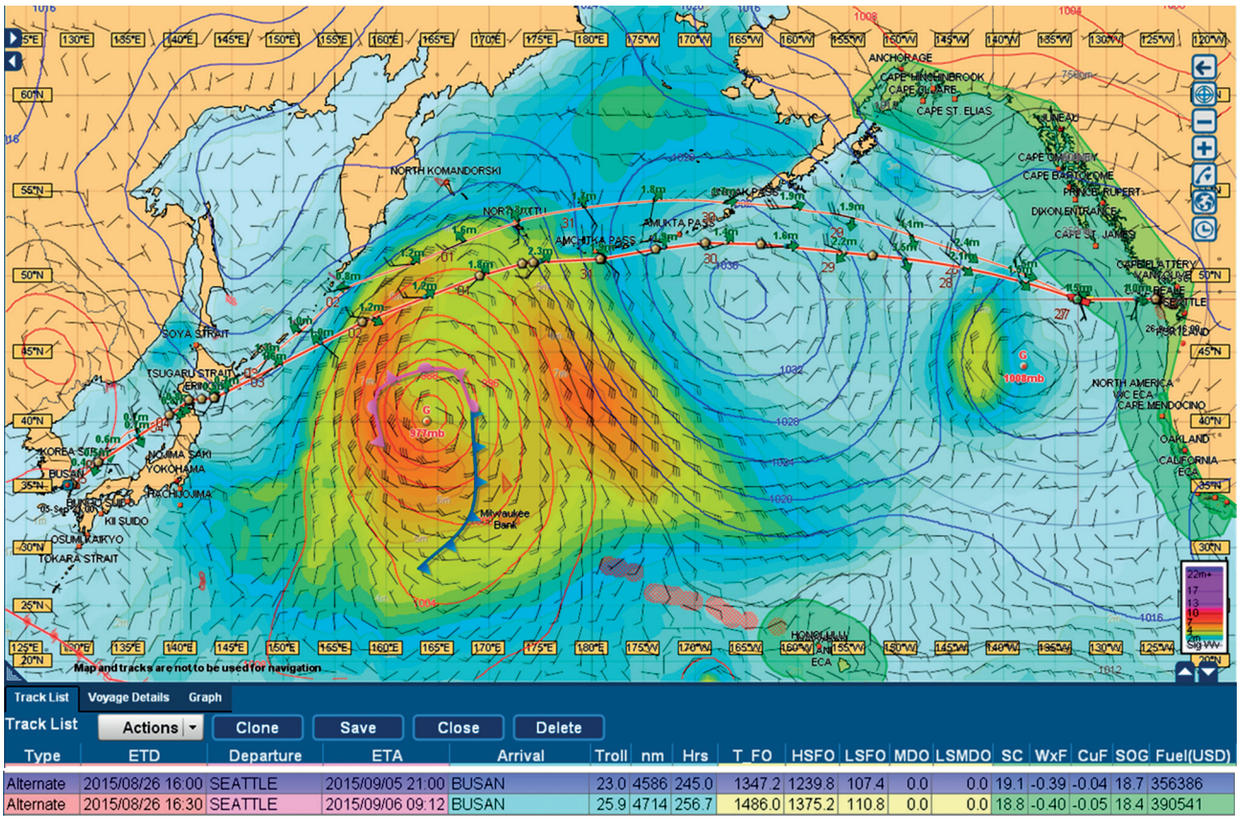

Figure 5.After voyage analysis – least fuel optimization (bold) and true route

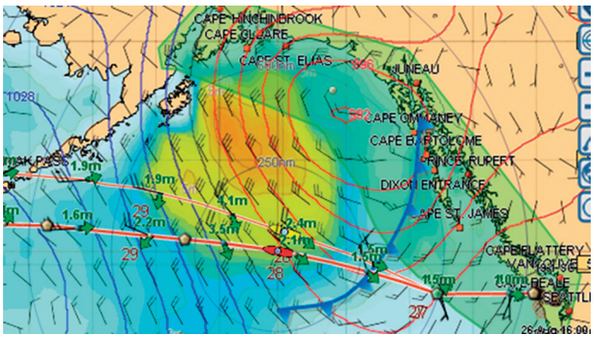

Figure 6. Weather conditions and ship's position in the Gulf of Alaska on Aug 28th. True route and after voyage optimization (bold)

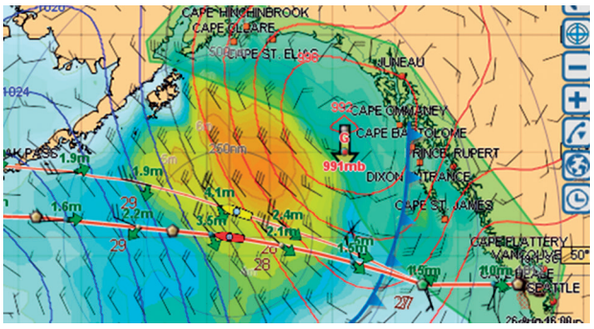

Figure 7. Weather conditions and ship's position in the Gulf of Alaska on Aug 28th. True route and after voyage optimization (bold)

by numerous amendments to the voyage schedule and required ETA.

Conclusions

A practical application of an onboard routing system Bon Voyage 7.0, a vessel route optimization and programming tool has been presented. Planning, programming, weather and operational optimization, as well as post-voyage analysis of the vessel route has been discussed, with the use of a true trans-pacific voyage of a post-Panamax container vessel. Onboard routing systems, like Bon Voyage, can be a huge asset for a navigator in carrying out the task of safe and economical, planning and programming of the ocean route for a ship.

References

1. Applied Weather Technologies (2014) Bon Voyage System (BVS 7.0), Voyage Optimization Software, User Manual. 140 Kifer Court, Sunnyvale CA 94086.
2. UK Hydrographic Office NP136 (2014) Ocean Passages for the World, 6th Edition.
3. UK Hydrographic Office NP41 (2014) Admiralty Sailing Directions, Japan Pilot, Volume I, 11th Edition.
4. Wiśniewski, B. (1991) *Problemy wyboru drogi morskiej statku*. Gdańsk: Wydawnictwo Morskie.

Reviewers in 2016

1. Dr hab. inż. Teresa Abramowicz-Gerigk, Gdynia Maritime University, Poland
2. Dr hab. inż. Jarosław Artyszuk, Associate Professor, Maritime University of Szczecin, Poland
3. Dr hab. inż. Andrzej Banaszek, West Pomeranian University of Technology, Szczecin, Poland
4. Dr hab. inż. Artur Bejger, Associate Professor, Maritime University of Szczecin, Poland
5. Michael Bergmann, Director Maritime Industry, Comite International Radio Maritime (CIRM), Grosskrotzenburg, Germany
6. Dr hab. inż. Mariusz Borawski, West Pomeranian University of Technology, Szczecin, Poland
7. Prof. dr hab. inż. Zbigniew Burciu, Gdynia Maritime University, Poland
8. Dr hab. inż. Tomasz Cepowski, Associate Professor, Maritime University of Szczecin, Poland
9. Prof. dr hab. inż. Adam Charchalis, Gdynia Maritime University, Poland
10. Dr hab. inż. Leszek Chybowski, Maritime University of Szczecin, Poland
11. Dr hab. inż. Krzysztof Czaplewski, Associate Professor, Gdynia Maritime University, Poland
12. Dr inż. Janusz Cieloszyk, West Pomeranian University of Technology, Szczecin, Poland
13. Prof. dr hab. inż. Romuald Cwilewicz, Gdynia Maritime University, Poland
14. Dr inż. Lech Dorobczyński, Maritime University of Szczecin, Poland
15. Prof. dr Daniel Duda, Polish Naval Academy, Gdynia, Poland
16. Prof. dr hab. inż. Marka Dzida, Gdańsk University of Technology, Poland
17. Dr inż. Łukasz Dziemba, Silesian University of Technology, Gliwice, Poland
18. Dr.-Ing. Evelin Engler, Institut für Kommunikation und Navigation – DLR, Neustrelitz, Germany
19. Prof. dr hab. inż. Andrzej Felski, Gdynia Maritime University, Poland
20. Dr hab. inż. Włodzimierz Filipowicz, Associate Professor, Gdynia Maritime University, Poland
21. Dr hab. inż. Wiesław Galor, Associate Professor, Maritime University of Szczecin, Kazimierz Wielki University, Bydgoszcz, Poland
22. Dr hab. inż. Mirosław K. Gerigk, Associate Professor, Gdańsk University of Technology, Poland
23. Dr Agnieszka Gozdek, Szczecin University, Poland
24. Dr inż. Zygmunt Górski, Associate Professor, Gdynia Maritime University, Poland
25. Dr hab. inż. Andrzej Grządziela, Associate Professor, Polish Naval Academy, Gdynia, Poland
26. Prof. dr hab. inż. Lucjan Gucma, Maritime University of Szczecin, Poland
27. Dr hab. inż. Maciej Gucma, Maritime University of Szczecin, Poland
28. Prof. dr hab. inż., dr h.c. Stanisław Gucma, Maritime University of Szczecin, Poland
29. Dr Sambor Guze, Gdynia Maritime University, Poland
30. Prof. dr hab. inż. Jacek Januszewski, Gdynia Maritime University, Poland
31. Prof. dr inż. Mirosław Jurdziński, Gdynia Maritime University, Poland
32. Dr inż. Jacek Karliński, Politechnika Wrocławska, Poland
33. Dr hab. Lech Kasyk, Associate Professor, Maritime University of Szczecin, Poland
34. Prof. dr hab. Krzysztof Kołowrocki, Gdynia Maritime University, Poland
35. Dr inż. Karol Korcz, Gdynia Maritime University, Poland
36. Dr inż. Jerzy Kowalski, Gdynia Maritime University, Poland
37. Dr inż. Maciej Kozak, Maritime University of Szczecin, Poland
38. Prof. dr. sc. Srećko Krile, University of Dubrovnik, Croatia
39. Dr hab. inż. Renata Krzyżyńska, Associate Professor, Politechnika Wrocławska, Poland
40. Prof. dr hab. Jan Kulczyk, Politechnika Wrocławska, Poland
41. Dr hab. inż. Lesław Kyzioł, Associate Professor, Gdynia Maritime University, Poland
42. Piotr Laskowski, Head of Research Infrastructure, National Centre for Nuclear Reserch, Świerk, Poland
43. Prof. dr hab. inż. Józef Lisowski, Gdynia Maritime University, Poland
44. Prof. dr hab. inż. Ewgenij Łusznikow, Maritime University of Szczecin, Poland
45. Dr hab. inż. Artur Makar, Associate Professor, Polish Naval Academy, Gdynia, Poland
46. Kmdr dr inż. Waldemar Mironiuk, Polish Naval Academy, Gdynia, Poland
47. Dr hab. inż. Jakub Montewka, Associate Professor, Gdynia Maritime University, Poland; Aalto University and Finnish Geospatial Research Institute, Finland
48. Junmin Mou, Ph.D, Navigation School, Wuhan University of Technology, China

Maritime University of Szczecin

The Maritime University of Szczecin (MUS) continues the tradition of marine-related education at Szczecin's maritime schools that was established in 1947. Since then, it has developed dynamically and maintained the highest standards in all areas of research and education.

MUS is recognized by the maritime industry as an important research centre developing marine engineering, navigation, transportation engineering and many other fields. MUS provide research services by ***Green Energy*** **– laboratory of wind power plants,** ***Marine Fuel and Lubricating Oils Laboratory***, ***Maritime Risk Analysis Center*** **and** ***Marine Power Plants Laboratory*****.**

Experts at the University develop innovative concepts like the LNG terminal in Świnoujście. The **European LNG Training Centre** (at MUS) provides the necessary training and awards the required qualifications for operating the terminal LNG equipment and LNG tankers.

The Baltic Fishing Training Centre in Kołobrzeg is a new MUS unit, established in June 2013. There are plans to set up a European Maritime Education Centre in co-operation with other universities of the Baltic states. This project involves two MUS training units, the Marine Traffic Engineering Centre and the Marine Rescue Centre. These units, equipped with several state-of-the-art simulators, will be run a broad training courses for Polish and foreign seafarers of all ranks.

The Marine Rescue Training Centre, one of the largest and best equipped centers of its type in Poland, offers training courses covering areas such as safety, life rescue, health security and environment protection. Participants are trained to respond in extreme emergency situations.

The Training Centre for Marine Officers runs training qualifications and specialized courses for merchant and fishing fleets officers.

The education of mariners calls for thorough onboard seamanship training. Part of this training takes place aboard the modern research-training vessel **Nawigator XXI**.

MUS graduates, with an excellent academic background of theoretical knowledge and practical skills, become specialists recognized in Europe and internationally. At present, students can choose a program at one of our three faculties, all conferring bachelor, master and doctoral degrees in Polish, or in English (selected programs).

Faculty of Engineering and Transport Economics

The Faculty educates personnel highly qualified in production management and engineering, port and fleet operations, transport logistics and systems. The programs are specially designed suit the needs of future prospective employers: forwarding, transport and logistics firms, operators in seaports and inland ports.

The following fields of study are available:

- Management and production engineering
- Transport
- Logistics

Faculty of Marine Engineering

The Faculty of Marine Engineering offers courses in two major fields:

- Mechanical engineering
- Mechatronics

These program's focus on theoretical and practical issues relating to the maritime industry, maintenance and operation of marine power plants, electric power systems, diagnostics of shipboard and industrial machines, and wind farms.

Faculty of Navigation

The Faculty teaching staff, many holding scientific degrees or professional titles combined with substantial experience and expertise of Master Mariner or Chief Officer, ensure the highest standards of academic education in accordance with the requirements of the STCW Convention. The faculty researchers focus on navigation safety, marine traffic engineering, navigation automation and the optimization of ocean routes, geomatics and hydrography.

The following fields of study are available:

- Navigation
- Transport
- Geodesy and cartography
- Computer science

Maritime University of Szczecin
1–2 Wały Chrobrego St., 70-500 Szczecin, Poland
tel. +48 91 4809400, www.am.szczecin.pl

We got a ministry grant for our quarterly development

We hereby inform, that the quarterly *Zeszyty Naukowe Akademii Morskiej w Szczecinie, Scientific Journals of the Maritime University of Szczecin* following Decision No. 790/P-DUN/2016 of 17 June 2016 received funding for the years from 2016 to 2017 from the Ministry of Science and Higher Education of Poland for the activities of promoting science.

The project includes the following tasks:

1. Digitalization of 72 volumes of the Scientific Journals published between 1973–2003 and their distribution on the Open Access basis (task type: digitalization of publications and scientific monographs to provide and maintain access to them through the Internet).

2. Translations and proofreading by a native speaker (task type: creating the English version of publications).

3. Publications of foreign, distinguished scientists and their participation in the scientific board (task type: participation of foreign, distinguished scientists in the scientific board of the journal).

4. Development of web-based editorial module for exchange of articles in the editor – author – reviewer system (task type: participation of foreign, distinguished scientists in the scientific board of the journal).

The tasks will be carried out in the period from 1 January 2016 to 31 December 2017.

Ministry of Science and Higher Education
Republic of Poland

Ministerstwo Nauki i Szkolnictwa Wyższego